ENERGY EFFICIENT ERROR-CORRECTING CODING FOR WIRELESS SYSTEMS

Xiaoying Shao

De promotiecommissie:

voorzitter en secretaris:

Prof.dr.ir. J. van Amerongen	Universiteit Twente

promotor:

Prof.dr.ir. C.H. Slump	Universiteit Twente

leden:

Prof.dr.ir. B. Nauta	Universiteit Twente
Prof.dr. P.J.M. Havinga	Universiteit Twente
Prof.dr.ir. A.B. Smolders	Technische Universiteit Eindhoven
Dr.ir. M.J. Bentum	Universiteit Twente
Dr.ir. F.M.J. Willems	Technische Universiteit Eindhoven

This research is financially supported by the Dutch Ministry of Economic Affairs under the IOP Generic Communication - Senter Novem Program.

Signals & Systems group,
EEMCS Faculty, University of Twente
P.O. Box 217, 7500 AE Enschede, the Netherlands

Printed by Gildeprint B.V., Enschede, The Netherlands
Typesetting in LaTeX2e

ISBN 978-90-365-3023-1
DOI 10.3990/1.9789036530231

ENERGY EFFICIENT ERROR-CORRECTING CODING FOR WIRELESS SYSTEMS

DISSERTATION

to obtain
the degree of doctor at the University of Twente,
on the authority of the rector magnificus,
prof.dr. H. Brinksma,
on account of the decision of the graduation committee,
to be publicly defended
on Thursday the 20th of May 2010 at 13.15.

by

Xiaoying Shao
born on the 3rd of October 1980
in Wenzhou, China

Dit proefschrift is goedgekeurd door:

De promotor: Prof.dr.ir. C.H. Slump

To my father

Shao, Yunsheng (1946 ∼ 2006)

Contents

Summary

The wireless channel is a hostile environment. The transmitted signal does not only suffers multi-path fading but also noise and interference from other users of the wireless channel. That causes unreliable communications. To achieve high-quality communications, error correcting coding is required to mitigate the noise and interference encountered during the signal transmission. However, the current design of error correcting codes does not take the power consumption in ADCs into account. ADCs consume about 50% of the total base-band power. The power-efficiency of ADCs does not increase in the same speed as the baseband signal processing. Digital signal processing follows Moore's law. Given the same specification, the power consumed in ADCs halves every 2.7 years but the power consumption in the baseband signal processing decreases a factor of 10 every 5 years. In the case of RF signal processing, the power efficiency is limited by the semi-conductor technology. Therefore, ADCs are the main bottleneck for an energy-efficient wireless receiver.

Quantized channels arise in practical communication systems where ADCs are used to sample the analog transmitted signals. Conventional narrow-band systems usually do not take quantization into account, since a large number of quantization levels is used. In this case the difference between the quantized and unquantized channel can be neglected. To lower the resolution of ADCs in the narrow-band wireless system, the design of the error correcting coding should consider the quantization effect. This thesis describes the design of a coding scheme for the quantized channel. The approach is based on multi-level coding and binary block codes to achieve the theoretical limits in the narrow-band wireless channel.

Wide-band wireless systems often employ OFDM to ease the equalizer in the receiver. OFDM has a high *Peak-to-Average Power Ratio* (PAPR) which is the main disadvantage of OFDM. When signal peaks in the OFDM signal are clipped, all sub-carriers are affected. Because the wide-band wireless channel is often modeled as a frequency selective fading channel, some part of the channel may suffer from deep fading and can not afford any distortion. Consequently, the communication is unreliable. That urges the usage of high-resolution ADCs in OFDM systems. Current OFDM systems

employ fixed high-resolution ADCs which are designed for the worst-case scenario. However, the worst-case scenario does not happen often. This thesis proposes to apply resolution adaptive ADCs in the OFDM system. In such a case, the ADC can be designed for each channel condition instead of fixing for the worst-case scenario. Correspondingly, the power consumption in ADCs reduces.

A further resolution reduction in ADCs can be achieved by designing an energy efficient error correcting coding for the OFDM system. The error correction coding in the current OFDM system is based on the joint coding scheme, which encodes the source data over all the sub-carriers in parallel. The joint coding scheme works better than separate coding, as it employs the fact that sub-carriers with high energy can compensate for sub-carriers with low-energy. Its drawback is each sub-carrier must be decoded, also the ones in deep fading. Hence, the maximum level of the noise floor endured by the joint coding scheme is limited to the dynamic range of the channel. Correspondingly, the minimum resolution of the ADC required by the joint coding scheme in a certain channel condition is dependent on the dynamic range of the channel. A way to reduce the dynamic range of the channel is to neglect the deep-fading part of the channel and to exploit the high-energy part only. Obviously, the joint-coding scheme can not apply this. Therefore, we propose in this thesis an energy-efficient error correction scheme based on fountain codes for OFDM systems. Fountain codes can reconstruct the original source file by only collecting enough fountain-encoded packets. It does not matter which packet is received as we only need to receive enough packets. In other words, fountain-encoded packets are independent with respect to each other. Since fountain codes are designed for erasure channels, error correction codes are required to transfer the noisy wireless channel into an erasure channel. That inspires us to exchange the code rate of error correction codes with the number of sub-carriers to be discarded. In this case, the resolution of ADCs and thus the power consumption can be reduced even more.

Samenvatting

Draadloze communicatie vindt plaats in een ongecontroleerde omgeving. Het signaal lijdt niet alleen onder reflecties, maar ook ruis en interferentie spelen een belanglijke rol. Dit maakt de communicatie in principle onbetrouwbaar. Om hoge kwaliteit communicatiediensten te garanderen is fout corrigerende code nodig om de ruis en interferentie te beperken die zich bij de signaaloverdracht voordoet. Echter, bij het huidige ontwerp van foutcorrectiecodes wordt geen rekening gehouden met het stroomverbruik van de *Analog-Digitaal Convertor* (ADC). ADCs verbruiken ongeveer 50% van het totale basis band stroomverbruik. De efficiëncy van ADCs blijft achter op de ontwikkelingen van de digitaal signaalverwerking. Het energieverbruik van de ADCs halvert per 2.7 jaar, het energieverbruik van de digitaal signaalverwerking neemt af met een factor 10 per 5 jaar. De energie efficiëncy bij RF signaal verwerking wordt hoofdzakelijk beperkt door de technologie. Daarom zijn ADCs het belangrijkste knelpunt voor energie-zuinige draadloze ontvangers.

Gekwantiseerde kanalen ontstaan in communicatie systemen waar ADCs worden gebruikt om analoge signalen te discretiseren. In conventionele systemen met een relatief smalle bandbreedte wordt meestal geen rekening gehouden met kwantisatie effecten, aangezien een groot aantal kwantisatie niveaus wordt gebruikt. In dit geval kan het verschil tussen het gekwantiseerde en ongekwantiseerde kanaal worden verwaarloosd. Bij het verlagen van de ADC resolutie moet bij het ontwerp van de foutcorrectieregeling codeer de kwantisatie ruis worden meegenomen. In dit proefschrift ontwerpen we een coderingsschema voor het gekwantiseerde kanaal. Dit wordt gedaan met Multi-level codering en Binary Block codering om zo de theoretische limiet van het smalbandige draadlose kanaal te bereiken.

In breedband draadloze systeem wordt vaak gebruik gemaakt van *Orthogonal Frequency Division Multiplexing* (OFDM) om de ververking in de ontvanger te ontlasten. Het belangrijkste nadeel van OFDM is het hoog *Peak-to-Average Power Ratio* (PAPR). Het afkappen van de signaalpieken in het OFDM signaal beinvloed alle draaggolven. Omdat het breed-band draadloze kanaal vaak wordt gemodelleerd als een Frequency Selective Fading kanaal lijdt een deel van het kanaal onder sterke

verzwakking en kan het zich geen vervorming veroorloven. Dit resulteert in onbetrouwbare communicatie. Dit vereist het gebruik van hoge-resolutie ADCs in het OFDM-systeem. Huidige OFDM systemen gebruiken vaste hoge resolutie ADCs die zijn ontworpen voor het meest ongunstigste scenario. Echter, dit scenario komt niet vaak voor. In dit proefschrift stellen we voor om adaptieve ADCs te gebruiken in OFDM-systemen. In een dergelijk geval kan de ADC worden aangepast voor iedere kanaal conditie. Dit resulteert in een gereduceerd stroomverbruik van de ADC.

Een verdere verlaging van de resolutie van ADCs kan worden bereikt door het ontwerpen van een energie-efficiënte foutcorrigerende code voor het OFDM-systeem. De foutcorrectie codering in het huidige OFDM-systeem is gebaseerd op het gezamenlijke codeer principe, die de bron van gegevens over alle draaggolven codeert. Het gezamenlijke codering schema werkt beter dan het afzonderlijke codering schema. Dit omdat het gebruik maakt van het feit dat hoge energie draaggolven lagere energie draaggolven kunnen compenseren. Het nadeel is dat elke draaggolf een gelijke behandeling nodig heeft. Vandaar dat het maximale niveau van de ruisvloer bij het gezamenlijke codering schema gelimiteerd is tot het dynamisch bereik van het kanaal. Een manier om het dynamische bereik van het kanaal te reduceren is het verwaarlozen van het "deep-fading" gedeelte van het kanaal en de focus te leggen op het hoog energetische gedeelte. Uiteraard kan het gezamenlijke-codeer schema dit niet bereiken. Daarom stellen we in dit proefschrift voor om een energie-efficiënte foutcorrectie-regeling gebaseerd op "Fountain" codes voor OFDM-systemen te gebruiken. "Fountain" codes kunnen het originele bronbestand slechts door het verzamelen van een voldoende aantal Fountain-gecodeerde pakketten reconstrueren. Het maakt niet uit welk pakket wordt ontvangen, zolang er maar voldoende pakketten zijn ontvangen. Met andere woorden, Fountain-gecodeerde pakketten zijn onafhankelijk ten opzichte van elkaar. Aangezien de Fountain codes zijn ontworpen voor "erasure" kanalen, zijn foutcorrectie codes nodig om het ruis kanaal om te zetten in een "erasure" kanaal. Dit inspireerde ons om de coderingscapaciteit van de fout correctie code in te zette van het kunnen negeren van draaggolven met zeer zwakke transmissie. In dit geval kan de resolutie van de ADCs verder worden gereduceerd.

Chapter 1

Introduction

1.1 Wireless Communications

Wireless communication consists of a transmitter, a receiver and the wireless channel in between, as shown in Figure 1.1. The goal of wireless communications is to transmit information from the transmitter to the receiver successfully, by means of electromagnetic (EM) waves in a wireless channel.

The EM spectrum typically used in wireless communication ranges from around tenths of KHz to tenths of GHz. A frequently occurring problem with EM wave propagation in this frequency range is *signal multipath* [1]. The EM waves transport the signal from the transmitter to the receiver via different paths of varying lengths. Due to the different delays of these propagation paths, the transmitted signal arrives at the receiver via multiple paths at different delays [1] [2] [3]. Besides, the transmitted signal via different propagation paths suffers different attenuation factors. Each received component via a different path has a different arrival time τ_i, amplitude A_i and phase ϕ_i. The different components will interfere with each other. Depending on the phase differences, the interference is constructive or destructive. The strength of the received signal depends strongly on the location of the objects and the transmitter and the receiver. The receiver can be located in a position, where it does not receive any signal at all. This phenomena is called multipath fading.

The transmitted signal does not only suffer the multi-path fading but also the noise and interference from the wireless channel, which can cause errors and affect the quality of communication. To achieve reliable communication, channel coding (i.e. error correcting coding) has to be applied in wireless communication systems. The function of the discrete channel encoder is to introduce, in a controlled manner, some

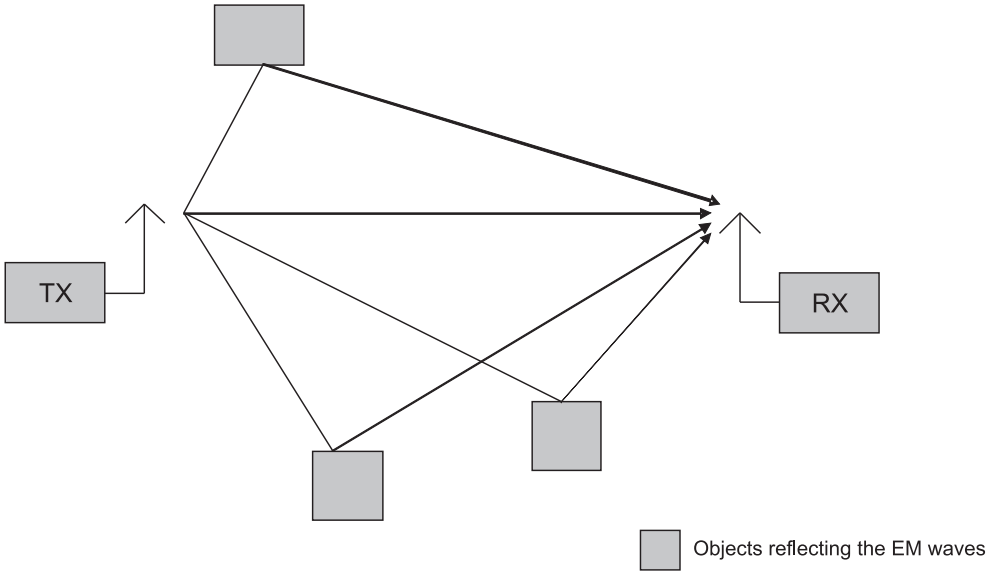

Fig. 1.1: Multipath propagation between the transmitter and the receiver.

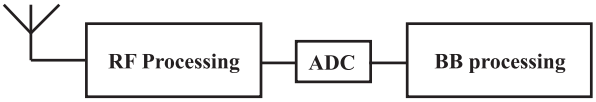

Fig. 1.2: A wireless receiver.

redundancy in the binary information sequence, which can be used at the receiver to overcome the effect of the noisy wireless channel [1]. The encoding process generally is to map a sequence of k source bits into a unique sequence of n encoded bits. Then, the output of the channel encoder is mapped to an analog waveform which suits for transmission over a communication channel using a digital modulator. Afterwards, the digital modulated signal is upconverted to the EM wave at *radio frequency* (RF).

At the receiver, the received RF signal has to be converted back to digital format by *Analog-to-Digital Converters* (ADCs), as seen in Figure 1.2. Before decoding the received signal, equalization (i.e. converting the multi-path channel effect) needs to be done. The complexity of equalization in wireless systems is determined by their transmission bandwidth. When the bandwidth is small, the symbol duration[1] is usually larger than the maximum delay spread of the channel[2]. In such case, the channel has a constant (i.e. flat) frequency response over the transmission band.

[1]The duration of the analog waveform corresponding to a digital data symbol is called the symbol duration.

[2]The maximum delay spread of the channel is defined as the difference between the maximum and the minimum delays among different paths.

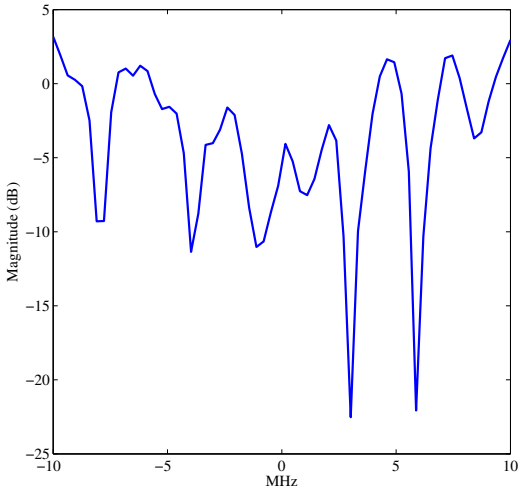

Fig. 1.3: Frequency selective channel.

When the bandwidth is large, the symbol duration is smaller than the maximum delay spread of the channel. In this case, *intersymbol interference* (ISI) occurs, which can significantly degrade the system performance. The channel responses at different frequencies in the transmission band are different. This is called a frequency selective fading channel, as shown in Figure 1.3. Equalizing the narrow-band signal is much simpler than equalizing the wide-band signal. To ease the equalization of the wide-band communication systems, *Orthogonal Frequency Modulation Division* (OFDM) technology is widely used in this context. The key idea of OFDM is to divide the whole transmission band into a number of parallel flat-fading sub-channels (also called sub-carriers) [4] [5]. In this case, equalization can be performed at small complexity.

OFDM enables an easy implementation of wireless systems at a high data rate. The channel capacity of a wireless system can be increased by increasing the channel bandwidth and/or increasing the amount of the transmission power. Bandwidth is not always available and increasing the transmission power increases the power consumption of the system and the interference to other users. Research in [6] and [7] has shown that the capacity of wireless channel can be increased by the use of multiple antennas at the transmitter and the receiver. A communication system using multiple antennas at the transmitter and the receiver is called a *multiple input multiple output* (MIMO) communication system. The capacity gain is reached by using a technique called spatial multiplexing.

1.2 MIMO in a Mass Market

The work reported in this thesis was carried within the "MIMO in a mass market" project [8], which in the period 2006-2010 brought together the University of Twente, Eindhoven University of Technology and Delft University of Technology, to meet the challenge of extending the performance of WLAN system-behavior. The focus of the project was on high data rate, large coverage and robustness to interferences with cheap and power-efficient implementations on the application of multiple-antenna techniques [8].

In indoor environments such as homes, offices and hospitals, wireless communication technology is spreading rapidly. This evolution is reflected in an increasing number of wireless connections, in an increasing diversity of communication standards, and, last but not least, in increasing data rates per communication link, supported in part by the emergence of multi-antenna technologies. The growing interest in low-weight wireless appliances, pervasive computing and ambient technology gives further impetus to this development, and poses new challenges with respect to power dissipation and cost price. Cost and battery power are known to be essential constraints for mass-market products. It may be too expensive to implement complete transmitter and receiver chains for each antenna. Particularly for bit rates above a few hundreds of Mbit/s, the power consumption in the ADC would also prohibit the use of multiple high resolution ADCs. Furthermore, the vast number of radio devices sharing the scarce radio spectrum will lead to serious interferences and coverage challenges that must be resolved simultaneously with the cost and power challenges for these new mass markets to materialize. That brings the research question to this thesis: **Can we design an energy-efficient wireless indoor communication system for a mass market which is robust to the noise and interferences encountered in the signal transmission?**

1.3 The Research Work

1.3.1 The Research Question

Wireless communication enables high mobility, but it brings us battery-powered wireless receivers, the noisy multi-path fading channel, the interference from other users, and etc. For battery-powered wireless receivers, the power consumption is still an issue. As we can see in Figure 1.4, there are three parts consuming power in wireless receivers: the RF signal processing, the ADC and the baseband (BB) signal processing. The power reduction in these three parts has the following trend:

- The power consumption in the RF signal processing reduces slowly and is limited by the technology.

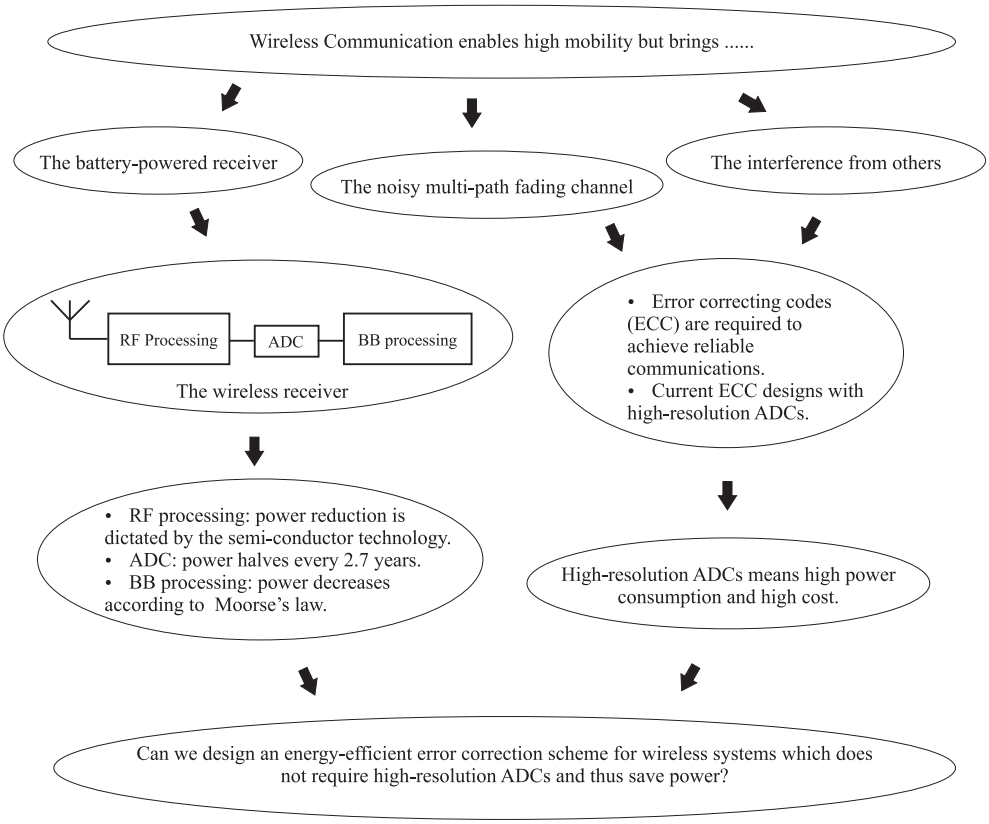

Fig. 1.4: The research question of the thesis.

- The power consumption in the ADC halves every 2.7 years [9].
- The power consumption in the BB signal processing decreases a factor of 10 every 5 years, according to Moorse's law [10].

The ADC can consume 50% of the total amount of baseband power [11], so the ADC is the main bottleneck for a power-efficient wireless receiver. A commonly used figure of merit that includes the power dissipation of the ADC is the "energy per conversion" figure of merit given by [12]:

$$\mathrm{FOM} = \frac{\mathrm{P}}{\mathrm{f_s} \cdot 2^{\mathrm{ENOB}}} \tag{1.1}$$

where P is the power consumption of the ADC, $\mathrm{f_s}$ is the sampling rate of the ADC and ENOB is the effective number of bits in the ADC. FOM shows that the tradeoff between precision and power. The above equation presents that the power consumption of the ADC halves for each reduced bit given the same $\mathrm{f_s}$. However, the quantization noise increases by decreasing ENOB. That may affect the quality of communications.

As mentioned earlier, error correction codes are applied in wireless systems to mitigate the effect of the noise and interference encountered in the wireless channel. However, error correction codes adopted in current high-data-rate wireless systems require high-resolution ADCs to achieve the good performance. Therefore, the research question of this thesis is equivalent to the following one: "**Can we design an energy-efficient error correction scheme for wireless systems which allows the receiver to use low resolution ADCs but still achieve the same quality of communication comparing to the current method?**".

1.3.2 The Contributions

Current wireless systems are not energy-efficient because they require high-resolution ADCs. High-resolution ADCs cost more power and money than low-resolution ADCs. In order to reduce the resolution of ADCs with the same Quality of Service (QoS), we should design an energy-efficient error correction scheme for wireless systems which does not require high-resolution ADCs. Error correction coding is designed according to the channel characteristics. Here, we discuss how we design the energy-efficient error correction scheme for narrow-band systems and wide-band systems separately.

1.3.2.1 Energy Efficient Error-Correcting Coding for Narrow-band Systems

Quantized channels arise in practical communication systems where ADCs are used to sample analog signals corresponding to the transmitted data. Conventional narrow-band systems usually do not take quantization into account, which is reasonable since

Fig. 1.5: System model showing the transmission over one subchannel in the OFDM system with ideal synchronization

a large number of quantization levels is used. In this case the difference between the quantized and unquantized channel can be neglected. To lower the resolution of ADCs in the narrow-band wireless system, we need to take the quantization effect into account. In this thesis, we investigate reliable communication over quantized channels from the information theoretical point of view. With a proper design of the quantization scheme, we study how much capacity will be lost using a coarse quantization in ADCs comparing to the case with high-resolution ADCs. Furthermore, we design in this thesis an error correction code for the quantized AWGN channel to achieve the theoretical limit.

1.3.2.2 Energy Efficient Error-Correcting Coding for Wide-band Systems

The wide-band wireless channel is always in a hostile environment. Therefore, it is a challenge to communicate both reliably and with a high throughput. OFDM has become a popular scheme for recent wireless systems which operate at a high data rate [13] [14] [15]. The main advantage of OFDM over the single-carrier scheme is its ability to eliminate ISI without complex equalization filters in the receiver [2]. OFDM has a high *Peak-to-Average Power Ratio* (PAPR) which is one of the main disadvantages of OFDM [16]. When signal peaks in the OFDM signal are clipped, all sub-carriers are affected.

In order to show the quantization effect in the OFDM system, let us first introduce the system model as shown in Figure 1.5. In the system, $\mathrm{X_k}$ is the symbol to be transmitted over the k-th sub-carrier, $\mathrm{x_n}$ is the n-th transmitted symbol in the time domain, $\mathrm{r_n}$ is the n-th received symbol in the time domain, $\mathrm{y_n}$ is the n-th quantized symbol and $\mathrm{Y_k}$ is the received signal over the k-th sub-carrier. We denote N as the number of sub-carriers and $\mathrm{N_q}$ as the number of quantization levels.

In this section, we assume the channel is noiseless which means that the received symbol $\mathrm{r_n}$ equals to the transmitted symbol $\mathrm{x_n}$. Every block of complex symbols transmitted over N sub-carriers is denoted by:

$$\mathbf{X} = [\mathrm{X}_0, \mathrm{X}_1, \cdots, \mathrm{X}_{\mathrm{N}-1}]$$

To communicate over this quantized channel, we map a sequence of d binary digits

into one of $\mathrm{M} = 2^{\mathrm{d}}$ symbols defined as:

$$\mathrm{s_m} = \phi(\mathrm{b_0}, \cdots, \mathrm{b_{d-1}}) \quad \mathrm{m} = 0, 1, \cdots, \mathrm{M} - 1 \tag{1.2}$$

where $(\mathrm{b_0}, \cdots, \mathrm{b_{d-1}})$ are the binary digits and ϕ is defined as:

$$\phi : \mathbf{GF}(2)^{\mathrm{d}} \rightarrow \mathbb{R} \tag{1.3}$$

We refer to ϕ as the *modulation map* and it defines the signal constellation $\mathcal{S}$:

$$\mathcal{S} = \{\mathrm{s_m} \in \mathbb{R} : \mathrm{s_m} = \phi(\mathrm{b_0}, \cdots, \mathrm{b_{d-1}})\} \tag{1.4}$$

We select two $\mathrm{s_m}$ from $\mathcal{S}$ as $\mathfrak{Re}\{\mathrm{X_k}\}$ and $\mathfrak{Im}\{\mathrm{X_k}\}$ respectively to construct $\mathrm{X_k}$ by:

$$\mathrm{X_k} = \mathrm{s_{m1}} + j\mathrm{s_{m2}} \tag{1.5}$$

which tells that X_k is mapped from a sequence of 2d binary digits. The modulation scheme that map 2d bits into one of $2^{2\mathrm{d}}$ complex constellation symbols is called *Quadrature Amplitude Modulation* (QAM) [1].

By taking the *Inverse Discrete Fourier Transform* (IDFT) of $\mathbf{X}$, we have the transmitted symbols in the time domain expressed as [2]:

$$\mathrm{x_n} = \frac{1}{\sqrt{\mathrm{N}}} \sum_{\mathrm{k}=0}^{\mathrm{N}-1} \mathrm{X_k} e^{j\frac{2\pi}{\mathrm{N}}\mathrm{kn}} \quad \mathrm{n} = 0, 1, \cdots, \mathrm{N} - 1 \tag{1.6}$$

According to the IEEE 802.11a standard [17], $\mathrm{x_n}$ is transmitted at a rate of 20 MSPS (mega samples per second). After the transmission over the channel, the real part and imaginary part of $\mathrm{x_n}$ are sampled at a sampling rate of 20 MHz assuming that there is no adjacent interference and the synchronization is perfect in the baseband. Then, they are quantized by quantizers respectively and we have:

$$\mathrm{y_n} = \mathcal{Q}(\mathfrak{Re}\{\mathrm{x_n}\}) + j\mathcal{Q}(\mathfrak{Im}\{\mathrm{x_n}\}) \tag{1.7}$$

We refer $\mathcal{Q}$ as the *quantization map* and is defined as:

$$\mathcal{Q} : \mathbb{R} \rightarrow \mathbf{Z} \tag{1.8}$$

where $\mathbf{Z} \in \mathbb{N}$ and represents the output of the quantizer. A quantization map is surjective and $\mathcal{Q}$ also defines an inverse quantization map which is defined as the set function $\mathcal{Q}^{-1}$:

$$\mathcal{Q}^{-1}(\mathrm{i}) = \{x_\mathrm{n} \in \mathbb{R} : \mathcal{Q}(\mathrm{x_n}) = \mathrm{i}, \mathrm{i} \in \mathbf{Z}\} \tag{1.9}$$

We restrict ourselves to quantizers where each $\mathcal{Q}^{-1}(\mathrm{i})$ is of the form $\mathcal{I}_\mathrm{i} = (a, b]$ for $a, b \in \mathbb{R}$. In this case $\{\mathcal{I}_\mathrm{i}\}$ partitions $\mathbb{R}$ and the quantizer is defined by the set of intervals $\{\mathcal{I}_\mathrm{i}\}$.

The quantization mapping function $\mathcal{Q}$ can also be expressed as:

$$\mathrm{y} = \mathcal{Q}(\mathrm{x}) = \mathrm{x} + \mathrm{n} \tag{1.10}$$

where $\mathrm{n} \in \mathbb{R}$ is called as the quantization noise. The quantization function is a *non-linear* function and the quantization noise is *signal-dependent*. (1.7) can be rewritten as:

$$\mathrm{y_n} = \mathrm{x_n} + \mathrm{n_n} \tag{1.11}$$

where the quantization noise $\mathrm{n_n} \in \mathbb{C}$ and its real and imaginary part are independent identical distributed (i.i.d.) and uniform distributed. We assume that the received signal is uniformly quantized. In such a case, $\mathrm{n_n}$ is uniformly distributed with zero mean and a variance of $\frac{\Delta^2}{6}$, where Δ is the uniform quantization step [18].

The quantized outputs are transformed back into the frequency domain by the *Discrete Fourier Transform* (DFT) [2]:

$$\begin{aligned} \mathrm{Y_k} &= \frac{1}{\sqrt{\mathrm{N}}} \sum_{\mathrm{n}=0}^{\mathrm{N}-1} \mathrm{y_n} e^{-j\frac{2\pi}{\mathrm{N}}\mathrm{kn}} \\ &= \frac{1}{\sqrt{\mathrm{N}}} \sum_{\mathrm{n}=0}^{\mathrm{N}-1} (\mathrm{x_n} + \mathrm{n_n}) e^{-j\frac{2\pi}{\mathrm{N}}\mathrm{kn}} \\ &= \mathrm{X_k} + \mathrm{N_k} \quad \mathrm{k} = 0, 1, \cdots, \mathrm{N}-1 \end{aligned} \tag{1.12}$$

where $\mathrm{N_k}$ is the quantization noise in the frequency domain. In other words, it shows the quantization effect of the OFDM systems. Due to the Central Limit Theorem, $\mathrm{N_k}$ is a Gaussian-distributed random variable with zero mean and a variance of $\frac{\Delta^2}{6}$. Due to the frequency selectivity of the wide-band channel, some sub-carriers suffer deep fading which can not afford more distortion. Consequently, unreliable communication occurs. That urges to use high-resolution ADCs in OFDM systems.

Still, the use of high-resolution ADCs can not guarantee the high quality of communication which require the assistance of error correction codes. In the current generation of wireless systems (e.g. IEEE 802.11a system [17], DVB systems [19] [20]), the *For-*

ward Error Correction (FEC) layer is based on the joint coding scheme. With this method, source data is encoded over all the sub-carriers. The joint coding scheme works better than the separate coding scheme, as it employs the fact that sub-carriers with high energy can compensate sub-carriers with low-energy [2]. Its drawback is that each sub-carrier has to be decodable. Hence, the maximum level of noise floor endured by the joint coding scheme is limited to the dynamic range of the channel. Correspondingly, the minimum resolution of the ADC required by the joint coding scheme in a certain channel condition is dependent on the dynamic range of the channel. One way to reduce the dynamic range of the channel is to neglect the deep-fading part of the channel but only to take care of the high-energy part. Obviously, the joint-coding scheme can not achieve it [see Chapter 3, 4, 5 and 6]. Furthermore, the joint decoder is not able to predict whether the received packet is decodable even with the perfect channel knowledge. That urges to employ a fixed high-resolution ADC in OFDM systems. Although this solution works well in practical systems, it is not energy-efficient for two reasons:

- Fixed high-resolution ADCs that are used in the current wireless receivers, are designed for the worst case scenarios.
- Packets which have encountered "bad" conditions are still processed by the entire receiver chain.

In this thesis, we propose an opportunistic error correction scheme based on resolution adaptive ADCs and fountain codes to mitigate the effects of a wireless channel at a lower power consumption in ADCs compared to the current OFDM-based wireless system. With resolution adaptive ADCs, the resolution of ADCs is adapted to each channel condition instead of being fixed to the high-resolution required for the worst-case scenarios. As a result, the power consumption of the ADC is reduced under most, i.e. non worst-case, channel conditions.

A further resolution reduction of the ADC can be achieved by discarding some part of the channel with deep fading. The current OFDM-based wireless systems do not support this idea, as all sub-bands are considered equally important by the FEC layer. However, the opportunistic error correction method based on fountain codes does not have this disadvantage. By using fountain codes, the receiver can recover the original data by collecting enough fountain-encoded packets. It does not matter which packets are received, only a minimum amount of packets have to be received correctly [21]. In other words, fountain-encoded packets are independent with respect to each other. That inspires us to transmit a fountain-encoded packet over a sub-band of a channel and transmit enough packets to be able to decode. Thus, multiple packets are transmitted simultaneously, using frequency division multiplexing. The receiver discards fountain-encoded packets which are transmitted over the sub-band with deep fading. Correspondingly, the power consumption in ADCs decreases.

The opportunistic error correction scheme is especially designed for OFDM-based systems to lower power consumption in ADCs. In this thesis, we analyze its performance from *the power consumption point of view* and *the robustness to the noise and interference point of view* for the following applications:

- the *Single Input Single Output* (SISO) point-to-point system like the IEEE 802.11a system [17], see *Chapter 3 and 6*.
- the broadcasting systems like OFDM-based DVB systems [19] [20] [22], see *Chapter 4*.
- the MIMO point-to-point system like the IEEE 802.11n system [23], see *Chapter 5*.

1.4 Structure of the Thesis

The main chapters of this thesis are Chapters 2, 3, 4, 5, 6. Each of those chapters consists of one or two papers in the format of their original published or submitted version. They are structured as shown in Figure 1.6, depending on whether the wireless channel is narrow-band or wide-band and on whether the wireless communication system is a SISO point-to-point system, a broadcasting system and a MIMO point-to-point system. As the title of the thesis suggests, we design energy efficient error-correcting schemes for different wireless systems. In Chapter 2, we focus on the single-carrier narrow-band wireless systems, while in Chapter 3-6, we move to the multi-carrier wide-band wireless systems.

- In Chapter 2, we investigate reliable communication over quantized channels from the information theoretical point of view. With properly designing a quantization scheme, $d+1$ or $d+2$ quantized bits are already enough when d source bits are mapped into conventional *Pulse Amplitude Modulation* (PAM) and transmitted over an *Additive White Gaussian Noise* (AWGN) channel. Moreover, we design an error correction code for the quantized AWGN channel, which can be applied in the narrow-band wireless system. With the combination of the multi-level coding and the *Low-Density Parity-Check* (LDPC) codes, a low bit error rate for a block length of 10^4 bits is achieved at 1.5 dB from the Shannon limit for $R \approx 1.5$ bit/use and at 1.4 dB from the Shannon limit for $R \approx 2$ bit/use.

- In Chapter 3, we design an energy-efficient error correction scheme for SISO-OFDM systems. It is based on resolution adaptive ADCs and fountain codes. With the channel knowledge, the ADC can be designed for each channel realization. The key part of the proposed system is that the dynamic range of ADCs can be reduced by discarding sub-carriers that are attenuated by the channel. Correspondingly, the power consumption in ADCs can be decreased. With this approach, more than 70% of the energy consumption in the ADCs can be saved compared with the conventional IEEE 802.11a WLAN system under the same channel conditions and throughput. In addition, it requires 7.5 dB less SNR than the 802.11a system. In this chapter, we also investigate its performance in the real-world. Measurement results show that the FEC layer used in the WLAN system consumes at least 26 times of the amount of power in ADCs comparing to the proposed cross-layer method.

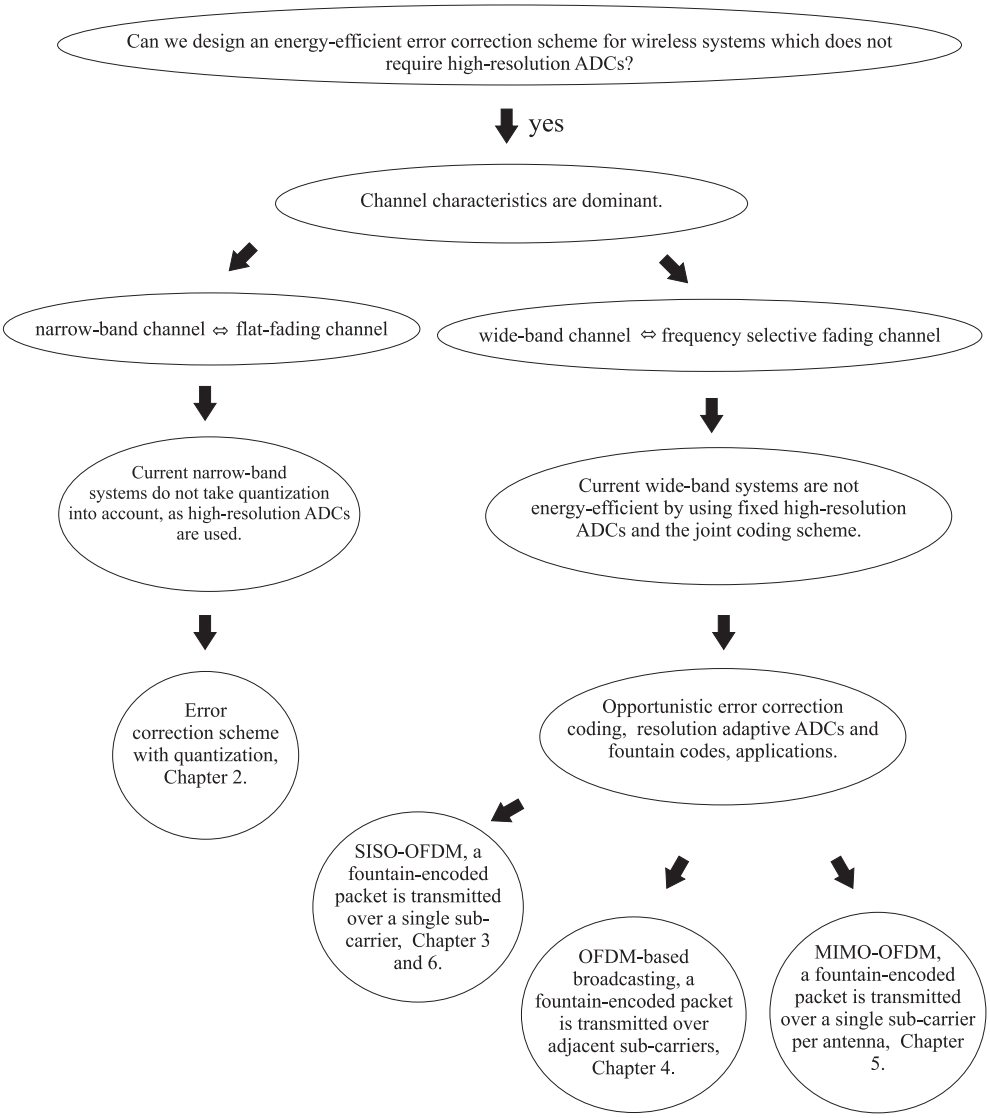

Fig. 1.6: The structure of the thesis.

- In Chapter 4, we apply the opportunistic error correction scheme based on fountain codes for OFDM-based broadcasting systems. To apply fountain codes in mobile TV, we divide a block of source bits into a set of packets, which are encoded by a fountain code. A fountain-encoded packet is transmitted over a sub band of the channel. Thus, multiple packets are transmitted simultaneously, using frequency division multiplexing. The receiver discards fountain-encoded packets which are transmitted over the sub band with deep fading. Correspondingly, the power consumption in ADCs decreases. With this new approach, around 84% of the energy consumption in ADCs can be saved compared with the conventional mobile TV system under the same channel conditions. To achieve a data rate of 9.5 Mbits/s, this new approach has a SNR gain of at least 10 dB with perfect channel knowledge and 11 dB with non-perfect channel knowledge in comparison to the current FEC layer in the DVB-T2 standard. With a low-complexity interpolation-based channel estimation algorithm, opportunistic error correction offers us a QEF (Quasi Error Free) quality with a maximum DF (Doppler Frequency) of 40 Hz but the current DVB-T2 FEC layer can only provide a BER of 10^{-7} quality after BCH decoding with a maximum DF of 20 Hz.

- In Chapter 5, we apply the opportunistic error correction scheme based on fountain codes for MIMO-OFDM systems. The key idea is to transmit a fountain-encoded packet over one single sub-carrier per antenna and to transmit enough packets to be able to reconstruct the original file. Comparing to the IEEE 802.11n standard, this approach allows around 83% of power saving in ADCs for a 2×2 system and 90% for a 4×4 system. With the current FEC scheme defined in the IEEE 802.11n standard, a 4×4 system requires twice the amount of power in ADCs as a 2×2 system when receiving the same amount of information with the same power. However, using opportunistic error correction in a 4×4 system costs only around 1.4 times amount of energy in ADCs comparing to a 2×2 system. Furthermore, we analyze its performance in the aspect of mitigating the noise and interference. At the same code rate, simulation results show that opportunistic error correction works better (i.e. requires lower SNR) than the FEC layers defined in the IEEE 802.11n standard. Comparing to RCPC with interleaving, the SNR gained by opportunistic error correction decreases as the multiplexing gain increases. In addition, we evaluate their performance in the real world. This novel approach does not have the same SNR gain in practice as in the simulation, comparing to the FEC layers in the IEEE 802.11n standard. Measurement results show that this new scheme survives in the most channel conditions (i.e. 92%) with respect to RCPC with interleaving (i.e. 86%) and the LDPC code from the IEEE 802.11n standard (i.e. around 80%).

- In Chapter 6, we analyze why and when opportunistic error correction works better than the traditional joint coding scheme adopted by the current OFDM system. Opportunistic error correction based on fountain codes is especially designed for the OFDM-based wireless system. The key point of this approach is the tradeoff

between the code rate of error correction codes and the number of sub-carriers to be discarded. That saves power in the ADC by quantizing the received signal coarsely. Correspondingly, this new method can afford higher level of noise floor than the joint coding scheme which is adopted by the current OFDM system. With the same code rate, it has a SNR gain of around 8.5 dB over Channel Model A with respect to the joint coding scheme used in the current WLAN system [24]. However, it is not clear whether this scheme has advantages over the joint coding scheme in the narrow-band wireless system (e.g. the flat-fading channel or the channel with a low dynamic range). In this chapter, we investigate when opportunistic error correction works best for OFDM systems in the simulation and in the real world. Simulation results show that, with the same code rate, it only performs better than the joint coding scheme when the dynamic range of the channel $\mathcal{D}$ is larger than 10 dB. Their performance difference becomes larger as $\mathcal{D}$ increases. Comparing to the LDPC code from the IEEE 802.11n standard at the same code rate, this novel approach gains a SNR of at least 11 dB over the TGn channel at 5 MHz, 10 MHz and 20 MHz. Furthermore, practical measurements show that it is more robust to the imperfections in the real world than the joint coding scheme. More measurements succeed in opportunistic error correction than in the joint coding scheme. This new scheme works better in practice than the joint coding scheme over the wireless channel at any $\mathcal{D}$. With respect to the joint coding scheme, on average, this novel approach gains a SNR of around 1.5 dB at $\mathcal{D} \in$ (0,10] dB, around 1.7 dB at $\mathcal{D} \in$ (10,20] dB and around 3.8 dB at $\mathcal{D} \in$ (20,30] dB.

- In Chapter 7, the conclusions are given.

1.5 Publications by the Author

1.5.1 Journals

1. X. Shao, R. Schiphorst and C.H. Slump, "An Opportunistic Error Correction Layer for OFDM Systems", EURASIP Journal on Wireless Communications and Networking, 2009.
   See Chapter 3.1.

2. X. Shao, C.H. Slump, "Opportunistic Error Correction for OFDM-based DVB Systems", submitted to IEEE Transactions on Broadcasting, 2010.
   See Chapter 4.2.

3. X. Shao, C.H. Slump, "Opportunistic Error Correction for MIMO-OFDM Systems: from Theory to Practice", submitted to IEEE Transactions on Wireless Communications, 2010.
   See Chapter 5.2.

4. X. Shao, C.H. Slump, "Opportunistic Error Correction : When does it Work Best for OFDM Systems?", submitted to IEEE Transactions on Communications, 2010.
See Chapter 6.2.

1.5.2 Conference Proceedings

1. X. Shao and H.S. Cronie, "Modulation and Coding for Quantized Channels", in Proceedings of SPS-DARTS 2007, the third annual IEEE Benelux/DSP Valley Signal Processing Symposium, 21-22 Mar 2007, Antwerp, Belgium. pp. 179-183.
See Chapter 2.

2. X. Shao, R. Schiphorst and C.H. Slump, "Opportunistic Error Correction for WLAN Applications", in Proceedings of the 4th IEEE International Conference on Wireless Communications, Networking and Mobile Computing, Oct 2008, Da Lian, China.
See Chapter 3.1.

3. X. Shao and C.H. Slump, "Practical Evaluation of Opportunistic Error Correction", in Proceedings of IEEE Global Telecommunications Conference (GLOBECOM), Dec 2009, Honolulu, USA.
See Chapter 3.2.

4. X. Shao, R. Schiphorst and C.H. Slump, "Energy Efficient Error Correction in Mobile TV", in Proceedings of IEEE International Conference on Communications (ICC), Jun 2009, Dresden, Germany.
See Chapter 4.1.

5. X. Shao and C.H. Slump, "Opportunistic Error Correction for MIMO", in Proceedings of the 20th IEEE Symposium on Personal, Indoor and Mobile Radio Communications (PIMRC), Sep 2009, Tokyo, Japan.
See Chapter 5.1.

6. X. Shao and C.H. Slump, "A Novel Cross Coding Scheme for OFDM Systems", in Proceedings of IEEE Information Theory Workshop on Information Theory (ITW), Oct 2009, Taomina, Italy.
See Chapter 6.1.

7. X. Shao and C.H. Slump, "Quantization Effects in OFDM Systems", in Proceedings of the 29th Symposium on Information Theory in the Benelux, 29-30 May 2008, Leuven, Belgium. pp. 93-103.

8. X. Shao, H.S. Cronie, F.W. Hoeksema and C.H. Slump, "Fountain Codes for Fre-

quency Occupancy Information Dissemination", in Proceedings of the 17th Annual Workshop on Circuits, 23-24 Nov 2006, Veldhoven, The Netherlands. pp. 196-203.

9. T. Zijnge, X. Shao, R. Schiphorst and C.H. Slump, "Raptor Codes for Use in Opportunistic Error Correction", in Proceedings of the 31st Symposium on Information Theory in the Benelux, 11-12 May 2010, Rotterdam, the Netherlands.

10. X. Shao and C.H. Slump, "Another Approach to Save Energy in Wireless Receivers", *submitted to* the IEEE Global Telecommunications Conference (GLOBECOM), Dec 2010, Miami, USA.

11. X. Shao and C.H. Slump, "A Robust Cross Coding Scheme for OFDM Systems", *submitted to* the 2010 International Symposium on Information Theory and its Applications (ISITA), Oct 2010, Taiwan.

Chapter 2

Modulation and Coding for Quantized Channels

[1]**Abstract** High-resolution Analog-to-Digital (AD) converters are widely used in telecommunication systems. The power consumption at the receiver is proportional to the resolution of AD converter. Therefore, it is of great interest to investigate whether it is possible to use the low-resolution AD converters in reliable communications. In this paper, we investigate reliable communication over quantized channels from the information theoretical point of view. We show that with properly designing a quantization scheme, $d+1$ or $d+2$ quantized bits are already enough when d source bits are mapped into conventional Pulse Amplitude Modulation (PAM) and transmitted over Additive White Gaussian Noise (AWGN) channel. Moreover, we show that combined with multi-level coding and low-density parity-check codes, a low bit error rate for a block length of 10^4 is achieved at 1.5 dB from the Shannon limit for $R \approx 1.5$ bit/use and at 1.4 dB from the Shannon limit for $R \approx 2$ bit/use.

[1]This chapter is partly based on the published paper [25]: *X. Shao and H.S. Cronie, "Modulation and Coding for Quantized Channels", in Proceedings of SPS-DARTS 2007, the third annual IEEE Benelux/DSP Valley Signal Processing Symposium, 21-22 Mar 2007, Antwerp, Belgium. pp. 179-183.*

2.1 Introduction

In this paper we investigate reliable and bandwidth efficient communication over quantized channels. Quantized channels arise in practical communication systems where analog-to-digital (AD) converters are used to sample analog signals corresponding to the transmitted data. Conventional coded modulation systems usually do not take quantization into account, which is reasonable since a large number of quantization levels is used. In this case the difference between the quantized and unquantized channel can be neglected. The dynamic change of the channel urges the use of high-resolution AD converters [26], [27]. However, for e.g. mobile communication systems the power consumption at the receiver is proportional to the resolution of the AD converter. Hence it is of interest to lower the resolution of the AD converter.

In this paper we consider quantized channels from an information theoretical point of view. We investigate information theoretical limits of transmission over quantized channels. The main question we try to answer is as follows. If we wish to transmit reliably at a rate of R bit/use, do we actually require more than R quantization bits? In this paper we show that for the additive white Gaussian noise (AWGN) channel, reliable transmission at a rate of R bit/use is possible with $R+1$ or $R+2$ quantization bits without sacrificing transmission power.

We also derive a coded modulation scheme based on multi-level coding and binary linear block codes which can be used to achieve the theoretical limits. We show that with a proper design of the low-resolution quantization scheme, the theoretical limit of the quantized AWGN channel with conventional pulse amplitude modulation (PAM) can be made very close to the theoretical limit of the unquantized AWGN channel with conventional PAM constellation scheme. We present simulation results to verify these claims.

The organization of the paper is as follows. First, we introduce the system model in section 2.2. Second, we investigate the use of quantization from an information theoretical point of view in section 2.3. Furthermore, we present a scheme which can be used to communicate over the quantized channel in this section. As an example we design a set of low-density parity-check (LDPC) codes for the quantized AWGN channel and present simulation results in section 2.4. We end with conclusions in section 2.5.

2.2 System Model

We consider communication over the memoryless continuous AWGN channel which is defined by [1]:

$$r(t) = x(t) + n(t) \tag{2.1}$$

where the channel input $x(t)$ is disturbed by additive noise $n(t)$ which has a zero-mean and power spectral density $\phi_{nm}(f) = \frac{1}{2}N_0$ W/Hz. To communicate over this channel we map a sequence of $d = \log_2 M$ binary digits into one of $M = 2^d$ symbols:

$$x_m = \phi(x_1, \ldots, x_d) \quad m = 0, 1, \cdots, M-1 \tag{2.2}$$

where $\phi(\cdots)$ is defined as:

$$\phi : GF(2)^d \rightarrow \mathbb{R} \tag{2.3}$$

We refer to ϕ as the *modulation map* and it defines the signal constellation $\mathcal{X}$ and mapping from binary digits to constellation symbols:

$$\mathcal{X} = \{x_m \in \mathbb{R} : x_m = \phi(x_1, \ldots, x_d)\} \tag{2.4}$$

In this case, the baseband signal waveform of the channel input can be represented as:

$$x(t) = x_m g(t) \tag{2.5}$$

where $g(t)$ is a real-valued signal pulse and has unit energy over the symbol interval T which is:

$$E_g = \int_0^T g^2(t)dt \tag{2.6}$$

The energy expended per channel use is defined as the mathematical expectation of $x^2(t)$:

$$\begin{aligned} E_s &= \int_0^T x^2(t)dt \\ &= \int_0^T x_m^2 g^2(t)dt \\ &= E[x_m^2] \end{aligned} \tag{2.7}$$

The received signal $r(t)$ is filtered by a matched filter whose impulse response is:

$$h(t) = g(T-t) \quad 0 \leq t \leq T \tag{2.8}$$

The outputs of these filters are:

$$\begin{aligned} y(t) &= \int_0^t r(\tau)h(t-\tau)d\tau \\ &= \int_0^t r(\tau)g(T-t+\tau)d\tau \\ &= \int_0^t x(\tau)g(T-t+\tau)d\tau + \int_0^t n(\tau)g(T-t+\tau)d\tau \end{aligned} \tag{2.9}$$

If we sample the output of the filters at $t = T$, we have:

$$\begin{aligned} y_m(T) &= \int_0^T x(\tau)g(\tau)d\tau + \int_0^T n(\tau)g(\tau)d\tau \\ &= x_m(T) + n_m(T) \end{aligned} \tag{2.10}$$

where $x_m(T)$ is:

$$\begin{aligned} x_m(T) &= \int_0^T x(\tau)g(\tau)d\tau \\ &= \int_0^T x_m g^2(\tau)d\tau \\ &= x_m \end{aligned} \tag{2.11}$$

and $n_m(T)$ is defined as:

$$n_m(T) = \int_0^T n(t)g(t)dt \tag{2.12}$$

$n_m(T)$ also has a zero-mean and variance is:

$$\begin{aligned} \mathbf{E}[n_m^2(T)] &= \int_0^T \int_0^T \mathbf{E}[n(t)n(\tau)]g(t)g(\tau)dtd\tau \\ &= \frac{1}{2}N_0 \int_0^T \int_0^T \delta(t-\tau)g(t)g(\tau)dtd\tau \\ &= \frac{1}{2}N_0 \int_0^T g^2(t)dt \\ &= \frac{1}{2}N_0 \end{aligned} \tag{2.13}$$

We refer $y_m(T)$ as y_m and $n_m(T)$ as n_m, so we have:

$$y_m = x_m + n_m \tag{2.14}$$

which is called as *the memoryless discrete AWGN channel*. In this paper, we suppose the match filter and the sampling are perfect and focus on the quantization effect in the memoryless discrete AWGN channel. We will refer *the memoryless discrete AWGN channel* to *the AWGN channel* in the following sections.

The channel output y_m is quantized by a quantization map $\mathcal{Q}$ which is defined as:

$$\mathcal{Q} : \mathbb{R} \to A \tag{2.15}$$

where $A \subset \mathbb{N}$ and represents the output of the quantized channel. As we will see later it is not necessary to associate the elements of A with the real numbers. The elements just represent the channel outputs. A quantization map is surjective and $\mathcal{Q}$ also defines an inverse quantization map which is defined as the set function $\mathcal{Q}^{-1}$:

$$\mathcal{Q}^{-1}(i) = \{y_m \in \mathbb{R} : Q(y_m) = i, i \in A\} \tag{2.16}$$

We restrict ourselves to quantizers where each $\mathcal{Q}^{-1}(i)$ is of the form $\mathcal{I}_i = (a, b]$ for $a, b \in \mathbb{R}$. In this case $\{\mathcal{I}_i\}$ partitions $\mathbb{R}$ and the quantizer is defined by the set of intervals $\{\mathcal{I}_i\}$. The goal is to make $|A|$ as small as possible and still achieve a reasonable mutual information between the input bits and the quantized channel output. With these definitions the quantized channel is defined as:

$$z_m = \mathcal{Q}(\phi(x_1, \ldots, x_d) + N), \tag{2.17}$$

where z_m is the channel output and takes values from A. Figure 2.1 shows an overview of the system model we have defined so far. In the next section we study this system from an information theoretical point of view and derive a scheme to communicate reliably over the quantized channel.

2.3 Quantization and Mutual Information

In this section we study the effect of quantization from an information theoretical point of view. Moreover, we consider the AWGN channel as an example where we

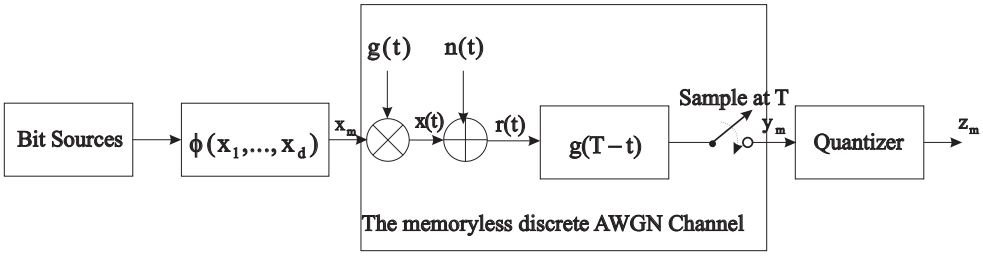

Fig. 2.1: The system model

restrict ourselves to conventional pulse amplitude modulation (PAM) signal constellations.

We are interested in the mutual information $I((x_1,\ldots,x_d);z_m)$ between $(x_1,\ldots,x_d)$ and z_m. First, note that the following sequence of random variables forms a Markov chain:

$$(x_1,\ldots,x_d) \rightarrow x_m \rightarrow y_m \rightarrow z_m \tag{2.18}$$

We can express $I((x_1,\ldots,x_d),x_m;z_m)$ as [28]:

$$\begin{aligned} I((x_1,\ldots,x_d),x_m;z_m) &= I(x_m;z_m) + I((x_1,\ldots,x_d);z_m|x_m) \\ &= I((x_1,\ldots,x_d);z_m) + I(x_m;z_m|(x_1,\ldots,x_d)), \end{aligned} \tag{2.19}$$

where we have used the chain rule of mutual information. Since $(x_1,\ldots,x_d) \rightarrow x_m \rightarrow z_m$ forms a Markov chain as well it follows that [29]:

$$I((x_1,\ldots,x_d);z_m|x_m) = 0 \tag{2.20}$$

Moreover, x_m is a function of $x_1,\ldots,x_d$ which implies that [30]:

$$I(x_m;z_m|(x_1,\ldots,x_d)) = 0 \tag{2.21}$$

With equation 2.19 we have the following equality:

$$I((x_1,\ldots,x_d);z_m) = I(x_m;z_m), \tag{2.22}$$

which shows that the mutual information of interest is fully defined by the signal constellation and the distribution of the constellation symbols. Next, we consider the mutual information between x_m and z_m. From the chain rule of mutual information

it follows that [28]:

$$\begin{aligned} I(x_m;(y_m,z_m)) &= I(x_m;y_m) + I(x_m;z_m|y_m) \\ &= I(x_m;z_m) + I(x_m;y_m|z_m). \end{aligned} \tag{2.23}$$

Since $x_m \rightarrow y_m \rightarrow z_m$ forms a Markov chain $I(x_m;z_m|y_m) = 0$ from which follows that:

$$I(x_m;z_m) = I(x_m;y_m) - I(x_m;y_m|z_m). \tag{2.24}$$

Given a channel there exists an input distribution which achieves the maximum value C of $I(x_m;y_m)$. For the AWGN channel this distribution is the Gaussian distribution. A particular choice of modulation leads to a certain $I(x_m;y_m)$. Moreover, when the output of the channel is quantized, the quantity of interest is $I(x_m;z_m)$ which is upperbounded by $I(x_m;y_m)$ as shown in equation 2.24. In this paper we consider the design of coded modulation schemes for the AWGN channel for which $I(x_m;z_m)$ is as close as the capacity of the AWGN channel as possible. Moreover, the number of quantization levels is only slightly larger than $\log_2(R)$, where R is the rate at which we transmit. We will see that in some cases a proper design of the quantizer gives a value of $I(x_m;z_m)$ which is quite close to the value of $I(x_m;y_m)$.

2.3.1 Uniform Quantization for AWGN with PAM Constellations

Now we consider uniform quantization for the AWGN channel where conventional PAM constellations are used. A PAM constellation with 2^d constellation symbols is defined as [1]:

$$\mathcal{S}_{\text{PAM}-2^d} = \{x_m \in \mathbb{R} : x_m = 2m - 1 - 2^d, m = 1, 2, \cdots, 2^d\} \tag{2.25}$$

In this case the constellation symbols are selected with equal probability and E_s is given by:

$$E_s = \frac{4^d - 1}{3} \tag{2.26}$$

One can normalize these constellation such that $E_s = 1$.

We define a uniform interval quantizer with 2^m levels and spacing q as an interval

quantizer for which the set of quantization levels is given by [31], [32], [33]:

$$\begin{aligned}\{\mathcal{I}_i : i = 1 \dots 2^m\} = \\ q \cdot \{(-\infty, -2^{m-1}+1], (-2^{m-1}+1, -2^{m-1}+2], \dots \\ , (2^{m-1}-2, 2^{m-1}-1], (2^{m-1}-1, \infty)\}\end{aligned} \tag{2.27}$$

Given these definitions we can express the mutual information between the channel input and the quantized channel output as [28]:

$$\begin{aligned}I(x_m; z_m) = \\ \sum_{x \in \mathcal{S}} \sum_{i \in A} P(z_m = i, x_m = x) \log_2 \frac{P(z_m = i | x_m = x)}{\sum_{x' \in \mathcal{S}} P(z_m = i, x_m = x')},\end{aligned} \tag{2.28}$$

where $P(z_m = i, x_m = x)$ is given by:

$$\begin{aligned}P(z_m = i, x_m = x) = \\ P(z_m = i | x_m = x) P(x_m = x) = 2^{-d} P(z_m = i | x_m = x),\end{aligned} \tag{2.29}$$

and $P(z_m = i | x_m = x)$ can be computed as follows:

$$\begin{aligned}P(z_m = i | x_m = x) &= P(y \in \mathcal{Q}^{-1}(i) | x_m = x) \\ &= \int_{\mathcal{Q}^{-1}(i)} dy P_{y_m | x_m}(y | x)\end{aligned} \tag{2.30}$$

Consider the case that E_s/σ^2 is equal to 5 dB where $I(x_m; y_m) = 1$ bit/dimension and we transmit over the AWGN channel using a PAM-4 constellation which is defined as $\mathcal{S} = \{-3, -1, 1, 3\}$. Suppose that we use a uniform interval quantizer to quantize the channel output into 2^m levels where m is equal to 2, 3 or 4. Figure 2.2 shows a plot of $I(x_m; z_m)$ as a function of q for these values of m and the case where no quantization is used. The figure also shows the Shannon limit of the AWGN channel. We observe that there is a loss in rate compared to the case where no quantization is used. However, with a proper spacing q and a m slightly larger than d the loss in rate can be made small. Furthermore, one does not have to use a uniform interval quantizer. The quantization levels can be chosen in such a way to give a higher value of $I(x_m; z_m)$.

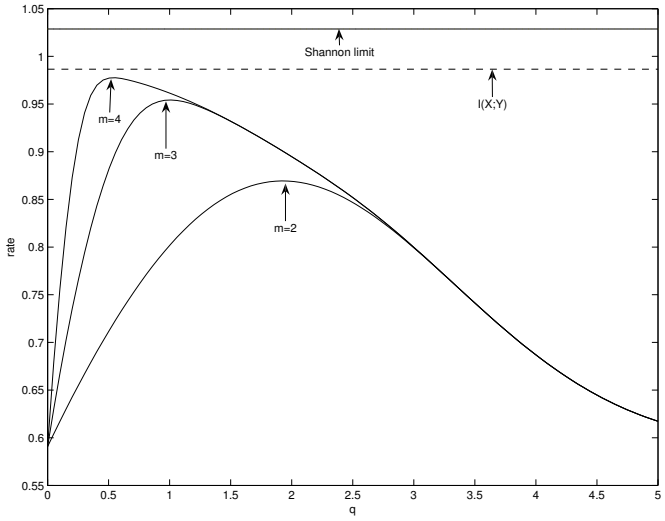

Fig. 2.2: Uniform quantized interval q with $d = 2$, PAM constellation and SNR=5dB

2.3.2 Non-uniform Quantization for AWGN with PAM Constellations

Non-uniform interval quantizer with 2^m levels is defined as an interval quantizer having non-equal spacing and the set of quantization levels given by [31], [32], [33]:

$$\begin{aligned} \{\mathcal{I}_i : i = 1 \dots 2^m\} = \\ \{(-\infty, -q_n], \dots, (-q_i, -q_{i-1}], \dots, (-q_1, 0], \\ (0, q_1], \dots, (q_{i-1}, q_i], \dots, (q_n, +\infty)\} \end{aligned} \tag{2.31}$$

where $i = 1, 2, \dots, n$ and $n = 2^{m-1} - 1$. The set of quantization levels is found by using a numerical maximization of the mutual information between the channel input and the quantized channel output.

2.3.3 Comparisons

Here we show the difference of the quantization effect between the uniform quantization scheme and the non-uniform quantization scheme. Assume that d bits are

Table 2.1: Optimum Quantization Set for $d = 2$ and $m = 3$

	q_1	q_2	q_3
Uniform	1.0	2.0	3.0
Non-uniform	0.64	1.71	2.37

Table 2.2: Optimum Quantization Set for $d = 2$ and $m = 4$

	q_1	q_2	q_3	q_4	q_5	q_6	q_7
Uniform	0.5	1.0	1.5	2.0	2.5	3.0	3.5
Non-uniform	0.31	0.79	1.29	1.75	2.06	2.38	2.87

mapped into a conventional PAM constellation symbol x_m which is transmitted over the AWGN channel, then the received symbol y_m is quantized into m bits where m is equal to $d + 1$ or $d + 2$.

Consider the case that $d = 2$. We transmit source bits by using a PAM-4 constellation over the AWGN channel where SNR = 10 dB. The optimum quantization sets of both schemes are shown in table 2.1 and 2.2. Figure 2.3 shows a plot of $I(x_m; z_m)$ as a function of E_b/N_0 using the quantization set of table 2.1 and 2.2 for the uniform quantization scheme and the non-uniform quantization scheme with 3 and 4 quantized bits. The figure also shows the capacity of unquantized AWGN channel with conventional PAM constellation and the Shannon limit of AWGN channel. From the figure, we can see that there is a loss in capacity due to the quantization but the loss is small especially when $m = 4$. Moreover, non-uniform quantization scheme works slightly better than uniform quantization scheme in this case.

For the case that $d = 3$, we assume that source bits are mapped into a conventional PAM-8 constellation which is defined as $\mathcal{S} = \{-7, -5, -3, -1, 1, 3, 5, 7\}$ and transmitted over the AWGN channel where SNR = 13 dB. Table 2.3 and 2.4 are the optimum quantization set in this case. Figure 2.5 shows the quadrature signal constellation and the quantization scheme of table 2.3 and 2.4 which are generated by using each dimension independently.

Figure 2.4 shows how the quantized channel capacity changes with E_b/N_0 for both quantization schemes with 4 or 5 quantized bits. Both schemes have almost the same performance for the case of $m = 5$ and the loss between the quantized channel limit and the unquantized channel limit can be neglected in this case, but for $m = 4$ the non-uniform quantization scheme works better the uniform quantization scheme.

Table 2.3: Optimum Quantization Set for $d = 3$ and $m = 4$

	q_1	q_2	q_3	q_4	q_5	q_6	q_7
Uniform	1.0	2.0	3.0	4.0	5.0	6.0	7.0
Non-uniform	0.75	1.58	2.54	3.52	4.50	5.44	6.55

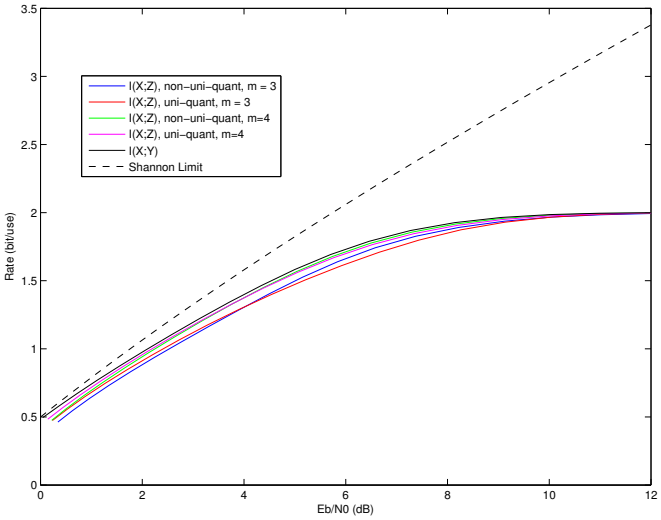

Fig. 2.3: The capacity limit of the quantized channel with PAM-4 constellation

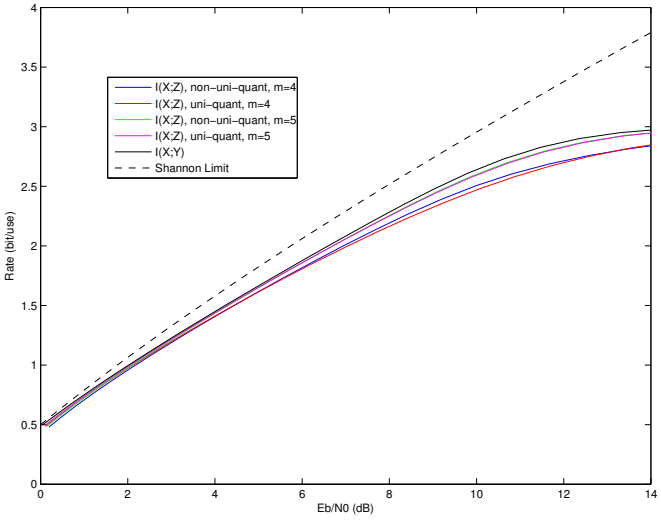

Fig. 2.4: The capacity limit of the quantized channel with PAM-8 constellation

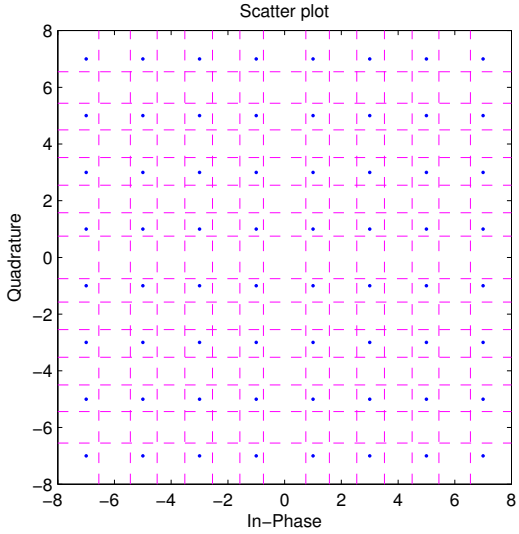

(a) $m = 4$

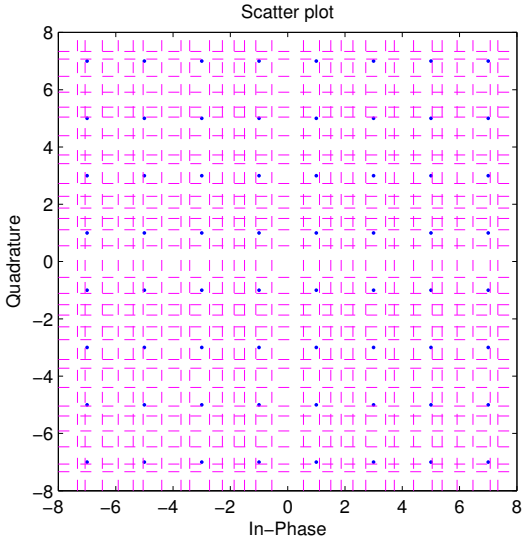

(b) $m = 5$

Fig. 2.5: The quadrature PAM signal constellation with 64 symbols and the optimum quantization schemes of table 2.3 and 2.4 with $d = 3$ and SNR $= 13$ dB.

From figure 2.3 and 2.4, we can draw a conclusion: when we transmit d bits, we only require $d + 1$ or $d + 2$ quantized bits from information theoretical point of view. In

Table 2.4: Optimum Quantization Set for $d = 3$ and $m = 5$

	q_1	q_2	q_3	q_4	q_5	q_6	q_7
Uniform	0.5	1.0	1.5	2.0	2.5	3.0	3.5
Non-uniform	0.55	1.11	1.51	1.87	2.28	2.73	3.42
q_8	q_9	q_{10}	q_{11}	q_{12}	q_{13}	q_{14}	q_{15}
4.0	4.5	5.0	5.5	6.0	6.5	7.0	7.5
3.72	4.40	5.05	5.39	5.91	6.47	7.07	7.34

the next section, we derive a coding scheme to achieve reliable communication at a rate close to $I(X;Z)$.

2.4 Code Design

Section 2.3 has proved from information theoretical point of view that the quantized channel limit is quite close to the unquantized channel limit even when $m = d + 1$. Error-correcting codes can be used to achieve reliable communication at a rate close to the constraint capacity.

A scheme that uses binary error-correcting codes is derived by considering the chain rule of mutual information in equation 2.23. We encode each sequence of x_i by a binary error-correcting code and each x_i is multiplied by a coefficient α_i then added together which is defined as:

$$x = \alpha_1 x_1 + \alpha_2 x_2 + \ldots + \alpha_d x_d \tag{2.32}$$

This method is called the multi-level coding (MLC) [34], [35]. At the receiver, we can decode the sequence of x_1 first then pass the decision to the next decoder which decodes the sequence of x_2. This procedure continues till all sequences are decoded. It is called the multi-stage decoding (MSD) [36]. The overview of this system is shown in figure 2.6.

LDPC codes are powerful binary error-correcting codes. Now, we design LDPC codes for quantized channel to achieve reliable communication at a rate close to the Shannon limit. We assume that source bits are mapped into conventional PAM constellation defined by equation 2.25 which means that $\{\alpha_i\}$ is defined by [1]:

$$\alpha_i = 2^{d-i} \tag{2.33}$$

where $i = 1, 2, .., d$. The received symbol is quantized into $d + 1$ bits by using the

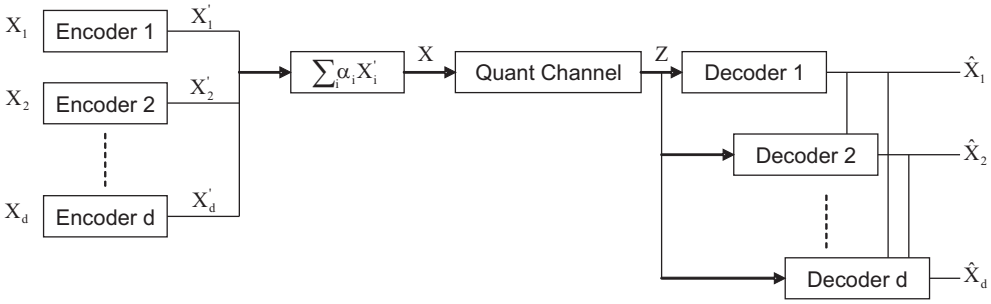

Fig. 2.6: Multilevel Coding and Multi-stage Decoding

non-uniform quantization scheme. We have designed LDPC codes for the quantized channels of $x_1, \ldots, x_d$ by a method based on density evolution [37], [38], [39]. We take $d = 2$ and $d = 3$ as an example to design LDPC codes as follows. For both cases, a block length of 10^4 was used and the code graph was constructed randomly. Furthermore, we decoded 100 blocks for each code which means 10^6 bits were decoded and the maximum variable node degree of the LDPC codes is 100.

Consider the case that $d = 2$. LDPC codes are designed for the AWGN channel where SNR = 10 dB and the non-uniform quantization scheme of table 2.1 where the target rate R is equal to 1.5322. The degree distributions for the variable nodes and the check nodes of both levels are shown in table 2.5. The code rate for level one to two are 0.785 and 0.57, respectively. The total rate at which we transmit is 1.355 in this case and the rate loss comparing to the target rate is 0.1772 bit/use. The simulation results are shown in figure 2.3. As we can see, an average BER $< 10^{-4}$ is achieved at 1.5 dB from the Shannon limit of the quantized AWGN channel for $R = 1.355$ bit/use.

For the case of $d = 3$, we design LDPC codes for the AWGN channel of SNR = 13 dB and the quantization scheme of table 2.3 where the target rate $R = 2.0$ bit/use. Table 2.6 is the set of degree distribution for level one to three and figure 2.4 shows the simulation results. The code rates for level one to three are 0.82, 0.63 and 0.37, respectively; and the rate loss between the total rate and the target rate is 0.18. In this case, an average BER $< 10^{-4}$ can be achieved at 1.4 dB from the capacity of the quantized AWGN channel.

LDPC codes have better performation for longer block length [37]. If the block length is increased, the gap to the Shannon limit of the quantized AWGN channel might be smaller than the gap we got from the simulation.

Table 2.5: Good LDPC Codes for Quantized Channel and $d = 2$ with code rate $R_1 = 0.785$ and $R_2 = 0.57$

x_1	λ_{x_1}	x_2	λ_{x_2}
2	0.140194	2	0.145849
3	0.156555	3	0.153525
6	0.0653432	6	0.0933067
7	0.141968	7	0.104362
17	0.170344	15	0.0336706
34	0.0492009	16	0.109157
36	0.0388888	32	0.0935713
37	0.0182293	33	0.0373538
39	0.0287644	100	0.229205
88	0.164533		
89	0.030926		

x_1	ρ_{x_1}	x_2	ρ_{x_2}
27	0.5	13	0.3
28	0.5	14	0.7

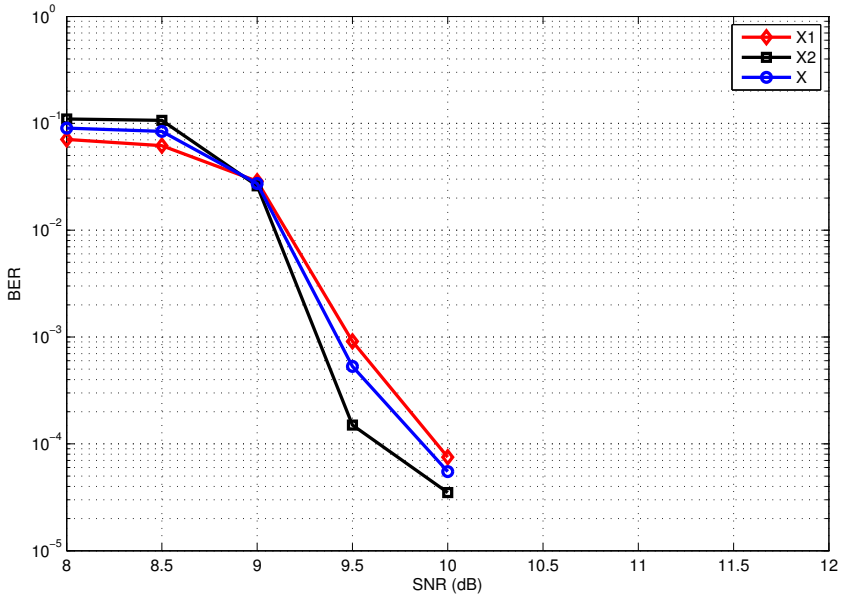

Fig. 2.7: Simulation results for $d = 2$ of table 2.5 using a block length of 10^4.

Table 2.6: Good LDPC Codes for Quantized Channel and $d = 3$ with code rate $R_1 = 0.82$, $R_2 = 0.63$ and $R_3 = 0.37$

x_1	λ_{x_1}	x_2	λ_{x_2}	x_3	λ_{x_3}
2	0.14729	2	0.145206	2	0.20161
3	0.153184	3	0.147201	3	0.15427
6	0.0940388	6	0.0638489	6	0.17203
7	0.107035	7	0.12743	7	0.0086804
16	0.0.140748	18	0.053874	13	0.044735
17	0.0260029	19	0.136699	14	0.089985
33	0.0349379	100	0.3257	29	0.029141
35	0.0476994			30	0.10223
38	0.0560525			100	0.19732
86	0.0472956				
87	0.145726				

x_1	ρ_{x_1}	x_2	ρ_{x_2}	x_3	ρ_{x_3}
32	0.7	16	0.5	8	1.0
33	0.3	17	0.5		

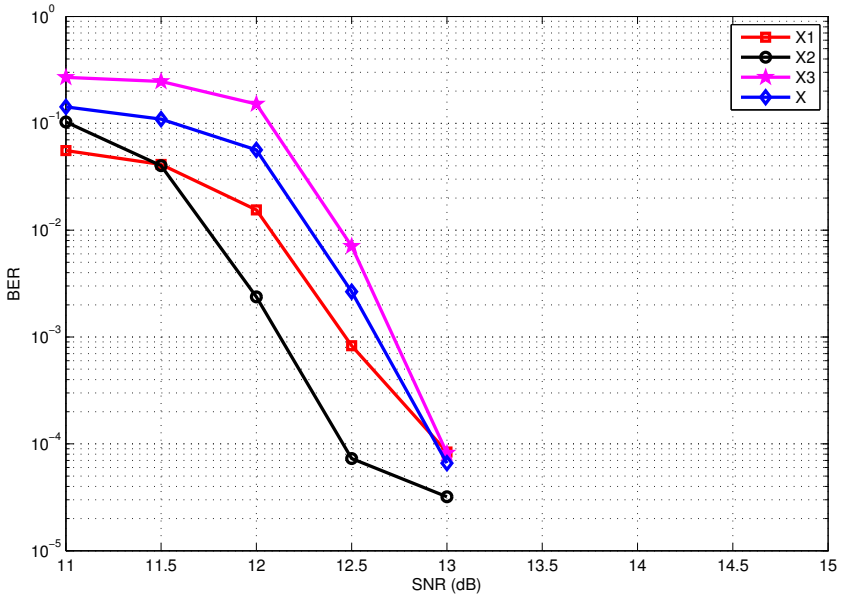

Fig. 2.8: Simulation results for $d = 3$ of table 2.6 using a block length of 10^4.

2.5 Conclusions

We have presented a method to design optimum quantization scheme with low resolution which can make a constrained capacity of the quantized AWGN channel as close to the constrained capacity of the unquantized AWGN channel as possible. We have shown the effect of quantization from an information theoretical point of view and showed that it is possible to transmit d source bits but only require $d+1$ quantized bits. As an example, we have designed LDPC codes for the cases of $d=2$ and $d=3$ with $d+1$ quantized bits, respectively. For the block length of 10^4, a low bit error rate is achieved at only 1.5 dB from the Shannon limit for $d=2$ and at 1.4 dB for $d=3$. Therefore, reliable communication is possible to use a low-resolution quantizer in the AWGN channel.

Chapter 3

Energy Efficient Error Correction for SISO-OFDM Systems

3.1 An Opportunistic Error Correction Layer for OFDM Systems

[1]**Abstract** In this paper, we propose a novel cross layer scheme to reduce the power consumption of ADCs in OFDM systems. The ADCs in a receiver can consume up to 50% of the total baseband energy. Our scheme is based on resolution-adaptive ADCs and fountain codes. In a wireless frequency selective channel some sub-carriers have good channel conditions and others are attenuated. The key part of the proposed system is that the dynamic range of ADCs can be reduced by discarding sub-carriers that are attenuated by the channel. Correspondingly, the power consumption in ADCs can be decreased. In our approach, each sub-carrier carries a fountain-encoded

[1]This section is the published paper [40]: *X. Shao, R. Schiphorst and C.H. Slump, "An Opportunistic Error Correction Layer for OFDM Systems", EURASIP Journal on Wireless Communications and Networking, 2009.* Part of this section is also published in [41]: *X. Shao, R. Schiphorst and C.H. Slump, "Opportunistic Error Correction for WLAN Applications", in Proceedings of the 4th IEEE International Conference on Wireless Communications, Networking and Mobile Computing, Oct 2008, Da Lian, China.*

packet. To protect fountain-encoded packets against bit errors, a LDPC code has been used. The receiver only decodes sub-carriers (i.e. fountain-encoded packets) with the highest SNR. Others are discarded. For that reason a LDPC code with a relatively high code rate can be used. The new error correction layer does not require perfect channel knowledge, so it can be used in a realistic system where the channel is estimated. With our approach, more than 70% of the energy consumption in the ADCs can be saved compared with the conventional IEEE 802.11a WLAN system under the same channel conditions and throughput. In addition, it requires 7.5 dB less SNR than the 802.11a system. To reduce the overhead of fountain codes, we apply message passing and Gaussian elimination in the decoder. In this way, the overhead is 3% for a small block size (i.e. 500 packets). Using both methods results in an efficient system with low delay.

3.1.1 Introduction

The wireless channel is a very hostile environment. Therefore, it is a challenge to communicate both reliably and with a high throughput. In this paper, we investigate a novel error correction layer based on *fountain codes*, *Orthogonal Frequency-Division Multiplexing* (OFDM) and adaptive analog-to-digital conversion to mitigate the effects of a wireless channel at a lower power consumption compared to traditional solutions.

OFDM has become a popular scheme for recent WLAN standards which operate at a high bit rate [13] [14] [15]. The main advantage of OFDM over the single-carrier scheme is its ability to eliminate *Inter-Symbol Interference* (ISI) without complex equalization filters in the receiver [2]. OFDM has a high *Peak-to-Average Power Ratio* (PAPR), therefore it requires *Analog-to-Digital Converters* (ADC) with a high dynamic range. These high resolution ADCs can take up to 50% of the baseband power [11].

In the current generation of WLAN equipment (based on IEEE 802.11a [17]), the *Forward Error Correction* (FEC) layer is based on *Rate Compatible Punctured Codes* (RCPC). These codes have good performance for random bit-errors, but poorer performance for burst bit errors. For that reason, an interleaver is applied to randomize the burst errors of the wireless channel. On the other hand, the wireless channel is changing in time. This means that some packets are received with a "good" channel and others over a "bad" channel. The error correction layer based on RCPC has been designed in such a way that for most channel realizations the *Bit-Error Rate* (BER) is zero. For a small part of the channel, bit errors will occur and retransmission is necessary. Although this solution works well in practical systems, it is not energy-efficient for two reasons:

- Packets which have encountered "bad" conditions are still processed by the entire receiver chain.
- Fixed high-resolution ADCs are used in the current WLAN systems, designed for worst case scenarios.

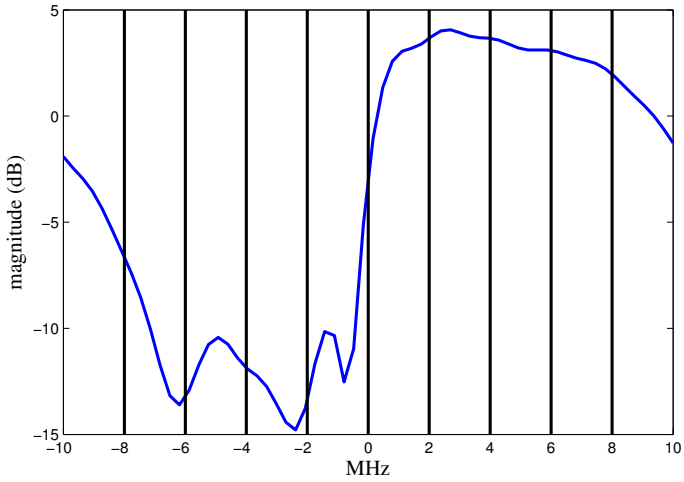

Fig. 3.1: Example of the baseband transfer function of a frequency selective Channel *model* A.

In this paper we propose a new error correction layer, which does not have these disadvantages. It is an opportunistic error correction layer because it processes only "good" packets. Also, it is a low power-consumption scheme as the resolution of the ADC is adapted to the minimum for each scenario instead of being designed for worst case situations.

A further resolution reduction of the ADC can be achieved by discarding those parts of the channel with deep fading. Taking Figure 3.1 as an example, the dynamic range of the whole channel is around 18.8 dB. From this figure, we can see that deep fading does not happen everywhere and only occurs in the frequency band of -8∼0 MHz. By discarding this 8 MHz sub-band, the dynamic range of the channel is reduced to around 10.4 dB. The current WLAN standards do not support this approach, as all sub-bands are considered equally important by the FEC layer.

Therefore, we propose a novel FEC layer based on fountain codes that allows us to discard those parts of the channel with deep fading. In [42], MacKay describes the encoder of a fountain code as a metaphorical fountain that produces a stream of encoded packets. Anyone who wishes to receive the encoded file holds a bucket under the fountain and collects enough packets to recover the original data. It does not matter which packets are received, only a minimum amount of packets have to be received correctly [42]. In other words, the fountain-encoded packets are independent with respect to each other.

To apply fountain codes in WLAN systems, we divide a block of source bits into a set of packets which are encoded by a fountain code. A fountain-encoded packet is transmitted over a sub-carrier. Thus, multiple packets are transmitted simultaneously,

using frequency division multiplexing. In our system the transmitter generates an abundance of packets and the receiver can discard fountain-encoded packets which are transmitted over the sub-carriers with deep fading. Correspondingly, the power consumption in the ADCs decreases.

The proposed method is an opportunistic error correction layer because it does not process all received packets but only processes "good" packets. This error correction is able to cope with discarding packets because fountain-encoded packets are independent of each other. Also, less power is consumed as the resolution of the ADC is adapted to the minimum required in each case, compared to using a fixed-resolution ADC. Thus, it is a novel cross-layer approach which integrates the error correction into the physical layer of an OFDM system.

The outline of this paper is as follows. We propose two techniques which together form the new error correction layer and reduce the power consumption: fountain codes and a resolution-adaptive ADC. First, fountain codes are discussed, which is followed by the resolution-adaptive ADC. A practical example is given in this paper considering the IEEE 802.11a system. In section 3.1.4, a description is given of the IEEE 802.11a system model and includes our proposed modifications. Finally, the simulation results are described, which compare the conventional 802.11a system with our modifications. The paper ends with conclusions and future work.

3.1.2 Fountain Codes

The proposed error correction layer is generic: any fountain codes (e.g. *Luby Transform* (LT) codes [43], Raptor codes [44], etc) can be applied in it. In this paper, we use LT codes in the proposed error correction layer.

Consider a file of size K packets $s_1, s_2, \cdots, s_K$ to be encoded by a fountain code. A 'packet' has m bits and is considered as an elementary unit here. At each clock cycle, indexed by n, the encoder randomly chooses several packets, and computes the bitwise sum (XOR) of these source packets to generate the corresponding transmitted packet. The number of packets used is random, as well as the selection of the packets used. The fountain code can supply us with a stream of packets based on source packets $s_1, s_2, \cdots, s_K$. In practical situations, however, only a fixed number of packets N are generated.

At the receiver side enough packets have to be received for successful decoding. The required number of received packets N is slightly larger than the number of source packets K and is defined by:

$$N = K(1 + \varepsilon) \tag{3.1}$$

where ε is the percentage of extra packets and is called the overhead.

After receiving N packets, the receiver can recover the source packet using the *message passing* algorithm which has a linear decoding cost. By using message passing to

decode LT codes, the practical block size for LT codes with small ε (e.g. within 5%) is on the order of 10^4 or higher, which prevents the fountain scheme from efficiently supporting real-time applications (i.e. low delay) [45]. For low failure probability (e.g. 1%), using messaging-passing decoding, the practical overhead for small block size (i.e. on the order of 10^3) is much larger than in theory [42]. In [41], the authors show that the practical overhead of LT codes is 14% when $K = 2000$, which limits the application of LT codes in practical systems to $K \leq 2000$. The practical overhead becomes smaller for a larger number of source packets. Although larger packets decrease the overhead, this also results in more delay. In addition, if the message-passing decoding fails, it does not mean that the source packets are not recoverable. Gaussian elimination can also be used for decoding, if the matrix G can be transformed into an up-converted matrix.

However, Gaussian elimination has higher complexity compared to the message-passing algorithm. The decoding cost of using the message-passing algorithm scales as $K \log_e K$ and the cost of using the Gaussian elimination algorithm is on the order of K^3 [42]. In [46], the authors propose a fast Gaussian elimination algorithm over GF(2) with reduced cost $O(K^2)$. The message-passing algorithm has lower decoding costs (computational complexity) but requires more overhead (i.e. fountain-encoded packets) for successful decoding compared to the Gaussian elimination. Therefore, we can combine both methods to give low overhead and a reasonable complexity. Gaussian elimination is applied after the message passing algorithm. Packets which can not be retrieved by message passing will be decoded by Gaussian elimination. By using both methods, the number of source packets can be small and the practical overhead is reduced as shown in Figure 3.2. From this figure, we can see that the overhead of using the message-passing plus Gaussian elimination for $K = 500$ can be reduced from 42% to 3% in comparison to only message-passing decoding. Furthermore, the complexity of this scheme is increased to $O(K_1 \log_e K_1) + O(K - {K_1}^2)$, where K_1 is the number of source packets recovered by the message-passing algorithm and $K - K_1$ is the number of source packets recovered by the Gaussian elimination algorithm. For $K = 500$, on average around 250 source packets can be decoded by the message passing algorithm and the rest of the packets can be recovered by Gaussian elimination. In this case, the complexity is around 6×10^4, which is around 25% of the complexity of only using Gaussian elimination algorithm for decoding. However, the overhead by using both methods can be reduced from 42% to 3% compared with the overhead of only using message passing.

As mentioned before, fountain-encoded packets are assumed to be transmitted over the *Erasure Channel*, which means that the encoded packet is either received error free or not received at all. However, wireless channels are not erasure channels. To convert the wireless channel into an erasure channel, *error correction codes* are applied to each fountain-encoded packet in practical systems [42]. Both the *Low Density Parity Check* (LDPC) codes [47] and Turbo codes [48] are good error correction codes which allow the transmission data rate close to the Shannon limit, but the complexity of LDPC codes is lower than Turbo codes and the performance of LDPC codes is better than Turbo codes for short-length blocks [49]. Therefore, in this paper LDPC codes are

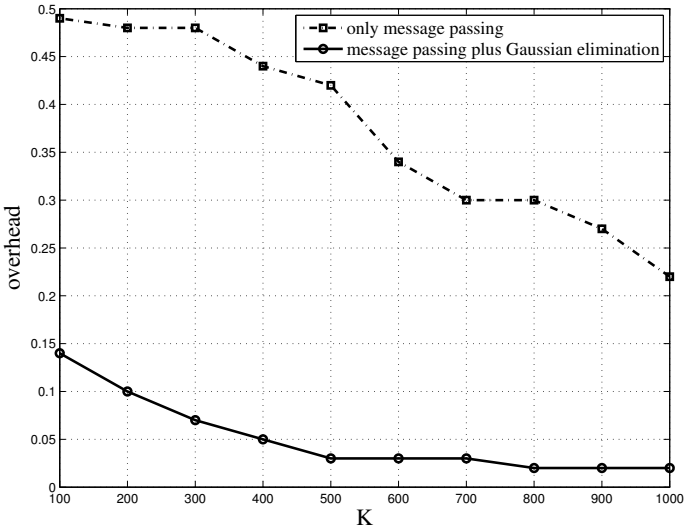

Fig. 3.2: The overhead of fountain codes (LT codes, c = 0.03, $\delta = 0.3$). fountain-encoded packets are transmitted over the erasure channel with the erasure probability of 20%. The dash-dot curve is the overhead of LT codes only using message passing decoding and the solid curve is the overhead of LT codes using message passing algorithm and Gaussian elimination together to decode.

used together with *Cyclic Redundancy Check* (CRC) to make the wireless channel behave like an erasure channel.

Our FEC encoding scheme is performed as follows. First, a fountain-encoded packet is created. Then, a CRC is added. Finally, the packet is encoded by a LDPC code to combat bit errors introduced by the channel.

At the receiver, each fountain-encoded packet is first LDPC decoded if its energy is equal to or higher than a threshold (i.e. corresponding to BER $\leq 10^{-5}$). The received packet is discarded if its energy is below the threshold. If the LDPC decoding fails, the received packet is discarded as well. If the LDPC decoding succeeds, the CRC is used to identify any errors undetected by the LDPC codes. If the CRC decoder detects an error, the receiver assumes that the whole packet has been lost. Once the receiver gets N surviving fountain-encoded packets, it starts to recover the source data.

3.1.3 Resolution-Adaptive ADC

Wireless channels in OFDM systems are fading channels and are modeled as frequency selective channels [2] [1]. An example is depicted in Figure 3.1. If a "bad" channel[2] is encountered, the required dynamic range of the ADC is higher than for a "good" one[3]. In addition, the ADC power consumption can be almost 50% of the total baseband power consumption [11]. This means that a resolution-adaptive ADC can potentially save power. An CMOS implementation of such an ADC is described in [50]. In this implementation, the power consumption scales linearly with the number of quantization levels.

3.1.3.1 Minimum Number of Quantization Levels

In OFDM receivers, demodulation of the sub-carriers is performed in the frequency domain. For that reason, it is not beforehand clear, how many ADC bits are necessary for proper decoding. In [18], the authors have derived a relation between the quantization noise in the time domain and frequency domain. However, results are shown only for non-fading channels. In this section, we present a scheme to design an optimum low-resolution ADC for frequency selective channels.

Because the quantization noise depends on the signal, we first analyze the statistical characteristics of the ADC input r_n. The channel is supposed to be noiseless, so the output at the n^{th} moment r_n is defined as:

$$r_n = \sum_{l=0}^{L-1} h_l x_{n-l} \tag{3.2}$$

where L is the number of channel taps, h_l the channel taps and x the transmitted signal. We assume that the quantization noise is dominant, so other noise (e.g. thermal noise) is ignored in this paper. From [18], we know that x_n can be modeled as a complex Gaussian-distributed random variable with zero-mean and a variance of 1. The elements in vector $[x_0, x_1, \cdots, x_{\mathrm{N}-1}]$ are mutual independent.

According to the *central limit theorem* [51], the sum of a sequence of independent, identically distributed random variables tends to be Gaussian-distributed, so the probability density function of r_n can be described as:

$$f(r_n) \approx \frac{1}{\pi} e^{-\frac{|r_n|^2}{\sum_l |h_l|^2}} \tag{3.3}$$

In other words, $r_n \sim \mathcal{CN}(0, \sum_l |h_l|^2)$.

[2] A "bad" channel means in our definition a large difference in energy between sub-carriers i.e. a large dynamic range of the ADC is required.

[3] A "good" channel on the other hand is when e.g. flat fading occurs.

The ADC output y_n is expressed by:

$$y_n = \mathcal{Q}(r_n) = \sum_l h_l x_{n-l} + n_n \tag{3.4}$$

where n_n is the quantization noise in the time domain. From [18], we know that n_n is uniformly distributed with zero mean and a variance of $\frac{\Delta^2}{6}$, where Δ is the uniform quantization step.

Due to the additional cyclic prefix in each OFDM symbol, the convolution in Equation 3.4 can be considered as a *cyclic convolution* [2]. So, after the OFDM demodulation, we can write Y_k as:

$$\begin{aligned} Y_k &= \frac{1}{\sqrt{\mathrm{N}}} \sum_n y_n e^{-j\frac{2\pi}{\mathrm{N}}nk} \\ &= \frac{1}{\sqrt{\mathrm{N}}} \sum_n \sum_l \left(h_l x_{n-l} + n_n\right) e^{-j\frac{2\pi}{\mathrm{N}}nk} \\ &= \frac{1}{\sqrt{\mathrm{N}}} \sum_n x_{n-l} e^{-j\frac{2\pi}{\mathrm{N}}(n-l)k} \sum_l h_l e^{-j\frac{2\pi}{\mathrm{N}}lk} \\ &\quad + \frac{1}{\sqrt{\mathrm{N}}} \sum_n n_n e^{-j\frac{2\pi}{\mathrm{N}}nk} \\ &= H_k X_k + N_k \end{aligned} \tag{3.5}$$

where N_k is the quantization noise in the frequency domain and H_k is the fading over the k-th sub-carrier defined by:

$$H_k = \sum_l h_l e^{-j\frac{2\pi}{\mathrm{N}}lk} \tag{3.6}$$

In [18], the authors have shown that N_k is a Gaussian distributed random variable with zero mean and a variance of $\frac{\Delta^2}{6}$. Thus, for each sub-carrier, the variance of the quantization noise is the same, but the Signal-to-(quantization)-Noise Ratio (SNR) is different due to different fading:

$$\mathrm{SNR}_k = \frac{|H_k|^2}{\frac{\Delta^2}{6}} \tag{3.7}$$

Error correcting codes can be applied to mitigate the effects of quantization and each

code has a certain SNR threshold to achieve BER at a certain order (e.g. 10^{-4}) or lower. So, the quantization step Δ can be determined once the error correcting code is chosen and the channel is estimated.

In practical systems, the ADC resolution is finite. This means that for the same channel, the required dynamic range of the ADC is larger for higher code rates.

If some clipping is allowed, the number of quantization levels N_q is given by [18]:

$$N_q = 2\lceil \frac{\mathrm{C}}{\Delta} \rceil \tag{3.8}$$

where C is equal to $3\sigma_{r_n}$. Once the channel is fixed, N_q is only dependent on Δ. In such a case, Δ depends not only on the applied error correction codes in the system, but also on how the encoded bits are transmitted. Assume that the fountain-encoded packets are transmitted over a wireless channel as shown in Figure 3.1 and that a packet is received correctly when SNR $\geq$ 12 dB. There are two schemes to transmit these fountain-encoded packets:

- Scheme I is to transmit each packet over all sub-carriers like current WLAN systems, which means that the SNR of the worst sub-carrier should be at least equal to 12 dB. In this case, the required number of quantization levels N_q is 54 for the example in Figure 3.3.
- Scheme II is to transmit each packet over one sub-carrier. Since each fountain-encoded packet is independent, it does not matter if we discard some packets which are transmitted over "bad" sub-carriers. From Figure 3.3, we can see that by discarding 15 sub-carriers, N_q can be reduced to 38 in comparison to Scheme I.

3.1.3.2 Power Consumption

The power consumption of the ADC is proportional to the number of quantization levels N_q which is related to the Effective Number Of Bits (ENOB) by:

$$N_q = 2^{\mathrm{ENOB}} \tag{3.9}$$

Thus, N_q is a measurement for the power consumption:

$$\mathrm{P} = \sum_{i=0}^{M_c-1} \alpha_i N_{qi} \mathcal{M} \tag{3.10}$$

where M_c is the number of channel realizations, α_i is the percentage of the i-th channel realization where useful information is transmitted, N_{qi} is the number of quantization

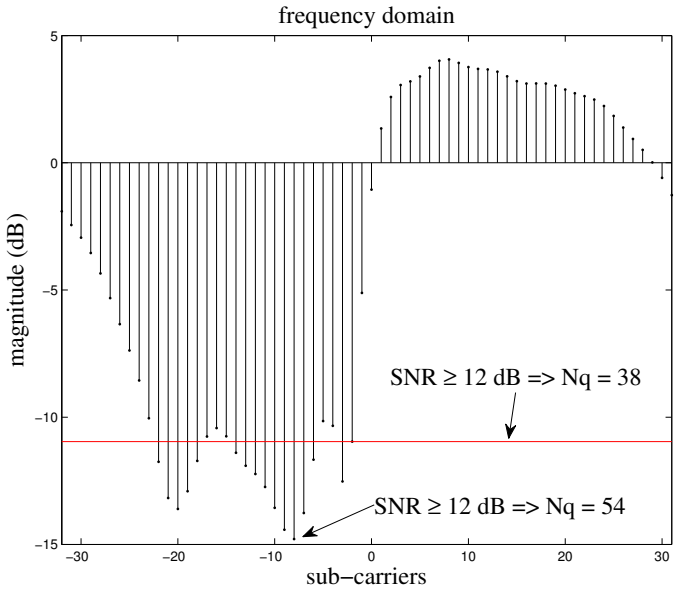

Fig. 3.3: The difference in the number of ADC levels N_q between the transmission Scheme I and the transmission Scheme II. In this example, $N_q = 54$ levels are required for the transmission Scheme I such that each fountain packet is transmitted over all sub-carriers; N_q can be reduced to 38 levels when 15 sub-carriers are discarded in the transmission Scheme II where each fountain packet is transmitted over one sub-carrier only.

levels used in the i-th channel realization, and $\mathcal{M}$ is the number of samples per MAC frame.

When Scheme II is applied, the power consumption of the ADC can be reduced by discarding "bad" sub-carriers. However, discarding transmitted packets over "bad" sub-carriers leads to an increase in the number of the transmitted packets. Therefore, there is a tradeoff in the power consumption of the ADC between the number of lost sub-carriers and the number of transmitted packets.

So far, we have designed the quantization scheme for OFDM systems over the frequency selective channels under the assumption of the perfect channel knowledge. However, in practical systems, the channel can not be perfectly estimated, which affects the design of quantization scheme. We will discuss this influence in the next section.

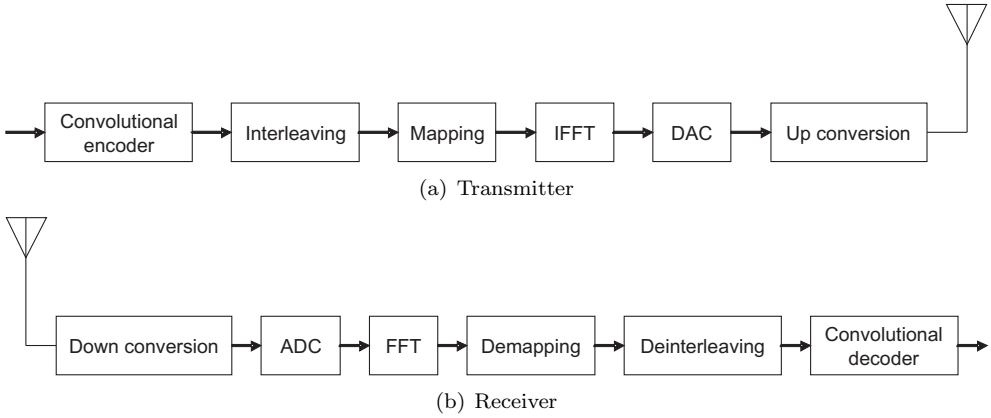

(a) Transmitter

(b) Receiver

Fig. 3.4: Conventional 802.11a transmitter (top) and receiver (bottom)

3.1.4 System Model

As mentioned earlier, our opportunistic error correction layer is based on fountain codes and resolution-adaptive ADCs which have been explained in the above sections. This proposed error correction layer can be applied in OFDM systems. The IEEE 802.11a system is taken as an example of an OFDM system in this paper.

In this section, the system model of an IEEE 802.11a transceiver is discussed as shown in Figure 3.4. It is a simplified model with focus on the (de)modulation and (en/dec)coding of the bit stream. This means that we assume for example that there is no adjacent channel interference.

The FEC layer in current IEEE 802.11a system is based on RCPC. RCPC has a good performance for random bit errors. An Interleaver is used to remove the burst errors. Although this solution works well in practical systems, it is not optimal. First, packets that have encountered a "bad" channel condition are still processed by the entire receiver chain. Although the IEEE 802.11a standard uses a form of adaptive modulation, it only consists of 6 modes which is a very coarse form. The transmitter tries continuously to use the highest code rate, but adaptation is relatively slow and each mode is designed for the 'average' channel. This means that for most packets, the code rate and hence capacity can be increased. Furthermore, the resolution of the applied ADCs is fixed for a 802.11a system.

In Figure 3.5, we show the new error correction layer that mitigates both problems. The key idea is to generate additional packets by the fountain encoder. First, the source packets are encoded by the fountain encoder. Then, a CRC checksum is added to each fountain-encoded packet and LDPC encoding is applied. The code rate of the LDPC code is chosen relatively high as only packets with high SNR have to be decoded, others are discarded. Each encoded packet is transmitted on one sub-carrier of the OFDM system. At the receiver side, we assume that the synchronization is

perfect and the channel is estimated by an adaptive ADC with high resolution. After that, the adaptive ADC can be reduced to the minimum necessary resolution for each channel realization. In the transmitter, more fountain-encoded packets are created than necessary for decoding. The receiver has now the freedom to discard some of the received packets. A further resolution reduction can be achieved by discarding the packets which are transmitted over "bad" sub-carriers.

If the SNR of the sub-carrier is equal to or above the threshold, the received fountain-encoded packet will go through LDPC decoding, otherwise it will be discarded. In our implementation, we choose a threshold of 12 dB for the used LDPC code. This means that the receiver is allowed to discard several sub-carriers (i.e. packets) to lower the dynamic range of the ADC and hence the power consumption. After the LDPC decoding, the CRC checksum is used to discard erroneous packets. As only packets with a high SNR are processed by the receiver, this will not happen very often.

In practical systems, the channel can not be perfectly estimated. High-resolution ADCs are applied to estimate the channel and the channel is estimated, for example by the *zero forcing* algorithm. A set of training symbols defined in [17] is used to estimate the channel, so we have:

$$Y_t = H_k X_t + N_h \tag{3.11}$$

where X_t is the training symbol, Y_t is the received training symbol, H_k is the k^{th} sub-carrier and N_h is the quantization noise from adaptive ADCs with high resolution. The k^{th} sub-carrier can be estimated by:

$$\begin{aligned} \hat{H_k} &= \frac{Y_t}{X_t} \\ &= H_k + \frac{N_h}{X_t} \end{aligned} \tag{3.12}$$

So, we can rewrite the output signal in the frequency domain after quantization defined in Equation 3.5 as:

$$\begin{aligned} Y_k &= H_k X_k + N_a \\ &= \hat{H_k} X_k - \frac{N_h}{X_t} X + N_a \\ &= \hat{H_k} X_k + N' \end{aligned} \tag{3.13}$$

where N_a is the quantization noise from resolution-adaptive ADCs. The variance of N' ($\sigma^2_{N'}$) is equal to $\sigma^2_{N_h} + \sigma^2_{N_a}$. Therefore, with the channel estimation error, the

SNR for each sub-carrier defined in Equation 3.7 can be updated as:

$$\begin{aligned} \mathrm{SNR}_k &= \frac{|\hat{H}_k|^2}{\sigma^2_{N'}} \\ &= \frac{|\hat{H}_k|^2}{\sigma^2_{N_h} + \sigma^2_{N_a}} \\ &= \frac{|\hat{H}_k|^2}{\sigma^2_{N_h} + \frac{\Delta^2}{6}} \end{aligned} \tag{3.14}$$

As we can see, the noise defined in the above equation is composed of the quantization noise from high-resolution ADCs for the channel estimation and from resolution-adaptive ADCs for the user data.

The channel estimation error will affect the SNR threshold for the correct LDPC decoding, as shown in Figure 3.6. From this figure we can see that the BER degradation can be neglected (within 0.1 dB gap for BER at the order of 10^{-5}), which means the received packets can still go through the LDPC decoder when SNR $\geq$ 12 dB. Though the channel estimation error does not influence the LDPC decoding too much, the number of quantization levels N_q will be affected, as the LDPC decoder needs to know the SNR defined in Equation 3.14. How N_q is influenced by the channel estimation error depends on the design method of quantization scheme. There are two design methods as follows:

- Method I: Assume $\sigma_a^2 > \sigma_h^2$ and the number of lost sub-carriers is fixed, so the quantization step Δ can be derived from Equation 3.14 and defined as:

$$\Delta = \sqrt{6\frac{|\hat{H}_k|^2}{\mathrm{SNR}_k} - \sigma_h^2} \tag{3.15}$$

  and N_q can be determined by Equation 3.8.
- Method II: Assume $\sigma_a^2 \gg \sigma_h^2$, Equation 3.14 can be rewritten as:

$$\mathrm{SNR}_k = \frac{|\hat{H}_k|^2}{\frac{\Delta^2}{6}} \tag{3.16}$$

  so Δ is defined as:

$$\Delta = \sqrt{6\frac{|\hat{H}_k|^2}{\mathrm{SNR}_k}} \tag{3.17}$$

  and N_q follows from Equation 3.8 as well. In this case, we will have smaller N_q

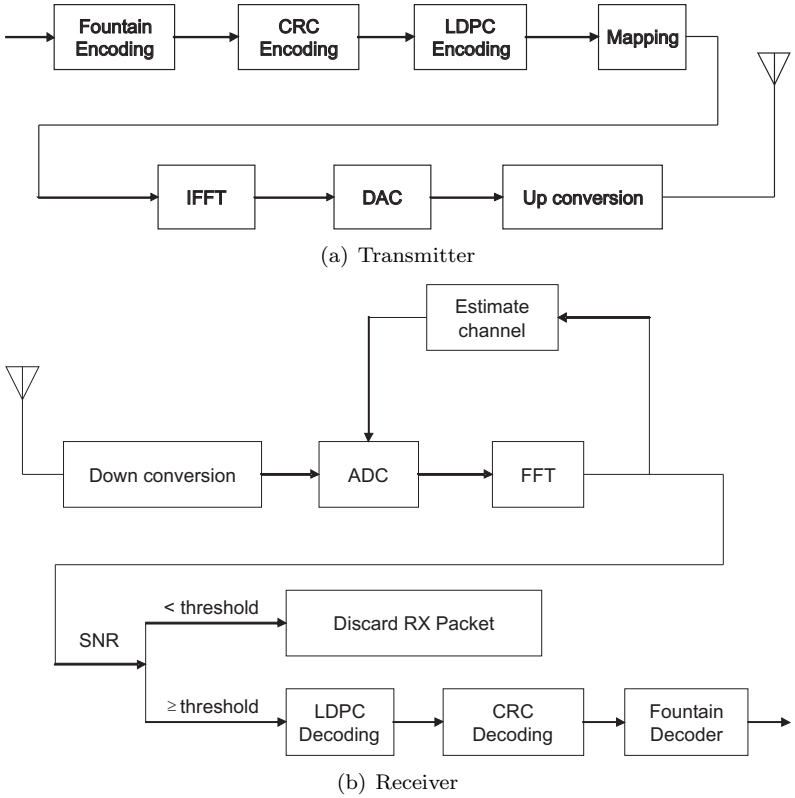

(a) Transmitter

(b) Receiver

Fig. 3.5: Proposed 802.11a transmitter (top) and receiver (bottom). In the transmitter, first source packets are encoded by fountain codes then LDPC and CRC are applied to each fountain-encoded packet; after that each encoded packet is transmitted over a sub-carrier. In the receiver, the channel is first estimated by high resolution ADCs then the resolution of ADCs are adapted to the minimum according to the estimated channel knowledge. Each received packet is decoded by LDPC and CRC if SNR $\geq$ threshold otherwise it will be discarded. When the receiver gets N fountain-encoded packets, it can recover the source file.

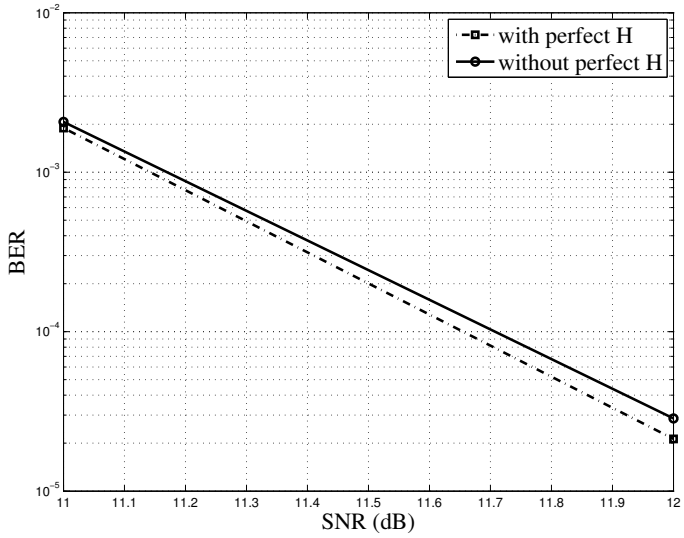

Fig. 3.6: BER of the (175,255) LDPC code. The dash-dot line is the BER curve with perfect channel knowledge and the solid line is the BER curve without perfect channel knowledge.

compared to Method I but we might lose more sub-carriers (i.e. packets) since the SNR defined in Equation 3.14 is smaller than the SNR we assume in Equation 3.17.

In order to see the influence of the channel estimation error and the performance of the quantization design Method I and II, we give an example as shown in Figure 3.7. In this example, we only consider 52 active sub-carriers defined in [17] and assume that no sub-carrier is discarded. In the case of perfect channel estimation, 248 quantization levels are required. When the channel is estimated by the zero forcing algorithm, the required N_q using Method I is 396 and using Method II 216 levels are needed which is less than the case of perfect channel estimation. But, one extra sub-carrier is discarded when Method II is applied, because this sub-carrier has lower SNR than the threshold (i.e. 12 dB). Obviously, Method II requires smaller N_q in comparison with Method I though in this case we might lose more sub-carriers than we expect. Method II is chosen to design the quantization scheme in this paper.

As we mentioned before, there is a tradeoff in the power consumption of ADCs between the number of lost sub-carriers and the number of transmitted packets. In Figure 3.8 the relation is depicted between power consumption (dynamic range) and the number of discarded sub-carriers with perfect channel knowledge and without. In each case the same amount of information was transmitted and decoded successfully by the receiver. Besides, the sub-carriers with the lowest energy are discarded. From this figure, we can also see that the channel estimation error does not really affect the total power consumption. For the perfect channel estimation, the minimum power consumption is reached when 14 sub-carriers are discarded. Without perfect channel

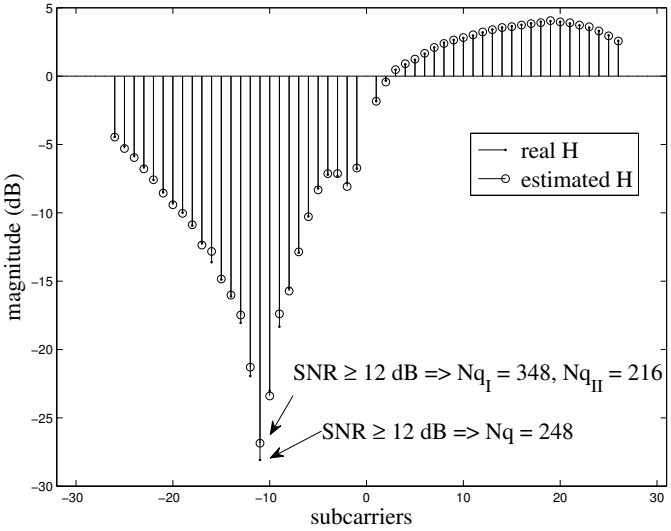

Fig. 3.7: The influence of the channel estimation error and the difference in N_q between the quantization design Method I and the quantization design Method II. In this example, we assume the worst sub-carrier has a SNR of 12 dB. $N_q = 248$ for the case with perfect channel knowledge. With the estimated channel knowledge, $N_q = 348$ for the quantization Method I and $N_q = 216$ for the quantization Method II.

knowledge, the lowest power consumption can be obtained when 15 sub-carriers are discarded.

In the next section, we compare both systems for the same bit rate.

3.1.5 Performance Analysis

In this section we compare three scenarios. Channel *model* A is used in all our simulations and we simulate at least 1 million bits per simulation. The first scenario, Scenario I, is a conventional IEEE 802.11a system with 16-QAM modulation and code rate $\frac{1}{2}$. This mode has a throughput of 24 Mbit/s (source bits). As the standard allows 10% packet loss [17], the effective throughput is $0.9 \cdot 24 = 21.6$ Mbit/s. Moreover, we assume that conventional ADCs are used, of which the resolution has been designed for 90% of the channel realizations. In Scenario II, the conventional ADCs are replaced by resolution-adaptive ADCs, which are designed to allow 10% packet loss. Finally, in Scenario III, we apply the new opportunistic error correction layer, which has the same effective throughput as Scenario II.

As discussed before, the channel estimation error can be neglected in case of using

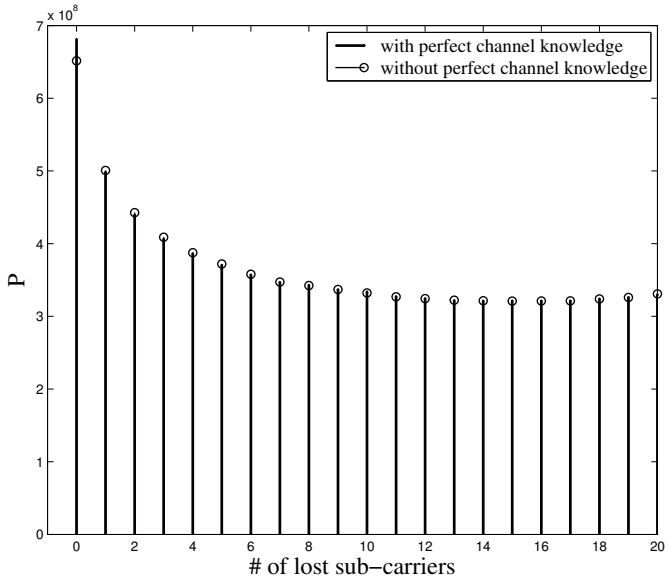

Fig. 3.8: Power consumption defined in Equation 3.10 versus the number of lost sub-carriers for a fountain code with a packet size of 168 bits. The dot points are with perfect channel knowledge and the circle points are without perfect channel knowledge.

high-resolution ADCs. In our simulations, we use the parameters of Table 3.1. The "SNR in frequency domain" is the minimal SNR for each sub-carrier. If this value is met, the Packet Error Rate (PER) will be less than 10%, as required by the standard [17]. Symbols are transmitted in bursts (i.e. MAC frame) and in 802.11a, 500 OFDM symbols are packed into one burst.

From Figure 3.8, one can derive that the minimal power consumption for Scenario III will be reached if about 15 sub-carriers can be discarded without perfect channel knowledge. So, the LDPC and CRC checksum have to be chosen in such a way that the total throughput is equal to Scenario I and about 15 sub-carriers are discarded by the receiver.

We replace the error correction layer by a 7-bit CRC checksum and a LDPC code (175,255) which has a code rate of 0.66. For the fountain code part, we use a LT code with parameters $c = 0.03$ and $\delta = 0.3$. The resulting fountain code packets are transmitted on separate sub-carriers and over multiple MAC frames. On average 14 sub-carriers can be discarded by the receiver, which is close to the optimal value if there is no perfect channel estimation.

Figure 3.9 shows the consumed power (per source bit) for each scenario versus the fountain code block length K under the condition of the non-perfect channel knowledge. For each simulation point 2000 fountain code bursts are transmitted. The

	Scenario I	**Scenario II**	**Scenario III**
ADC	normal	res. adapt.	res. adapt.
FEC	RCPC	RCPC	LDPC + Fount. codes
Code rate	0.5	0.5	0.66
Modulation	16-QAM	16-QAM	16-QAM
N_c	48	48	48
N	64	64	64
N_s	500	500	500
Effective throughput	21.6 Mbit/s	21.6 Mbit/s	21.6 Mbit/s
SNR in freq. domain	9.0 dB	9.0 dB	12.0 dB

Table 3.1: System setup comparison for three scenarios (N_c - the number of data carriers, N - the number of sub-carriers, N_s - the number of symbols per MAC frame)

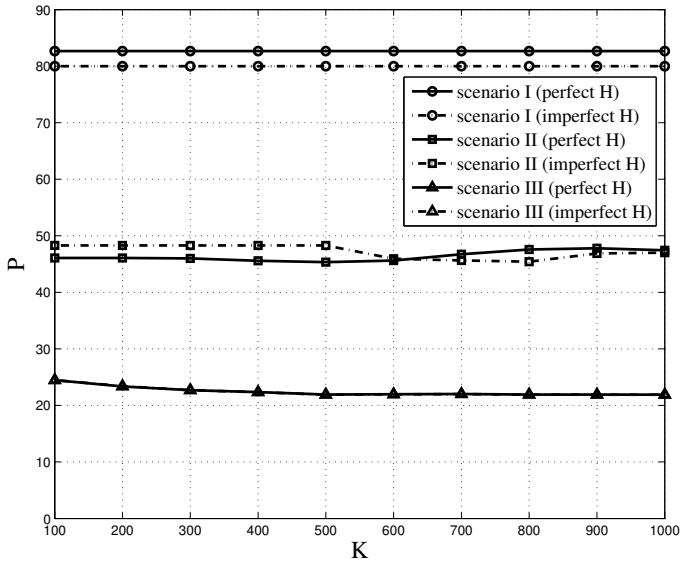

Fig. 3.9: The power consumption (defined in equation 3.10) per source bit. The curves with circle-mark are for Scenario I, the curves with square-mark are for Scenario II and the curves with triangle-mark are for Scenario III. The solid curve is with perfect channel knowledge and the dash-dot line is without channel knowledge.

power consumption in Scenario I is constant for each K since the conventional ADC is designed for worst case. In Scenario II, the power consumption on average is about 58% of the power consumed in Scenario I. The difference in the power consumption for different K in this scenario is due to the channel randomness. In Scenario III,

the power consumption for different K is inversely proportional to the overhead of LT codes. The average power consumption for receiving 1 source bit in Scenario III is about 48% of the average power consumed in Scenario II and about 28% of the average power consumed in scenario I.

Furthermore, Figure 3.9 shows the power consumption with perfect channel knowledge. As we can see, for each scenario, the consumed power has little difference between the perfect channel estimation and the non-perfect channel estimation. This difference depends on how accurate the channel is estimated. As we know, the zero forcing estimation algorithm assumes no noise in the received symbol which means this algorithm has better performance when SNR is higher. Figure 3.7 also shows that "good" sub-carriers can be more accurately estimated than "bad" sub-carriers. In Scenario III we only need to take care of "good" sub-carriers but we have to take care of all sub-carriers in Scenario I and II. From Equation 3.8, we can see that N_q is determined by the quantization step Δ. The threshold of the used LDPC is 12 dB which means Δ depends on *the wanted sub-carrier with the lowest energy* $H_{k'}$ as defined in Equation 3.14. In a word, N_q is determined by $H_{k'}$. $|H_{k'}|^2$ in Scenario III is larger than $|H_{k'}|^2$ in Scenario I and II. So, the difference in N_q between the perfect channel knowledge and the non-perfect channel knowledge is smaller in Scenario III than in Scenario I and II, as we can see in Figure 3.9. In this figure, in Scenario III both curves overlap but this does not happen in Scenario I and II. Therefore, the new error correction layer is less sensitive to the channel estimation error comparing to the conventional error correction layer.

Thus, the resolution-adaptive ADC can save around 42% power and the novel opportunistic error correction layer can save an additional 30% power consumption. In total, the new method reduces the power consumption in ADCs by 72% compared to the current 802.11a standard.

From Section 3.1.3, we can see that low power consumption means low SNR requirement. Compared to the RCPC codes, LDPC codes have better performance close to the Shannon limit. For that reason, LDPC codes have been adopted by the IEEE 802.11n standard. In order to check how our scheme performs with respect to the required SNR, we compare convolutional codes, LDPC codes from the IEEE 802.11n standard and our opportunistic error correction layer under the condition of the same effective throughput (i.e. 21.6 Mbits/s). Figure 3.10 shows the simulation results over the noisy Channel *model* A with perfect channel estimation when $K = 500$. For each simulation point, more than 1 million bits are transmitted. From this figure, we can see that the required SNR for convolutional codes is 23 dB when BER $= 2 \times 10^{-4}$. A similar value for this channel model is reported in [52]. Figure 3.10 shows that LDPC codes have a gain of around 4 dB comparing to convolutional codes. However, the proposed method has a gain of around 7.5 dB.

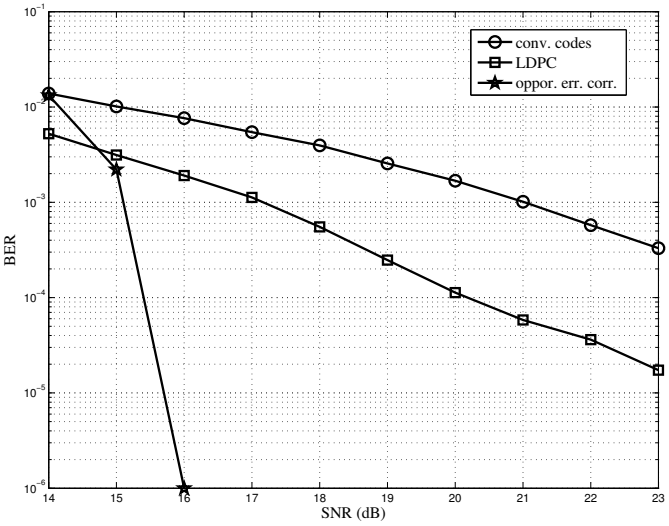

Fig. 3.10: FEC layers comparison over Channel *model* A with the same effective transmission data rate 21.6 Mbits/s (i.e. PER = 10%, BER = 2×10^{-4}). The SNR is in the time domain and the channel estimation is assumed to be perfect. The blue circle points are for convolutions codes; the red square points are for LDPC codes from 802.11n and the black star points are for opportunistic error correction layer (fountain codes + LDPC plus CRC). For SNR = 16 dB and higher, no errors are detected in the opportunistic error correction layer. So, for SNR = 16 dB, we represent BER = 0 by 10^{-6}.

3.1.6 Conclusions and Future Work

In this paper, we propose a novel cross-layer scheme which integrates the error correction into the physical layer. This new opportunistic error correction layer is designed for OFDM systems (e.g. IEEE 802.11a system) based on fountain codes and resolution-adaptive ADCs. Each fountain-encoded packet is transmitted over a subcarrier. By discarding fountain-encoded packets that have been transmitted over "bad" sub-carriers, the dynamic range of ADCs can be reduced. Correspondingly, the power consumption of ADCs can be lowered as well.

The ADCs in a receiver can consume up to 50% of the total baseband energy, so it is advantageous to lower its power consumption. The resolution-adaptive ADC can save on average around 42% energy consumption comparing to the conventional ADC. Fountain codes together with LDPC plus CRC codes can allow the power consumption in ADC to be decreased by an additional 30%. So, the new opportunistic error correction layer can reduce the power consumption in ADC by more than 70% compared with the conventional IEEE 802.11a system. In addition, it requires 7.5 dB less SNR than the 802.11a system.

Besides, we have shown that the new error correction layer is a robust scheme against the channel estimation errors. So, ADCs can also be adapted to the minimum resolution in a realistic system where the channel is estimated. Moreover, by using message passing algorithm and Gaussian elimination algorithm, the new error correction scheme can be applied to a small packet size (e.g. $K = 500$) with low overhead (e.g. 3%) which can make this new scheme efficient.

Here, we assume that there is no adjacent interference which does not happen in the real wireless channels. Further research focuses on the optimization of this new error correction for the wireless channel with adjacent interference.

3.2 Practical Evaluation of Opportunistic Error Correction

[4]**Abstract** In [40], we have proposed a novel cross-layer scheme based on resolution adaptive ADCs and fountain codes for the OFDM systems to lower the power consumption in ADCs. The simulation results show that it saves more than 70% power consumption in ADCs comparing to the current IEEE 802.11a system. In this paper, we investigate its performance in the real-world. Measurement results show that the FEC layer used in the IEEE 802.11a system consumes around 59 times of the amount of power in ADCs comparing to the LDPC codes from the IEEE 802.11n standard, whose power consumption in ADCs is around 26 times of the proposed cross-layer method. In addition, this new cross-layer approach only needs to process the well-received packets to save the processing power. The latter can not be applied in the current FEC schemes.

3.2.1 Introduction

Orthogonal Frequency Division Multiplexing (OFDM) has become a popular scheme for recent WLAN standards which operate at a high data rate [13]. OFDM has a high *Peak-to-Average Power Ratio* (PAPR), therefore it requires *Analog-to-Digital Converters* (ADC) with a high dynamic range. These high resolution ADCs can take up to 50% of the baseband power [11]. However, low power-consumption in battery-powered wireless receivers is a highly desirable feature.

[4]This section is the published paper [53]: *X. Shao and C.H. Slump, "Practical Evaluation of Opportunistic Error Correction", in Proceedings of IEEE Global Telecommunications Conference (GLOBECOM), Dec 2009, Honolulu, USA.*

In [40], we have proposed a novel error correction layer based on *adaptive ADCs* and *fountain codes* to mitigate the effects of a wireless channel at a lower power consumption level in ADCs comparing to traditional solutions. With this method, the resolution of ADCs is adapted to each channel condition instead of fixing to the high-resolution for the worse-case scenario. As a result, the power consumption of the ADC is reduced under most, i.e. non worst-case, channel conditions.

A further resolution reduction of the ADC can be achieved by using a novel opportunistic error correction scheme that integrates into the physical layer. This approach allows us to discard some part of the channel with deep fading. The current WLAN standards do not support this idea, as all sub-bands are considered equally important by the *Forward Error Correction* (FEC) layer. However, the opportunistic error correction method based on fountain codes does not have this disadvantage.

By using fountain codes, the receiver can recover the original data by collecting enough fountain-encoded packets. It does not matter which packets are received, only a minimum amount of packets have to be received correctly [42]. In other words, fountain-encoded packets are independent with respect to each other. By transmitting a fountain-encoded packet over a sub-band of a channel. Thus, multiple packets are transmitted simultaneously, using frequency division multiplexing. The receiver discards fountain-encoded packets which are transmitted over the sub-band with deep fading. Correspondingly, the power consumption in ADCs decreases.

The performance of this new scheme has been investigated by the C++ simulation in [40]. With the same effective throughput, the simulation results have shown that this new algorithm allows a reduction of more than 70% power consumption in ADCs comparing to the traditional IEEE 802.11a system [40].

C++ simulation, with its highly accurate double-precision numerical environment, is on the one hand a perfect tool for the investigation of the algorithms. On the other hand, many imperfections of the real-world are neglected (e.g. the quantization noise is assumed to be dominant and the channel noise is ignored in [40]). So, simulation may show a too optimistic receiver performance. The uncertainties in the real life are mainly simplified assumptions in the simulation like perfectly known noise levels, additive Gaussian noise, omitted synchronization, etc. Therefore, we want to evaluate the performance of the opportunistic error correction scheme in the real-world.

In this paper we test an approach based on resolution adaptive ADCs and fountain codes to reduce the power consumption of ADCs in the experimental communication testbed built by the Signals and Systems Group, University of Twente. Since the resolution adaptive ADC is not a on-the-shelf product yet, we requantize the signal from the ADCs by software to mimic the effect of resolution adaptive ADCs. In addition, we test how the imperfect synchronization affects the opportunistic error correction scheme based on fountain codes.

The outline of this paper is as follows. Opportunistic error correction layer is applied to lower the power consumption in wireless OFDM-based receivers. First, the basic idea of the opportunistic error correction scheme is described, which is followed by the

system setup. In Section 3.2.4, the measurement setup is depicted. We compare the FEC layer from the IEEE 802.11a standard [17] and the one from the IEEE 802.11n standard [23] with the opportunistic error correction layer in the measurements. Finally, the measurement results are analyzed. The paper ends with a discussion of the results.

3.2.2 Opportunistic Error Correction

Opportunistic error correction is based on fountain codes. In this paper, we use a kind of fountain codes, i.e. *Luby Transform* (LT) codes [43] in the proposed error correction layer. Other fountain codes (e.g. Raptor codes [44]) can also be applied.

Consider a block of size K packets $s_1, s_2, \cdots, s_K$ to be encoded by a fountain code. A packet has m bits and considered a unit. At each clock cycle, labeled by n, one fountain-encoded packet is generated by selecting a set of source packets randomly and computing the bitwise sum (XOR) of these source packets [42]. The fountain codes can supply an unlimited number of encoded packets based on $s_1, s_2, \cdots, s_K$. In practical systems, only a fixed number of packets N is generated.

At the receiver side, enough packets are required for successful decoding. The required number of received packets N is slightly larger than the number of source packets K and is defined as:

$$N = K(1 + \varepsilon) \tag{3.18}$$

where ε is the percentage of extra packets and is called the overhead.

After receiving N packets, the receiver can recover the source packets by the *message-passing* algorithm [54] which has a linear decoding cost. We have shown that decoding the fountain codes using the message-passing algorithm combined with Gaussian elimination allows small block sizes, e.g. $K = 500$, with small overhead $\varepsilon = 3\%$ in [40]. Small block sizes are needed to keep the decoding delay low, which is important in real-time applications such as WLAN applications.

Fountain codes are designed for *Erasure Channels*. However, wireless channels are noisy fading channels, not erasure channels. In practical systems, fountain codes are used in combination with other error correction algorithms to convert the noisy channels into erasure channels, often *Low-Density Parity-Check* (LDPC) codes [54]. In this paper, LDPC codes are used together with a *Cyclic Redundancy Check* (CRC) to make the wireless channel behave like an erasure channel.

Our FEC encoding scheme is performed in the following order. First, a fountain-encoded packet is created. Then, the CRC is added. Finally, the packet is encoded by the LDPC code.

At the receiver, each fountain-encoded packet is first LDPC decoded if its energy is above or equal to a threshold (i.e. corresponding to BER $\leq 10^{-5}$). The threshold

is determined by the channel energy, the channel noise and the quantization noise. So, the resolution of ADCs (i.e. the quantization noise) can affect the threshold in a given channel. If the system allows packets from the low-energy channel to be lost, the required resolution of ADCs can be reduced.

The received packet is discarded if its energy is below the threshold. If the LDPC decoding fails, the received packet is discarded as well. If the LDPC decoding succeeds, the CRC is used to identify any errors undetected by the LDPC codes. If the CRC decoder detects an error, the receiver assumes that the whole packet has been lost. Once the receiver gets N surviving fountain-encoded packets, it starts to recover the source data.

3.2.3 System Setup

The opportunistic error correction layer is based on resolution adaptive ADCs and fountain codes. This proposed cross layer can be applied in the OFDM system. In this paper, we evaluate its performance in the testbed, as shown in Fig. 3.11. It is assembled as a cascade of the following modules: PC, DAC, RF up-converter, power amplifier, antenna, and the reverse chain for the receiver. In the receiver, there is no power amplifier and band-pass RF filter before the down-converter but a low-pass baseband filter before the AD converter to remove the aliasing.

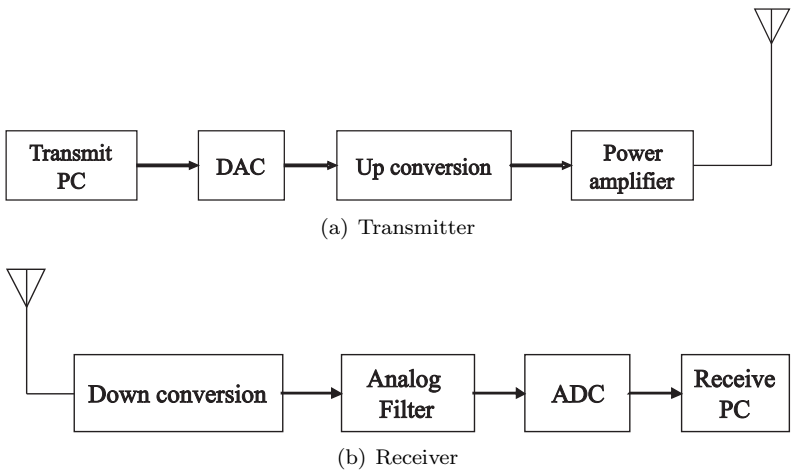

(a) Transmitter

(b) Receiver

Fig. 3.11: Block diagram of the testbed

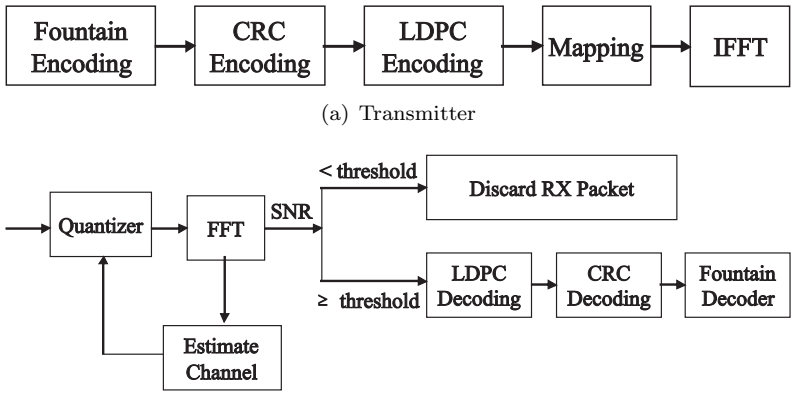

(a) Transmitter

(b) Receiver

Fig. 3.12: System model of opportunistic error correction layer: transmitter (top) and receiver (bottom).

3.2.3.1 The Transmitter

The data is generated offline in C++. The generation consists of the random source bits selection, the FEC encoding and digital modulation. Any FEC scheme and digital modulation can be applied. The FEC layer in the current IEEE 802.11a system is based on *Rate Compatible Punctured Codes* (RCPC). RCPC has a good performance for random bit errors. An interleaver is used to mitigate the burst errors. Although this solution works well in practical systems, it is not optimal. First, because packets that have encountered a low-energy channel are still processed by the decoders. It will waste processing power. In addition, the error correction layer is based on worst case scenarios. This means that for most packets, the code rate and hence capacity can be increased. Furthermore, the resolution of the applied ADCs is fixed for IEEE 802.11a receivers, which is designed for worst case conditions. However, worse case condition does not always happen.

In Fig. 3.12(a), the opportunistic error correction scheme is depicted to reduce the power consumption in ADCs. The key idea is to generate additional packets by the fountain encoder. First, a block of source bits are divided into a set of packets and encoded by the fountain encoder. Then, a CRC checksum is added to each fountain-encoded packet, and LDPC encoding is applied. On each sub-carrier, a fountain-encoded packet is transmitted. Thus, multiple packets are transmitted simultaneously, using frequency division multiplexing.

The generated data is stored in a file. A server software in the transmit PC uploads the file to the Adlink PCI-7300A board[5] which transmits the data to DAC (AD9761)[6] via the FPGA board. After the DAC, the baseband analog signal is upconverted to

[5]ADLINK, 80 MB/s High-Speed 32-CH Digital I/O PCI Card
[6]Analog Devices, 10-Bit, 40 MSPS, dual Transmit D/A Converter.

2.3 GHz by a Quadrature Modulator (AD8346)[7] and transmitted using a conical skirt monopole antenna.

3.2.3.2 The Receiver

The reverse process takes place in the receiver. The received RF signal is first down-converted by a Quadrature Demodulator (AD8347)[8], then pass the 8-th order low-pass Butterworth analog filter to remove the aliasing. The baseband analog signal is quantized by the ADC (AD9238)[9] and stored in the receive PC via the Adlink PCI board.

The received data is processed offline in C++. The receiver should synchronize with the transmitter and estimate the channel using the preambles and the pilots, which are defined in [17]. Timing and frequency synchronization is done by the Schmidl & Cox algorithm [55] and the channel is estimated by the *zero forcing* algorithm. With the estimated channel information, the resolution of the adaptive ADC can be reduced to the minimum for each channel realization. In addition, the *residual carrier frequency offset* is estimated by the four pilots in each OFDM symbol.

After the synchronization and the channel estimation, decoding can start. Fig. 3.12(b) depicts the opportunistic error correction decoding scheme. With the estimated channel knowledge, the SNR of each sub-carrier can be derived. If the SNR of the sub-carrier is equal to or above the threshold, the received fountain-encoded packet will go through LDPC decoding, otherwise it will be discarded. This means that the receiver is allowed to discard low-energy sub-carrier (i.e. packets) to lower the dynamic range of the ADC and hence the receiver is allowed to discard the erroneous packets. As only packets with a high SNR are processed by the receiver, this will not happen often. When the receiver collects enough fountain-encoded packets, it starts to recover the source data.

3.2.4 Measurements

Measurements are carried out in the corridor of the Signal and Systems Group, located at the 9th floor of Building Hogekamp in University of Twente, the Netherlands. The measurement setup is shown in Fig. 3.13. The transmitter (TX) was positioned in an open place in front of the elevator (i.e. the gray area in Fig. 3.13), while the receiver antenna (RX) was in the left/right side of the corridor (i.e. the cross positions in Fig. 3.13). The transmit antenna was moved arbitrarily in the gray area of Fig. 3.13. 56 measurements were done in this scenario with a non-line-of-sight situation. The average transmitting power is around -38 dBm and the distance

[7] Analog Devices, 2.5 GHz Direct Conversion Quadrature Modulator.
[8] Analog Devices, 800 MHz to 2.7 GHz RF/IF Quadrature Demodulator
[9] Analog Devices, Dual 12-Bit, 20/40/65 MSPS, 3V A/D Converter.

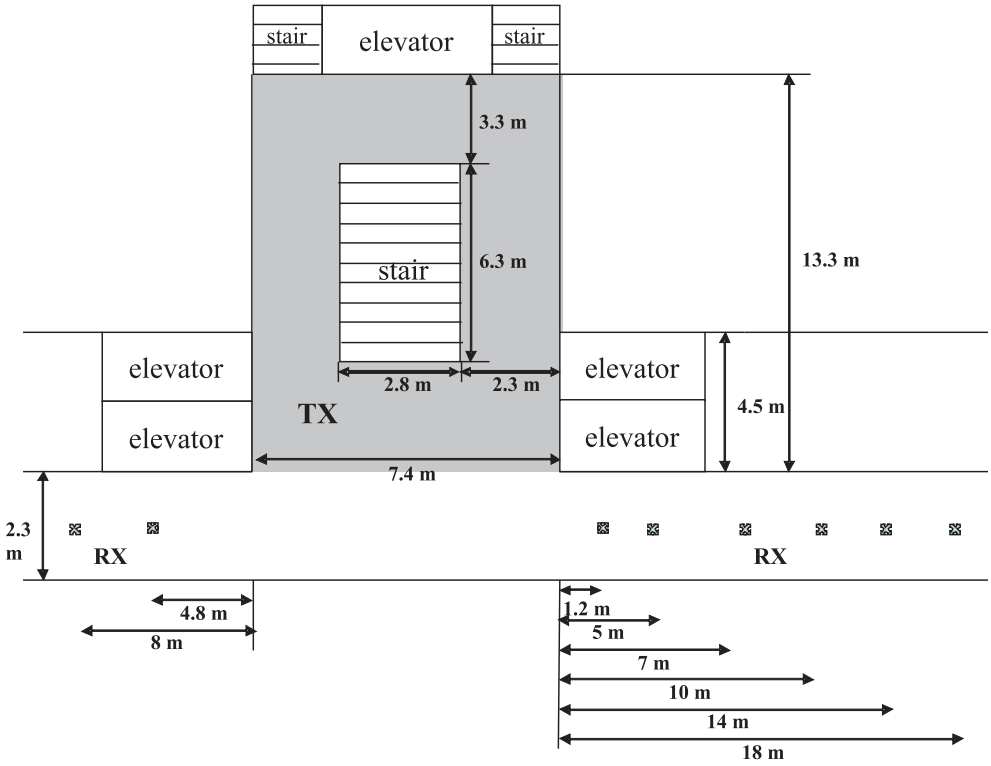

Fig. 3.13: Measurement Setup: antennas are 0.9 m above the concrete floor. The measurements are done in the corridor of the Signals and Systems Group. The receiver is positioned at left/right side of the corridor (i.e. the cross positions) and the transmitter is at the gray part as shown in the figure. The room contains one coffee machine, one garbage bin and one glass cabin.

between the transmitter and the receiver is around $7 \sim 25$ meters. The measurements were conducted at 2.3 GHz carrier frequency and 20 MHz bandwidth.

In order to investigate whether the opportunistic error correction layer performs better than the other FEC layers in the real-world, the following FEC layers are compared in the measurements:

- FEC I: convolutional codes ($R = \frac{1}{2}$) with interleaving defined in the IEEE 802.11a standard.
- FEC II: the (324,648) LDPC code from the IEEE 802.11n standard.
- FEC III: the opportunistic error correction layer based on fountain codes.

In [40], these FEC schemes have been compared in the C++ simulation. In the simulation, they can be compared by using the same source bits. Different channel bits can go through the same random frequency selective channels. However, it does not apply in the real environment. The wireless channel is time-variant even when the transmitter and the receiver are stationary (e.g. the moving of elevator with the closed door can affect the channel). Hence, we should compare them by using the same channel bits.

Because not every stream of random bits is a codeword of a certain coding scheme, it is not possible to derive its corresponding source bits from any sequence of random bits, especially for the case of FEC I and FEC III. Fortunately, the decoding of FEC II is based on the parity check matrix. Any stream of random bits can have its unique sequence of source bits with its corresponding syndrome matrix. The receiver can decode the received data based both on the parity check matrix and the syndrome matrix. So, FEC I can use the same channel bits with FEC II, same for FEC II and FEC III. In such case, they can be compared under the same channel condition (i.e. channel fading, channel noise and the distortion caused by the hardware.). During the measurements, both sequences of channel bits are transmitted in one burst (i.e. 2 blocks) in order to have their channels as similar as possible.

In the measurements, we transmit more than 300 blocks of source packets over the air. Each block consists of 88200 source bits. The source bits are encoded by FEC I and III, respectively. The encoded bits are shared with FEC II as just explained. Afterwards, they are mapped into QAM-16 symbols before the OFDM modulation.

FEC I, II and III are compared with the same effective throughput (i.e. 10% packet loss). One packet is 54 Bytes[10], so 10% packet loss is equivalent to a BER of 2.3×10^{-4}. For FEC I and II, the lost packets will be retransmitted. For FEC III, fountain codes replaces the retransmission protocol. With FEC III, each burst is encoded by a LT code (with parameters $c = 0.03$, $\sigma = 0.3$) and decoded by the message-passing algorithm and Gaussian elimination together. From [40], we know that 3% overhead is required to recover the source packets successfully. To each fountain-encoded packet, a 7-bit CRC is added before the (175,255) LDPC encoder is applied. Since the effective

[10] a common used value.

code rate in our measurements is $0.5 \times 0.9 = 0.45$, we can lose around 30%[11] of the total transmitted packets in FEC III.

At present, there is no feedback channel in our testbed. No retransmission can occur, so we use the corresponding BER value for the 10% packet loss in FEC I and II. In addition, the modulation scheme is fixed to QAM-16 in our measurements. Each measurement corresponds to the fixed position of the transmitter and the receiver. It is possible that some measurements might fail in decoding. If the received data per measurement has a BER lower than 10^{-3} in FEC I and II, we assume that the measurement succeeds otherwise we assume it fails. For the case of FEC III, if the packet loss is more than 30% as expected, we assume that the measurement fails.

3.2.5 Results

In total, 56 measurements have been done. There are 6 blocks of data transmitted over each measurement: 3 blocks for FEC I and II and 3 blocks for FEC II and III. Not every measurement succeeds in decoding. With FEC III, 68% of measurements succeed which is almost the same as FEC II (i.e. 66%). FEC I only has 45% of successful measurements and performs the worst comparing to FEC II and FEC III.

As mentioned earlier, the wireless channel is time-variant even when the transmitter and the receiver are placed at the same position. So, we are going to analyze the measurements for FEC I and II and the ones for FEC II and III separately.

3.2.5.1 FEC I vs. FEC II

From Fig. 3.14, we can see that more measurements succeed in FEC II (i.e. 64%) than in FEC I (i.e. 45%). With FEC I, 11% of the measurements need high-resolution ADCs. For the case of FEC II, only 5% of the measurements require high-resolution ADCs.

The successful measurements in FEC I also succeed in FEC II. In those 45% measurements, the received data from ADC is first checked in the software whether they can be requantized by a lower resolution ADC comparing to the ADC in the testbed. If it allows, it will be requantized by a resolution adaptive ADC then decoded by FEC I and FEC II, respectively. With the minimum resolution for each case, the average BER is 3.07×10^{-4} for FEC I and 1.24×10^{-4} for FEC II.

Fig. 3.15 shows that FEC I and II have different requirement for the minimum resolution of ADCs. In those 45% measurements, FEC II does not require high-

[11] $30\% \approx 1 - \frac{R}{R_1 \times R_2}$, where R is the effective code rate (i.e. 0.45), R_1 is the code rate of LT codes (i.e. $\frac{1}{1.03} \approx 0.97$) and R_2 is the code rate of the (175,255) LDPC code with 7-bit CRC (i.e. $\frac{168}{255} \approx 0.66$)

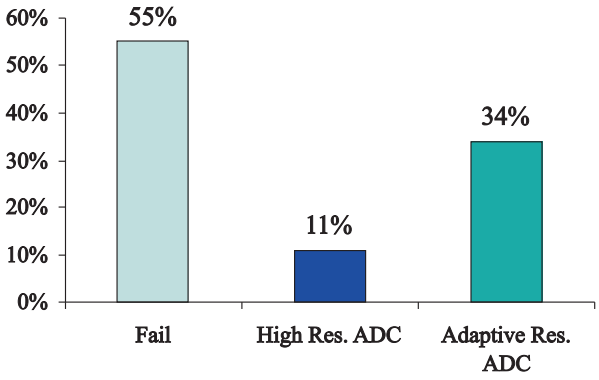

(a) FEC I

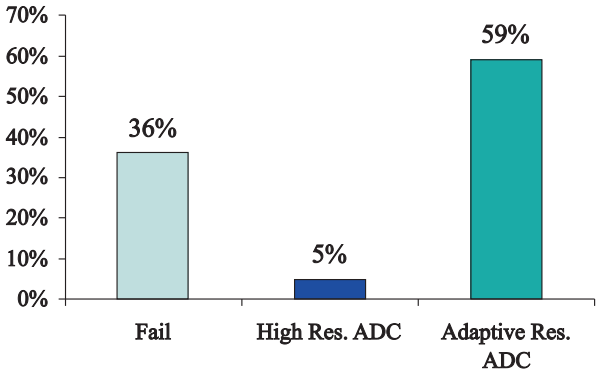

(b) FEC II

Fig. 3.14: Statistical analysis of the measurement data for FEC I (top) and FEC II (bottom). By using FEC I, 55% of measurements are failed, 11% of measurements require high-resolution ADCs and 34% of measurements can use resolution adaptive ADCs. For the case of FEC II, 36% of measurements are failed, 5% of measurements need high-resolution ADCs and 59% of measurements can use resolution adaptive ADCs.

resolution ADCs which are needed by FEC I. For a CMOS-integrated ADC, the power consumption scales linearly with the number of quantization levels [11]. On average, FEC I demands 1004 quantization levels but FEC II only needs 17 levels. Correspondingly, the power consumption in ADCs by using FEC I is around 59 times of that by using FEC II.

3.2.5.2 FEC II vs. FEC III

Fig. 3.16 is the statistical analysis of the measurement data shared by FEC II and III. From this figure, we can see that FEC III has slightly more successful measurements

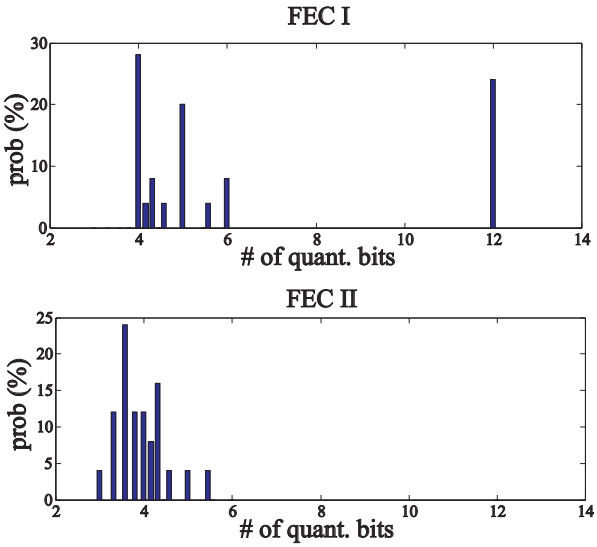

Fig. 3.15: Comparison in the number of quantization bits between FEC I (top) and FEC II (bottom). Both FEC schemes succeed in 45% of measurements. In those measurements, high-resolution ADCs are only required by FEC I.

(i.e. 68%) comparing to FEC II (i.e. 66%). In addition, the measurement data tells that high resolution ADCs are not necessary for FEC III once the measurement succeeds. However, it does not happen to FEC II. Around 25% of the successful measurements requires high-resolution ADCs (i.e. 12-bit ADC) by using FEC II.

Both FEC schemes only succeed in around 57% of the measurements. For those 57% successful measurements, the received digital data is first checked whether they can be requantized by a lower resolution ADC comparing to the one in the testbed. If possible, the received data will go through resolution adaptive ADCs in the C++ simulation and the lowest number of quantization bits will be found for each measurement data. With the minimum resolution for each scenario, FEC II has an average BER of 2.4×10^{-4} and FEC III is error free.

Fig. 3.17 shows the required number of quantization bits for FEC II and III in those 57% successful measurements. Around 12.5% of those successful measurements, high-resolution ADCs are needed in FEC II. The average number of quantization levels for FEC III is around 3.8% (i.e. 20 levels) of the case for FEC II (i.e. 528 levels). In other words, using FEC II consumes 26 times of power in ADCs comparing to FEC III.

From the measurement results, we find that FEC III works better than FEC II, especially in a channel with deep fading (i.e. the dynamic range of the channel is larger than 10 dB). The measurement results show that FEC II either needs high-resolution ADCs or fails in the channel with deep fading. Although FEC III might also fail in those deep fading channels, the measurement data shows that it performs

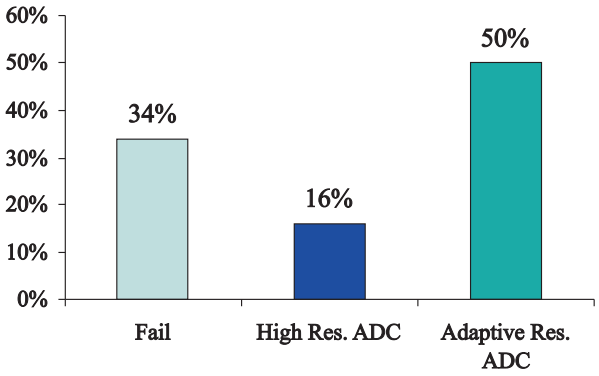

(a) FEC II

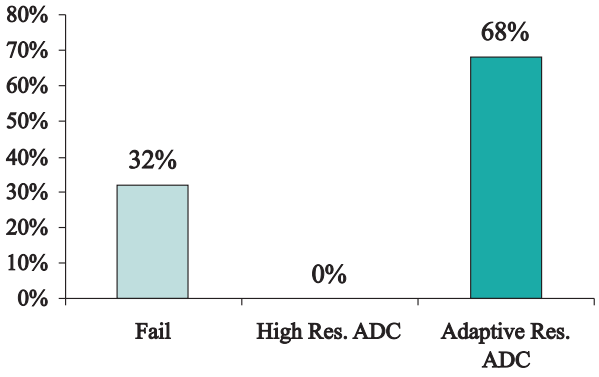

(b) FEC III

Fig. 3.16: Statistical analysis of the measurement data for FEC II (top) and FEC III (bottom). By using FEC II, 34% of measurements are failed, 16% of measurements require high-resolution ADCs and 50% of measurements can use resolution adaptive ADCs. For the case of FEC III, 32% of measurements are failed, no measurements need high-resolution ADCs and 68% of measurements can use resolution adaptive ADCs.

more efficient than FEC II.

Let us take one measurement as an example. In this measurement, both FEC II and III fail. Fig. 3.18 shows the estimated channel information of this measurement. As we can see, it has a dynamic range of more than 40 dB. With FEC II, around 89% of the encoded packets can not be decoded. With FEC III, about 65% of fountain-encoded packets are lost during the transmission. As mentioned earlier, we only allow 30% of fountain-encoded packets to be lost in order to recover the source data by fountain codes. So, FEC III also fails.

However, if we want to have reliable communication in such a channel without changing the mapping scheme and the code rate, we can retransmit the lost packets for FEC II and transmit more fountain-encoded packets to the receiver for the case of

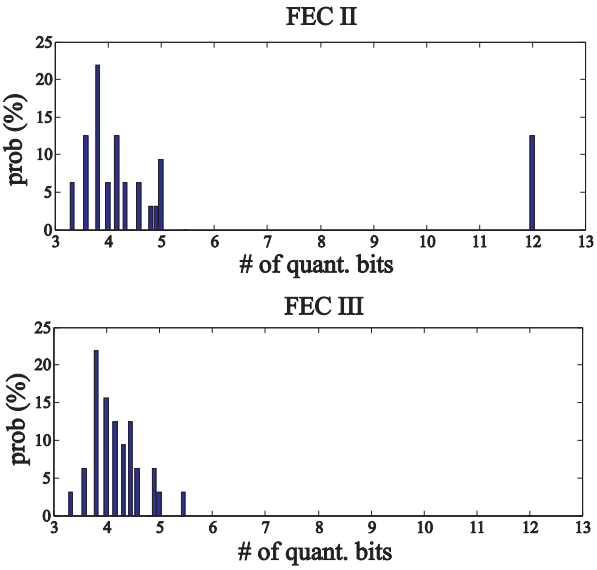

Fig. 3.17: Comparison in the number of quantization bits between FEC II (top) and FEC III (bottom). Both FEC schemes succeed in 57% of measurements. In those measurements, high-resolution ADCs are only required by FEC II.

FEC III once the required feedback channel is implemented. In such case, around 9 blocks of data need to be transmitted by using FEC II in order to receive 1 block of data correctly, but with FEC III only 2 blocks of fountain-encoded packets should be sent.

In addition, a packet encoded by FEC II is transmitted over all the sub-carriers. It can not be predicted whether the received packet is decodable with the estimated channel knowledge. So, all the received packets should be processed. However, it is not the case in FEC III. By using FEC III, each fountain-encoded packet is transmitted over one sub-carrier. Each sub-carrier can be modeled as a flat fading channel [40]. For the used LDPC code to convert the wireless channel into an erasure channel, it has a BER of 10^{-5} or lower when SNR $\geq$ 12dB. From Fig. 3.18(b), we can see that around $\frac{2}{3}$ data sub-carriers have SNR lower than 12 dB. That explains why we lose around 65% fountain-encoded packets during the transmission. Also, it means that we can discard the fountain-encoded packets whose SNR is lower than the threshold. Therefore, FEC III consumes less processing power than FEC II.

3.2.6 Conclusions

In this paper, we have compared the FEC layer from the IEEE 802.11a standard (i.e. FEC I) and the FEC layer from the IEEE 802.11n standard (i.e. FEC II) with

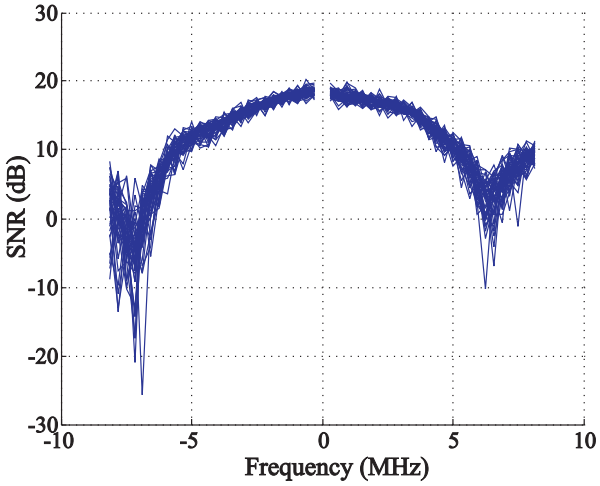

(a) The 48 estimated baseband channels

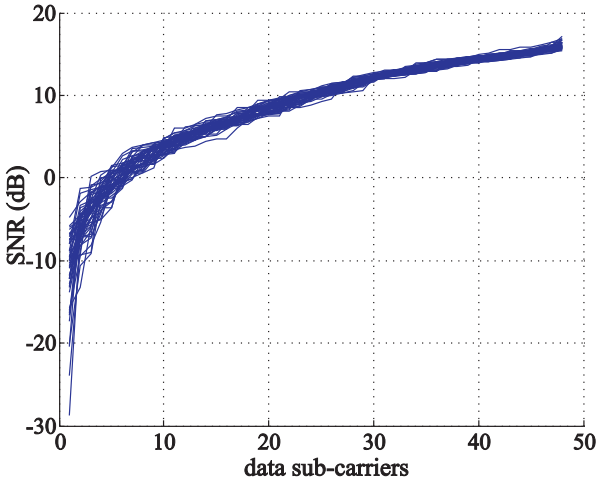

(b) The 48 data sub-carriers sorted by their energy

Fig. 3.18: The estimated baseband channels of a measurement, which is an example that FEC III performs more efficient than FEC II in the channel with deep fading. The channel is estimated every 64 OFDM symbols. One measurement consists of 3 blocks of data and each block consists of 1024 OFDM symbols. So, there are 48 estimated channels in one measurement. No data is transmitted at the DC frequency.

the opportunistic error correction scheme (i.e. FEC III) in the practical OFDM-based system. The real wireless channel is time-variant, so FEC I and II share the same channel bits to be compared in the same channel condition. Same for FEC II and FEC III. In 56 measurements, FEC III has the most successful measurements comparing to FEC I and II. Among those successful measurements, the received data is requantized by resolution adaptive ADCs. Measurement results show that FEC I consumes around 59 times of the amount of power in ADCs comparing to FEC II, whose power consumption in ADCs is around 26 times of FEC III. In addition, FEC III performs more efficiently than FEC II in the channel with deep fading. With FEC III, the receiver only needs to process the packet from the high-energy sub-carrier. Correspondingly, the processing power can be decreased which can not be achieved by using FEC I and II.

Chapter 4

Energy Efficient Error Correction for OFDM-based Broadcasting Systems

4.1 Energy Efficient Error Correction in Mobile TV

[1]**Abstract** The current error correction layer of digital mobile TV is designed for worst case scenarios, which often do not apply. In this paper, we propose a new opportunistic error correction layer based on fountain codes and a resolution adaptive ADC, which has been integrated into the OFDM-based physical layer. The key element in the new proposed system is that only packets are processed by the receiver which have encountered high-energy channels. Others are discarded. With this new approach, around 84% of the energy consumption in ADCs can be saved compared with the conventional mobile TV system under the same channel conditions.

[1]This section is the published paper [56]: *X. Shao, R. Schiphorst and C.H. Slump, "Energy Efficient Error Correction in Mobile TV", in Proceedings of IEEE International Conference on Communications (ICC), Jun 2009, Dresden, Germany.*

4.1.1 Introduction

Low power consumption in battery-powered digital mobile TV receivers is a highly desirable feature. Consumers expect their devices to operate for several hours on a single battery charge. In wireless LAN systems, the *Analog-to-Digital Converter* (ADC) can consume up to 50% of the total baseband power budget [11]. Similar numbers are expected for mobile TV systems, as both systems are based on *Orthogonal Frequency Division Multiplexing* (OFDM). In this paper, we propose a novel scheme to reduce the power consumption of the ADC by combining a resolution adaptive ADC architecture with opportunistic error correction.

The mobile wireless channel is a hostile environment. It suffers from time-varying multi-path propagation and high levels of man-made interference, such as from GSM and 3G wireless systems [19]. In effect, mobile TV channels are modeled as time-varying frequency selective channels. Because of the frequency-selective fading and the interference, the worst-case dynamic range of the received signal is very high, typically around 52 dB (TU6 channel[2]) in addition to the range needed for proper signal detection (SNR). Given a traditional fixed-resolution ADC, this high dynamic range leads to a high number of bits and therefore to high power consumption [57].

However, the worst-case conditions do not always apply. Therefore, we use a resolution adaptive ADC which selects the minimum number of bits according to the current channel. As a result, the power consumption of the ADC is reduced under most, i.e. non worst-case, channel conditions.

A further resolution reduction of the ADC can be achieved by using a novel opportunistic error correction scheme that integrates into the physical layer. This approach allows us to discard some part of the channel with deep fading. Take Figure 4.1 as an example, the dynamic range of the whole channel is around 13.5 dB. From this figure, we can see that the deep fading does not happen everywhere and only happens in the frequency band of -4∼-3 MHz and 2∼3 MHz. By discarding this 2 MHz sub band, the dynamic range of the channel is reduced to 10.7 dB.

The current mobile TV standards do not support this idea, as all sub bands are considered equally important by the *Forward Error Correction* layer (FEC). Therefore, we propose a novel FEC layer based on fountain codes that does not have this disadvantage. In [21], MacKay describes the encoder of a fountain code as a metaphorical fountain that produces a stream of encoded packets. Anyone who wishes to receive the encoded file holds a bucket under the fountain and collects enough packets to recover the original data. It does not matter which packets are received, only a minimum amount of packets have to be received correctly [21]. In other words, fountain-encoded packets are independent with respect to each other.

To apply fountain codes in mobile TV, we divide a block of source bits into a set of packets, which are encoded by a fountain code. A fountain-encoded packet is transmitted over a sub band of the channel. Thus, multiple packets are transmitted simultaneously, using frequency division multiplexing. The receiver discards fountain-encoded

[2]TU6 channel: the Typical Urban 6-path channel model.

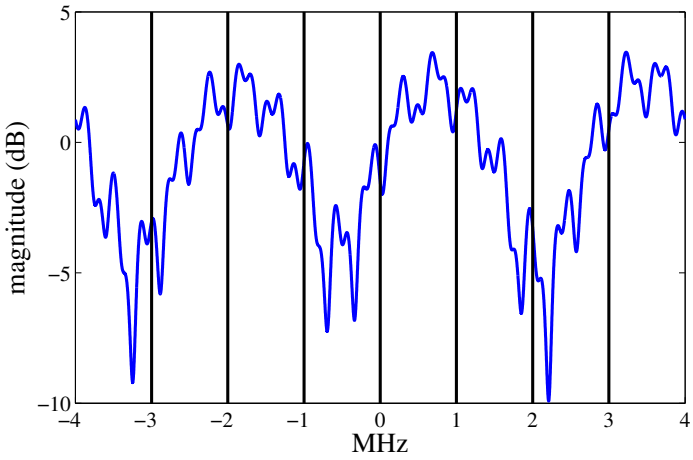

Fig. 4.1: Example of the baseband transfer function of a TU6 channel.

packets which are transmitted over the sub band with deep fading. Correspondingly, the power consumption in ADCs decreases.

In this paper, we propose an approach based on resolution adaptive ADCs and fountain codes to reduce the power consumption in ADCs. The proposed method is an opportunistic error correction layer because it does not process all received packets but only processes surviving packets. This error correction layer is able to cope with discarding packets because fountain-encoded packets are independent of each other. Also, less power is consumed as the resolution of ADC is adapted to the minimum for each case, compared to using the fixed-resolution ADC. Thus, it is a novel cross-layer approach which integrates the error correction into the physical layer of an OFDM system.

The outline of this paper is as follows. Fountain codes and a resolution adaptive ADC are applied to lower the power consumption in mobile TV receivers. First, fountain codes are discussed which is followed by the resolution adaptive ADC. In section 4.1.4, a description is given of the DVB-H system, which is a practical example of mobile TV. We compare the current DVB-H system with our proposed system in the simulation. Finally, the simulation results are analyzed. The paper ends with a discussion of the results.

4.1.2 Fountain Codes

In this paper, we use a kind of fountain codes, i.e. *Luby Transform* (LT) codes [43] in the proposed error correction layer. Other fountain codes (e.g. Raptor codes [44]) can also be applied.

Consider a block of size K packets $s_1, s_2, \cdots, s_K$ to be encoded by a fountain code. A packet has m bits and considered a unit. At each clock cycle, labeled by n, one fountain-encoded packet is generated by selecting a set of source packets randomly and computing the bitwise sum (XOR) of these source packets [21]. The fountain codes can supply an unlimited number of encoded packets based on $s_1, s_2, \cdots, s_K$. In practical systems, only a fixed number of packet N is generated.

At the receiver side, enough packets are required for successful decoding. The required number of received packets N is slightly larger than the number of source packets K and is defined as:

$$N = K(1 + \varepsilon) \tag{4.1}$$

where ε is the percentage of extra packets and is called the overhead.

After receiving N packets, the receiver can recover the source packets by the *message-passing* algorithm [54] which has a linear decoding cost. We have shown that decoding the fountain codes using the message-passing algorithm combined with Gaussian elimination allows small block sizes, e.g. $K = 500$, with small overhead $\varepsilon = 3\%$ in [58]. Small block sizes are needed to keep the decoding delay low, which is important in real-time applications such as mobile TV.

Fountain codes are designed for *Erasure Channels*. However, wireless channels are noisy channels, not erasure channels. In practical systems, fountain codes are used in combination with other error correction algorithms to convert the noisy channels into erasure channels, often *Low-Density Parity-Check* (LDPC) codes [54]. In this paper, LDPC codes are used together with a *Cyclic Redundancy Check* (CRC) to make the wireless channel behave like an erasure channel.

Our FEC encoding scheme is performed in the following order. First, a fountain-encoded packet is created. Then, the CRC is added. Finally, the packet is encoded by the LDPC code.

At the receiver, each fountain-encoded packet is first LDPC decoded if its energy is above or equal to a threshold (i.e. corresponding to BER $\leq 10^{-5}$). The received packet is discarded if its energy is below the threshold. If the LDPC decoding fails, the received packet is discarded as well. If the LDPC decoding succeeds, the CRC is used to identify any errors undetected by the LDPC codes. If the CRC decoder detects an error, the receiver assumes that the whole packet has been lost. Once the receiver gets N surviving fountain-encoded packets, it starts to recover the source data.

4.1.3 Resolution Adaptive ADC

In [59], the authors have designed an resolution adaptive ADC for IEEE 802.11a WLAN system and shown that adaptive resolution ADCs can save 38% power consumption in ADCs comparing with conventional high-resolution ADCs. For WLAN

receivers, ADC power consumption can be almost 50% of the total baseband power consumption [11]. For a mobile TV receiver, we expect that similar values. An CMOS implementation of such an ADC is described in [57]. In this implementation, the power consumption scales linearly with the number of quantization levels.

4.1.3.1 Minimum Number of Quantization Levels

The mobile TV channel is often modeled as a time-varying frequency selective channel. The TU6 channel model is representative for the typical mobile reception with the Doppler frequency above 10 Hz [19].

In OFDM receivers, demodulation of the sub carriers is performed in the frequency domain. For that reason, it is not beforehand clear, how many ADC bits are necessary for proper decoding. In [59], the authors have derived an relation between the quantization noise in the time domain and the frequency domain for frequency selective channels. Here, we briefly explain it following [59].

We assume that the channel is noiseless and the channel of one OFDM symbol is constant, so the channel output at the n^{th} moment r_n is defined as:

$$r_n = \sum_{l=0}^{L-1} h_l x_{n-l} \tag{4.2}$$

where L is the number of channel taps, h_l the channel taps and x the transmitted signal. We assume that the quantization noise is dominant, so other noise (e.g. thermal noise) is ignored in this paper. In [59], it has shown that r_n is Gaussian-distributed with a zero mean and a variance of $\sum_l |h_l|^2$.

The ADC output y_n is expressed by:

$$y_n = \mathcal{Q}(r_n) = \sum_l h_l x_{n-l} + n_n \tag{4.3}$$

where n_n is the quantization noise in the time domain. Because the quantization noise n_n depends on the signal r_n and the probability density function of r_n is symmetric to 0, n_n is uniform distributed with zero mean and a variance of $\frac{\Delta^2}{6}$, where Δ is the uniform quantization step [18].

After the OFDM demodulation, we have Y_k as [2]:

$$Y_k = H_k X_k + N_k \tag{4.4}$$

where N_k is the quantization noise in the frequency domain defined by [59]:

$$N_k = \frac{1}{\sqrt{\mathrm{N}}} \sum_n n_n e^{-j\frac{2\pi}{\mathrm{N}}nk} \tag{4.5}$$

and H_k is the fading over the k^{th} sub carrier defined by:

$$H_k = \sum_l h_l e^{-j\frac{2\pi}{\mathrm{N}}lk} \tag{4.6}$$

N_k is a Gaussian-distributed random variable with zero mean and a variance of $\frac{\Delta^2}{6}$ according to the *Central Limit Theorem* [59]. Thus, for each sub carrier, the variance of the quantization noise is the same, but the Signal-to-(quantization)-Noise Ratio (SNR) is different due to different fading:

$$\mathrm{SNR}_k = \frac{|H_k|^2}{\frac{\Delta^2}{6}} \tag{4.7}$$

If the clipping is allowed, the number of quantization levels N_q is determined by [18]:

$$N_q = 2\lceil \frac{\mathrm{C}}{\Delta} \rceil \tag{4.8}$$

where C is equal to $3\sigma_{r_n}$. Once the channel is fixed, N_q is only determined by Δ. In such case, Δ depends not only on the applied error correction codes in the system (i.e. SNR defined in Equation 4.7), but also on how the fountain-encoded packets are transmitted.

4.1.3.2 Transmission Scheme

In [59], the authors have shown that each fountain-encoded packet is transmitted over one sub carrier and the dynamic range of ADCs can be reduced by discarding the low-energy sub carriers for each channel realization. In the 802.11a WLAN system, the channel can be considered to be time-invariant over a MAC frame. In [59], the transmission of each fountain-encoded packet is finished within a MAC frame. Hence, the channel over one fountain-encoded packet transmission can be considered as a time-invariant flat fading channel. However, this does not apply in the mobile TV

system.

The mobile TV transmission system (e.g. DVB-H) should offer sufficient flexibility and scalability to allow the reception of the services at various speeds while optimizing transmission coverage [19]. In this paper, we focus on the 8k transmission mode which has a large area of the *Single-Frequency Network* (SFN) and maximum frequency efficiency [20]. Also, the 8k mode is more sensitive to the Doppler spread comparing to other transmission modes. In order to avoid the effects of the Doppler spread in adjusting resolution adaptive ADCs, we propose to transmit each fountain-encoded packet over a set of adjacent sub carriers. We denote such a set of sub carriers a *sub band*. In such case, the 8k sub carriers can be divided into a number of sub bands. Over each sub band, one fountain-encoded packet is transmitted. The energy of each sub band is equal to the lowest energy of the sub carrier in its sub band.

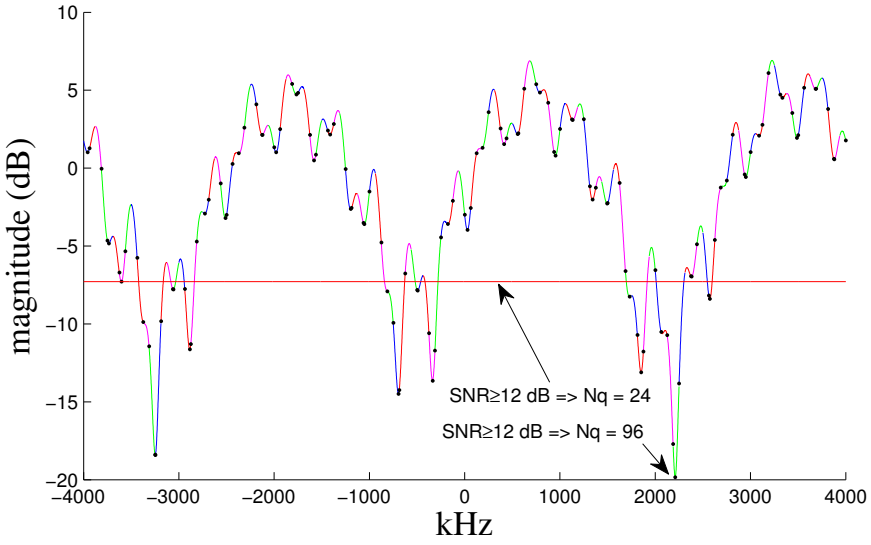

Fig. 4.2: An example of dividing TU6 channel into 128 sub bands. The black point is the sub carrier with the lowest energy every sub band, which defines the energy of its corresponding sub band.

Since each fountain-encoded packet is independent, it does not matter that we discard some packets which are transmitted over low-energy sub bands. For example, assume that the SNR of the high-energy sub band should be at least equal to 12 dB and fountain-encoded packets are transmitted over a wireless channel as shown in Figure 4.2. We discard low-energy sub bands and keep high-energy sub bands. We denote the number of low-energy sub bands as N_b. If we keep all sub bands (i.e. $N_b = 0$) in Figure 4.2, the required number of quantization levels N_q is 96; but if we discard 30 sub bands (i.e. $N_b = 30$), the required N_q can be reduced to 24.

4.1.3.3 Power Consumption

The power consumption of the ADC is proportional to the number of quantization levels N_q which is related to the *Effective Number Of Bits* (ENOB) by:

$$N_q = 2^{\mathrm{ENOB}} \tag{4.9}$$

Hence, N_q is a measurement of the power consumption P:

$$P = \sum_{i=0}^{M_c-1} \alpha_i N_{q_i} \mathcal{M} \tag{4.10}$$

where M_c is the number of OFDM symbols, α_i is the percentage of the i-th OFDM symbol where useful information is transmitted, N_{q_i} is the number of quantization levels used in the i-th OFDM symbol, and $\mathcal{M}$ is the number of samples per OFDM symbol.

The power consumption in ADCs can be reduced by discarding low-energy sub bands. However, discarding transmitted packets over low-energy sub bands results in an increase of the total number of transmitted packets. Therefore, there is a tradeoff in power consumption between the number of low-energy sub bands and the total number of transmitted packets.

So far, we design the quantization scheme for each OFDM symbol according to the current channel knowledge. However, in a practical mobile TV system (e.g. DVB-H), pilot symbols are only located in the scattered sub carriers, which means that the pilot data and user data are transmitted in the same OFDM symbol at the same time. In other words, it is impossible to adjust the resolution of ADCs to the minimum according to the current channel knowledge. Therefore, we have to use the channel knowledge of the previous OFDM symbol to adjust the resolution of ADCs for quantizing the current OFDM symbol, which will of course negatively affect the design of quantization scheme. We will discuss this influence in the next section.

4.1.4 System Model

The opportunistic error correction layer is based on fountain codes and resolution adaptive ADCs which have explained in the above sections. This proposed cross layer can be applied in mobile TV systems. In this paper, the DVB-H system is taken as an example of mobile TV systems.

The FEC layer in the current DVB-H system is based on *Reed Solomon* (RS) codes and *Rate Compatible Punctured Codes* (RCPC). These codes have a good performance

for random bit errors. Interleaver is employed to remove burst errors. Although this solution works well in practical systems, it is not optimal. First, because packets that have encountered a low-energy channel are still processed by the decoders. It will waste processing power. In addition, the error correction layer is based on worst case scenarios. This means that for most packets, the code rate and hence capacity can be increased. Furthermore, the resolution of the applied ADCs is fixed for DVB-H receivers, which is designed for worse case conditions. However, worse case conditions do not happen often.

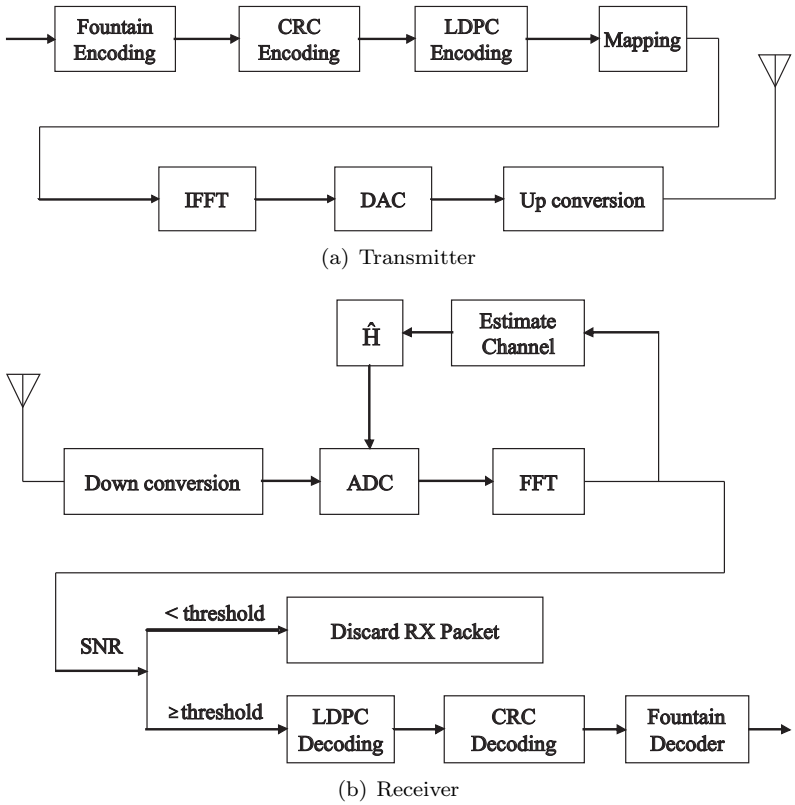

Fig. 4.3: Proposed DVB-H transmitter (top) and receiver (bottom).

In Figure 4.3, the proposed new error correction scheme is depicted to reduce the power consumption in ADCs. The key idea is to generate additional packets by the fountain encoder. First, the source packets are encoded by the fountain encoder. Then, a CRC checksum is added to each fountain-encoded packet and LDPC encoding is applied. On each sub band, a fountain-encoded packet is transmitted. Thus, multiple packets are transmitted simultaneously, using frequency division multiplexing.

At the receiver side, we assume that the synchronization and channel estimation are

perfect. With the perfect channel knowledge, the resolution of the adaptive ADCs can be reduced to the minimum for each channel realization. If the SNR of the sub band is equal to or above the threshold, the received fountain-encoded packet will go through LDPC decoding, otherwise it will be discarded. This means that the receiver is allowed to discard low-energy sub bands (i.e. packets) to lower the dynamic range of the ADC and hence the power consumption. After the LDPC decoding, the CRC checksum is used to discard the erroneous packets. As only packets with a high SNR are processed by the receiver, this will not happen often. When the receiver collects enough fountain-encoded packets, it starts to recover the source data.

In Figure 4.4, the relation is depicted between the average power consumption (dynamic range) of ADCs and the number of low-energy sub bands N_b, under the condition that the resolution of ADCs is adjusted according to the current channel knowledge. In each case, 1000 fountain-encoded packets are received and the low-energy sub bands are discarded. The number of the transmitted fountain-encoded packets is defined as $1000 \times \frac{\mathrm{N_a}}{\mathrm{N_a - N_b}}$, where $\mathrm{N_a}$ is the total number of active sub bands. When 41 sub bands are discarded, the minimum power consumption is achieved.

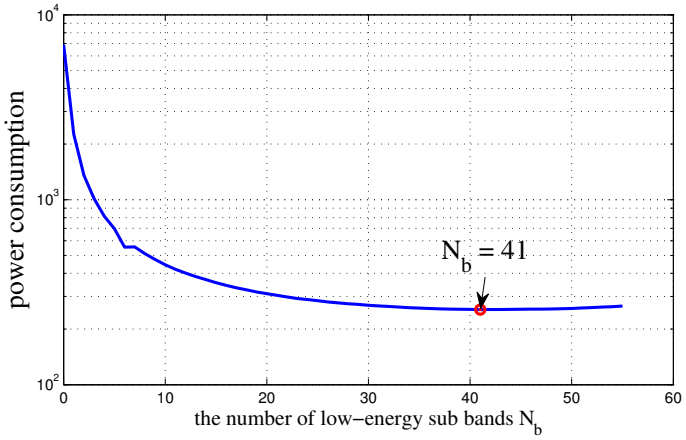

Fig. 4.4: The average power consumption versus the number of low-energy sub bands for receiving a burst of fountain-encoded packets. 64 sub carriers are grouped into a sub band and the total number of active sub bands is 106.

As mentioned in Section 4.1.3, it is impossible to adjust the resolution of ADCs according to the current channel knowledge. In order to apply the resolution adaptive ADCs in the DVB-H receiver, we propose to use the channel knowledge of the previous OFDM symbol to adjust the resolution of ADCs for the current OFDM symbol. In such case, we still achieve the lowest power consumption when we discard 41 sub bands. However, the actual number of lost sub bands might not be as same as we expected and this needs more analysis.

We assume that the channel is perfectly estimated and N_b sub bands are lost. We denote each sub band of the n^{th} OFDM symbol by H_{k_n} and we sort the sub band by

the energy, so we have:

$$|H_{(k+1)_n}| > |H_{k_n}| \tag{4.11}$$

Suppose that the fountain-encoded packet can be decoded correctly when SNR $\geq$ 12 dB. We design the quantization scheme for the $(n+1)^{th}$ OFDM symbol by making the $(N_b+1)^{th}$ sub band of the n^{th} OFDM symbol have a SNR of 12 dB, so we have:

$$\Delta = \sqrt{6\frac{|H_{(N_b+1)_n}|^2}{10^{1.2}}} \tag{4.12}$$

The SNR of the $(N_b+1)^{th}$ sub band in the $(n+1)^{th}$ OFDM symbol is defined by:

$$\begin{aligned} \mathrm{SNR}_{(N_b+1)_{(n+1)}} &= \frac{|H_{(N_b+1)_{(n+1)}}|^2}{\frac{\Delta^2}{6}} \\ &= 12 + 20\log_{10}\frac{|H_{(N_b+1)_{(n+1)}}|}{|H_{(N_b+1)_n}|} \end{aligned} \tag{4.13}$$

If $|H_{(N_b+1)_{(n+1)}}| \geq |H_{(N_b+1)_n}|$, $\mathrm{SNR}_{(N_b+1)_{(n+1)}} \geq 12$ dB; otherwise $\mathrm{SNR}_{(N_b+1)_{(n+1)}} <$ 12 dB. The difference between $|H_{(N_b+1)_{(n+1)}}|$ and $|H_{(N_b+1)_n}|$ determines whether the actual number of lost sub bands will be more than or less than or equal to N_b sub bands.

$\frac{|H_{(N_b+1)_{(n+1)}}|}{|H_{(N_b+1)_n}|}$ depends on the predefined number of low-energy sub bands N_b and the Doppler spread, as shown in Figure 4.5. From this figure, we can see that the gap is inversely proportional to N_b but proportional to the Doppler spread. For the case of $N_b = 0$, the range of $\frac{|H_{(N_b+1)_{(n+1)}}|}{|H_{(N_b+1)_n}|}$ is within $\pm$27 dB at the probability of 95% for 120 Hz Doppler spread and at 97.5% for 20 Hz Doppler spread; but when $N_b = 30$, the range can be reduced to $\pm$2.7 dB at 95% for 120 Hz and at 98% for 20 Hz Doppler spread. So, it is beneficial to discard more sub bands.

Due to the lack of a feedback channel, there is no chance to recover the fountain source packets if we lose more sub bands than we anticipated. To make sure that receivers get enough fountain-encoded packets, we can increase the designed resolution of ADC by a certain number of bits to compensate for the gap between $|H_{(N_b+1)_{(n+1)}}|$ and $|H_{(N_b+1)_n}|$. In such case, we should give 4.5 bits extra for $N_b = 0$ and only 0.45 bit extra for $N_b = 30$ to recover the source packets at least with the probability of 97.5%.

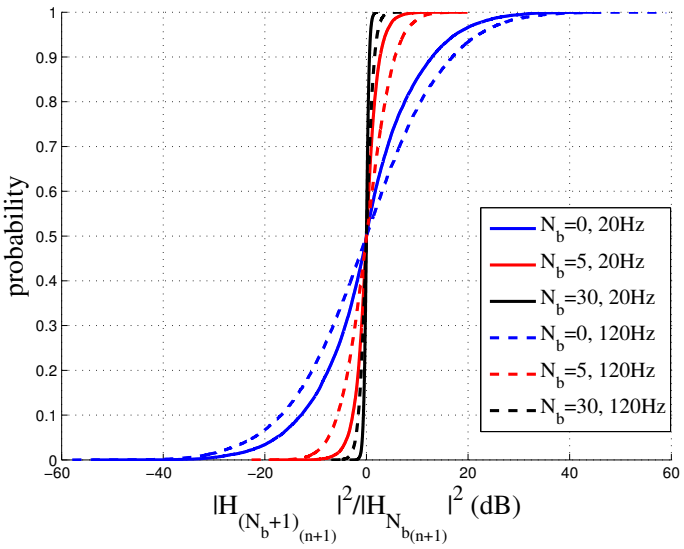

Fig. 4.5: The probability of $\frac{|H_{(N_b+1)(n+1)}|}{|H_{(N_b+1)n}|}$ for different N_b and different Doppler shift. Those probability curves are based on 2×10^4 TU6 channels with 20 Hz and 120 Hz Doppler shift.

4.1.5 Performance Analysis

In this section, we analyze the performance of our proposed opportunistic error correction layer. In the simulation, we transmit 1000 blocks of source packets to 1000 receivers over a TU6 channel with 120 Hz Doppler shift. Each block consists of 500 source packets with a length of 168 bits.

We compare two scenarios in the simulation. The first scenario, Scenario I, is a conventional DVB-H system with 16-QAM modulation and code rate $2/3 \times 3/4 = 1/2$ [20]. We allow that 1%[3] receivers have packet loss and the other ones will receive the packets correctly. Moreover, we assume that the conventional fixed-resolution ADCs are used.

In Scenario II, we apply the new opportunistic error correction layer, which has the same effective throughput as Scenario I. Each burst is encoded by a LT code (with parameters $c = 0.03$, $\sigma = 0.3$) and decoded by the message-passing algorithm and Gaussian elimination together. From [58], we know that 3% overhead is required to recover the source packets successfully. To each fountain-encoded packet, a 7-bit CRC is added then the (255,175) LDPC encoder is applied. Under the condition of the same effective throughput, we can lose 23 sub bands where the power consumption is closed to the minimum case with 41 lost sub bands as shown in Figure 4.4. For the resolution adaptive ADC, we use the perfect channel knowledge of the previous

[3]A common value used in coverage tools

	Scenario I	**Scenario II**
ADC	uniform	res. adapt.
FEC	RS+RCPC	LDPC + Fount. codes
Code rate	0.5	0.64
Modulation	16-QAM	16-QAM
N_c	6784	6784
N_s	106	106
SNR in freq. domain	9.0 dB	16.0 dB
N_b	0	23

Table 4.1: System setup comparison for two scenarios (N_c - the number of data carriers, N_s - the number of sub bands and N_b - the number of low-energy sub bands)

OFDM symbol to adjust the resolution of ADCs for the current OFDM symbol. In order to achieve the expected number of fountain-encoded packets (i.e. $N = 515$) with the probability of at least 99%, we will give some extra bits (i.e. 4 dB extra SNR).

In our simulations, we have used the parameters in Table 4.1 to compare the conventional and the proposed system. The "SNR in frequency domain" is the minimal SNR for all sub bands in Scenario I and the minimal SNR for all high-energy sub bands in Scenario II.

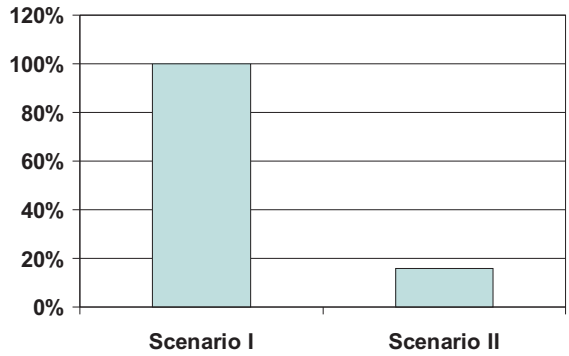

Fig. 4.6: Power consumption comparison between two Scenarios. The power consumption in ADCs of Scenario I is normalized to 100%.

Figure 4.6 shows the average power consumption in ADCs for the transmission of each block. We normalize the power consumption of Scenario I to 100%. From this figure, we can see that the power consumed in Scenario II is reduced to 16% in comparison with Scenario I.

In order to let the number of lost sub bands not be more than we expected (i.e. $N_b = 23$), we give 4 dB extra SNR to adjust the resolution of ADCs in Scenario II.

During the transmission of 1000 bursts, each receiver loses on average 1.1 sub bands and at maximum 13 sub bands every OFDM symbol, which means every receiver can recover the source packets correctly. So our system has a higher QoS at a lower power consumption compared to the conventional system where typically 1% of the receivers can not decode the mobile TV stream.

4.1.6 Conclusions

In this paper, we propose a novel cross-layer scheme which integrates the error correction into the physical layer. This new opportunistic error correction layer is especially designed for mobile TV (e.g. DVB-H) and broadcasting applications. It is based on fountain codes and resolution adaptive ADCs. Each fountain-encoded packet is transmitted over a sub band which consists of a set of sub carriers. By discarding fountain-encoded packets that have been transmitted over low-energy sub bands, the dynamic range of ADCs can be reduced. Correspondingly, the power consumption in ADCs can be decreased. The new cross-layer method results in up to 84% lower power consumption of the ADCs compared to the current standard. Moreover, it has higher coverage than the current standard.

4.2 Opportunistic Error Correction for OFDM-based DVB Systems

[4]**Abstract** DVB-T2 (second generation terrestrial digital video broadcasting) employs LDPC (Low Density Parity Check) codes combined with BCH (Bose-Chaudhuri-Hocquengham) codes, which has a better performance in comparison to convolutional and Reed-Solomon codes used in other OFDM-based DVB systems. However, the current FEC layer in the DVB-T2 standard is still not optimal. In this paper, we propose a novel error correction scheme based on fountain codes for OFDM-based DVB systems. The key element in this new scheme is that only packets are processed by the receiver which have encountered high-energy channels. Others are discarded. To achieve a data rate of 9.5 Mbits/s, this new approach has a SNR gain of at least 10 dB with perfect channel knowledge and 11 dB with non-perfect channel knowledge in comparison to the current FEC layer in the DVB-T2 standard. With a low-complexity interpolation-based channel estimation algorithm, opportunistic error correction offers us a QEF (Quasi Error Free) quality with a maximum DF (Doppler Frequency)

[4]This section is the submitted paper [60]: *X. Shao, C.H. Slump, "Opportunistic Error Correction for OFDM-based DVB Systems", submitted to IEEE Transactions on Broadcasting, 2010.*

of 40 Hz but the current DVB-T2 FEC layer can only provide a BER of 10^{-7} quality after BCH decoding with a maximum DF of 20 Hz.

4.2.1 Introduction

Orthogonal Frequency Division Multiplexing (OFDM) [61] [16] [15] has recently been proposed as modulation technology for current *Digital Video Broadcasting* (DVB) standards (e.g. DVB-T [20], DVB-T2 [22], DVB-H [62], etc) [63]. Although OFDM enables a rather straightforward implementation of a wireless receiver, it can not mitigate the effects of noise and interference encountered in the transmission of the signal through the wireless channel [64] [2]. Therefore, error correction codes are required to achieve reliable communications [28].

For a finite block length of data to be transmitted over a frequency selective channel, coding jointly over the sub-carriers yields a smaller error probability than can be achieved by coding separately over the sub-carriers at the same rate [2]. This theory has been applied in practical OFDM-based wireless systems (e.g. IEEE 802.11 a/n [17] [23], DVB-T, DVB-T2, etc). Let us take the DVB-T2 system as an example, source bits are encoded by *Low Density Parity Check* (LDPC) codes [65] [66] [67] together with *Bose-Chaudhuri-Hocquengham* (BCH) codes [68] [22]. An encoded packet is transmitted over all the sub-carriers like other DVB systems [62] [20] [22]. With the joint coding scheme [2], however, it is not beforehand known whether the received packet is decodable or not due to the frequency selective characteristics of the wireless channel. In such a case, the receiver tries to decode all the packets, also the ones that can not be decoded successfully. This may lead to a waste of processing power. Furthermore, the sub-band with the deepest fading, limits the level of the noise floor that can be endured by the system, as each part of the channel is considered to be equally important in the joint coding scheme. Therefore, we propose a novel error correction layer based on fountain codes for OFDM-based DVB systems that does not have this disadvantage.

In [21], MacKay describes the encoder of a fountain coder as a metaphorical fountain that produces an unlimited number of encoded packets. Anyone who wishes to receive the source file holds a bucket under the fountain and collects enough packets. The original file can be reconstructed from the received packets. It does not matter which packet is received. The only requirement is to receive a certain number of packets [69]. In other words, fountain-encoded packets are independent to one another. This inspires us to reduce the *Signal-to-Noise Ratio* (SNR) requirement of the system by discarding some frequency bands of the wireless channel with deep fading. To achieve this, we encode a fountain-encoded packet with error correction codes at a relatively higher code rate and transmit it over a sub-band. By discarding some packets transmitted over the sub-bands with low energy, the noise floor can be increased and is not limited any more by the sub-band with the lowest energy.

For WLAN systems, a fountain-encoded packet can be transmitted over a single sub-

carrier [70]. Multiple packets are transmitted simultaneously using frequency division multiplexing. With this method, the receiver does not have to decode all the packets but only process the well-received packets whose SNR is higher than a threshold (i.e. corresponding to BER $< 10^{-5}$ after decoding). The fountain decoder can recover the original file by only using the surviving packets. In such a case, the processing power can be reduced with respect to the traditional joint coding scheme. In addition, this method not only saves the processing power but also gives better performance comparing to the FEC layer used in the current WLAN system. With the same effective throughput (i.e. 21.6 Mbits/s), this new method offers us a SNR gain of 7.5 dB in comparison with the IEEE 802.11a system [70].

Unfortunately, these results can not be applied directly in any OFDM-based DVB systems. In the 802.11a WLAN system, the channel is considered to be time-invariant over a MAC frame. The transmission of each fountain-encoded packet in [70] is completed within a MAC frame. Hence, the channel over a fountain-encoded packet transmission can be considered as a time-invariant flat fading channel. However, this is not the case in the DVB system. The DVB transmission system should offer sufficient flexibility to allow the reception of the services at various velocities [19]. To avoid the effects of Doppler spread, we propose to transmit the fountain-encoded packets over a set of adjacent sub-carriers. We denote such a set of sub-carriers as a *sub-band*. The whole transmission band is divided into a number of sub-bands. Over each sub-band, one fountain-encoded packet is transmitted. The energy of each sub-band is considered equal to the lowest energy of the sub-carriers in its sub-band. If a packet is transmitted over a sub-band whose energy is higher than the threshold, it will be processed by the decoder otherwise it will be discarded. Correspondingly, the processing power is reduced assuming the power consumed in the SNR comparison is negligible.

In this paper, we propose a novel approach based on fountain codes for OFDM-based DVB systems. The main contribution of this paper is to investigate whether this new method can perform better (i.e. at a lower SNR) in DVB systems than the current FEC layer in the standard. If so, this new error correction scheme offers us a higher data rate than the current DVB systems under the same channel condition.

The outline of this paper is as follows. Opportunistic error correction is first depicted where we explain the whole idea and why we choose such a transmission scheme. In section 4.2.3, we describe the system model which shows how we apply this novel scheme in the DVB system. After that, we compare its performance with the FEC layer from the DVB-T2 system over a TU6 channel[5] [71]. The paper ends with a discussion of the conclusions.

[5]TU6 channel: the Typical Urban 6-path channel model

4.2.2 Opportunistic Error Correction

Opportunistic error correction is based on fountain codes. There are several kinds of fountain codes, e.g. *Luby Transform* (LT) codes [43], Raptor codes [44], Online codes [72]. Opportunistic error correction is compatible with any kind of fountain code.

4.2.2.1 Fountain Codes

With fountain codes, the transmitter can generate a potentially limitless supply of fountain-encoded packets. Each fountain-encoded packet is a bitwise summation (i.e. exclusive-or-ing) of a random set of source packets [21]. Not only the selection of source packets is random, but also the number of the selected source packets is random. The receiver can reconstruct the original file by collecting enough fountain-encoded packets. The number of packets required in the receiver N is slightly larger than the number of source packets K [21]:

$$N = (1 + \varepsilon)K \tag{4.14}$$

where ε is the percentage of extra packets and is called the overhead.

The mathematical principle behind fountain decoding is to solve K unknown parameters from N linear equations. It can in principle be solved by Gaussian elimination but this has a high complexity. Therefore, the message-passing algorithm [54] is usually chosen to decode fountain codes. The message-passing algorithm has a linear computation cost [21], but it requires a large ε for small block size. For example, the practical overhead of LT codes is 14% when $K = 2000$, which limits its application in the practical system [70]. By combining message-passing algorithm with Gaussian elimination, the overhead of LT codes is reduced to 3% when $K \geq 500$ [70].

With only fountain codes, we can not have opportunistic error correction for wireless systems. Fountain codes are designed for erasure channels over which the receiver either receive the packet without error or does not receive it at all. A wireless channel is not an erasure channel but a noisy fading channel, so good error correction codes should be used to make noisy channels behave like an erasure channel. Most of the time, the error correction code performs perfectly; occasionally, the decoder fails, and reports that it has failed, so the receiver knows the whole packet has been lost [21].

4.2.2.2 Transmission Schemes

Fountain codes can be applied to wireless channels, if they are combined with good error correction codes. The performance of this combination depends on how a packet

is transmitted. There are two schemes to transmit a fountain-encoded packet:

- **Scheme I** is to transmit a packet over all the sub-carrier.
- **Scheme II** is to transmit a packet over a single sub-carrier.

In the case of WLAN, the transmission scheme II is chosen. Because the WLAN system is mainly designed for the reception with Doppler frequency below 10 Hz (i.e. the pedestrian and indoor reception) [19], the system can be designed in such a way that the time needed to transmit a packet is much smaller than the coherence time. That means the channel over a fountain-encoded packet can be modeled as a flat fading channel. In this case, it is possible to predict whether the received packet is decodable using the channel knowledge (i.e. SNR). Only the well received packets are processed. Correspondingly, the processing power can be reduced. Over a finite block length, Scheme I yields a smaller *Bit Error Rate* (BER) but a larger *Packet-Error-Rate* (PER) than Scheme II [73]. Fountain codes only need enough error-free fountain-encoded packets to reconstruct the original file. Therefore, with fountain codes in the IEEE 802.11a system, Scheme II performs better (i.e. an SNR gain of 5 dB with QAM-16 modulation scheme) than Scheme I at the same code rate (i.e. $R = 0.5$) [73].

However, the DVB system is different from the WLAN system. In DVB, the receivers are moving at different velocities (corresponding to different Doppler spreads). Also, the DVB system utilizes a large number of sub-carriers ranging between 1k and 32k to have high spectrum efficiency. The higher the spectrum efficiency, the more sensitive to Doppler spread. In this paper, we focus on the 8k mode. To reduce the delay as much as possible, we make the fountain-encoded packet short such that it does not occupy the whole band-width with the transmission Scheme I. Due to Doppler spread, the channel over a packet is not a flat-fading channel regardless with Scheme I or with Scheme II. Which one to choose depends on the following:

- During the transmission of a packet, the channel should be as flat as possible.
- During the transmission of a packet, the dynamic range $\mathcal{D}$ of the channel should not be affected by the variation of Doppler spread.

Figure 4.7 shows the difference in $\mathcal{D}$ between the use of the transmission Scheme I and II. Obviously, Scheme II is more sensitive to the variation of Doppler Frequency (DF) than Scheme I. With Scheme I, around 80% of packets can be transmitted over a channel with $\mathcal{D} \leq 5$dB as DF varies from 10 to 70 Hz. With Scheme II, $\mathcal{D}$ increases with DF. When DF = 10Hz, only 10% packets can be transmitted over the channel with $\mathcal{D} \leq 5$dB; however, the percentage is decreased to around 3% for DF = 20Hz. For DF $\geq$ 30Hz, almost all the packets have to be transmitted over a channel with $\mathcal{D} > 5$dB. Therefore, we choose Scheme I to transmit a fountain-encoded packet in the DVB system.

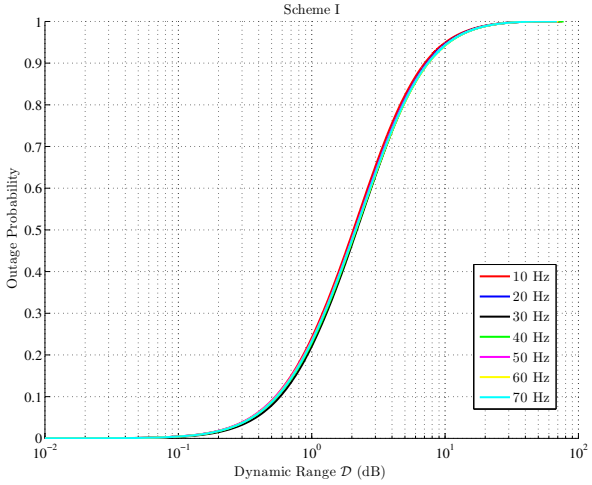

(a) Transmission Scheme I

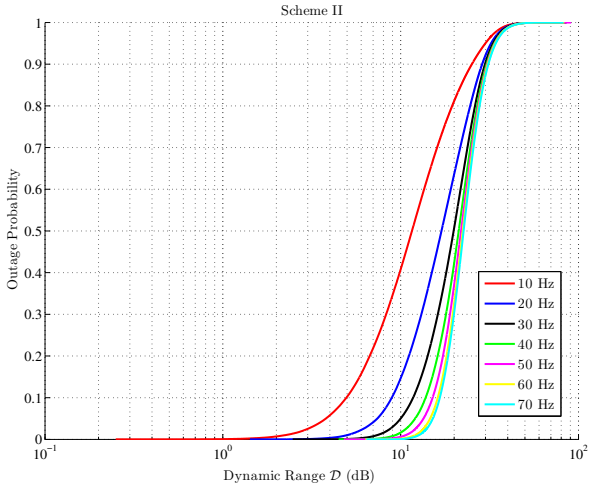

(b) Transmission Scheme II

Fig. 4.7: The cumulative probability of the channel's dynamic range $\mathcal{D}$ over a fountain-encoded packet: the transmission Scheme I (top) and the transmission Scheme II (bottom).

4.2.2.3 Opportunistic Error Correction

Opportunistic error correction is based on fountain codes and good error correction codes. In this paper, we employ LT codes as fountain codes and LDPC [74] plus *Cyclic Redundancy Check* (CRC) [75] to make the wireless channel behave like an erasure channel. To reduce the overhead of LT codes for small K, we use the message-passing

algorithm with Gaussian elimination to decode the LT codes.

Our FEC encoding scheme is performed in the following order: K source packets are encoded by LT codes first. To each fountain-encoded packet, a CRC is first added and the resulting packet is encoded by a LDPC code. Each packet is transmitted in a single sub-band. It is a cross-coding scheme over all the sub-bands, as source data is first encoded jointly over all the sub-bands by LT codes then encoded separately over a single sub-band by LDPC plus CRC codes. That is different from the FEC layer in the DVB standards, which is based on the joint coding scheme over all the sub-bands.

At the receiver, each fountain-encoded packet is first LDPC decoded when the SNR of its sub-band is equal to or higher than the threshold. The received packet is discarded if its energy is below the threshold. If LDPC decoding fails, the packet is discarded as well. If LDPC decoding succeeds, CRC is used to identify whether there are undetected errors from LDPC codes. If CRC decoding fails, the receiver also assumes that the whole packet has been lost. Once the receiver collects N surviving fountain-encoded packets, it starts to recover source data.

4.2.3 System Model

The opportunistic error correction scheme has been explained in the above section. The proposed approach can be applied in any OFDM-based DVB system. In this paper, the SISO DVB-T2 system is taken as an example of DVB systems.

The FEC layer in the current DVB-T2 system is based on LDPC codes and BCH codes. The concatenated LDPC-BCH codes assure a better protection than the FEC layer in the DVB-T system, which is based on convolutional and Reed-Solomon codes [22]. To reduce burst bit errors, interleaving is employed after the LDPC-BCH encoder in the DVB-T2 system. As mentioned earlier, the encoded packet is transmitted over all the sub-bands. Although this solution works well in practical systems, it is not optimal. Because it can not be beforehand predicted whether the received packet is decodable even with a perfect channel knowledge. Packets that have encountered a low-energy channel are still processed by the decoders. That can waste processing power. Also, the performance of this joint-coding approach is limited to the sub-bands with low energy, as it treats each part of the channel equally important.

In Figure 4.8, the proposed opportunistic error correction scheme is depicted. The key idea is to generate additional packets by fountain encoding. First, source packets are encoded by the fountain encoder. Then, a CRC checksum is added to each fountain-encoded packet and LDPC encoding is applied afterwards. On each sub-band, a packet is transmitted. Thus, multiple packets are transmitted simultaneously, using frequency division multiplexing. With this method, interleaving is not required.

At the receiver side, we assume that synchronization is perfect. A dynamic estimation of the channel is necessary after the demodulation of OFDM signals, as the wideband

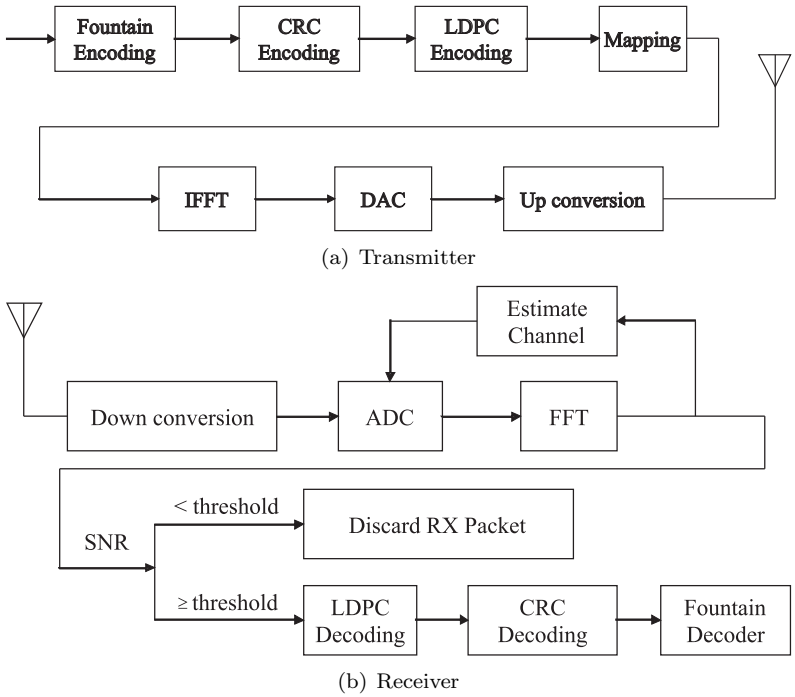

Fig. 4.8: Proposed DVB-T2 transmitter (top) and receiver (bottom).

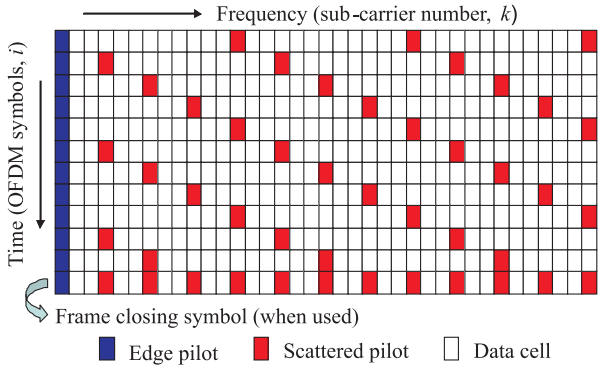

Fig. 4.9: Scattered pilot pattern *PP1* (SISO) [22].

mobile communication system transmits data over a time-variant frequency selective fading channel [61]. The channel estimation in the DVB system is based on a set of scattered pilots inserted into each OFDM symbol (i.e. the comb-type pilot). In total, there are 8 types of pilot patterns defined in the DVB-T2 standard [22]. In this paper, we utilize the *PPI* pattern to estimate the channel as shown in Figure 4.9.

The scattered pilots are estimated by the *zero-forcing* algorithm:

$$\hat{H}(i, k_p) = \frac{Y(i, k_p)}{X(i, k_p)} \tag{4.15}$$

where $Y(i, k_p)$ is the k_p-th received pilot tone and $X(i, k_p)$ is the k_p-th transmitted pilot tone at the i-th OFDM symbol.

With $\hat{H}(i, k_p)$, the channel information of the data sub-carriers can be estimated by interpolation. Generally it is a two-dimensional interpolation problem but it can be separated into a one-dimensional interpolation in time and in frequency for a low-complexity system implementation [76]. There are several types of interpolation algorithms, e.g. linear interpolation, second order interpolation, low-pass interpolation [77]. In this paper, for the sake of simplicity, the linear interpolation is used in the time domain and the low-pass interpolation is employed for the frequency domain.

In the time domain, the channel information at the k_p-th data-carrier of the i-th OFDM, $i_1 < i < i_2$, is estimated by [77]:

$$\hat{H}(i, k_p) = \hat{H}(i_1, k_p) + \frac{i - i_1}{i_2 - i_1}(\hat{H}(i_2, k_p) - \hat{H}(i_1, k_p)) \tag{4.16}$$

where $\hat{H}(i_1, k_p)$ and $\hat{H}(i_2, k_p)$ are the estimated channel information of scattered pilots at the i_1-th and i_2-th OFDM symbols, respectively. With $\hat{H}(i, k_p)$, the low-pass interpolation is performed in the frequency domain by inserting zeros into the original sequence. Then, a low-pass FIR filter is applied to minimize the mean-square error between the interpolated points and their ideal values [77]. So, the channel information of the k-th data sub-carrier at the i-th OFDM symbol is estimated by:

$$\hat{H}(i, k) = \sum_{l} C_l \hat{H}(i, k - l) \tag{4.17}$$

where C_l is the coefficient of the low-pass filter.

With the channel knowledge, the receiver can decide whether the received packet should be processed by the receiving chain. If the SNR of the sub-band is equal to or above the threshold, the received packet will go through the LDPC decoding otherwise it will be discarded. This means that not all the packets are processed by the receiver but only the well-received packets. Correspondingly, the processing power is reduced. If the channel is perfectly estimated, this can be done. However, the channel estimation is based on interpolation with limited accuracy. In such a case, the receiver can hardly predict correctly whether the received packet is decodable with a high probability. That degrades its performance. To avoid this, the receiver

will process all the fountain-encoded packets with the non-perfect channel estimation. The received packets can only survive if they pass LDPC decoding and CRC decoding successfully. When the receiver has collected enough fountain-encoded packets, it starts to recover the source data by using the message-passing algorithm and Gaussian elimination together.

4.2.4 Performance Comparison

In this section, we analyze the performance of opportunistic error correction in the OFDM-based DVB system. The DVB-T2 system is taken as an example of OFDM-based DVB systems, as the LDPC-BCH codes in the DVB-T2 standard work better than the convolutional and Reed Solomon codes in other OFDM-based DVB systems. We compare opportunistic error correction with the FEC scheme from the DVB-T2 standard in the simulation. For each simulation point, we transmit more than 1000 bursts of data (i.e. around 100 million bits) over a 8 MHz TU6 channel with a certain DF. Each burst consists of 512 source packets with a length of 168 bits. With the same data rate of 9.5 Mbits/s (i.e. QAM-16 modulation with code rate $R = 0.434$), a source file is encoded by opportunistic error correction and the LDPC-BCH code from the DVB-T2 standard, respectively. Afterwards, they are mapped into QAM-16 symbols before OFDM modulation.

With opportunistic error correction, each burst is encoded by a LT code (with parameters $c = 0.03$, $\sigma = 0.3$) and decoded by the message-passing algorithm and Gaussian elimination together. Only 3% overhead is required to reconstruct the original data successfully [70]. To each fountain-encoded packet, a 7-bit CRC is added before the (175,255) LDPC encoding is applied. Under the condition of the same code rate (i.e. $R = 0.434$), we are allowed to discard around 32% of the packets[6].

With the FEC layer defined in the DVB-T2 standard, source bits are first encoded by the (7032,7200) BCH code then by the (7200,16200) LDPC code. To reduce burst bit errors, bits are interleaved and de-multiplexed into cells afterwards [22]. The DVB-T2 system is designed to provide a "Quasi Error Free" (QEF) quality target [22]. The definition of QEF adopted for DVB-T2 is "less than one uncorrected error-event per transmission hour at the level of a 5 Mbit/s single TV service decoder", approximately corresponding to a Transport Stream Packet Error Ratio PER $< 10^{-7}$ (i.e. BER $< 10^{-11}$) before the de-multiplexer which is equivalent to BER $< 10^{-7}$ after LDPC decoding [22]. To keep simulation times reasonable, we choose a BER of 10^{-4} after LDPC decoding as the comparison criterion, which corresponds to approximately a BER of 10^{-7} after BCH decoding [78].

As stated earlier, the interpolation-based channel estimation mentioned in section 4.2.3 is not optimal, but it is employed by the practical DVB systems due to its low

[6] $32\% \approx 1 - \frac{R}{R_1 \times R_2}$, where R is the effective code rate (i.e. 0.434), R_1 is the code rate of LT codes (i.e. $\frac{1}{1.03} \approx 0.97$) and R_2 is the code rate of the (175,255) LDPC code with 7-bit CRC (i.e. $\frac{168}{255} \approx 0.66$)

implementation complexity. To show how robust both FEC layers are to the channel estimation errors, they are compared in two situations: *with perfect channel knowledge* and *with non-perfect channel knowledge*.

4.2.4.1 With Perfect Channel Knowledge

In this case, we assume that the receiver has a perfect knowledge of the channel. As shown in Figure 4.7, the dynamic range of sub-bands based on the transmission method I is not affected by Doppler spread. In other words, the BER performance does not change with Doppler frequency as revealed in the simulation. Figure 4.10 shows the simulation results over the TU6 channel. Obviously, our opportunistic error correction scheme performs much better than the FEC layer in the DVB-T2 standard. To reach a BER of 10^{-7} after BCH decoding (i.e. a BER of 10^{-4} after LDPC decoding), the current DVB-T2 system should have a SNR of at least 28 dB at a data rate of 9.5 Mbits/s. With our opportunistic error correction method, the proposed DVB-T2 system has error free when SNR = 18 dB. That means our method gains a SNR of more than 10 dB at a data rate of 9.5 Mbits/s for a BER of 10^{-7}. However, if we compare them under the QEF criterion, opportunistic error correction will gain a SNR of at least 14 dB with respect to the FEC layer in the DVB-T2 standard (i.e. a BER of 10^{-7} after LDPC decoding).

4.2.4.2 With Non-Perfect Channel Knowledge

In this part, we investigate the side-effect of the channel estimation error to both FEC schemes. As described in Section 4.2.3, the channel estimation in the DVB system is based on scattered pilot sub-carriers. The estimation accuracy of the pilot sub-carries directly affects the estimation of the data sub-carriers. In a frequency selective channel, it is very likely that some pilot sub-carriers will suffer deep fading. With the zero-forcing algorithm, this results in a huge estimation error which directly influences the channel estimation of data sub-carriers. In order to see the penalty of the noise on the pilot sub-carriers for both FEC schemes, we compare them over the TU6 channel *without noise* and *with noise*, separately.

1. *Noiseless Channel:* In this case, pilot sub-carriers are perfectly estimated and data sub-carriers are estimated by the interpolation algorithm as depicted in Section 4.2.3. Figure 4.11 shows the simulation results. Obviously, the BER performance degrades when DF increases. Opportunistic error correction is error free till DF = 40Hz but that does not happen in the DVB-T2 FEC layer. When DF = 50Hz, opportunistic error correction has higher BER than the FEC layer from the DVB-T2 standard. That is because opportunistic error correction does not have enough error-free packets to reconstruct the original file. Since there is no feed-back channel in the DVB systems, in this case the receiver either can not

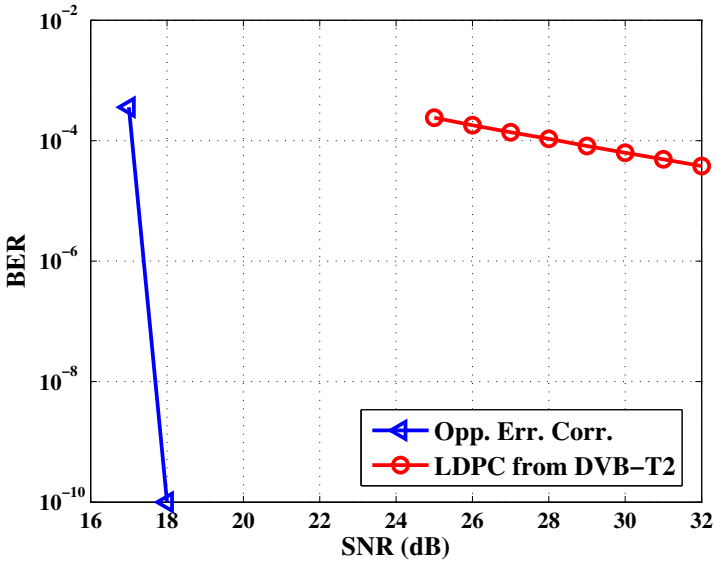

Fig. 4.10: BER comparison between opportunistic error correction and the (7200,16200) LDPC code from the DVB-T2 standard in the noisy TU6 channel with perfect channel estimation. For opportunistic error correction, no error occurs when SNR $\geq$ 18 dB. So for this point, we represent BER = 0 by 10^{-10}.

recover source data or use some packets in error[7] to reconstruct the original file. In our simulation, we choose the second option. If the fountain decoder utilizes packets in error, bit errors will propagate during the decoding. This is the disadvantage of using fountain codes as a FEC scheme without a feedback channel. However, the BER of the LDPC code from the DVB-T2 standard is 1.14×10^{-3} at DF = 50Hz and is also not acceptable. Only when DF $\leq$ 20Hz, the current DVB-T2 system has a BER less than 10^{-4} after LDPC decoding. Furthermore, it is impossible for the current DVB-T2 system to achieve the QEF target with the interpolation-based channel estimation at a data rate of 9.5 Mbits/s. But, opportunistic error correction can offer us the QEF quality using this low-accurate and low-complexity channel estimation algorithm. Therefore, we conclude that opportunistic error correction works better than the DVB-T2 FEC layer in the noiseless TU6 channel with the non-perfect channel knowledge.

2. *Noisy Channel:* In practice, the channel estimation does suffer from inaccuracies caused both by imperfect interpolation and by the presence of noise on the pilot cells. Figure 4.12 shows the practical performance of opportunistic error correction over a TU6 channel at DF $\leq$ 40Hz. As we can see, opportunistic error correction still provides us the error-free quality even with the non-perfect estimation

[7]Packets in error refer to those which can not pass the error correction decoding.

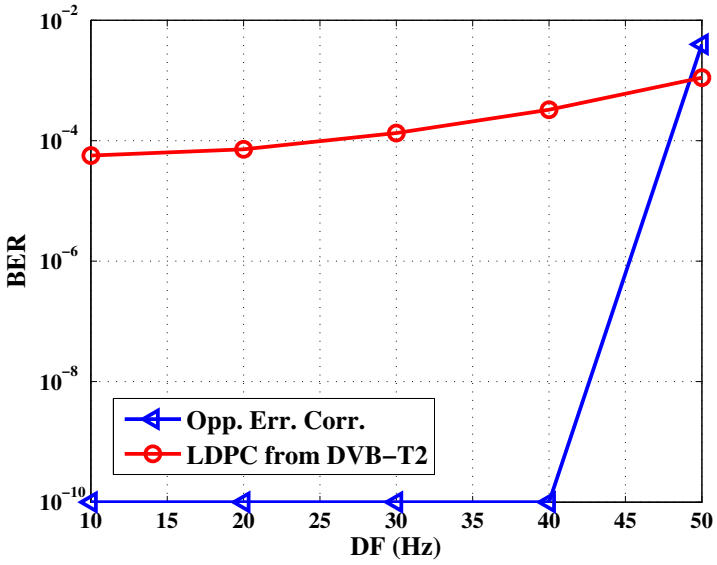

Fig. 4.11: BER comparison between opportunistic error correction and the FEC layer in the DVB-T2 standard in the noiseless TU6 channel with the non-perfect channel estimation. For opportunistic error correction, no error occurs when DF = 10Hz $\sim$ 40Hz. So for those points, we represent BER = 0 by 10^{-10}.

in the pilot cells. Larger DF requires higher SNR to achieve BER = 0. When DF $\leq$ 30Hz, there is 1 dB SNR loss as DF increases by 10 Hz. In the case of DF increase from 30Hz to 40Hz, there is a 7 dB SNR loss. A more accurate channel estimation algorithm is required for OFDM-based DVB systems when DF $\geq$ 30Hz.

As just discussed, it is impossible for the current DVB-T2 system to have a BER of 10^{-7} when DF $\geq$ 20Hz. So, we only investigate the practical performance of the (7200,16200) LDPC code over a noisy TU6 channel with DF $\leq$ 20Hz. The simulation results are shown in Figure 4.13. To achieve a BER of 10^{-7} after BCH decoding (i.e. a BER of 10^{-4} after LDPC decoding), it needs around 34 dB for DF = 10Hz and around 36 dB for DF = 20Hz at a data rate of 9.5 Mbits/s. It has a 2 dB SNR loss as the DF increases by 10 Hz which is twice as the opportunistic error correction. Furthermore, opportunistic error correction gains a SNR of more than 11 dB for DF = 10Hz and more than 12 dB for DF = 20Hz over a noisy TU6 channel with the non-perfect channel estimation.

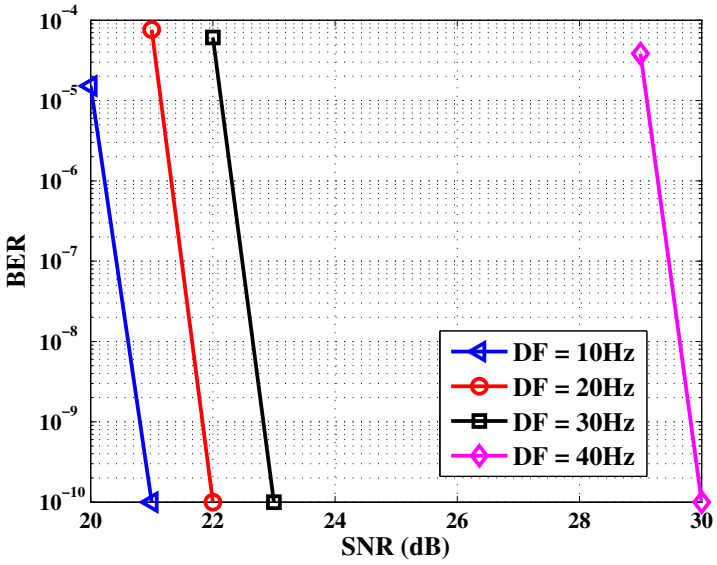

Fig. 4.12: BER performance of opportunistic error correction in the noisy TU6 channel with the non-perfect channel estimation. For DF = 10Hz, no error occurs at SNR = 21dB. So for this point, we represent BER = 0 by 10^{-10}. Same for DF = 20Hz $\sim$ 40Hz.

4.2.5 Conclusions

In this paper, we propose a novel error correction scheme based on fountain codes for OFDM-based DVB systems. It is called opportunistic error correction because the receiver is allowed to discard packets. By transmitting a fountain-encoded packet over a single sub-band, the receiver does not have to take care of all the sub-bands (i.e. all the received packets) but only the sub-bands with high energy (i.e. the packets with high SNR). Fountain codes can reconstruct the original file by only using the surviving packets. With the perfect channel knowledge, opportunistic error correction has a SNR gain of at least 10 dB in comparison to the FEC layer from the DVB-T2 standard at a data rate of 9.5 Mbits/s.

In addition, opportunistic error correction survives in the low-accuracy interpolation-based channel estimation when DF $\leq$ 40 Hz but that does not happen with the current DVB-T2 FEC layer. With this low-complexity channel estimation, opportunistic error correction offers us the QEF quality with a maximum DF of 40 Hz but the current DVB-T2 FEC layer can only provide a BER of 10^{-7} quality after BCH decoding with a maximum DF of 20 Hz. Furthermore, our new approach gives us a SNR gain of more than 11 dB with the non-perfect channel estimation over a noisy TU6 channel in comparison to the current FEC layer in the DVB-T2 standard. As the concatenated LDPC-BCH codes yields a better protection than the convolutional and Reed-Solomon codes used in other OFDM-based DVB systems [22], we can conclude

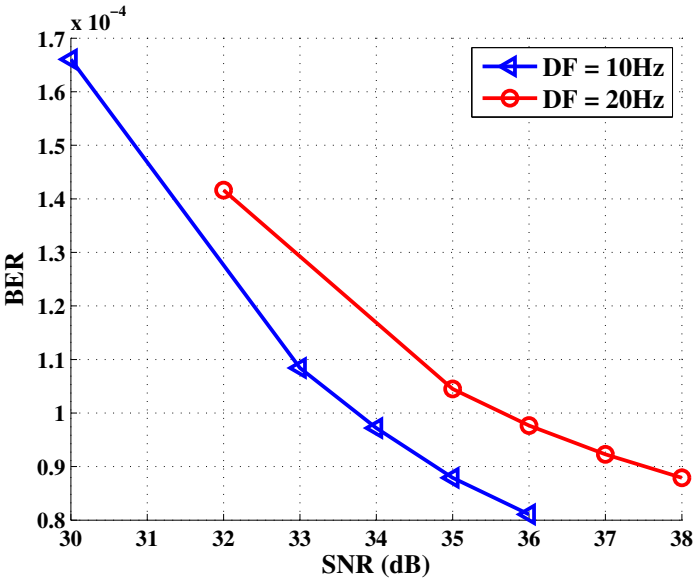

Fig. 4.13: BER performance of the (7200,16200) LDPC code from the DVB-T2 standard in the noisy TU6 channel with the non-perfect channel estimation.

that opportunistic error correction performs better over a TU6 channel than the FEC layer in current OFDM-based DVB systems. Therefore, we suggest to consider this new scheme as a candidate of the FEC layer for the next generation OFDM-based DVB systems.

In this paper, we assume that synchronization is perfect which does not happen in the real wireless channels. Further research focuses on the optimization of this new error correction for the wireless channel with non-perfect synchronization.

Chapter 5

Energy Efficient Error Correction for MIMO-OFDM Systems

5.1 Opportunistic Error Correction for MIMO

[1]**Abstract** In this paper, we propose an energy-efficient scheme to reduce the power consumption of ADCs in MIMO-OFDM systems. The proposed opportunistic error correction scheme is based on resolution adaptive ADCs and fountain codes. The key idea is to transmit a fountain-encoded packet over one single sub-carrier per antenna and to transmit more packets than needed for decoding. Comparing to the IEEE 802.11n standard, this approach allows around 83% of power saving in ADCs for a 2×2 system and 90% for a 4×4 system. With the current FEC scheme defined in the IEEE 802.11n standard, a 4×4 system requires twice amount of power in ADCs as a 2×2 system when receiving the same amount of information with the same power. However, using opportunistic error correction in a 4×4 system costs only around 1.4 times amount of energy in ADCs comparing to a 2×2 system.

[1]This section is the published paper [79]: *X. Shao and C.H. Slump, "Opportunistic Error Correction for MIMO", in Proceedings of the 20th IEEE Symposium on Personal, Indoor and Mobile Radio Communications (PIMRC), Sep 2009, Tokyo, Japan.*

5.1.1 Introduction

Multiple-Input Multiple-Output (MIMO) technology has attracted a lot of attention in wireless communications, due to its high data rate without additional bandwidth or transmitted power [2]. Combining *Orthogonal Frequency Division Multiplexing* (OFDM) with MIMO enables easy implementation of MIMO systems in wireless channels. OFDM has a high *Peak-to-Average Power Ratio* (PAPR), therefore it needs *Analog-to-Digital Converter* (ADC) with a high dynamic range, especially in MIMO-OFDM systems.

In this paper, we focus on a M×M MIMO-OFDM system with maximum multiplexing gain. At the transmitter, we assume that each antenna transmits one data stream and has unity transmission power. At the receiver, the signal arriving at each antenna is the combination of the signals from all the transmit antennas. So, the dynamic range of the ADCs is proportional to the number of antennas M. In wireless LAN systems, the ADC can consume up to 50% of the total baseband power budget [11]. Low power-consumption in battery-powered digital MIMO receivers is a highly desired feature. Therefore, we propose a novel scheme to reduce the power consumption of the ADC by combining a resolution adaptive ADC architecture with opportunistic error correction.

Fixed high-resolution ADCs are applied in current WLAN MIMO systems. The high-resolution ADCs are employed for worst-case channel conditions. However, worst-case channel conditions do not always happen. Therefore, we propose to use resolution adaptive ADCs whose resolution is adapted for each channel instead of being fixed for worst-case conditions. Correspondingly, the power consumption in ADCs is reduced.

A further resolution reduction of the ADC can be achieved by using a novel error correction scheme to be integrated into the physical layer. In the IEEE 802.11n standard [23], the *Forward Error Correction* (FEC) layer encodes source data across all transmit antennas and the full transmission band, which means that each part of those M parallel channels (after inverting the effect of the MIMO channel) is considered equally important. In such case, the resolution of ADCs is determined by the sub-band with the lowest energy of the M channels. Take Figure 5.1 as an example, the lowest energy of the 4 parallel channels is around -32 dB. From this figure, we can see that the deep fading does not happen everywhere and only happens in the frequency band of 7∼9 MHz. By discarding this 2 MHz sub-band, the lowest energy of this channel vector is reduced to around -20 dB. If we put the 4 channels together and sort them by energy, its lowest energy is increased to around -13 dB by also discarding 10% of bandwidth.

As just mentioned, the FEC scheme defined in the IEEE 802.11n standard does not allow us to discard part of a channel with deep fading. However, this can be achieved by using fountain codes. Fountain codes can reconstruct the source file by collecting enough packets. It does not matter which packet is received. We only need to receive a certain number of packets. Therefore, we propose to transmit a fountain-encoded packet over a sub-carrier per antenna. Multiple packets are transmitted

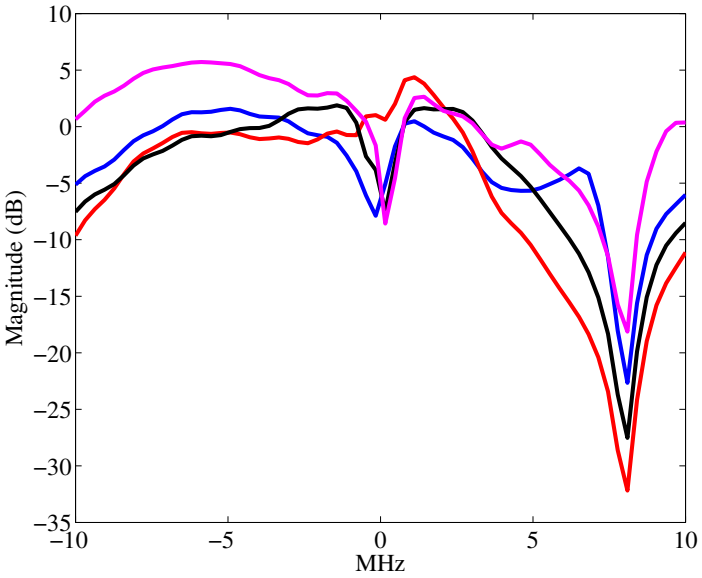

Fig. 5.1: Example of the baseband transfer function of a 4-by-4 Channel *model* A after inverting the effect of the MIMO channel.

simultaneously, using frequency division multiplexing and space division multiplexing. The receiver discards the sub-carriers with deep fading and recovers the source data by only collecting the well-received packets from the high-energy sub-carriers. With this approach, the quantization of the ADCs can be coarse.

The outline of this paper is as follows. We propose two techniques to reduce power consumption of ADCs: fountain codes and resolution adaptive ADCs. First, fountain codes are discussed which is followed by resolution adaptive ADCs for MIMO-OFDM systems. In Section 5.1.4, system models will be described. Finally, the simulation results will be analyzed, which compare the conventional 802.11n system with our approach. The paper ends with conclusions.

5.1.2 Fountain Codes

Opportunistic error correction is based on fountain codes. A fountain code has a similar property to a fountain of water: when you fill a cup from the fountain, you do not care about which drops of water fall in, but only want that your cup fills enough to quench your thirst [80].

With a fountain code, the transmitter can generate a potentially infinite supply of

fountain-encoded packets and the receiver can reconstruct the original file by collecting enough fountain-encoded packets. The number of fountain-encoded packets N required at the receiver is slightly larger than the number of source packets K [54]:

$$N = (1 + \varepsilon)K \tag{5.1}$$

where ε is the percentage of extra packets and is called the overhead.

The *message-passing* algorithm has been used to reconstruct source data from fountain-encoded packets due to its linear computation cost [54]. However, it requires a large ε for small block size. For example, the practical overhead of LT codes[2] [43] is 14% when $K = 2000$, which limits its application in practical systems [41]. In [40], we have shown that the overhead is reduced to 3% by using message-passing with Gaussian Elimination to decode LT codes for $K \geq 500$.

Fountain codes are specially designed for erasure channels. A wireless channel is not an erasure channel but a noisy fading channel. In order to apply fountain codes in wireless channels, error correction codes need to be utilized to make wireless channel behave like an erasure channel. In this paper, *Low-Density Parity-Check* (LDPC) codes together with *Cyclic Redundancy Check* (CRC) are used to convert the channel.

The opportunistic error correction scheme is performed as follows:

- At the transmitter, a fountain-encoded packet is created. Then the CRC is added. Finally, the packet is encoded by the LDPC code.
- At the receiver, each packet is first LDPC decoded if its energy is above or equal to a threshold (corresponding to BER $\leq 10^{-5}$). The received packet is discarded if its energy is below the threshold. If the LDPC decoding fails, the received packet is discarded as well. If the LDPC decoding succeeds, the CRC is used to identify any undetected errors from LDPC codes. If the CRC decoder detects an error, the receiver assumes that the whole packet has been lost. Once the receiver collects N surviving fountain-encoded packets, it starts to recover the original data.

5.1.3 Resolution Adaptive ADCs for MIMO-OFDM System

In MIMO-OFDM systems, signal detection is performed in the frequency domain after inverting the effect of the channel. It is not beforehand clear how many ADC bits are required for proper detection, because quantization happens in the time domain and before the effect of the MIMO channel is inverted. In this section, we derive a relation between the quantization noise in the time domain and the frequency domain for MIMO-OFDM systems. Afterwards, we present a scheme to design optimum low-resolution ADCs for MIMO-OFDM systems.

[2]LT code is a kind of fountain codes. In this paper, we use LT codes in our proposed scheme which is compatible with any fountain codes (e.g. Raptor codes [81]).

Notation: **bold** represents vector and matrix, *lower case* represents the signal in the time domain and *upper case* represents the signal in the frequency domain.

5.1.3.1 Minimum Number of Quantization Levels

Because the quantization noise is dependent on the signal, we first analyze the statistical characteristics of the ADC input $\mathbf{r}_n$. We assume that the quantization noise is dominant, so other noise (e.g. channel noise) is ignored in this paper. In such case, a M × M channel output at the n_{th} moment $\mathbf{r}_n$ can be written as:

$$\mathbf{r}_n = \sum_{l=0}^{L-1} \mathbf{h}_l \mathbf{x}_{n-l} \tag{5.2}$$

where $\mathbf{x} = [\mathrm{x}^{(1)}, \cdots, \mathrm{x}^{(m)}, \cdots, \mathrm{x}^{(\mathrm{M})}]$ is the transmitted vector, $\mathbf{h}_l$ is the M×M channel matrix at the l_{th}-path and L is the number of channel paths. From [18], we know that $\mathrm{x}^{(m)}$ can be modeled as a normal-distributed random variable with zero mean and a variance of 1. The elements in $\mathbf{x}$ are mutual independent, so it has zero mean and a unity variance matrix. In addition, $\mathbf{x}_n$ and $\mathbf{x}_{n'}$ are mutual independent, if $n \neq n'$.

As each element in $\mathbf{r}_n = [\mathrm{r}_n^{(1)}, \cdots, \mathrm{r}_n^{(m)}, \cdots, \mathrm{r}_n^{(\mathrm{M})}]$ is quantized separately, we analyze the statistical characteristics of $\mathrm{r}_n^{(m)}$ instead of $\mathbf{r}_n$. $\mathrm{r}_n^{(m)}$ can be expressed as:

$$\mathrm{r}_n^{(m)} = \sum_{l=0}^{L-1} \sum_{s=0}^{\mathrm{M}-1} h_l^{(m,s)} x_{n-l}^{(s)} \tag{5.3}$$

According to the *Central Limit Theorem*, the sum of a sequence of independent, identically distributed random variables tends to be Gaussian-distributed, so the probability density function of $\mathrm{r}_n^{(m)}$ can be described as:

$$f(\mathrm{r}_n^{(m)}) \approx \frac{1}{\pi \sigma^2_{\mathrm{r}_n^{(m)}}} \exp\left(-\frac{|\mathrm{r}_n^{(m)}|^2}{\sigma^2_{\mathrm{r}_n^{(m)}}} \right) \tag{5.4}$$

where $\sigma^2_{\mathrm{r}_n^{(m)}} = \sum_{l=0}^{L-1} \sum_{s=0}^{\mathrm{M}-1} |h_l^{(m,s)}|^2$. For simplicity, we assume that $\sum_{l=0}^{L-1} |h_l^{(m,s)}|^2 = \sum_{l=0}^{L-1} |h_l^{(m,s')}|^2 = 1$ $(s \neq s')$, so $\mathrm{r}_n^{(m)} \sim \mathcal{CN}(0, \mathrm{M})$. However, the discussion below holds more generally.

The ADC output $\mathrm{y}_n^{(m)}$ can be expressed as:

$$\mathrm{y}_n^{(m)} = \mathcal{Q}(\mathrm{r}_n^{(m)}) = \sum_{l=0}^{L-1} \sum_{s=0}^{\mathrm{M}-1} h_l^{(m,s)} x_{n-l}^{(s)} + \mathrm{n}_n^{(m)} \tag{5.5}$$

where $\mathrm{n}_n^{(m)}$ is the quantization noise in the time domain at the m_{th} antenna. With a uniform quantizer, $\mathrm{n}_n^{(m)}$ is uniformly distributed with zero mean and a variance of $\frac{\triangle^2}{6}$, where $\triangle$ is the uniform quantization step [18].

After OFDM demodulation, each sub-carrier can be considered as a narrow-band MIMO channel in the frequency domain:

$$\mathbf{Y}_k = \mathbf{H}_k \mathbf{X}_k + \mathbf{N}_k \tag{5.6}$$

where $\mathbf{X}_k = [\mathrm{X}_k^{(1)}, \cdots, \mathrm{X}_k^{(\mathrm{m})}, \cdots, \mathrm{X}_k^{(\mathrm{M})}]$ is the transmitted vector at the k_{th} sub-carrier and $\mathbf{N}_k = [\mathrm{N}_k^{(1)}, \cdots, \mathrm{N}_k^{(\mathrm{m})}, \cdots, \mathrm{N}_k^{(\mathrm{M})}]$ is the quantization noise in the frequency domain:

$$\mathbf{N}_k = \frac{1}{\sqrt{\mathrm{N}}} \sum_{n=0}^{\mathrm{N}-1} \mathbf{n}_n e^{-j\frac{2\pi}{\mathrm{N}}nk} \tag{5.7}$$

where N is the number of sub-carriers. The *Central Limit Theorem* shows that $\mathrm{N}_k^{(m)}$ is Gaussian-distributed with zero mean and a variance of $\frac{\triangle^2}{6}$ [18]. $\mathbf{H}_k$ is the fading matrix at the k_{th} sub-carrier defined by:

$$\mathbf{H}_k = \sum_{l=0}^{L-1} \mathbf{h}_l e^{-j\frac{2\pi}{\mathrm{N}}lk} \tag{5.8}$$

In order to detect the transmitted symbol from each transmitted antenna, we need to invert the effect of the MIMO channel. In this paper, the *zero-forcing* algorithm is used to do the inversion:

$$\hat{\mathbf{X}}_k = \mathbf{H}_k^{-1} \mathbf{Y}_k = \mathbf{X}_k + \mathbf{H}_k^{-1} \mathbf{N}_k \tag{5.9}$$

Thus, for the symbol $\mathrm{X}_k^{(m)}$ from the m_{th} antenna at the k_{th} sub-carrier, its *Signal-to-*

Noise Ratio (SNR) can be derived as:

$$\mathrm{SNR}_k^{(m)} = \left(\frac{\triangle^2}{6} \sum_{s=0}^{M-1} |\mathbf{H}_k^{-1}{}^{(m,s)}|^2 \right)^{-1} \tag{5.10}$$

The above equation shows the quantization effects in MIMO-OFDM system. To communicate reliably, error correction coding is used to mitigate the quantization effect. Different coding has different SNR threshold to achieve a BER at a certain order or lower (e.g. 10^{-4}). So, the quantization step $\triangle$ can be derived once an error correction code is chosen and the channel is estimated. If clipping is allowed, the number of quantization levels N_q can be determined by [18]:

$$N_q = 2\lceil \frac{\mathrm{C}}{\triangle} \rceil \tag{5.11}$$

where $\mathrm{C} = 3\sigma_{\mathrm{r}_n^{(m)}} = 3\sqrt{\mathrm{M}}$. Here, we can see that the dynamic range of ADCs is proportional to M, so does N_q.

From Equation 5.10 and 5.11, we can see that N_q is determined by M, $\triangle$ and the channel. Once the MIMO system is chosen and the channel is fixed, N_q depends on $\triangle$. In such case, $\triangle$ depends not only on the used error correction code but also on how an encoded packet is transmitted.

5.1.3.2 Power Consumption

In general, the power consumption of ADCs is proportional to the number of quantization levels N_q. The power consumption of the ADC implemented by CMOS scales linearly with N_q [11]. Thus, we can write the ADC's power consumption P as:

$$\mathrm{P} = \sum_{i=0}^{M_c-1} \sum_{m=0}^{\mathrm{M}-1} \alpha_i N_{q_i}^{(m)} \mathcal{M} \tag{5.12}$$

where M_c is the number of channel realizations, α_i is the percentage of the i-th channel realization where useful information is transmitted, $N_{qi}^{(m)}$ is the number of quantization levels used in the i-th channel realization and at the m-th antenna, and $\mathcal{M}$ is the number of samples per MAC frame.

Once an error correction code is chosen, Equation 5.10, 5.11 and 5.12 tell us that the power consumption of ADCs depends on the sub-carrier with the lowest energy. By

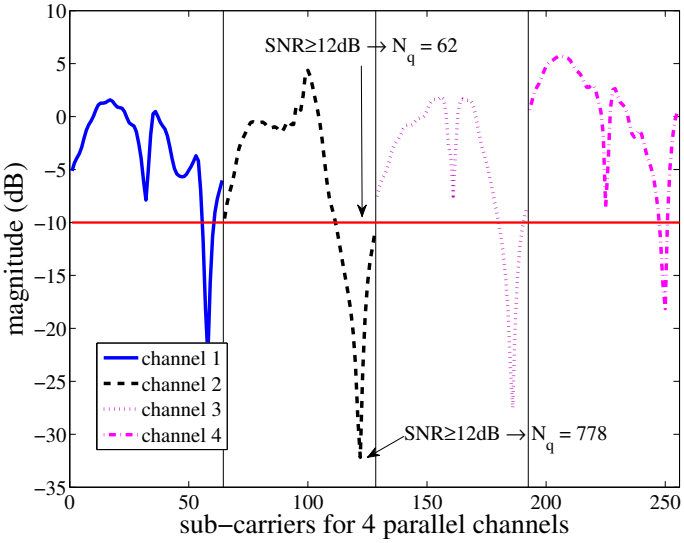

Fig. 5.2: The difference in the number of ADC levels N_q between transmission *Method I* and transmission *Method II*.

transmitting one fountain-encoded packet over a sub-carrier per antenna, the power consumption of ADCs can be reduced by discarding packets from the sub-carriers with deep fading. For example, assume that a fountain-encoded packet is transmitted over a 4-by-4 channel as Figure 5.1. *Method I* is to transmit it across all the antennas and all the sub-carriers as defined in [23] and *Method II* is to transmit it over one sub-carrier per antenna. Suppose the fountain-encoded packet can be received correctly when its SNR $\geq$ 12dB. Figure 5.2 shows that *Method I* needs 778 levels but *Method II* only requires 62 levels in ADC by discarding 18% of the sub-carriers. However, discarding packets over the low-energy sub-carriers means increasing the total number of transmitted packets which might increase the total power consumption in ADCs. Therefore, there is a tradeoff in the power consumption between the number of lost sub-carriers and the total number of transmitted packets which will be analyzed in the following section.

5.1.4 System Model

The opportunistic error correction scheme is based on fountain codes and resolution adaptive ADCs which have been explained in the above sections. This novel method can be applied in MIMO-OFDM systems. In this paper, we take the IEEE 802.11n system as an example of MIMO-OFDM systems.

The current IEEE 802.11n standard is based on *Rate Compatible Punctured Codes* (RCPC). RCPC has good performance for random bit errors but not for burst bit errors, so interleaving is applied to reduce burst errors. Each RCPC-encoded packet is transmitted based on *Method I*. Although this solution works good in practice, it is not optimal from a power consumption point of view:

- Packets encountered by a "bad" channel are still processed by the receiver.
- Fixed high-resolution ADCs are used in all antennas.

Those problems can be solved by using the opportunistic error correction scheme, as shown in Figure 5.3. The key idea is to transmit fountain-encoded packets based on *Method II* and generate additional packets by the fountain encoder. At the transmitter, the source file is first divided into a stream of source packets which are encoded by a LT code (with parameter $c = 0.03$, $\sigma = 0.3$). Then, each fountain-encoded packet is added by a 7-bit CRC checksum and encoded by a (175,255) LDPC code. Afterwards, it is transmitted over a sub-carrier of a transmitted antenna.

At the receiver, the resolution of ADCs is adapted into the minimum with the estimated channel knowledge and the number of lost sub-carriers. After OFDM demodulation and inverting the effect of the MIMO channel, the receiver can only process the packets from high-energy sub-carriers (i.e. SNR $\geq$ threshold) by checking its SNR defined in Equation 5.10. The received packet survives if it has successful LDPC decoding and CRC checking. Once the receiver has got enough packets, it reconstructs the original file by fountain decoding.

As discussed in Section 5.1.3, discarding more sub-carriers does not mean less power consumption in ADCs. Assume that the receiver needs to collect 1000 fountain-encoded packets and the received packet will be discarded if its SNR is less than 12 dB. With a HT (i.e. High Throughput) mode defined in [23], 52 sub-carriers are used to transmit fountain-encoded packets. As the quantization noise is the dominant noise, resolution adaptive ADCs are designed in such way that N_b[3] sub-carriers have a SNR lower than 12 dB. Figure 5.4 shows the tradeoff between the power consumption in ADCs and N_b with perfect channel knowledge. As we can see, a 4×4 system consumes more power in ADCs than a 2×2 system to receive the same amount of fountain-encoded packets. Their difference is reduced when $N_b > 0$.

The power consumption of ADCs in both systems first decreases then increases when N_b becomes larger. The 2×2 system consumes the minimum power in ADCs with 17 lost sub-carriers while the 4×4 system needs to discard 19 sub-carriers. Before arriving the minimum point, the decreasing speed becomes slower when N_b increases. Comparing to $N_b = 0$, the power consumption in the 2×2 system is reduced by around 62% when $N_b = 5$, 69% when $N_b = 10$ and 71% when $N_b = 17$. Similar valued holds for the 4×4 system, whose power consumption in ADCs is decreased by around 73% with 5 lost sub-carriers, 78% with 10 lost sub-carriers and 80% with 19 sub-carriers lost comparing to the case of no lost sub-carrier. Obviously, the power saving in ADCs is mainly contributed by discarding 5 lowest-energy sub-carriers. In

[3] N_b: the number of lost sub-carriers

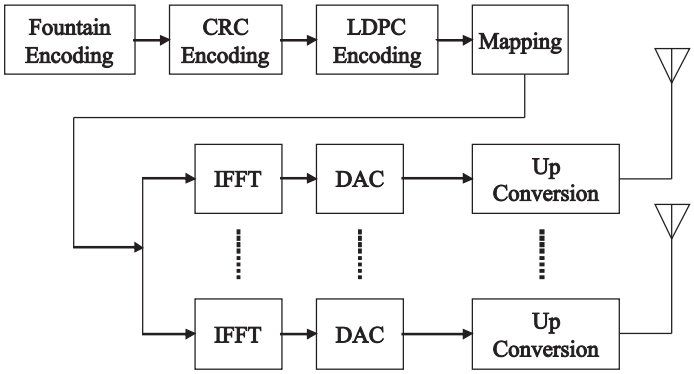

(a) Transmitter

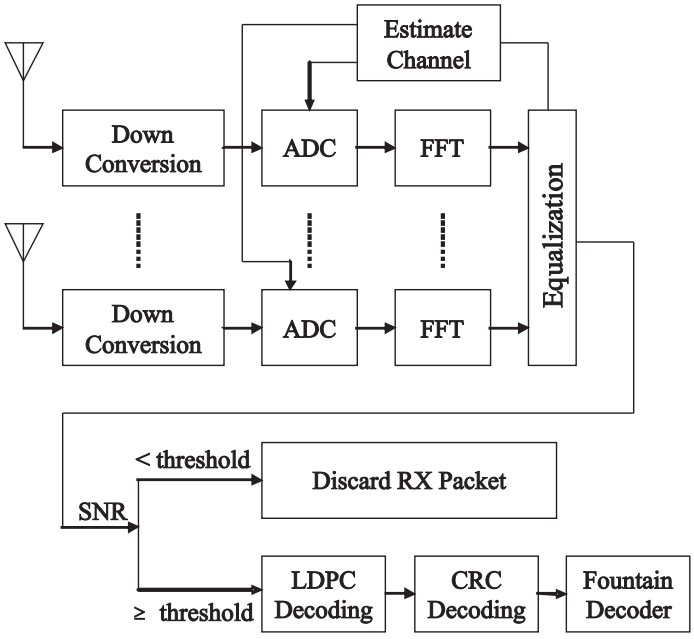

(b) Receiver

Fig. 5.3: Proposed IEEE 802.11n transmitter (top) and receiver (bottom).

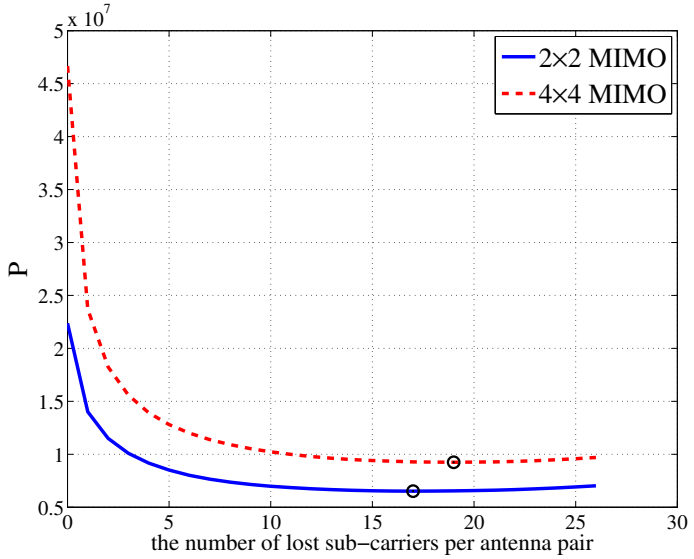

Fig. 5.4: Power consumption defined in Equation 5.12 versus the number of lost sub-carriers for receiving 1000 fountain-encoded packets.

addition, the 4×4 system has more power saving in ADCs than the 2×2 system given a N_b.

5.1.5 Performance Analysis

In this section, we analyze the performance of opportunistic error correction scheme by comparing the following scenarios. **Scenario I** is a RCPC with interleaving from the IEEE 802.11n standard with $R_{\mathrm{I}} = 0.5$. Fixed-resolution ADCs are used in Scenario I. As the standard allows 10% packet loss, the resolution of ADCs in Scenario I is designed for 90% channel realizations. In **Scenario II**, we replace fixed-resolution ADCs in Scenario I by resolution adaptive ADCs. **Scenario III** is the opportunistic error correction scheme based on fountain codes and resolution adaptive ADCs. In Scenario III, the code rate of LT code R_{LT} is around 0.97 and the code rate of LDPC plus CRC $R_{\mathrm{LDPC-CRC}}$ is around 0.66, so its total code rate R_{III} is around 0.64. To have the same effective throughput, Scenario III is allowed to discard around 30% (i.e. $0.5 \times 0.9/0.64$) of data sub-carriers. In addition, QAM-16 is the mapping scheme and 52 sub-carriers are used to transmit data as defined in [23].

Figure 5.5 shows the simulation results for a 2×2 system and a 4×4 system. In both systems, Scenario I costs the most power in ADCs comparing to Scenario II and III. Scenario III saves around 65% ADCs' power in a 2×2 system (79% for a 4×4

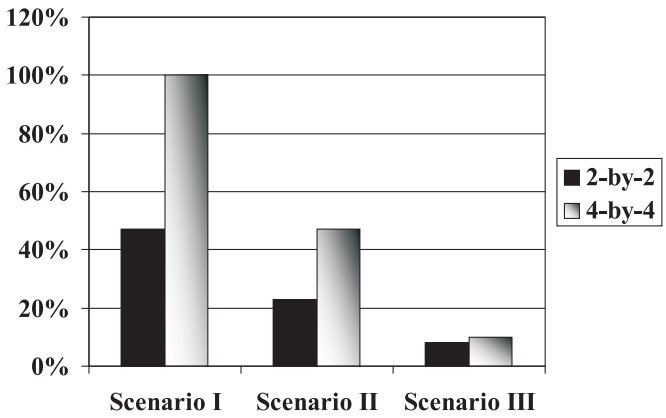

Fig. 5.5: Comparison in power consumption between Scenario I, II and III for a 2×2 system and a 4×4 system. Scenario I: RCPC with fixed-resolution ADCs, Scenario II: RCPC with resolution adaptive ADCs, Scenario III: opportunistic error correction (i.e. fountain codes with resolution adaptive ADCs). The power consumption of Scenario I in a 4×4 system is normalized to 1.

system) comparing to Scenario II, which consumes around 49% of the power in ADCs with respect to Scenario I in a 2×2 system (47% for a 4×4 system). As we can see, Scenario III in a 4×4 system has more energy saving than in a 2×2 system in comparison with Scenario I and II.

In addition, receiving the same amount of information in a 2×2 system consumes more power in ADCs than in a 4×4 system. With RCPC, the power consumption in ADCs using a 4×4 system is around twice as much as the case of using a 2×2 system no matter whether using fixed-resolution ADCs or resolution adaptive ADCs. However, this does not happen in the opportunistic error correction scheme. In Scenario III, receiving the same amount of information using a 4×4 system consumes around 1.4 times amount of power in ADCs as a 2×2 system. Furthermore, the receiver does not need to process all the received packets but only process the well-received packets in Scenario III, which does not apply in Scenario I and II.

5.1.6 Conclusions

In this paper, we propose an energy-efficient scheme based on fountain codes and resolution adaptive ADCs for MIMO-OFDM systems to save power consumption in ADCs. The ADCs in a receiver can consume up to 50% of the total baseband energy, so the need to lower its power consumption is clear. The resolution adaptive ADCs saves around 49% power in a 2×2 system and 47% power in a 4×4 system comparing

to fixed-resolution ADCs. Fountain codes together with LDPC plus CRC codes allow another 34% energy saving in a 2×2 system and 43% in a 4×4 system comparing to RCPC. In total, our proposed approach gives a power saving in ADCs of around 83% in a 2×2 system and a saving of around 90% in a 4×4 system.

Furthermore, the power consumption in ADCs is proportional to M by receiving the same amount of information and with the same transmission power. With RCPC, a 4×4 system costs about twice the power in ADCs comparing to a 2×2 system. However, fountain codes allow a 4×4 system to consume around 1.4 times of the amount of power in ADCs with respect to a 2×2 system.

5.2 Opportunistic Error Correction for MIMO-OFDM: From Theory to Practice

[4]**Abstract** Opportunistic error correction based on fountain codes is especially designed for the MIMO-OFDM system. The key point of this new method is the tradeoff between the code rate of error correcting codes and the number of sub-carriers in the channel vector to be discarded. By transmitting one fountain-encoded packet over a single sub-carrier per antenna, the ADC is allowed to only take care of the sub-carriers with high energy in the channel vector. In such case, the power in the ADC is reduced by quantizing the received signal coarsely. Correspondingly, this approach can afford higher level of noise floor than the joint coding scheme adopted by the current MIMO-OFDM system. In this paper, we evaluate its performance in the aspect of mitigating the noise and interference. At the same code rate, simulation results show that opportunistic error correction works better (i.e. requires lower SNR) than the FEC layers defined in the IEEE 802.11n standard. Comparing to RCPC with interleaving, the SNR gained by opportunistic error correction decreases as the multiplexing gain increases. Furthermore, we evaluate their performance in the real world. This novel approach does not have the same SNR gain in practice as in the simulation, comparing to the FEC layers in the IEEE 802.11n standard. Measurement results show that this new scheme survives in most of the channel conditions (i.e. 92%) with respect to RCPC with interleaving (i.e. 86%) and the LDPC code from the IEEE 802.11n standard (i.e. around 80%).

[4]This section is the submitted paper [82]: *X. Shao and C.H. Slump, "Opportunistic Error Correction for MIMO-OFDM Systems: from Theory to Practice", submitted to IEEE Transactions on Wireless Communications, 2010.*

5.2.1 Introduction

Multiple-Input Multiple-Output (MIMO) technology has attracted a lot of attention in wireless communications, due to its high data rate without additional band-width or transmission power [2] [83] [84] [85]. Combining *Orthogonal Frequency Division Multiplexing* (OFDM) with MIMO enables a relative easy implementation of MIMO systems in the wireless channel [86] [87]. However, the high *Peak-to-Average Power Ratio* (PAPR) is seen as one of its main disadvantages [88] [89]. When signal peaks in the OFDM signal are clipped, all the sub-carriers are affected [90]. Due to the frequency selectivity of the wireless channel, sub-carriers with deep fading can not afford any distortion. Consequently, unreliable communication happens. Therefore, OFDM requires *Analog-to-Digital Converters* (ADCs) with a high dynamic range, especially in MIMO-OFDM systems.

In this paper, we focus on a M $\times$ M MIMO-OFDM system with the maximum multiplexing gain. At the transmitter, we assume that each antenna transmits one data stream and has unity transmission power. At the receiver, the signal arriving at each antenna is the combination of the signals from all the transmit antennas. So, the dynamic range of the ADCs is proportional to the number of antennas M. Besides, the resolution of the ADCs is also proportional to the dynamic range of the M parallel channels (after inverting the effect of the MIMO channel) due to the traditional coding scheme.

To achieve reliable communication at a high data rate, error correction codes have to be employed in MIMO-OFDM systems [91] [28] [92]. Over a finite block length, coding jointly over all the sub-carriers yields a smaller error probability that can be achieved by coding separately over the sub-carriers at the same rate [2]. This theory has been applied in practical SISO-OFDM and MIMO-OFDM systems, such as WLAN and DVB systems [17] [23] [62] [20] [22]. In MIMO-OFDM systems like the IEEE 802.11n system [23], source data is encoded across all the transmit antennas and all the transmission band. The joint coding scheme utilizes the fact that sub-carriers with high-energy can compensate for those with low-energy for the M parallel channels, but its drawback is that each sub-carrier must be decoded. With the joint coding scheme [2], the maximum level of the noise floor (NF) is limited to the dynamic range of the M parallel channels. That shows the resolution of ADCs is proportional to the dynamic range of the channel vector.

The power consumption of ADCs is proportional to the resolution and the sampling rate [12]. Given the same sampling rate, higher resolution ADCs consume more energy. In wireless LAN systems, the ADC can consume up to 50% of the total base-band power budget [11]. Low power-consumption in battery-powered digital MIMO receivers is a highly desired feature. To reduce the power consumption in ADCs, the question we should answer is: *Can we design a system in such a way that sub-carriers with deep fading in the M parallel channels can be ignored but still achieve reliable communication?* Obviously, the joint coding scheme can not solve this problem. But, fountain codes [21] can help us to achieve it.

In this paper, we propose an energy-efficient error correction scheme based on fountain codes to reduce the power consumption in ADCs for MIMO-OFDM systems. Fountain codes can reconstruct the source file by collecting enough packets. It does not matter which packet is received. We only need to receive a certain number of packets. Therefore, we propose to transmit a fountain-encoded packet over a sub-carrier per antenna. Multiple packets are transmitted simultaneously, using frequency division multiplexing and spacial division multiplexing. Because of fountain codes, the receiver does not have to take care of all the parts of the M parallel channels. So, the receiver discards the sub-carriers with deep fading and recovers the source data by only collecting the well-received packets from high-energy sub-carriers. With this approach, the quantization of the ADCs can be coarse. Correspondingly, this novel coding scheme can afford a higher noise floor level.

In this paper, we investigate the performance of opportunistic error correction with respect to mitigating noise and interference. It will be verified over the TGn[5] MIMO channel model [94] in C++ simulation. However, C++ simulation, with its highly accurate double-precision numerical environment, is on the one hand a perfect tool for the investigation of the algorithms. On the other hand, many imperfections of the real-world are neglected. So, simulation may show a too optimistic receiver performance. The uncertainties in the real life are mainly simplified assumptions in the simulation like perfectly known noise levels, additive Gaussian noise, omitted synchronization, etc. Therefore, we also will evaluate the performance of the opportunistic error correction scheme in the real-world.

The outline of this paper is as follows. We first discuss the advantages and disadvantages between the joint coding scheme and the separate coding scheme for the MIMO-OFDM channel. Then, opportunistic error correction is depicted in Section 5.2.3. In Section 5.2.4, we describe the system model by showing how we apply this novel coding scheme in MIMO-OFDM systems. After that, we compare its performance with the *Forward Error Correction* (FEC) layers from the IEEE 802.11n standard [23] over a TGn channel in the simulation. Furthermore, we evaluate its performance in the practical system. The paper ends with a discussion of the conclusions.

5.2.2 Coding over MIMO-OFDM Channels

MIMO systems increase the capacity of rich scattering wireless channels enormously by using multiple antennas at both the transmitter and the receiver [95] [96]. The wireless channel is a hostile environment and often modeled as a frequency selective fading channel. Combining MIMO with OFDM provides an effective solution to frequency selective fading channels. MIMO-OFDM transforms a frequency selective MIMO system into a number of flat fading MIMO systems on different sub-carriers.

[5]The TGn channel model is used by the High Throughput Task Group [93]. "TG" stands for Task Group and "n" stands for the IEEE 802.11n standard.

Still, to achieve reliable communication at a high data rate, error correction codes are required in MIMO-OFDM systems.

In MIMO-OFDM systems, decoding is done after the effect of the MIMO channel is inverted. Correspondingly, coding is performed in the frequency domain of the M parallel channels. Whether source bits are encoded jointly or separately over all the sub-carriers of the channel vector depends on the transmission scheme. There are two schemes to transmit an encoded packet [97]:

- **Scheme I** is to transmit a packet over all the transmitted antennas and over all the sub-carriers like the IEEE 802.11n standard. In such a case, the coding is jointly over all the sub-carriers of those M parallel channels.

- **Scheme II** transmits a packet over a single sub-carrier per antenna. Using this scheme, the coding is carried out separately over all the sub-carriers of the channel vector.

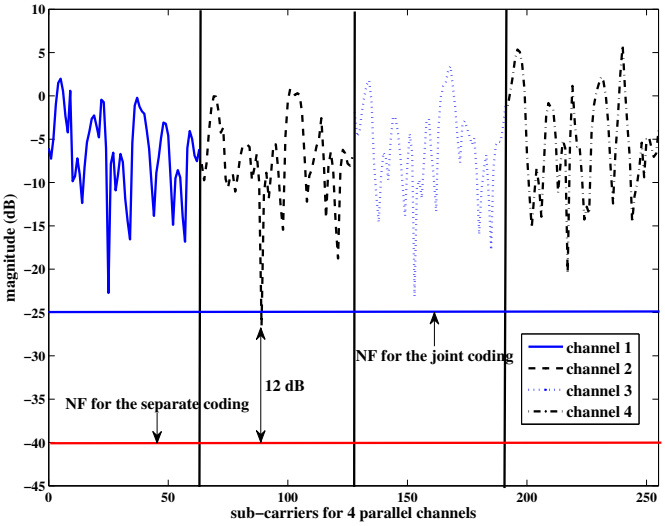

Fig. 5.6: The difference in the required NF between the joint coding scheme and the separate coding scheme.

For a finite block length, coding jointly over all the sub-carriers yields a smaller error probability than can be achieved by coding separately at the same rate [2]. Using the joint coding scheme, sub-carriers with high energy can compensate for those in deep fading. The maximum NF endured by the joint coding is limited to the dynamic range of the M parallel channels, while the maximum NF for the separate coding scheme depends on the sub-carrier with the lowest energy. Let us take an example to show their difference in the required NF. Assume that some encoded packets are

transmitted over a 4×4 channel as shown in Figure 5.6 and that a packet is received correctly when the SNR $\geq$ 12 dB. In this example, the maximum NF for the joint coding is -25 dB. For the separate coding, the maximum NF is determined by the sub-carrier with the lowest energy (i.e. -40 dB in this example). This shows the joint coding scheme performs better than the separate coding scheme in the same NF [2]. Therefore, the current MIMO-OFDM systems utilize the joint coding scheme such as the IEEE 802.11n system [23].

However, the joint coding scheme is not energy-efficient. With this coding method, it is not beforehand known whether the received packet is decodable with a high probability or not at all, which may lead to a waste of processing power. This does not happen in the separate coding scheme, since each sub-carrier can be modeled as a flat fading channel. With the separate coding scheme, the receiver is able to process the well-received packets. Also, because each sub-carrier is considered to be equally important, the NF in the joint coding scheme is limited to the dynamic range of the channel ($\mathcal{D}$). Higher $\mathcal{D}$ means lower NF. Correspondingly, higher resolution ADCs need to be used. If we are allowed to discard sub-carriers with deep fading, the NF can be further increased. In such a case, the received signal can be quantized coarsely. To achieve this, we propose a novel cross coding scheme based on fountain codes which will be explained in the next section.

5.2.3 Opportunistic Error Correction

Opportunistic error correction is based on fountain codes. A fountain code has a similar property as a fountain of water: when you fill a cup from the fountain, you do not care about what drops of water fall in, but you only want that your cup fills enough to quench your thirst [80]. In other words, fountain-encoded packets are independent with respect to each other. Fountain codes are designed for erasure channels. To apply fountain codes in wireless channels, good error correction codes should be used to make noisy wireless channels behave like an erasure channel. The key point of opportunistic error correction is to trade the code rate of error correction codes with the sub-carriers in deep fading over M parallel channels. By using an error correcting code with a relatively high code rate to encode one fountain-encoded packet and transmitting it over a single sub-carrier per antenna, some parts of the channel vector with deep fading can be discarded. That corresponds to a reduction in the dynamic range of the channel vector. Consequently, lower resolution ADCs can be used in comparison to the joint coding scheme. Besides, using Scheme II to transmit fountain-encoded packets gives the advantage of the separate coding scheme (i.e. saving the processing power).

Figure 5.7 shows how opportunistic error correction works in MIMO-OFDM systems. With a fountain code, the transmitter can generate a potentially infinite supply of fountain-encoded packets. In this paper, the transmitter generates N_t fountain-encoded packets. Each packet is encoded by an error correction code to convert the

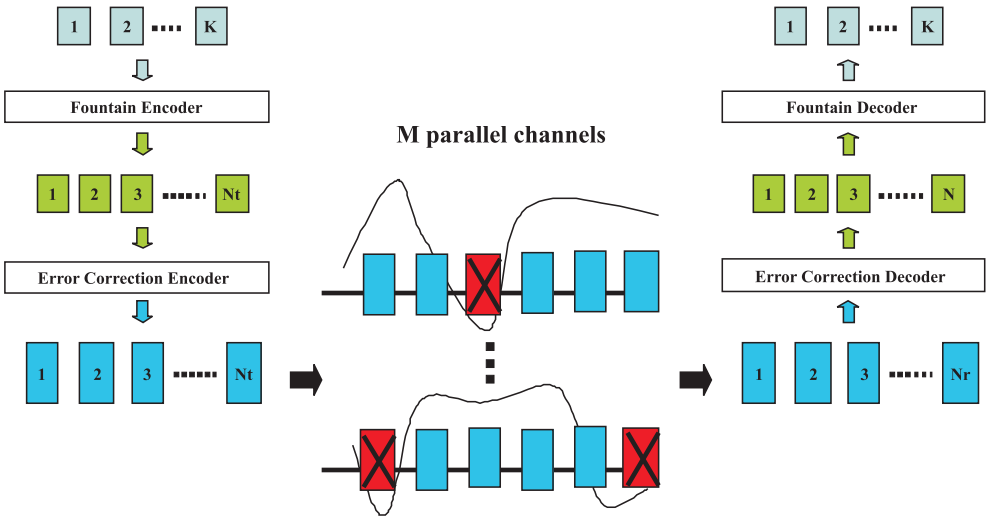

Fig. 5.7: Opportunistic error correction for an M × M MIMO-OFDM system.

wireless channels into erasure channels. After that, each packet is transmitted over a single sub-carrier per antenna. Multiple packets are transmitted simultaneously, using frequency division multiplexing and spacial division multiplexing. For MIMO-OFDM systems, decoding is always done after inverting the effect of the MIMO channel. Equivalently, fountain-encoded packets are transmitted over a single sub-carrier of the channel vector.

At the receiver, the channel vector is first estimated. With the channel knowledge, the receiver makes a decision about which packet can go through the whole receiving chain. We assume that N_r ($N_r \leq N_t$) fountain-encoded packets can go through the error correction decoding. Packets only survive if they succeed in the error correction decoder. The number of fountain-encoded packets N ($K < N \leq N_r$) required at the fountain decoder is slightly larger than the number of source packets K:

$$N = (1 + \varepsilon)K \tag{5.13}$$

where ε is the percentage of extra packets and called the overhead.

The mathematical principle behind the fountain decoding is to solve K unknown parameters from N linear equations. It can be solved by Gaussian elimination which has a high complexity. Therefore, the message-passing algorithm [54] is usually chosen to decode fountain codes. The message-passing algorithm has a linear computation cost [42], but it requires a larger ε for small block size. For example, the practical overhead of LT codes is 14% when $K = 2000$, which limits its application in the practical system [40]. By combining message-passing algorithm with Gaussian elimination, the

overhead of LT codes is reduced to 3% when $K \geq 500$ [40].

In this paper, we use *Luby-Transform* (LT) codes [43] as fountain codes and the (175,255) LDPC code [74] with a 7-bit *Cyclic Redundancy Check* (CRC) [75] as error correction codes in the proposed opportunistic error correction. This new scheme is generic. Any fountain codes can be used (e.g. Raptor codes [81] and online codes [72]). Also, any error correction code (e.g. Turbo codes [98]) can be applied in it. To have a small ε for small K, we choose to decode LT codes by combing the message passing algorithm and Gaussian elimination in this paper.

5.2.4 System Model

The opportunistic error correction scheme is based on fountain codes which have been explained in the above section. This novel method can be applied in the MIMO-OFDM system. In this paper, we take the IEEE 802.11n system as an example of MIMO-OFDM systems.

The current IEEE 802.11n standard gives two options for the FEC layer. One is based on *Rate Compatible Punctured Codes* (RCPC) and the other one is based on LDPC codes [65] [66] [67]. RCPC has good performance for random bit errors but performs less for burst bit errors. So, interleaving is applied before the RCPC encoding to reduce burst bit errors. Each encoded packet is transmitted based on Scheme I. Although this solution works well in practice, it is not optimal from the power consumption point of view:

- The maximum level of NF (i.e. the lowest resolution of ADCs) is limited to the dynamic range of the parallel channel vector.
- Packets encountered by a "bad" channel are still processed by the receiver.

Those problems can be solved by using opportunistic error correction, as shown in Figure 5.8. The key idea is to generate additional packets by the fountain encoder and transmit each packet over a single sub-carrier per antenna. In such case, the dynamic range of the parallel channel vector can be reduced by discarding the sub-carriers with deep fading. Besides, the receiver does not have to process all the packets but only the well-received packets.

At the transmitter, the source file is first divided into a set of source packets which are encoded by a LT code. Then, each fountain-encoded packet is added by a 7-bit CRC checksum and encoded by the (175,255) LDPC code. Afterwards, they are mapped into complex symbols before the OFDM modulation.

The M × M channel output at the n_{th} moment $\mathbf{r}_n = [\mathrm{r}_n^{(1)}, \cdots, \mathrm{r}_n^{(m)}, \cdots, \mathrm{r}_n^{(\mathrm{M})}]$ can be written as:

$$\mathbf{r}_n = \sum_{l=0}^{L-1} \mathbf{h}_l \mathbf{x}_{n-l} + \mathbf{n}_n \tag{5.14}$$

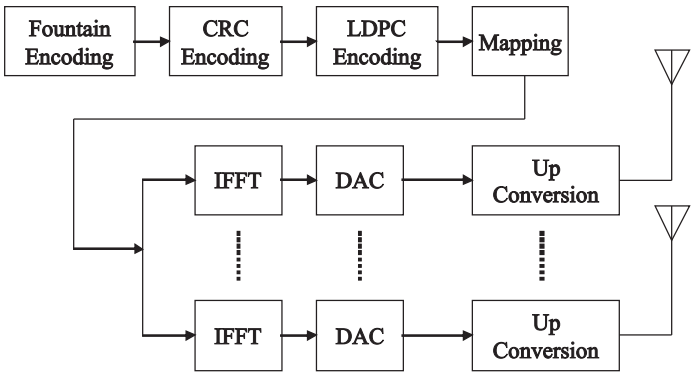

(a) Transmitter

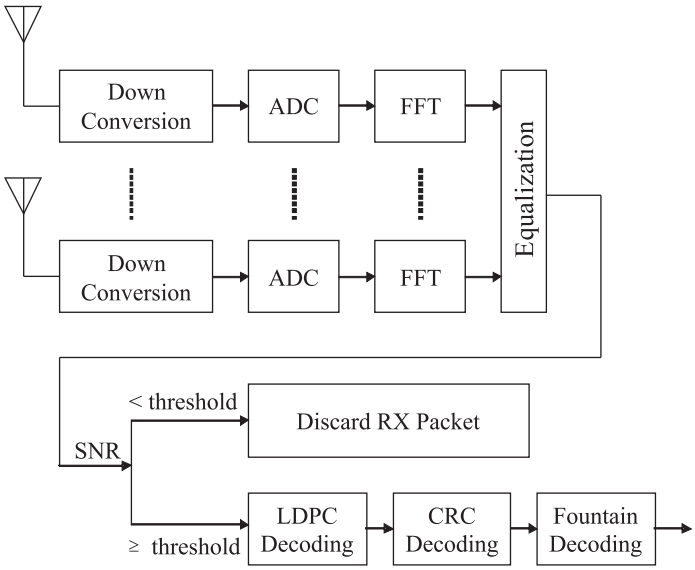

(b) Receiver

Fig. 5.8: The application of opportunistic error correction to the IEEE 802.11n system: the transmitter (top) and the receiver (bottom).

where $\mathbf{x} = [\mathrm{x}^{(1)}, \cdots, \mathrm{x}^{(m)}, \cdots, \mathrm{x}^{(\mathrm{M})}]$ is the transmitted vector, $\mathbf{h}_l$ is the $\mathrm{M} \times \mathrm{M}$ channel matrix at the l_{th}-path and L is the number of channel paths. From [18], we know that $\mathrm{x}^{(m)}$ can be modeled as a Gaussian-distributed random variable with zero mean and a variance of 1. The elements in $\mathbf{x}$ are mutual independent, so it has zero mean and a unity covariance matrix. In addition, $\mathbf{x}_n$ and $\mathbf{x}_{n'}$ are mutual independent if $n \neq n'$. $\mathbf{n}_n$ is the channel noise vector (including the quantization noise, the thermal noise and the interference) in the time domain. We assume that the elements in $\mathbf{n}_n$ are mutual independent, so it has zero mean and a covariance matrix of $\sigma^2\mathbf{I}$. Therefore,

the SNR of the signal at the m_{th} received signal is defined as:

$$\text{SNR}_{\text{r}_n^{(m)}} = \frac{\text{M}}{\sigma^2} \tag{5.15}$$

Given the same $\text{SNR}_{\text{r}_n^{(m)}}$, the level of NF (i.e. σ^2) increases by 3 dB if M doubles.

At the receiver, synchronization and channel estimation can be done using the preambles and the pilots, which are defined in [23]. In this paper, we use the *zero forcing* algorithm [99] to estimate the channel. Each sub-carrier can be considered as a narrow-band MIMO channel:

$$\mathbf{Y}_k^p = \mathbf{H}_k \mathbf{X}_k^p + \mathbf{N}_k^p \tag{5.16}$$

where $\mathbf{X}_k^p = [\text{X}_k^{p(1)}, \cdots, \text{X}_k^{p(\text{M})}]$ is the preamble at the k_{th} sub-carrier and $\mathbf{N}_k^p = [\text{N}_k^{p(1)}, \cdots, \text{N}_k^{p(\text{M})}]$ is the noise in the frequency domain:

$$\mathbf{N}_k^p = \frac{1}{\sqrt{\text{N}}} \sum_n \mathbf{n}_n^p e^{-j\frac{2\pi}{\text{N}}nk} \tag{5.17}$$

where N is the number of sub-carriers. According to the *Central Limit Theorem*, $\text{N}_k^{p(m)}$ is Gaussian-distributed with zero mean and a variance of σ^2 [79]. $\mathbf{H}_k$ is the fading matrix at the k_{th} sub-carrier defined by:

$$\mathbf{H}_k = \sum_{l=0}^{L-1} \mathbf{h}_l e^{-j\frac{2\pi}{\text{N}}lk} \tag{5.18}$$

which can be estimated by the zero-forcing algorithm as [2]:

$$\begin{aligned} \hat{\mathbf{H}}_k &= \mathbf{Y}_k^p \mathbf{X}_k^{p\dagger} \\ &= \mathbf{H}_k + \mathbf{N}_k^p \ \mathbf{X}_k^{p\dagger} \end{aligned} \tag{5.19}$$

where $\mathbf{X}_k^{p\dagger}$ is the pseudoinverse of the matrix $\mathbf{X}_k^p$.

In order to detect the transmitted symbol from each transmitted antenna, equalization needs to be done. In this paper, the zero-forcing algorithm is used to invert the effect

of the MIMO channel:

$$\begin{aligned}\hat{\mathbf{X}}_k &= \hat{\mathbf{H}}_k^{\dagger}\mathbf{Y}_k \\ &= \left(\mathbf{H}_k + \mathbf{N}_k^p\ \mathbf{X}_k^{p\dagger}\right)^{\dagger}(\mathbf{H}_k\mathbf{X}_k + \mathbf{N}_k)\end{aligned} \tag{5.20}$$

With the perfect channel estimation, the above equation can be simplified as:

$$\hat{\mathbf{X}}_k = \mathbf{X}_k + \mathbf{H}_k^{\dagger}\mathbf{N}_k \tag{5.21}$$

Thus, for the symbol $\hat{\mathrm{X}}_k^{(m)}$ from the m_{th} antenna at the k_{th} sub-carrier, its *Signal-to-Noise Ratio* (SNR) can be derived as:

$$\mathrm{SNR}_k^{(m)} = \left(\sigma^2 \sum_{s=0}^{M-1} \left|\mathbf{H}_k^{\dagger\,(m,s)}\right|^2\right)^{-1} \tag{5.22}$$

In such a case, the receiver can decide which packets should go through the receiving chain. Only if its SNR is equal to or above the threshold, the received packet will go through the LDPC decoder otherwise it will be discarded. Correspondingly, the processing power can be reduced.

However, the channel estimation and the equalization are based on the zero-forcing algorithm whose accuracy and complexity are low. In such a case, the receiver can hardly predict correctly whether the received packet is decodable with a high probability, as we can see in Equation 5.20 by the presence of the term $\mathbf{N}_k^p\ \mathbf{X}_k^{p\dagger}$. That degrades its performance. To avoid it, the receiver will process all the fountain-encoded packets with non-perfect channel estimation. The received packets can only survive if they pass the LDPC decoder and the CRC decoder successfully. When the receiver collects enough fountain-encoded packets, it starts to recover the source data by using the message-passing algorithm and Gaussian elimination algorithm.

5.2.5 Performance Analysis in Simulations

In this section, we analyze the performance of opportunistic error correction scheme in MIMO-OFDM systems by comparing the following FEC schemes:

- FEC I: RCPC with interleaving from the IEEE 802.11n standard.
- FEC II: LDPC codes from the IEEE 802.11n standard with $n = 648$.
- FEC III: opportunistic error correction.

The IEEE 802.11n system is taken as an example of MIMO-OFDM systems. 52 subcarriers are used to transmit data as defined in [23]. To have the same code rate (i.e. $R = 0.5$), FEC III is allowed to discard around 21%[6] in the simulation. For each simulation point, we transmit more than 1000 bursts of data (i.e. more than 100 million bits) over a 20 MHz downlink TGn channel. Each burst consists of 630 source packets with a length of 168 bits. The source file is encoded by FEC I, II and III, respectively. With FEC III, each burst is encoded by a LT code (with parameter $c = 0.03$, $\sigma = 0.3$) and decoded by the message-passing algorithm and Gaussian elimination together. Only 3% overhead is required to reconstruct the original data successfully [40]. To each fountain-encoded packet, a 7-bit CRC is added before the (175,255) LDPC encoding is applied. Before the OFDM modulation, the encoded bits are mapped into QAM-16 symbols.

In total, we compare them in three types of MIMO-OFDM systems: the 2×2 system, the 4×4 system and the 8×8 system. Figure 5.9 shows the simulation results with perfect synchronization and channel estimation. From this figure, we can see the follows.

- In the case of FEC I, it has a BER of 10^{-5} or lower when SNR $\geq$ 31.5 dB in the 2×2 system, SNR $\geq$ 34.5 dB in the 4×4 system and SNR $\geq$ 38 dB in the 8×8 system. FEC I has a SNR loss of around 3 dB when M doubles. Given the same level of noise floor, Equation 5.15 shows that SNR increases by 3 dB if M doubles. Hence, the maximum NF endured by FEC I is not affected if the multiplexing gain doubles.

- In the case of FEC II, it reaches a BER of 10^{-5} or lower when SNR $\geq$ 34 dB in the 2×2 system, SNR $\geq$ 37.5 dB in the 4×4 system and SNR $\geq$ 46.5 dB in the 8×8 system. When M increases from 2 to 4, FEC II could survive in the same NF to achieve a BER of 10^{-5} or lower (i.e. a SNR gain loss of around 3.5 dB). However, the maximum NF in the 8×8 system has to be 6 dB lower than in the 4×4 system for FEC II to have a BER of 10^{-5} or lower.

- In the case of FEC III, it can achieve error free when SNR $\geq$ 24 dB in the 2×2 system, SNR $\geq$ 31 dB in the 4×4 system and SNR $\geq$ 36 dB in the 8×8 system. FEC III loses more than 3 dB when M doubles. To have the error-free quality, the maximum NF for FEC III has to be decreased as M increases. When M changes from 2 to 4, NF has to be decreased by 4 dB. When M doubles from 4 to 8, NF has to be decreased by 2 dB.

- With respect to FEC I, FEC III has a SNR gain of around 8.5 dB in the 2×2 system, around 4.5 dB in the 4×4 system and around 2.5 dB in the 8×8 system. The SNR gain decreases with M.

- In comparison with FEC II, FEC III has a SNR gain of around 10 dB in the 2×2

[6] $21\% \approx 1 - \frac{R}{R_1 \times R_2}$, where R is the effective code rate (i.e. 0.5), R_1 is the code rate of LT codes (i.e. $\frac{1}{1.03} \approx 0.97$) and R_2 is the code rate of the (175,255) LDPC code with 7-bit CRC (i.e. $\frac{168}{255} \approx 0.66$)

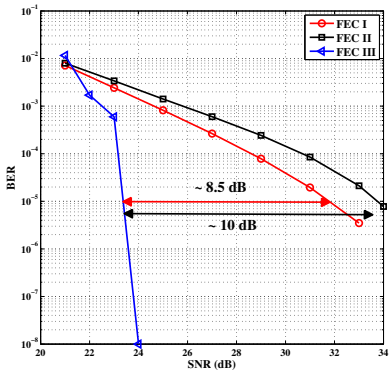

(a) 2-by-2 with perfect H

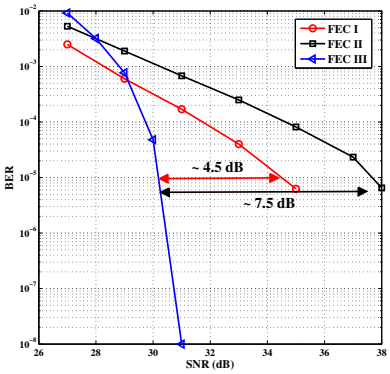

(b) 4-by-4 with perfect H

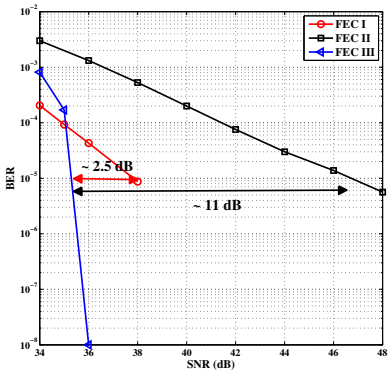

(c) 8-by-8 with perfect H

Fig. 5.9: Performance comparison between FEC I, II and III at $R = 0.5$ over the TGn channel at 20 MHz. We compare them in three systems: the 2×2 system, the 4×4 system and the 8×8 system. FEC III can achieve error-free when the fountain decoder received enough fountain-encoded packets. We represent BER $= 0$ by 10^{-8} in the above figures

system, around 7.5 dB in the 4×4 system and around 11 dB in the 8×8 system. The SNR gain decreases when M increases from 2 to 4 and increases as M changes from 4 to 8.

The maximum NF endured by FEC I is not affected by M; while the maximum NF for FEC III has to be decreased as M increases. Still, FEC III requires lower SNR than FEC I and II to achieve BER $\leq 10^{-5}$ in three MIMO-OFDM systems. Therefore, we can conclude that opportunistic error correction (i.e. FEC III) works best in those three types of MIMO-OFDM systems comparing to the joint coding scheme (i.e. FEC I and II) in the IEEE 802.11n standard.

5.2.6 Practical Evaluation

The C++ simulation results in the above section show the performance of opportunistic error correction in comparison to the joint coding scheme (i.e. FEC I and II) for three types of MIMO-OFDM systems. However, simulation may show a too optimistic receiver performance. In this section, we evaluate its performance in practice to investigate whether opportunistic error correction is more robust to the real-world's imperfections.

5.2.6.1 System Setup

The practical experiments are done in the experimental communication testbed designed and realized by Signals and Systems Group [100], University of Twente, as shown in Figure 5.10. It is a 2×2 MIMO system, which is assembled as a cascade of the following modules: PC, DACs, RF up-converters, power amplifiers, antennas, and the reverse chain for the receiver. In the receiver, there are no power amplifiers and band-pass RF filters before the down-converters but two low-pass baseband filters before the ADCs to remove the aliasing.

- **The Transmitter**

  The data is generated offline in C++. The generation consists of the random source bits selection, the FEC encoding and the digital modulation as we depict in Section 5.2.4. The generated data is stored in a file. A server software in the transmit PC uploads the file to the Adlink PCI-7300A board[7] which transmits the data to DAC (AD9761)[8] via the FPGA board. After the DAC, the baseband analog signal is upconverted to 2.3 GHz by a Quadrature Modulator (AD8346)[9] and transmitted using two conical skirt monopole antennas.

- **The Receiver**

  The reverse process takes place in the receiver. The received RF signal is first downconverted by a Quadrature Demodulator (AD8347)[10], then passes the 8-th order low-pass Butterworth analog filter to remove the aliasing. The baseband analog signal is quantized by the ADC (AD9238)[11] and stored in the receive PC via the Adlink PCI board.

  The received data is processed offline in C++. The receiver should synchronize with the transmitter and estimate the channel using the preambles and the pilots, which

[7] ADLINK, 80 MB/s High-Speed 32-CH Digital I/O PCI Card
[8] Analog Devices, 10-Bit, 40 MSPS, dual Transmit D/A Converter.
[9] Analog Devices, 2.5 GHz Direct Conversion Quadrature Modulator.
[10] Analog Devices, 800 MHz to 2.7 GHz RF/IF Quadrature Demodulator
[11] Analog Devices, Dual 12-Bit, 20/40/65 MSPS, 3V A/D Converter.

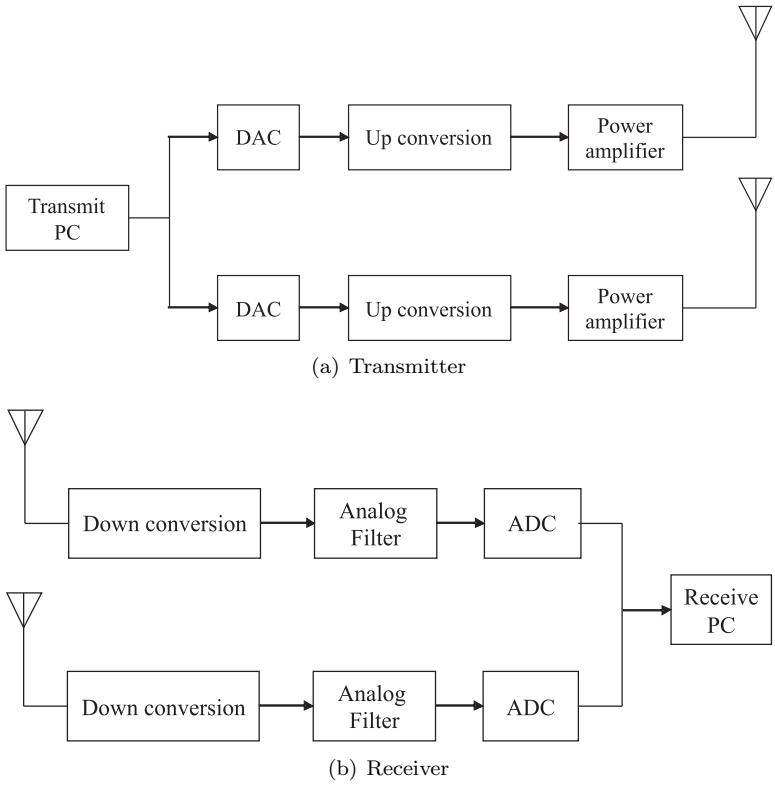

Fig. 5.10: Block diagram of the 2×2 MIMO testbed.

are defined in [23]. Timing and frequency synchronization is done by the Schmidl & Cox algorithm [55] and the channel is estimated by the *zero forcing* algorithm. In addition, the *residual carrier frequency offset* is estimated by the four pilots in each OFDM symbol [101]. Before the decoding starts, the effect of the MIMO channel has to be inverted with the estimated channel knowledge. As shown in Equation 5.20, the real SNR of $\hat{\mathbf{X}}_k$ can not be estimated reliably. That degrades the performance of opportunistic error correction if we only process the packets with a high estimated SNR. Hence, we process all the received fountain-encoded packets in practice.

5.2.6.2 Experiment Setup

Experiments are carried out in the corridor of Signals and Systems Group, located at the 9th floor of Building Hogekamp in University of Twente, the Netherlands. The experiment setup is shown in Fig. 5.11. The transmitter (TX) was positioned in front of the elevator (i.e. one of the circle positions in Fig. 5.11), while the receiver antenna

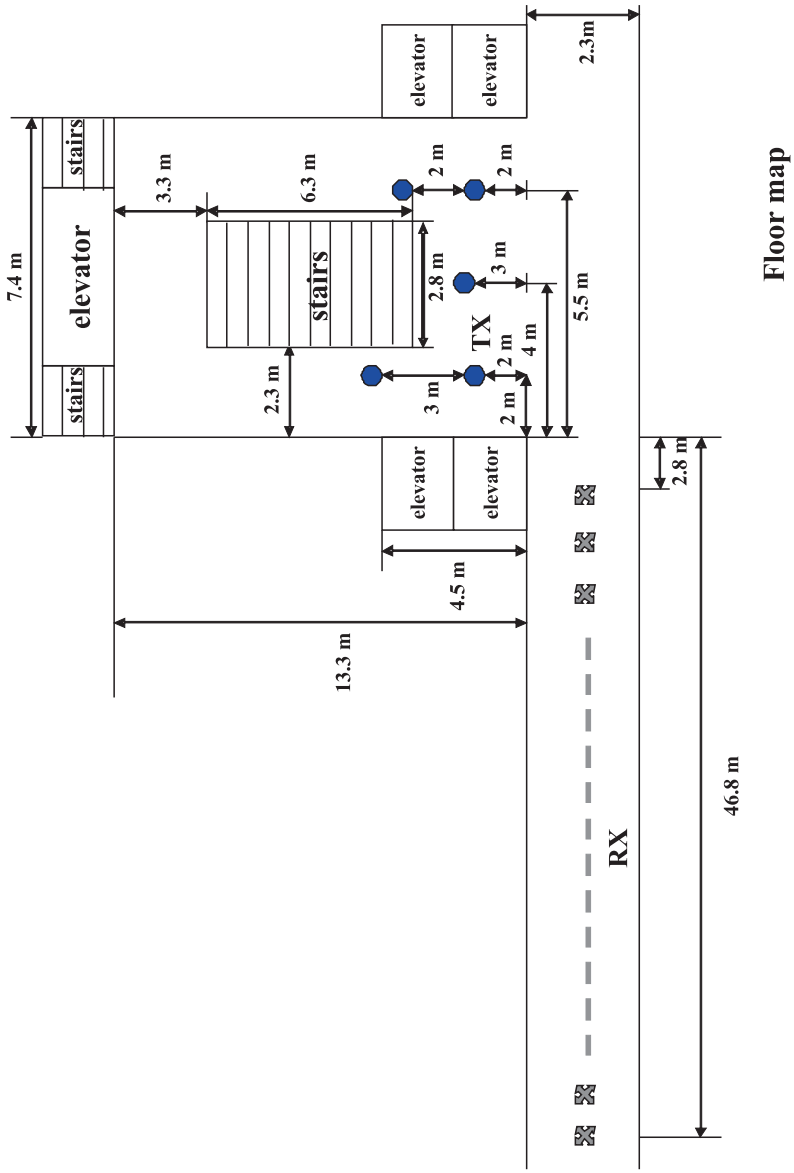

Fig. 5.11: Experiment Setup: antennas are 0.9 m above the concrete floor. The experiments are done in the corridor of the Signals and Systems Group. The receiver is positioned at left side of the corridor (i.e. the cross positions) and the transmitter is at the circle positions as shown in the figure. The hall contains one coffee machine, one garbage bin and one glass cabin.

(RX) was in the left side of the corridor (i.e. the cross positions in Fig. 5.11). 180 experiments were done in this scenario with a non-line-of-sight situation. The average

transmitting power is around -10 dBm and the distance between the transmitter and the receiver is around $6 \sim 52.5$ meters. The experiments were conducted at 2.3 GHz carrier frequency and 10 MHz bandwidth[12].

In Section 5.2.5, these FEC schemes have been compared in the C++ simulation. In the simulation, they can be compared by using the same source bits. Different channel bits can go through the same random frequency selective channels. However, it does not apply in the real environment. The wireless channel is time-variant even when the transmitter and the receiver are stationary (e.g. the moving of the elevator with the closed door can affect the channel). Hence, we should compare them by using the same channel bits.

Because not every stream of random bits is a codeword of a certain coding scheme, it is not possible to derive its corresponding source bits from any sequence of random bits, especially for the case of FEC I and FEC III. Fortunately, the decoding of FEC II is based on the parity check matrix. Any stream of random bits can have its unique sequence of source bits with its corresponding syndrome matrix. The receiver can decode the received data based both on the parity check matrix and the syndrome matrix. So, FEC I can use the same channel bits with FEC II, same for FEC II and FEC III. In such case, they can be compared under the same channel condition (i.e. channel fading, channel noise and the distortion caused by the hardware.). During the experiments, both sequences of channel bits are transmitted in one burst (i.e. 2 blocks) in order to have their channels as similar as possible.

In the experiments, we transmit more than 2500 blocks of source packets over the air. Each block consists of 105840 source bits. The source bits are encoded by FEC I and III, respectively. The encoded bits are shared with FEC II as just explained. Afterwards, they are mapped into QPSK[13] symbols before the OFDM modulation.

Each experiment corresponds to the fixed position of the transmitter and the receiver. It is possible that some experiments might fail in decoding. Due to the lack of the feedback channel in the testbed, no retransmission can occur. In this paper, we assume that the experiment fails if the received data per measurement has a BER higher than 10^{-3} by using FEC I and II. For the case of FEC III, if the packet loss is more than 21% as expected, we assume that the experiment fails.

[12] Due to the limit of the testbed, 10 MHz is the maximum bandwidth for the 2×2 system.

[13] Choosing QPSK instead of QAM-16 in the experiments is due to the limit of the testbed, whose minimum noise floor is around -25 dB (i.e. the maximum SNR $\approx$ 25 dB). Figure 5.9 shows that the required SNR for the 2×2 system should be at least 24 dB for FEC III to achieve error free. For FEC I and II, the required SNR is even higher to have a BER of 10^{-5} or lower. With the non-perfect synchronization and channel estimation, a higher SNR is expected in the real world than in the simulation to achieve the same order of BER. Therefore, we choose a lower order of modulation scheme to have more successful experiments to compare FEC I, II and III in the real world.

5.2.6.3 Experiment Results

In total, 180 experiments have been done. There are 14 blocks of data transmitted over each experiment: 7 blocks for FEC I and II and 7 blocks for FEC II and III. As mentioned earlier, the wireless channel is time-variant even when the transmitter and receiver are placed at the same position. So, we are going to analyze the experiments for FEC I and II and those for FEC II and III separately.

- **FEC I vs. FEC II**

  Not every experiment succeeds in decoding. FEC I fails in 14% of experiments while FEC II fails in 21% of experiments, as we can see in Figure 5.12. This concludes that FEC I works in more channel conditions than FEC II.

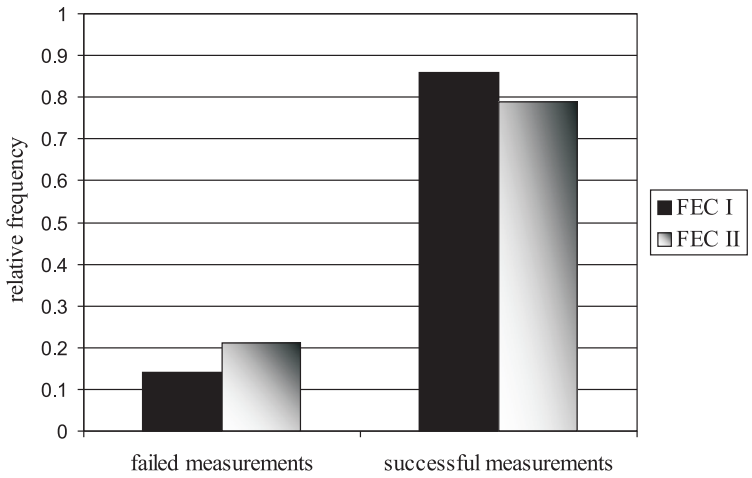

Fig. 5.12: Histogram of the experiment results for FEC I and II. By using FEC I, around 14% of experiments are failed. For the case of FEC II, around 21% of experiments are failed.

Both FEC schemes succeeds in 142 experiments, where the SNR of the signal at two receive antennas ranges from 17 dB to 25 dB. In order to investigate whether FEC I can endure higher NF than FEC II as shown in the simulation results, we add extra white noise to the received signal in the software. It is difficult to have the same SNR range in all measurements, so we evaluate the practical performance by analyzing the statistical characteristics of experiment results. Here, we define $\mathrm{SNR_I}$ as the minimum SNR for FEC I and $\mathrm{SNR_{II}}$ as the minimum SNR for FEC II to reach a BER of 10^{-3} or lower. The difference between $\mathrm{SNR_{II}}$ and $\mathrm{SNR_I}$ is expressed as:

$$\Delta_1 = \mathrm{SNR_{II}} - \mathrm{SNR_I} \tag{5.23}$$

If $\Delta_1 > 0$ (i.e. $\text{SNR}_{\text{II}} > \text{SNR}_{\text{I}}$), FEC II needs higher SNR (i.e. lower level of NF) to achieve BER $< 10^{-3}$ than FEC I. $\Delta_1 < 0$ is for the opposite case.

Figure 5.13 shows the statistical characteristics of SNR_{I}, SNR_{II} and Δ_1. Both SNR_{I} and SNR_{II} have a wide range: $\text{SNR}_{\text{I}} \in [10, 24]$ dB and $\text{SNR}_{\text{II}} \in [9, 25]$ dB. This presents that different channel condition requires different NF to achieve BER $< 10^{-3}$. In the simulation, all the channel conditions have the same level of NF. Given the same NF (i.e. SNR) in those 142 experiments, SNR_{I} should be 24 dB and SNR_{II} needs to be 25 dB to have all those experiments with BER $< 10^{-3}$. In this case, FEC I has a SNR gain of 1 dB over FEC II. Furthermore, Figure 5.13(b) shows whether FEC I performs better than FEC II in every experiment. Δ_1 ranges from -2 dB to 5 dB. Around 86% of experiments have Δ_1 within 1 dB. The average Δ_1 is around 0.06 dB. That leads to the following conclusion. In comparison with FEC II, FEC I has a SNR gain of 1 dB with the same NF in all experiments (i.e. 142 experiments) and an average SNR gain of around 0.06 dB when every experiment has its own maximum NF.

- **FEC II vs. FEC III**

Figure 5.14 is the statistical analysis of the experiment data shared by both FEC II and III. From this figure, we can see that FEC II fails in 19% of experiments and FEC III fails only in 8% of experiments. Figure 5.12 and 5.14 presents that opportunistic error correction (i.e. FEC III) survives in more channel conditions than the joint coding scheme (i.e. FEC I and II).

FEC II and III succeeded in 145 experiments. In those experiments, the SNR of the signal at two receive antennas ranges from 17 dB to 25 dB. Same as the above section, we add extra white noise to the received signal in the software. We define SNR_{III} as the minimum SNR for FEC III to reach the error-free quality. The difference between SNR_{II} and SNR_{III} is expressed as:

$$\Delta_2 = \text{SNR}_{\text{II}} - \text{SNR}_{\text{III}} \tag{5.24}$$

If $\Delta_2 > 0$ (i.e. $\text{SNR}_{\text{II}} > \text{SNR}_{\text{III}}$), FEC II needs higher SNR (i.e. lower level of NF) to achieve BER $< 10^{-3}$ than FEC III to have the error-free quality. $\Delta_2 < 0$ is for the opposite case.

Figure 5.15 shows the statistical characteristics of SNR_{II}, SNR_{III} and Δ_2. SNR_{II} and SNR_{III} have a wide range: $\text{SNR}_{\text{II}} \in [9, 24]$ dB and $\text{SNR}_{\text{III}} \in [11, 24]$ dB. The maximum values of SNR_{II} and SNR_{III} are the same (i.e. 24 dB). Hence, with the same NF in those 145 experiments, FEC III has no SNR gain comparing to FEC II. However, the minimum SNR_{II} is 9 dB but the minimum SNR_{III} is 11 dB. That means that FEC II requires less SNR to achieve BER $< 10^{-3}$ than FEC III to reach error free in some experiments. Figure 5.15(b) presents whether FEC II performs

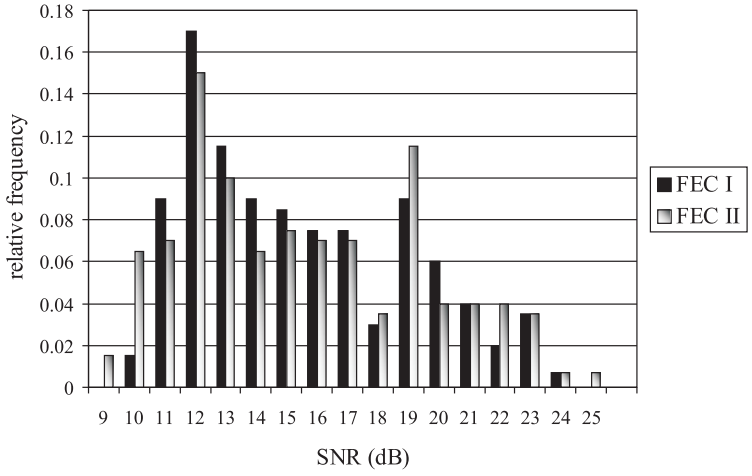

(a) Histogram of $\mathrm{SNR_I}$ and $\mathrm{SNR_{II}}$.

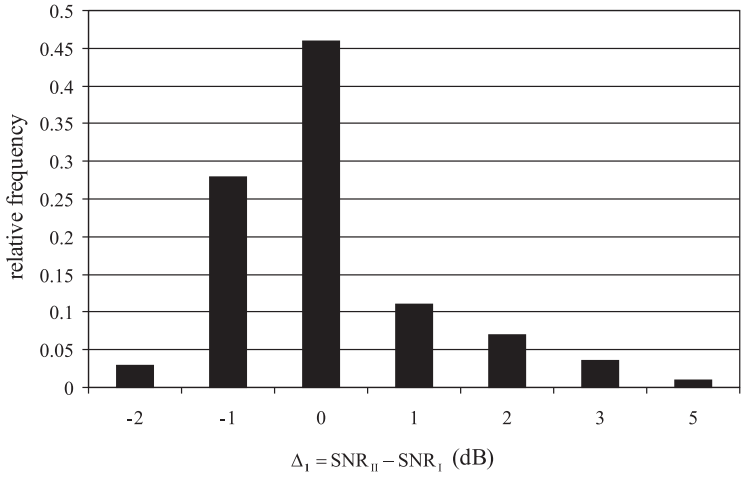

(b) Histogram of Δ_1.

Fig. 5.13: Histogram of $\mathrm{SNR_I}$, $\mathrm{SNR_{II}}$ and Δ_1.

better than FEC III in every experiment. Δ_2 ranges from -3 dB to 6 dB. Around 78% of experiments have Δ_2 in the range of $[-2, 0]$ dB, which means that FEC II does not require higher SNR than FEC III to reach the required BER. On average, Δ_2 is around -0.4 dB. Therefore, we can conclude that FEC III can survive in more channel conditions than FEC II, but the average SNR required by FEC III

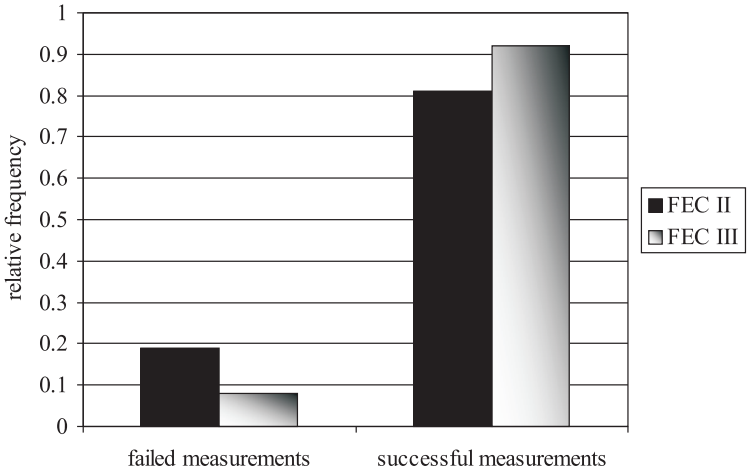

Fig. 5.14: Histogram of the experiment data for FEC II and III. By using FEC II, around 19% of experiments are failed. For the case of FEC III, around 8% of experiments are failed.

is larger than FEC II in the successful experiments.

5.2.7 Conclusions

Opportunistic error correction based on fountain codes is designed for MIMO-OFDM systems to reduce the power consumption in ADCs. Fountain codes are designed for erasure channels. To apply fountain codes to the wireless channel, error correcting codes have to be used in every fountain-encoded packet. The key idea of this scheme is the tradeoff between the code rate of error correcting codes and the sub-carriers in deep fading. By transmitting a fountain-encoded packet over a single sub-carrier per antenna, fountain codes can reconstruct the original file by only using the packets transmitted over the sub-carriers with high-energy. In such case, the ADC does not have to take care of each part of those M parallel channels. The received signal can be quantized coarsely. The coarse quantization means a higher level of noise floor.

In this paper, we have investigated its performance over the TGn channel in the aspect of mitigating the noise and the interference. In the simulation, we compare three FEC layers in different MIMO-OFDM systems with the same coding rate (i.e. $R = 0.5$) and the modulation scheme (i.e. QAM-16): RCPC with interleaving from the IEEE 802.11n standard (i.e. FEC I), the (324,648) LDPC code from the IEEE 802.11n standard (i.e. FEC II) and opportunistic error correction based on fountain codes (i.e. FEC III). FEC III works better than FEC I and II in the simulation. With

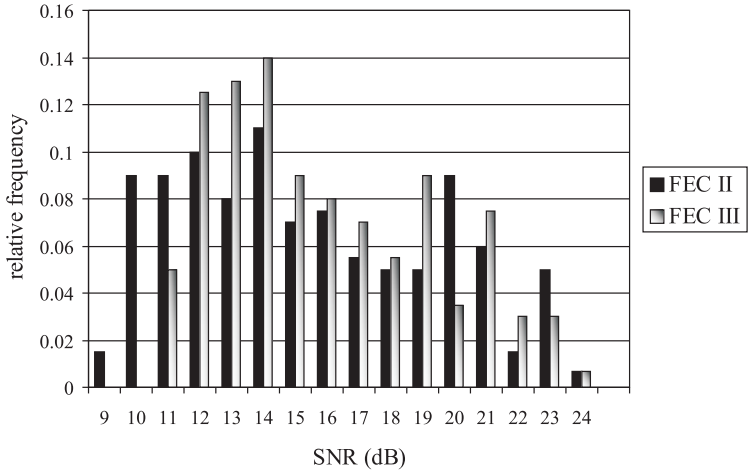

(a) Histogram of $\mathrm{SNR_{II}}$ and $\mathrm{SNR_{III}}$.

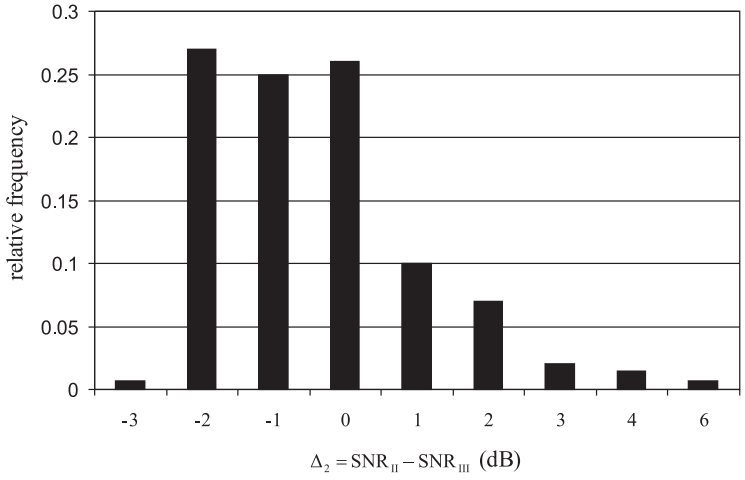

(b) Histogram of Δ_2.

Fig. 5.15: Histogram of $\mathrm{SNR_{II}}$, $\mathrm{SNR_{III}}$ and Δ_2.

respect to FEC I, FEC III has a SNR gain of around 8.5 dB in the 2×2 system, around 4.5 dB in the 4×4 system and around 2.5 dB in the 8×8 system. Their SNR difference decreases with M. However, in comparison with FEC II, FEC III has a SNR gain of around 10 dB in the 2×2 system, around 7.5 dB in the 4×4 system and around 11 dB in the 8×8 system. The SNR gain decreases when M increases

from 2 to 4 then increases as M changes from 4 to 8.

Furthermore, we have evaluated their performance in practice. The real wireless channel is time-variant, so FEC I and II share the same channel bits to have the same channel condition. Same for FEC II and III. In total, we have done 180 experiments. Due to the limit of the testbed, we choose QPSK instead of QAM-16 as the modulation scheme to have more successful experiments. Still, not all the experiments succeed. FEC III survive in the most experiments (i.e. 92%) which is followed by FEC I (i.e. 86%) and FEC II (i.e. around 80%). Correspondingly, FEC III works in more channel conditions than FEC I and II. To investigate whether FEC III endure higher level of NF than FEC I and II in the rest successful experiments, we add extra noise to the measurement data. To let FEC I and II have BER $< 10^{-3}$ in 142 successful experiments under the same NF, FEC I has a SNR gain of 1 dB comparing to FEC II. If we allow every experiment to have its own maximum NF, FEC I has an average SNR gain of around 0.06 dB over FEC II. For the case of FEC II and III, they succeed in 145 experiments. With the same level of NF, FEC II requires the same level of noise level as FEC III to let all 145 experiments reach the required BER (i.e. BER $< 10^{-3}$ for FEC II and BER $= 0$ for FEC III). However, FEC III has an average SNR loss of around 0.4 dB if the level of NF in every experiment is adjusted to the maximum value.

Chapter 6

Opportunistic Error Correction: When and Why does it work best for OFDM systems?

6.1 A Novel Cross Coding Scheme for OFDM Systems

[1]**Abstract** In wireless OFDM-based systems, coding jointly over all the sub-carriers simultaneously performs better than coding separately per sub-carrier. However, the joint coding is not always optimal. In this paper, we propose a novel coding scheme based on fountain codes, which combines the separate coding and the joint coding over all the sub-carriers. The key element in the new proposed system is that each

[1]This section is the published paper [73]: *X. Shao and C.H. Slump, "A Novel Cross Coding Scheme for OFDM Systems", in Proceedings of IEEE Information Theory Workshop on Information Theory (ITW), Oct 2009, Taomina, Italy.*

fountain-encoded packet is transmitted over a single sub-carrier. The packets can be discarded if they have encountered a low-energy channel. Fountain codes can recover the source data by using only the surviving packets. With this new approach, we have a gain of around 8.5 dB comparing to the FEC layer used in current WLAN standards (i.e. the IEEE 802.11a standard and the IEEE 802.11n standard).

6.1.1 Introduction

It is a challenge to communicate both reliably and at a high throughput, because the wireless channel is a hostile environment which suffers from time-varying multi-path propagation and high levels of man-made interference. To overcome the multi-path effect, *Orthogonal Frequency Division Multiplexing* (OFDM) has become a popular scheme for recent wireless systems which operate at a high bit rate [13]. For the effects of the noise and interference encountered in the transmission of the signal through the wireless channel, *Error Correction Coding* is used as a means of utilizing wireless channels at full capacity [92].

In [2], the authors mention that over a finite block length, coding jointly over the sub-carriers yields a smaller error probability than can be achieved by coding separately over the sub-carriers at the same rate. This theory has been applied in practical OFDM-based wireless systems. In the current *Forward Error Correction* (FEC) layer for OFDM systems (e.g. WLAN, DVB, DAB, etc), the source bits are encoded jointly across the sub-carriers. However, coding can also be done in a crosswise way, which combines the separate coding and the joint coding over all the sub-carriers. It is unknown whether the cross coding approach performs better or worse than the joint coding scheme in OFDM systems. Hence, it is of interest to investigate the performance of the cross coding scheme for OFDM systems.

In this paper, we propose a novel cross FEC layer based on fountain codes, which is called *Opportunistic Error Correction Layer*. In [42], MacKay describes the encoder of a fountain code as a metaphorical fountain that produces a stream of encoded packets. Anyone who wishes to receive the encoded file holds a bucket under the fountain and collects enough packets to recover the original data. It does not matter which packets are received, only a minimum amount of packets have to be received correctly [42]. In other words, fountain-encoded packets are independent with respect to each other.

To apply fountain codes in the OFDM system, we divide a block of source bits into a set of packets, which are encoded by a fountain code. Because fountain codes are only designed for erasure channels, we have to apply error correction codes to convert the wireless channel into an erasure channel. A fountain-encoded packet is transmitted over a sub-carrier. Thus, multiple packets are transmitted simultaneously, using frequency division multiplexing. The receiver discards fountain-encoded packets which are transmitted over the sub-carriers with deep fading. In other words, the

receiver does not have to process all the received packets but only the packets from high-energy channels. The processing power is reduced correspondingly.

There are two coding steps in the opportunistic error correction layer. First, the source packets are coded jointly over all the sub-carriers by fountain codes; then, each fountain-encoded packet is encoded individually over a sub-carrier by error correction codes. This is different from the traditional FEC layer. In this paper, we investigate the performance of this new cross coding scheme for the wireless systems.

The outline of this paper is as follows. First, the different coding schemes for wireless channels are discussed; this is followed by the opportunistic error correction layer. In Section 6.1.4, a description is given of the IEEE 802.11a system, which is a practical example of an OFDM system. We compare the current FEC layers with the opportunistic error correction layer in the simulation. Finally, the simulation results are analyzed. The paper ends with a discussion of the results.

6.1.2 Coding for Wireless Channels

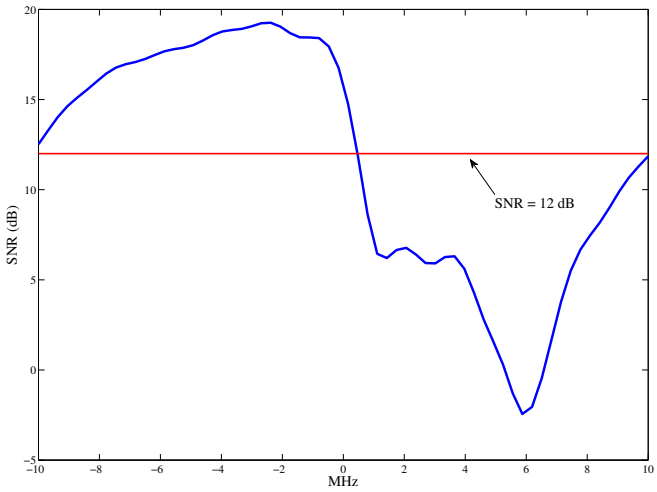

Fig. 6.1: Example of the baseband transfer function of a frequency selective Channel *model* A [102].

The wireless channel is a hostile environment and often modeled as a frequency selective channel. The multi-path effect results in *Inter-Symbol Interference* (ISI). OFDM has become a fruitful approach to communicate over frequency selective channels [2]. In the OFDM system, each sub-carrier can be considered as a flat fading channel.

However, due to the channel noise or interference, reliable communication still can not be guaranteed by only using OFDM.

Error correction codes have been applied in wireless systems for reliable communications. In OFDM systems, coding is performed in the frequency domain. Whether the source data is encoded jointly or separately over all the sub-carriers depends on the transmission mode. There are two modes to transmit an encoded packet:

- Mode I is to transmit each encoded packet over one sub-carrier. In such case, the coding is performed separately over all the sub-carriers.
- Mode II is to transmit each encoded packet over all the sub-carriers like current WLAN systems. With this method, the coding is done jointly over all the sub-carriers.

Indeed, over a finite block length, coding jointly over all the sub-carriers yields a smaller error probability than can be achieved by coding separately at the same rate [2]. That is because the sub-carrier with high energy can compensate for the sub-carrier with deep fading. This is also shown in the simulation results of Section 6.1.5.

From the power consumption point of view, however, the joint coding over all the sub-carriers is not optimal. With the joint coding, the receiver has to process all the received packet as it is not beforehand known from the channel knowledge, whether a packet is decodable or not. Take Figure 6.1 as an example, 1000 packets are transmitted over this channel. Each packet has 175 bits and encoded by a (175,255) LDPC code [47]. QAM-16 is used as the mapping scheme and the channel estimation is assumed to be perfect. With the transmission Mode I, the receiver has to process all the 1000 packets and only 17 packets can be decoded correctly. With the transmission Mode II, the receiver can only process "good" packets which are transmitted over the sub-carriers with high energy, since each sub-carrier can be considered as a flat fading channel. For the LDPC code used in this example, it has a BER of 10^{-5} or lower when SNR $\geq$ 12dB. In such case, the receiver only need to decode 500 packets in this example, which can all be decoded correctly in this example. Therefore, Mode II has lower processing power than Mode I. In addition, Mode II has less packets in error than Mode I in some "bad" channels like Figure 6.1.

Low power consumption in battery-powered wireless receivers is highly desirable. In order to lower the processing power with a low BER, we propose a novel cross coding approach based on fountain codes (i.e. opportunistic error correction layer) for wireless OFDM-based systems. The opportunistic error correction layer is based on Mode II but it is not a separate coding scheme. It is a combination of the separate coding and the joint coding over all the sub-carriers. We will discuss this new coding scheme in the next section.

6.1.3 Opportunistic Error Correction

The [2]***Abstract*** opportunistic error correction layer is based on fountain codes. In this paper, we use a kind of fountain codes, i.e. *Luby Transform* (LT) codes [43] in the proposed error correction layer. Other fountain codes (e.g. Raptor codes [44]) can also be applied.

Consider a block of size K source packets $s_1, s_2, \cdots, s_K$ to be encoded by a fountain code. A "packet" has m bits and is considered as a unity. At each clock cycle, labeled by t, one fountain-encoded packet is generated by selecting a set of source packets randomly and computing the bitwise sum (XOR) of these source packets [42]. The fountain codes can supply unlimited packets. In practical systems, only a fixed number of packets N_t is generated.

At the receiver side, a certain amount of packets is required for successful decoding. The required number of received packets N is slightly larger than the number of source packets K and defined as:

$$N = K(1 + \varepsilon) \tag{6.1}$$

where ε is the percentage of extra packets and is called the overhead.

After receiving N packets, the receiver can recover the source packets by the *message-passing* algorithm [54] which has a linear decoding cost. By using the message-passing algorithm, the practical block size of LT codes with small overhead ε (i.e. within 5%) is on the order of 10^4 or higher which prevents the fountain scheme from efficiently supporting the real-time applications (i.e. low delay) [45]. In [40], the authors have shown that the small block size (i.e. $K = 500$) of LT codes with small ε (i.e. 3%) can be achieved by using message-passing and Gaussian elimination together for decoding. Gaussian elimination is applied after the message-passing algorithm. Combining both methods for decoding can have lower overhead and higher computation complexity in comparison with only using the message-passing algorithm to decode. For $K = 500$, the complexity of using both methods is around of 25% of the complexity of only using message-passing decoding, but the overhead of using both methods can be reduced from 42% to 3% [40]. In this paper, we combine both methods to decode LT codes.

Fountain codes are designed for communication over *Erasure Channels*, which means that the encoded packet is either received error free or not received at all. However, the wireless channels are not erasure, but fading and noisy channels. In practical systems, fountain codes are used in combination with other error correction algorithms to convert the noisy channels into erasure channels, often *Low-Density Parity-Check* (LDPC) codes [54]. In this paper, LDPC codes together with *Cyclic Redundancy Check* (CRC) are employed to convert the channel.

[2]This section is the submitted paper [103]: X. Shao, C.H. Slump, "Opportunistic Error Correction : When does it Work Best for OFDM Systems?", submitted to IEEE Transactions on Communications, 2010.

Our FEC encoding scheme is performed in the following order: K source packets are encoded by fountain codes first. To each fountain-encoded packet, a CRC is first added and the packet is encoded by a LDPC code. So, the source data is first encoded jointly over all the sub-carriers by fountain codes, then encoded separately over one sub-carrier by LDPC plus CRC codes.

At the receiver, each fountain-encoded packet is first LDPC decoded when the SNR is equal to or higher than the threshold (i.e. BER $\leq 10^{-5}$). The received packet is discarded if its energy is below the threshold. If the LDPC decoding fails, the received packet is discarded as well. If the LDPC decoding succeeds, the CRC is used to identify the undetected error from LDPC codes. If the CRC decoder fails, the receiver also assumes that the whole packet has been lost. Once the receiver has collected N surviving fountain-encoded packets, it starts to recover the source data.

6.1.4 System Model

The opportunistic error correction layer is based on fountain codes which have been explained in the above sections. This proposed cross layer can be applied in the OFDM systems. In this paper, the IEEE 802.11a system is taken as an example of OFDM systems.

The FEC layer in the current IEEE 802.11a system is based on *Rate Compatible Punctured Codes* (RCPC) [17]. Although this solution works well in practical systems, it is not optimal. First, because packets that have encountered a low-energy channel are still processed by the decoders. This is a waste of processing power. In addition, this FEC layer is based on worst case scenarios. However, worst case conditions do not happen all the time. This means that for most packets, the code rate and hence capacity can be increased.

In Figure 6.2, the proposed new error correction scheme is depicted. The key idea is to generate additional packets by the fountain encoder. First, the source packets are encoded by the fountain encoder. Then, a CRC checksum is added to each fountain-encoded packet and LDPC encoding is applied. On each sub-carrier, a fountain-encoded packet is transmitted. Thus, multiple packets are transmitted simultaneously, using frequency division multiplexing.

At the receiver side, we assume that the synchronization and channel estimation are perfect. If the SNR of the sub-carrier is equal to or above the threshold, the received fountain-encoded packet will go through LDPC decoding, otherwise it will be discarded. This means that the receiver is allowed to discard low-energy sub-carriers (i.e. packets) to lower the processing power consumption. After the LDPC decoding, the CRC checksum is used to discard the erroneous packets. As only packets with a high SNR are processed by the receiver, this will not happen often. When the receiver has collected enough fountain-encoded packets, it starts to recover the source data.

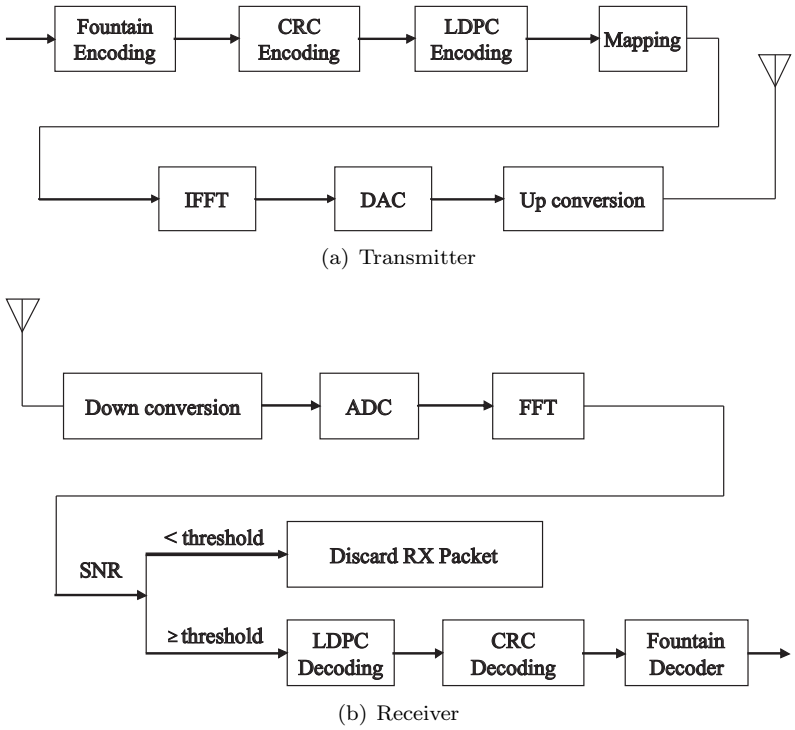

Fig. 6.2: Proposed IEEE 802.11a transmitter (top) and receiver (bottom).

6.1.5 Performance Analysis

In this section, we analyze the performance of our proposed opportunistic error correction layer. We compare four FEC schemes by simulation as follows:

- FEC I: RCPC with $R = 0.5$ from the IEEE 802.11a standard [17].
- FEC II: LDPC codes with $R = 0.5$ from the IEEE 802.11n standard [23] (n=648).
- FEC III: fountain codes with the (175,255) LDPC code plus 7-bit CRC using the transmission Mode I, which is the opportunistic error correction layer.
- FEC IV: fountain codes with the (175,255) LDPC codes plus 7-bit CRC using the transmission Mode II.

In the simulation, we transmit 8000 blocks of source packets over Channel *model* A. Each block consists of 590 source packets with a length of 168 bits. With the same code rate of $R = 0.5$, the source packets are encoded by FEC I, II, III and IV, respectively. Afterwards, they are mapped into QAM-16 symbols before the OFDM modulation.

For the case of FEC III and IV, each burst is encoded by a LT code (with parameters $c = 0.03$, $\sigma = 0.3$) and decoded by the message-passing algorithm and Gaussian

elimination together. From [40], we know that 3% overhead is required to recover the source packets successfully. To each fountain-encoded packet, a 7-bit CRC is added, then the (175,255) LDPC encoder is applied. Under the condition of the same code rate (i.e. $R = 0.5$), we are allowed to discard 21%[3] of transmitted packets. In FEC III, we transmit one packet per sub-carrier. In this case, we are allowed to discard 10 sub-carriers (i.e 21% of 48 data sub-carriers). In FEC IV, we transmit each fountain-encoded packet over all the data sub-carriers. Same as FEC III, we are allowed to have 21% packet loss in FEC IV.

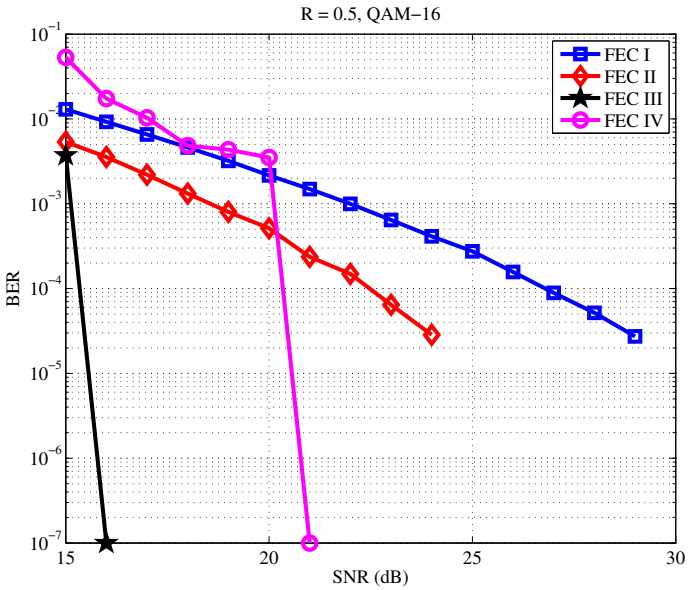

Fig. 6.3: Performance comparison between FEC I, II, III and IV at R = 0.5 (without interleaving in FEC I and II). For SNR = 16 dB or higher, no errors are detected in FEC III. So, for SNR = 16 dB, we represent BER = 0 by 10^{-7}. Same for FEC IV.

Figure 6.3 shows the simulation results with perfect channel knowledge. From this figure, we can see the followings:

- FEC I has a BER of 10^{-5} or lower when SNR $\geq$ 29dB.
- FEC II has a BER of 10^{-5} or lower when SNR $\geq$ 24dB.
- FEC III is error free when SNR $\geq$ 16dB.
- FEC IV is error free when SNR $\geq$ 21dB.

So, FEC III has a gain of around 13.5 dB comparing with FEC I, 8.5 dB comparing to FEC II and 5 dB comparing to FEC IV.

[3] $21\% \approx 1 - \frac{R}{R_1 \times R_2}$, where R is the effective code rate (i.e. 0.5), R_1 is the code rate of LT codes (i.e. $\frac{1}{1.03} \approx 0.97$) and R_2 is the code rate of the (175,255) LDPC code with 7-bit CRC (i.e. $\frac{168}{255} \approx 0.66$)

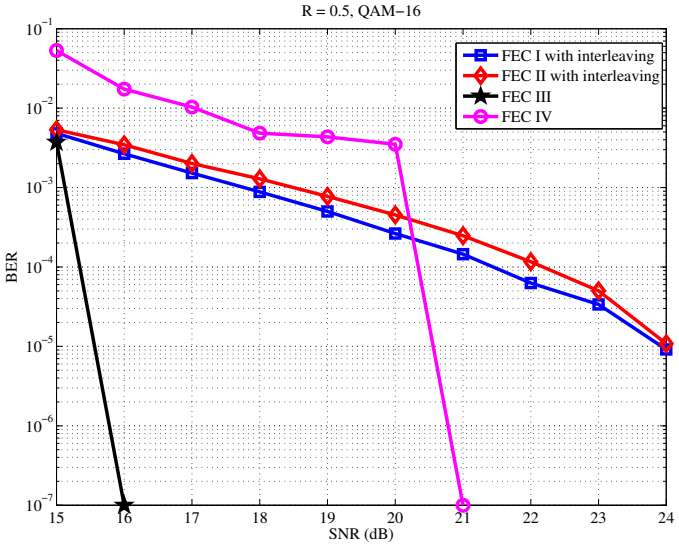

Fig. 6.4: Performance comparison between FEC I, II, III and IV at R = 0.5 (with interleaving in FEC I and II). For SNR = 16 dB or higher, no errors are detected in FEC III. So, for SNR = 16 dB, we represent BER = 0 by 10^{-7}. Same for FEC IV.

As we know, RCPC has a good performance for random bit errors. Interleaving is employed to mitigate burst errors. To improve the performance of FEC I, an interleaver is added before the RCPC encoder. Also, an interleaver is inserted in FEC II to check whether interleaver can increase the performance of LDPC codes. Figure 6.4 shows the simulation results. Both FEC I and II with interleaving have a BER of 10^{-5} or lower when SNR $\geq$ 24dB. In this case, FEC III has a gain of 8.5 dB comparing to FEC I and II. In addition, interleaving makes FEC I behave slightly better than FEC II and gives a gain of 5 dB to FEC I but no gain to FEC II.

From Figure 6.3 and 6.4, we can see that FEC III works better than the other FEC schemes. FEC III has a different transmission mode than the others. In FEC III, each packet is transmitted over one sub-carrier. In the OFDM system, each sub-carrier can be modeled as a flat fading channel. With the channel knowledge, the receiver knows how many sub-carriers (i.e. packets) will be lost. Actually, the surviving sub-carriers have a higher SNR than the threshold of the used LDPC codes, which means that the channel capacity of the surviving sub-carriers can not be fully utilized. But if one fountain-encoded packet is transmitted over all the sub-carriers, the subcarrier with high energy can compensate for the subcarrier with deep fading. In this sense, transmission Mode II should have a smaller error probability than Mode I for the same code rate, which is stated in [2]. In order to show this, we compare FEC III and FEC IV without using fountain codes in the same simulation condition as Figure 6.3 and 6.4. Figure 6.5 shows the BER performance of both transmission modes. We

can see that the transmission Mode II has a lower BER than the transmission Mode I at the same code rate when SNR = 15 $\sim$ 16dB.

However, Figure 6.3 and 6.4 do not show the same result as Figure 6.5. In Figure 6.3 and 6.4, FEC III has a lower BER than FEC IV at SNR = 15 dB. When SNR = 16 dB, FEC III is error free but FEC IV still has a BER of around 10^{-2}. By using fountain codes, the receiver does not care about the total number of errors in the received packets but only cares about the total number of the error-free packets. Figure 6.6 shows the outage probability P_{out} of the packet loss ϵ:

$$\mathrm{P}_{out} = \mathbb{P}\{\text{the percentage of packet loss} < \epsilon\} \tag{6.2}$$

In this figure, we can see that FEC III has a lower packet loss than FEC IV when we allow more than 7% packet loss. Therefore, from Figure 6.5 and Figure 6.6 we conclude that the transmission Mode I has a larger BER comparing transmission mode II but the errors exist in less number of packets than the transmission mode II when the packet loss is larger than 7%. As mentioned earlier, we allow 21% packet loss in FEC III and IV in order to have the same code rate of FEC I and II. Fountain codes can recover the source data once the receiver has collected enough error-free fountain-encoded packets. That explains why FEC III works better than FEC IV. Also, because of this and the characteristics of fountain codes, FEC III works better than FEC I and FEC II.

6.1.6 Conclusions

In this paper, we propose a novel cross-coding approach based on fountain codes for OFDM systems, which combines the separate coding and the joint coding over all the sub-carriers. It is called the opportunistic error correction layer, because it does not process all the received packets but only the packets from high-energy channels. In such a case, the processing power consumption can be reduced correspondingly. This new method has a gain of 8.5 dB in comparison with the current FEC layer used in the IEEE 802.11a system and the LDPC codes with interleaving used in the IEEE 802.11n system. Also, it has a gain of 5 dB comparing with the case that each fountain-encoded packet is transmitted over all the sub-carriers.

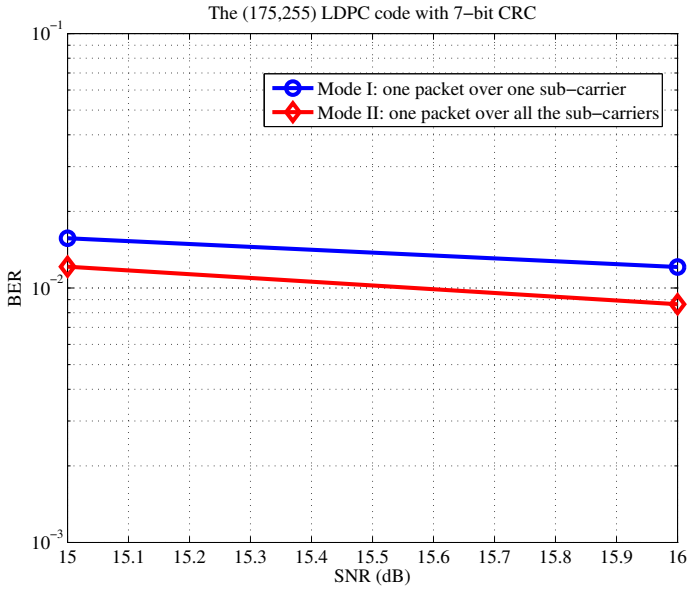

Fig. 6.5: Comparison in BER between the transmission Mode I and Mode II using the (175,255) LDPC code with 7-bit CRC.

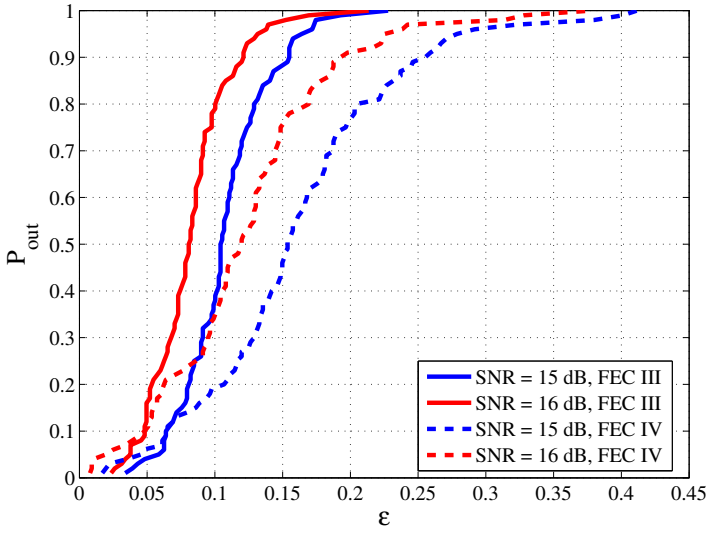

Fig. 6.6: Comparison in the outage probability of the packet loss between the transmission Mode I and Mode II using the (175,255) LDPC code with 7-bit CRC.

6.2 Opportunistic Error Correction: When does it Work Best for OFDM Systems?

[4]**Abstract** Opportunistic error correction based on fountain codes is especially designed for the OFDM-based wireless system. The key point of this approach is the tradeoff between the code rate of error correction codes and the number of sub-carriers to be discarded. That saves power in the ADC by quantizing the received signal coarsely. Correspondingly, this new method can afford a higher level of the noise floor than the joint coding scheme which is adopted by the current OFDM system (e.g. the IEEE 802.11a system, DVB systems). Simulation results have shown that opportunistic error correction performs better than the joint coding scheme over the wide-band channel (i.e. the frequency selective fading channel). However, it is not clear whether this scheme has advantages over the joint coding scheme in the narrow-band wireless system (e.g. the flat-fading channel or the channel with a low dynamic range). In this paper, we investigate when opportunistic error correction works best for OFDM systems in the simulation and in the real world. Simulation results show that, with the same code rate, it only performs better than the joint coding scheme if the dynamic range $\mathcal{D}$ of the channel is larger than 10 dB. Their performance difference becomes larger as $\mathcal{D}$ increases. Comparing to the LDPC code from the IEEE 802.11n standard at the same code rate, this novel approach gains a SNR of at least 11 dB over the TGn channel at 5 MHz, 10 MHz and 20 MHz. Furthermore, practical measurements show that it is more robust to the imperfections in the real world than the joint coding scheme. More measurements succeed in opportunistic error correction than in the joint coding scheme. This new scheme works better in practice than the joint coding scheme over the wireless channel with any $\mathcal{D}$. With respect to the joint coding scheme, on average, this novel approach gains a SNR of around 1.5 dB at $\mathcal{D} \in$ (0,10] dB, around 1.7 dB at $\mathcal{D} \in$ (10,20] dB and around 3.8 dB at $\mathcal{D} \in$ (20,30] dB.

6.2.1 Introduction

The wireless channel is a hostile environment and often modeled as a frequency selective channel [99] [1]. *Orthogonal Frequency Division Multiplexing* (OFDM) has become a fruitful approach to communicate over such channels, as it enables a rather straightforward equalization in wireless receivers [2] [86] [87]. However, the nearly Gaussian distribution of OFDM signals is seen as one of its main disadvantages [88] [89]. When signal peaks in the OFDM signal are clipped, all sub-carriers are affected [90] [104]. Equivalently, the Fourier Transform makes all sub-carriers suffer the same noise floor. Due to the frequency selectivity of wireless channels, sub-carriers

[4]This section is based on the submitted paper [103]: *X. Shao, C.H. Slump, "Opportunistic Error Correction : When does it Work Best for OFDM Systems?", submitted to IEEE Transactions on Communications, 2010.*

with deep fading can not afford any distortion. That leads to unreliable communication. Therefore, high-resolution ADCs are required in OFDM receivers.

In OFDM systems, the high-quality communication at a high data rate can not be guaranteed by only using high resolution ADCs. To achieve reliable communication, error correction codes are employed in OFDM systems [91] [28] [92]. Over a finite block length, coding jointly yields a smaller error probability than can be achieved by coding separately over the sub-carriers at the same rate [2]. This theory has been applied in practical OFDM systems like WLAN and DVB systems [17] [23] [62] [20] [22]. The joint coding scheme utilizes the fact that sub-carriers with high-energy can compensate for those with low-energy, but its drawback is that no sub-carrier can be discarded in the decoding. That means the resolution of ADCs is proportional to the dynamic range of the channel. Hence, the resolution of ADCs has to be high for channels with a high dynamic range. For the separate coding scheme, the requirement for ADCs is even higher to have all received packets decodable.

The power consumption of ADCs is proportional to the resolution and the sampling rate [12]. Given the same sampling rate, higher resolution ADCs consume more energy [9]. This is not a desirable characteristic for battery-powered wireless receivers. Quantizing the received OFDM signal coarsely can reduce the power consumption in ADCs. To achieve this, the question we should answer is: *Can we design a system in such a way where sub-carriers with deep fading can be ignored but still achieve reliable communications?* The answer is yes. In [24], we propose a novel cross coding scheme based on fountain codes for OFDM-based wireless systems, combining the separate coding and the joint coding over all the sub-carriers. Fountain codes [21] are designed for erasure channels. To apply them in wireless communications, error correction codes are required to convert wireless channels into an erasure channel. The key point of this approach is to use a relatively high code rate to encode each fountain-encoded packet and transmit it over a single sub-carrier. By transmitting enough number of packets, packets can be discarded if they are transmitted over low-energy sub-carriers. That allows us to ignore sub-carriers with deep fading. Fountain codes can reconstruct the original file if a certain number of fountain-encoded packets is received. In such a case, we can allow the increase of the noise floor of the wireless receiver. Correspondingly, the resolution of ADCs can be reduced. The power consumption in CMOS-based ADCs is linearly proportional to the number of quantization levels [11]. With the same effective throughput, simulation results show that this new cross coding scheme saves around 52% of energy in ADCs comparing to the joint coding defined in the IEEE 802.11a system [40].

Because the receiver does not have to process all the received packets, this cross coding scheme is called *opportunistic error correction*. It consists of fountain codes and error correction codes. Basically, it trades the code rate of error correction codes with the number of sub-carriers to be discarded. That saves power in ADCs by quantizing the received OFDM signal coarsely. In other words, opportunistic error correction can afford higher level of noise floor than the joint coding scheme. In [24], we have shown that opportunistic error correction has a better performance than the joint coding over frequency selective channels. With the same code rate, it has a *Signal-to-Noise*

Ratio (SNR[5]) gain of around 8.5 dB over Channel Model A [105] comparing to the *Forward Error Correction* (FEC) layer based on the joint coding scheme in current WLAN standards [24].

However, this new method might not perform better than the joint coding scheme over a narrow-band channel (i.e. a flat-fading channel), as all sub-carriers suffer the same fading. Opportunistic error correction employs a relatively higher code rate to encode each fountain-encoded packet with respect to the joint coding scheme. Given the same type of error correction codes, the one with higher code rate always needs higher SNR to decode correctly. If opportunistic error correction utilizes the same type of error correction codes as the joint coding scheme, it would not perform better than the joint coding scheme over the flat-fading channel. This may apply to the wireless channel with a low dynamic range. Therefore, it is of great interest to investigate at what dynamic range of the channel this new cross coding scheme shows its advantage over the joint coding scheme. This will tell us what kind of communication environment needs this novel approach.

In this paper, we evaluate the performance of opportunistic error correction in the WLAN systems for different dynamic ranges of wireless channels. Its performance analysis is based on simulation results and practical measurements. That will give a good insight whether this new algorithm is robust to the imperfections of the real-world which are neglected in simulations.

The paper is organized as follows. Opportunistic error correction is first depicted where we explain why this new method is suitable for OFDM systems and how it works. In section 6.2.3.1, we describe the system model by showing how we apply this novel scheme in OFDM systems. After that, we compare its performance with FEC layers from WLAN systems over a TGn[6] channel [93] in the simulation. Besides, we evaluate its performance in the practical system in section 6.2.4. The paper ends with a discussion of conclusions.

6.2.2 Opportunistic Error Correction

OFDM enables a relative easy implementation of wireless receivers [4], but it does not guarantee reliable communication over the noisy wireless channel. Therefore, error correction codes have to be employed in wireless systems. In OFDM systems, coding is performed in the frequency domain. Whether source data is encoded jointly or separately over all the sub-carriers depends on the transmission mode. There are two modes to transmit an encoded packet [97]:

- **Mode I** is to transmit a packet over a single sub-carrier. In such case, the coding is done separately over all the sub-carriers.

[5]In this paper, SNR is equivalent to *Carrier-to-Noise Ratio.*

[6]The TGn channel model is used by the High Throughput Task Group [93]. "TG" stands for Task Group and "n" stands for the IEEE 802.11n standard.

- **Mode II** is to transmit a packet over all the sub-carriers. With this method, the coding is performed jointly over all the sub-carriers.

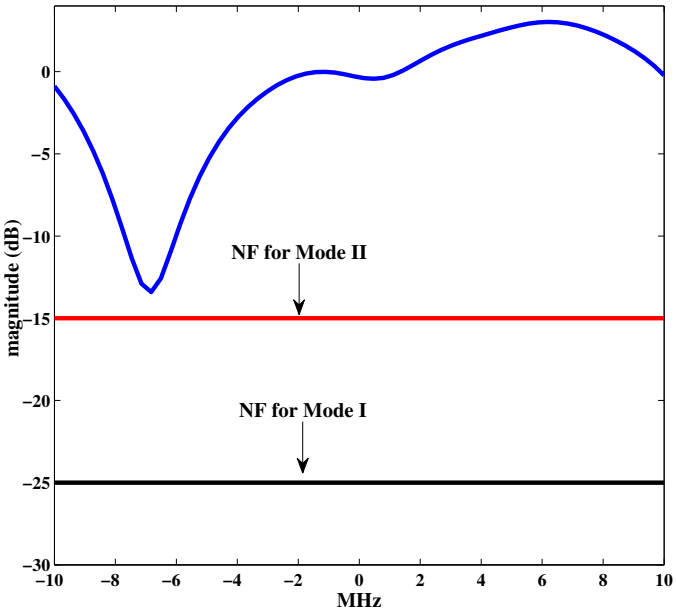

Fig. 6.7: Example of the difference in NF required by the seperate coding scheme (i.e. Mode I) and the joint coding scheme (i.e. Mode II).

Both transmission modes have advantages and disadvantages. Using Mode I, the receiver can predict whether the received packet is decodable since each sub-carrier can be modeled as a flat-fading channel. The packets transmitted over the sub-carriers with low energy can be discarded without going through the whole receiving chain. Correspondingly, the processing power can be reduced. This can not be applied in Mode II. But Mode I endures a lower Noise Floor (**NF**) than Mode II to achieve the same quality of communication. Assuming that some encoded packets are transmitted over a wireless channel as shown in Figure 6.7 and that a packet is received correctly when the SNR $\geq$ 12 dB. In this example, the maximum NF for Mode I is -25 dB which is determined by the sub-carrier with the lowest energy. Comparing to Mode I, Mode II can survive in a higher NF (i.e -15 dB in this example), as sub-carriers with high energy can compensate for those with low energy. Higher NF means lower resolution ADCs (i.e. lower power consumption) can be used in the wireless receiver. Correspondingly, Mode II performs better than Mode I in the same NF [2]. Hence, current OFDM systems (e.g. WLAN, DVB systems) utilize the joint coding scheme.

However, Mode II is still not optimal as there might be a waste of processing power. Also, because each sub-carrier is considered to be equally important, the NF in Mode

II is limited to the dynamic range of the channel[7] ($\mathcal{D}$). Higher $\mathcal{D}$ means lower NF. If we are allowed to discard sub-carriers with deep fading, the dynamic range of channel can be reduced. In such case, the NF can be further increased. To achieve this, we proposed a novel cross coding scheme based on fountain codes in [24], as it combines the joint coding scheme and the separate coding scheme together.

Opportunistic error correction is specially designed for OFDM systems. It is based on fountain codes. A fountain code has a similar property to a fountain of water: when you fill a cup from the fountain, you do not care about which drops of water fall in, but you only want that your cup fills enough to quench your thirst [80]. In other words, fountain-encoded packets are independent to each other. This allows us to discard some parts of wireless channel with deep fading by transmitting one fountain-encoded packet over a single sub-carrier. That also gives the advantage of the separate coding scheme (i.e. save processing power).

Figure 6.8 shows how opportunistic error correction works. With a fountain code, the transmitter can generate an in-principle infinite sequence of fountain-encoded packets. In this paper, the transmitter generates N_t number of fountain-encoded packets. Then, each packet is encoded by an error correction code to make wireless channels behave like an erasure channel. Afterwards, each packet is transmitted over a single sub-carrier.

At the receiver side, the channel is first estimated. With the channel knowledge, the receiver makes a decision about which packets are to be decoded. We assume that N_r ($N_r \leq N_t$) fountain-encoded packets can go through the error correction decoding. Packets only survive if they succeed in the error correction decoder. The fountain decoder can reconstruct the original file by collecting enough packets. The number of fountain-encoded packets N ($K < N \leq N_r$) required at the receiver is slightly larger than the number of source packets K [42]:

$$N = (1 + \varepsilon)K \tag{6.3}$$

where ε is the percentage of extra packets and is called the overhead. For high throughput, ε is expected to be as small as possible. However, fountain codes (e.g. *Luby-Transform* (LT) codes [43]) require a large ε for small block size by only using the *message-passing* algorithm to decode. For example, the practical overhead of LT codes is 14% when $K = 2000$, which limits its application in the practical system [41]. In [40], we have shown that the overhead is reduced to 3% by combining the message passing algorithm and Gaussian Elimination to decode LT codes for $K \geq 500$.

In this paper, we use LT codes in the proposed error correction layer. This new scheme is generic: any fountain codes (e.g. LT codes, Raptor codes [81] and online codes [72]) can be applied in it. To have a small ε for small block size, we choose to decode LT codes by combining the message passing algorithm and Gaussian elimination in this paper.

[7] In this paper, we assume that all the channels have the same energy.

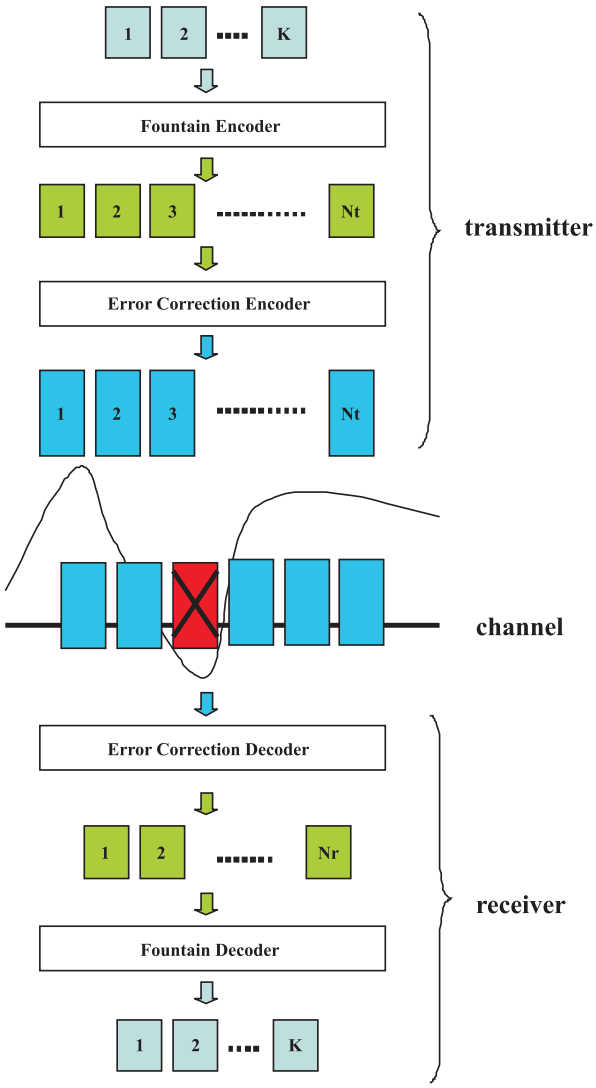

Fig. 6.8: Pictural diagram of opportunistic error correction for OFDM systems

6.2.3 Performance Analysis in Simulation

In this section, we analyze the performance of opportunistic error correction in the simulation. In [24] and [40], we have shown that this new approach works better over Channel Model A than the traditional joint coding scheme from WLAN standards. To investigate whether this novel cross coding scheme also works in other channel models, we choose the TGn channel [93] as the channel model in this paper. Before checking its overall performance in the TGn channel, let us look at the statistical characteristics of

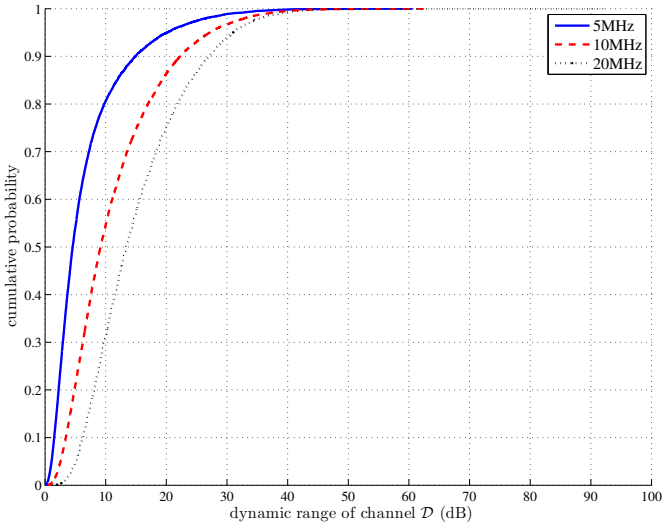

Fig. 6.9: The cumulative distribution curves of the dynamic range $\mathcal{D}$ for the TGn channel at 5 MHz, 10 MHz and 20 MHz

TGn channels' dynamic range $\mathcal{D}$ at different transmission bandwidths (BW). Figure 6.9 shows the cumulative probability of $\mathcal{D}$ for TGn channels at 5 MHz, 10 MHz and 20 MHz. Although they have different BW, their $\mathcal{D}$ mainly distributes in the range of $0 \sim 40$ dB (i.e. at a probability of 99%). In this section, we analysis the performance of opportunistic error correction over the TGn channel model at different $\mathcal{D}$ and its overall performance at different BW.

6.2.3.1 System Model

The opportunistic error correction layer is based on fountain codes which have been explained in the above section. This proposed cross layer can be applied in any OFDM-based wireless systems. In this paper, the IEEE 802.11a system is taken as an example of OFDM systems.

In Figure 6.10, the proposed new error correction scheme is depicted. The key idea is to generate additional packets by the fountain encoder. First, source packets are encoded by the fountain encoder. Then, a CRC checksum is added to each fountain-encoded packet and the LDPC encoding is applied. On each sub-carrier, a fountain-encoded packet is transmitted. Thus, multiple packets are transmitted simultaneously, using frequency division multiplexing.

At the receiver side, we assume that synchronization and channel estimation are

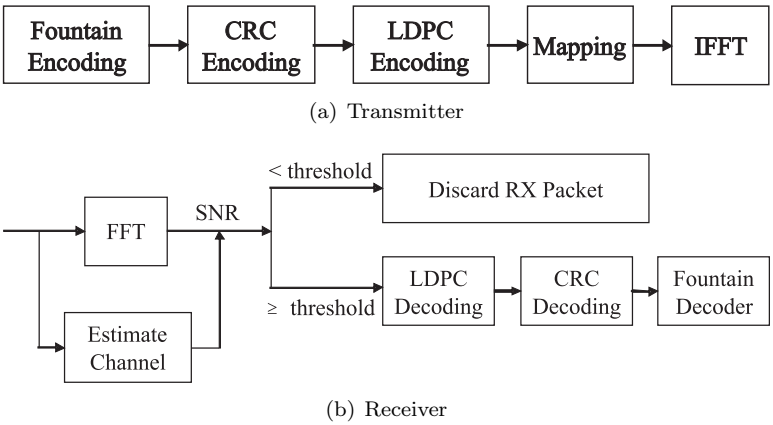

Fig. 6.10: Proposed IEEE 802.11a transmitter (top) and receiver (bottom).

perfect in the simulation. If the SNR of the sub-carrier is equal to or above the threshold, the received fountain-encoded packet will go through the LDPC decoding, otherwise it will be discarded. This means that the receiver is allowed to discard low-energy sub-carriers (i.e. packets) to lower the processing power consumption. After the LDPC decoding, the CRC checksum is used to discard the erroneous packets. As only packets with a high SNR are processed by the receiver, this will not happen often. When the receiver has collected enough fountain-encoded packets, it starts to recover the source data.

6.2.3.2 Simulation Results

In this section, we compare three FEC schemes in simulation as follows:

- FEC I: LDPC codes at $R = 0.5$ with interleaving from the IEEE 802.11n standard [23] (n=648).
- FEC II: fountain codes with the (175,255) LDPC code [47] plus 7-bit CRC using the transmission Mode I, which is the opportunistic error correction layer.
- FEC III: fountain codes with the (175,255) LDPC code plus 7-bit CRC using the transmission Mode II.

The three FEC schemes are simulated as function of the dynamic range $\mathcal{D}$ and/or the bandwidth BW by transmission of 1000 bursts of data (i.e. around 100 million bits) over the TGn channel. Each burst consists of 583 source packets with a length of 168 bits. With the same code rate of $R = 0.5$, source packets are encoded by FEC I, II and III, respectively. Afterwards, they are mapped into QAM-16 symbols before the OFDM modulation.

For the case of FEC II and III, each burst is encoded by a LT code (with parameters $c = 0.03$, $\sigma = 0.3$) and decoded by the message-passing algorithm and Gaussian elimination together. From [40], we know that 3% overhead is required to recover the source data successfully. To each fountain-encoded packet, a 7-bit CRC is added, then the (175,255) LDPC encoder is applied. Under the condition of the same code rate (i.e. $R = 0.5$), we are allowed to discard 21%[8] of the transmitted packets. In FEC II, we transmit one packet per sub-carrier. In this case, we are allowed to discard 10 sub-carriers (i.e. 21% of 48 data sub-carriers). In FEC III, we transmit each fountain-encoded packet over all the data sub-carriers. Similar to FEC II, we are allowed to have a 21% packet loss in FEC III.

- Channel at different dynamic range

  In total, we compare them under 6 situations: the flat-fading channel (i.e. the AWGN channel), $\mathcal{D} \in$ (0,10] dB, $\mathcal{D} \in$ (10,20] dB, $\mathcal{D} \in$ (20,30] dB, $\mathcal{D} \in$ (30,40] dB and $\mathcal{D} \in$ (40,$+\infty$) dB. Figure 6.11 shows the simulation results. In the case of the flat-fading channel, we see that FEC I performs better (i.e. a SNR gain of around 2 dB) than FEC II and III as expected. That is because FEC I employs lower code rate of LDPC codes (i.e. $R = 0.5$) comparing to the LDPC code used in FEC II and III. The same performance has been observed in the case of $\mathcal{D} \in$ (0,10] dB, as we can see in Figure 6.11(b). Hence, we can say that the joint coding scheme (i.e. FEC I) performs better than the cross coding scheme (i.e. FEC II) at $\mathcal{D} \in$ [0,10] dB. Furthermore, there is no difference in the performance between the transmission Mode I and II with fountain codes (i.e. between FEC II and III) at $\mathcal{D} \in$ [0,10] dB.

  FEC II starts to show its advantage over the joint coding scheme (i.e. FEC I and III) when $\mathcal{D}$ is higher than 10 dB.

  - Comparing to FEC I at a BER of 10^{-5} or lower, FEC II has a SNR gain of around 1 dB at $\mathcal{D} \in$ (10,20] dB, around 6 dB at $\mathcal{D} \in$ (20,30] dB, around 10.5 dB at $\mathcal{D} \in$ (30,40] dB and around 13.5 dB at $\mathcal{D} \in$ (40,$+\infty$) dB. From Figure 6.11(c) to 6.11(f), we can see that the performance of FEC I degrades (i.e. a SNR loss of around 6 dB) as $\mathcal{D}$ increases by 10 dB. That does not apply to FEC II. FEC II is more robust to the variation of $\mathcal{D}$. Only when the dynamic range of the channel $\mathcal{D}$ changes from (10,20] dB to (20,30] dB, FEC II loses around 2 dB in SNR to achieve the error-free quality. From $\mathcal{D} \geq 20$ dB, there is no performance loss as $\mathcal{D}$ increases.

  - Comparing to FEC III at the error-free quality, FEC II has a SNR gain of 1 dB at $\mathcal{D} \in$ (10,20] dB, 3 dB at $\mathcal{D} \in$ (20,30] dB, 7 dB at $\mathcal{D} \in$ (30,40] dB and 11 dB at $\mathcal{D} \in$ (40,$+\infty$) dB. The performance of FEC III degrades (i.e. a SNR loss of 4

[8] $21\% \approx 1 - \frac{R}{R_1 \times R_2}$, where R is the effective code rate (i.e. 0.5), R_1 is the code rate of LT codes (i.e. $\frac{1}{1.03} \approx 0.97$) and R_2 is the code rate of the (175,255) LDPC code with 7-bit CRC (i.e. $\frac{168}{255} \approx 0.66$)

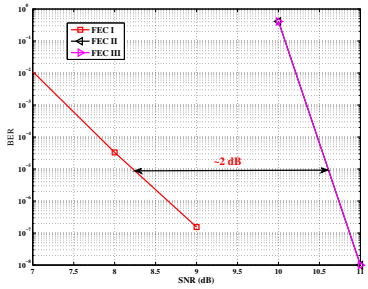

(a) the flat-fading channel

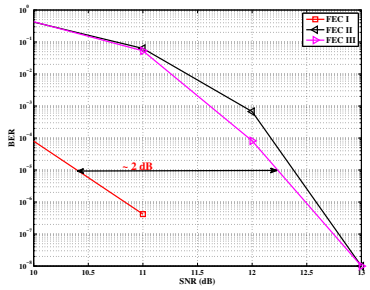

(b) $\mathcal{D} \in$ (0,10] dB

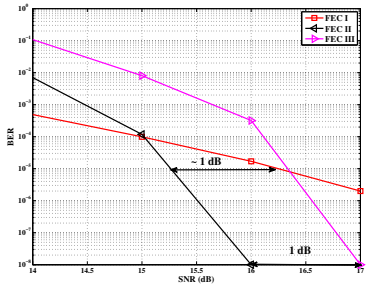

(c) $\mathcal{D} \in$ (10,20] dB

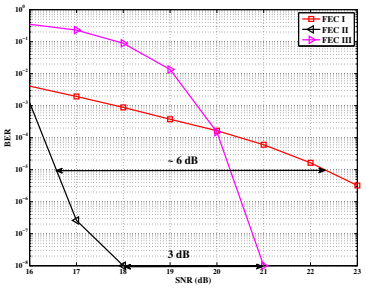

(d) $\mathcal{D} \in$ (20,30] dB

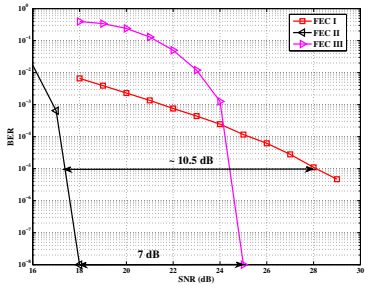

(e) $\mathcal{D} \in$ (30,40] dB

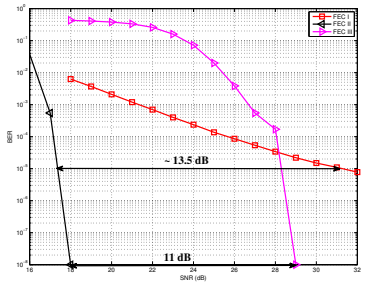

(f) $\mathcal{D} \in$ (40,+∞) dB

Fig. 6.11: Performance comparison in the simulation between FEC I, II and III at $R = 0.5$ over the TGn channel at different $\mathcal{D}$ ranges. FEC II and III can achieve error-free when the fountain decoder receives enough number of fountain-encoded packets. We represent BER $= 0$ by 10^{-8} in the above figures.

dB) as $\mathcal{D}$ increases by 10 dB. That is less than the case of FEC I (i.e. a SNR loss of 6 dB at every 10 dB increase in $\mathcal{D}$). Therefore, we can conclude that fountain codes make the error correction coding scheme more robust to the variation of $\mathcal{D}$.

As mentioned before, the key point of opportunistic error correction (i.e. FEC II) is to exchange the code rate of the used error correction codes with the number of discarded sub-carriers. The simulation results in Figure 6.9 conclude that there is no benefit to have this tradeoff when the dynamic range of the channel $\mathcal{D}$ is within 10 dB. The profit starts for $\mathcal{D} \geq 10$ dB and increases with $\mathcal{D}$.

- Channels at different Bandwidth

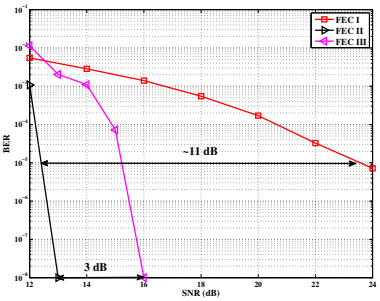

(a) 5 MHz

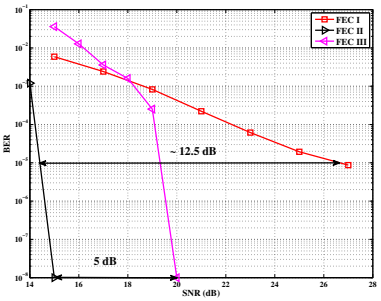

(b) 10 MHz

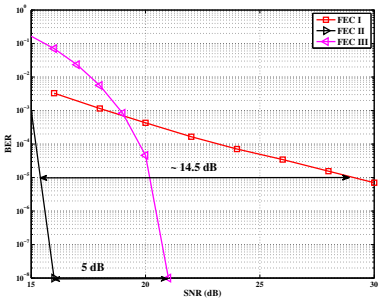

(c) 20 MHz

Fig. 6.12: Performance comparison between FEC I, II and III at $R = 0.5$ over the TGn channel at different bandwidths (i.e. 5 MHz, 10 MHz and 20 MHz). FEC II and III can achieve error-free decoding when the fountain decoder receives enough fountain-encoded packets. We represent BER $= 0$ by 10^{-8} in the above figures.

In this part, we compare them over the TGn channel with different bandwidth: 5 MHz, 10 MHz and 20 MHz. Figure 6.9 has presented that different bandwidth has different probability distribution of $\mathcal{D}$. The average $\mathcal{D}$ increases with the channel bandwidth. Simulation results are shown in Figure 6.12, where we can see that FEC II works much better than the joint coding scheme (i.e. FEC I and III) at any

BW. The performance of FEC I, II and III degrades when BW increases. FEC I loses around 3 dB when BW doubles. When BW changes from 5 MHz to 10 MHz, there is a SNR loss of around 2 dB in FEC II and around 4 dB in FEC III. Both FEC II and III lose 1 dB when BW increases from 10 MHz to 20 MHz. In a word, FEC II is less sensitive to the variation of BW than FEC I and III. Comparing with FEC I at BER of 10^{-5} or lower, FEC II has a SNR gain of around 11 dB at BW = 5 MHz, around 12.5 dB at BW = 10 MHz and around 14.5 dB at BW = 20 MHz. The SNR gain increases with BW. With respect to FEC III at the error-free quality, FEC II gains a SNR of 3 dB at BW = 5 MHz, 5 dB at BW = 10 MHz and 20 MHz.

In general, FEC II and III performs better than FEC I at BW = 5 MHz, 10 MHz and 20 MHz. The reason behind is as follows. Due to the variation of the channel, a burst data encounters several channels with different $\mathcal{D}$. For the case of FEC II and III, if some part of fountain-encoded packets are lost more than expected in a channel with $\mathcal{D}_1$, fountain codes still can recover the original data when the other part of fountain-encoded packets is lost less than expected in the channel with $\mathcal{D}_2$. However, this does not apply to FEC I.

6.2.4 Practical Evaluation

The C++ simulation results in the above section have shown the performance of opportunistic error correction in comparison with the joint coding scheme (i.e. FEC I and III) over the TGn channel with different $\mathcal{D}$ and BW, respectively. C++ simulation, with its highly accurate double-precision numerical environment, is on the one hand a perfect tool for the investigation of the algorithms. On the other hand, many imperfections of the real-world are neglected (e.g. perfect synchronization and channel estimation are assumed in Section 6.2.3, which does not happen in the real-world). So, simulation may show a too optimistic receiver performance. In this section, we evaluate its performance in practice to investigate whether opportunistic error correction is more robust to the real-world's imperfections.

6.2.4.1 System Setup

The practical measurements are done in the experimental communication testbed designed and built by Signals and Systems Group [100], University of Twente, as shown in Figure 6.13. It is assembled as a cascade of the following modules: PC, DAC, RF up-converter, power amplifier, antenna, and the reverse chain for the receiver. In the receiver, there is no power amplifier and band-pass RF filter before the down-converter but a low-pass baseband filter before the ADC to remove the aliasing.

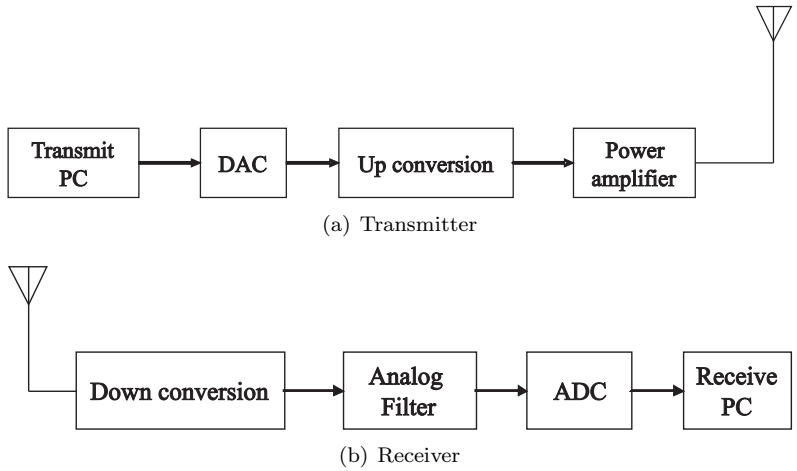

(a) Transmitter

(b) Receiver

Fig. 6.13: Block diagram of the testbed

- The Transmitter

  The data is generated offline in C++. The generation consists of the random source bits selection, the FEC encoding and the digital modulation as we depict in Section 6.2.3.1. The generated data is stored in a file. A server software in the transmit PC uploads the file to the Adlink PCI-7300A board[9] which transmits the data to DAC (AD9761)[10] via the FPGA board. After the DAC, the baseband analog signal is upconverted to 2.3 GHz by a Quadrature Modulator (AD8346)[11] and transmitted using a conical skirt monopole antenna.

- The Receiver

  The reverse process takes place in the receiver. The received RF signal is first downconverted by a Quadrature Demodulator (AD8347)[12], then filtered by the 8th order low-pass Butterworth analog filter to remove the aliasing. The baseband analog signal is quantized by the ADC (AD9238)[13] and stored in the receive PC via the Adlink PCI board.

  The received data is processed offline in C++. The receiver should synchronize with the transmitter and estimate the channel using the preambles and the pilots, which are defined in [17]. Timing and frequency synchronization is done by the Schmidl & Cox algorithm [55] and the channel is estimated by the *zero forcing*

[9] ADLINK, 80 MB/s High-Speed 32-CH Digital I/O PCI Card
[10] Analog Devices, 10-Bit, 40 MSPS, dual Transmit D/A Converter.
[11] Analog Devices, 2.5 GHz Direct Conversion Quadrature Modulator.
[12] Analog Devices, 800 MHz to 2.7 GHz RF/IF Quadrature Demodulator
[13] Analog Devices, Dual 12-Bit, 20/40/65 MSPS, 3V A/D Converter.

algorithm. In addition, the *residual carrier frequency offset* is estimated by the four pilots in each OFDM symbol [101]. After the synchronization and the channel estimation, decoding can start as we describe in Section 6.2.3.1.

6.2.4.2 Measurement Setup

Measurements are carried out in the corridor of Signals and Systems Group, located at the 9th floor of Building Hogekamp in University of Twente, the Netherlands. The measurement setup is shown in Fig. 6.14. The transmitter (TX) was positioned in front of the elevator (i.e. one of the circle positions in Fig. 6.14), while the receiver antenna (RX) was in the left side of the corridor (i.e. the cross positions in Fig. 6.14). 89 measurements were done in this scenario with a non-line-of-sight situation. The average transmitting power is around -10 dBm and the distance between the transmitter and the receiver is around $6 \sim 52.5$ meters. The measurements were conducted at 2.3 GHz carrier frequency and 20 MHz bandwidth.

In section 6.2.3, these FEC schemes have been compared in the C++ simulation. In the simulation, they can be compared by using the same source bits. Different channel bits can go through the same random frequency selective channel. However, it does not apply in the real environment. The wireless channel is time-variant even when the transmitter and the receiver are stationary (e.g. the moving of elevator with the closed door can affect the channel). Hence, we should compare them by using the same channel bits.

Because not every stream of random bits is a codeword of a certain coding scheme, it is not possible to derive its corresponding source bits from any sequence of random bits, especially for the case of FEC II and FEC III. Fortunately, the decoding of FEC I is based on the parity check matrix. Any stream of random bits can have its unique sequence of source bits with its corresponding syndrome matrix. The receiver can decode the received data based both on the parity check matrix and the syndrome matrix. So, FEC I can use the same channel bits with FEC II. In such case, they can be compared under the same channel condition (i.e. channel fading, channel noise and the distortion caused by the hardware.). Therefore, we only compare the joint coding scheme from the IEEE 802.11n standard (i.e. FEC I) with opportunistic error correction (i.e. FEC II) in the real-world.

In the measurements, FEC I and II are compared with the same code rate (i.e. $R = 0.5$). More than 600 blocks of source packets are transmitted over the air. Each block consists of 97944 bits. The source bits are encoded by FEC II. The encoded bits are shared by FEC I as just explained. Afterwards, they are mapped into QPSK symbols[14] before the OFDM modulation.

[14]The choice for QPSK instead of QAM-16 in the measurements is due to the noise floor of the testbed, whose noise floor is around -20 dB (i.e. SNR $\approx$ 20 dB). Figure 6.11 shows that the required SNR for $\mathcal{D} \in$ (20,30] dB should be at least 20 dB for FEC I to achieve a BER of 10^{-4} or lower.

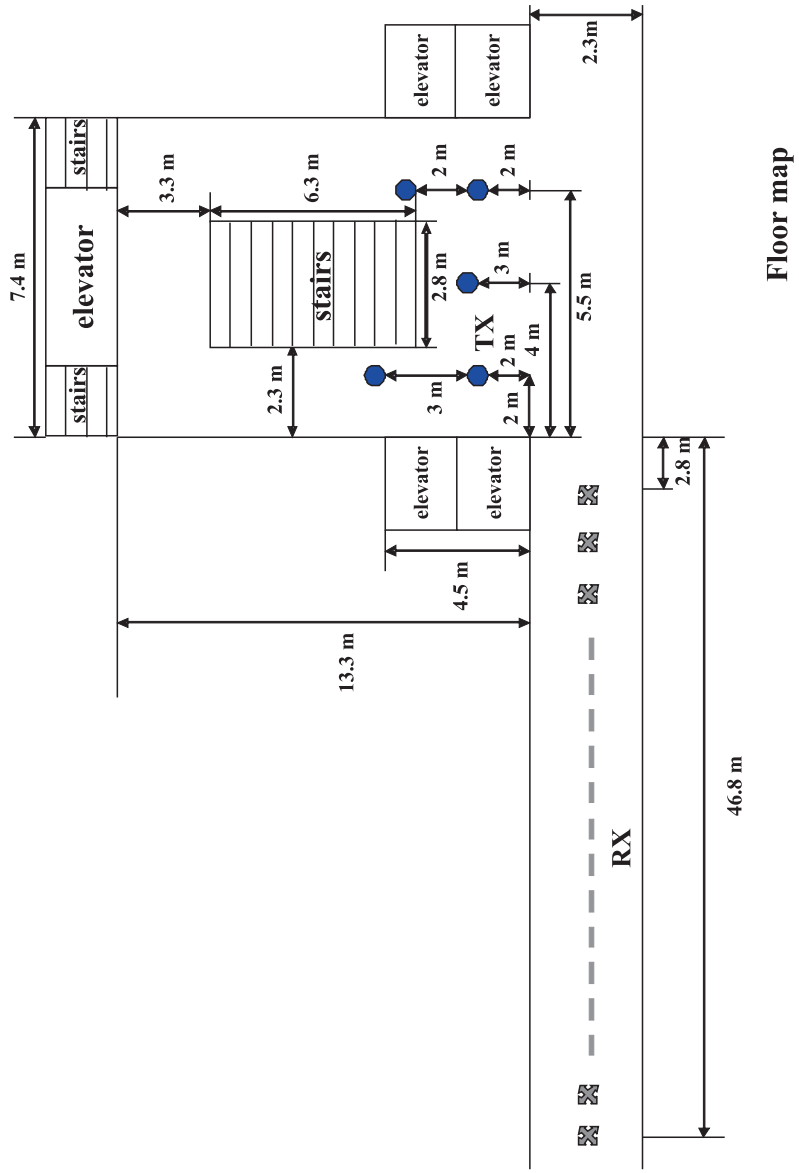

Fig. 6.14: Measurement Setup: antennas are 0.9 m above the concrete floor. The measurements are done in the corridor of the Signals and Systems Group. The receiver is positioned at left side of the corridor (i.e. the cross positions) and the transmitter is at the gray part as shown in the figure. The room contains one coffee machine, one garbage bin and one glass cabin.

With the non-perfect synchronization and channel estimation, a higher SNR is expected in the real

Each measurement corresponds to the fixed position of the transmitter and the receiver. It is possible that some measurements might fail in decoding. Due to the lack of a feedback channel in the testbed, no retransmission can occur. In this paper, we assume that the measurement fails if the received data per measurement has a BER higher than 10^{-3} by using FEC I. For the case of FEC II, if the packet loss is more than 21% as expected, we assume that the measurement fails.

6.2.4.3 Measurement Results

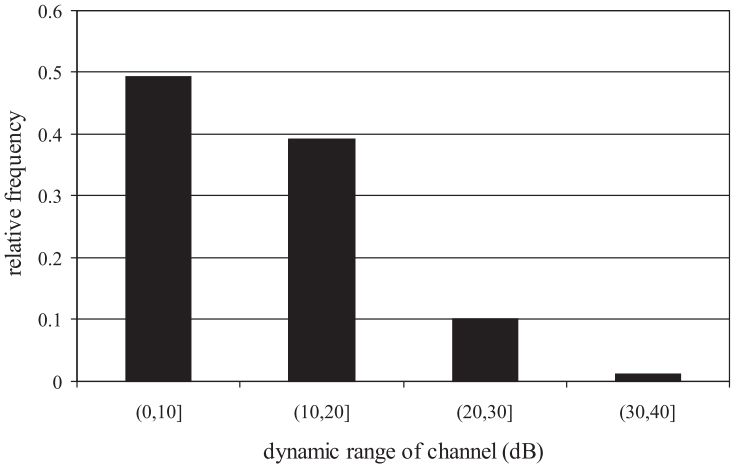

Fig. 6.15: The probability distribution of the estimated dynamic range $\mathcal{D}$ for the channel over 89 measurements.

In total, 89 measurements have been done. There are 7 blocks of data transmitted in each measurement. The estimated $\mathcal{D}$ of the channel over those 89 measurements distributes in the range of $0 \sim 40$ dB, as shown in Figure 6.15. As we can see, around 50% of the measurements have $\mathcal{D} \in$ (0,10] dB; around 39% of the measurements have $\mathcal{D} \in$ (10,20] dB; around 10 % of the measurements have $\mathcal{D} \in$ (20,30] dB; around 1 % of the measurements have $\mathcal{D} \in$ (30,40] dB.

FEC II succeeds in all the measurements but that does not happen to FEC I. Figure 6.16 shows the percentage of the successful measurements for each $\mathcal{D}$. With FEC I, the probability of the successful measurements decreases as $\mathcal{D}$ increases. In the simulation, FEC I works better than FEC II at $\mathcal{D} \in$ (0,10] dB, but it does not happen in the real-life. FEC I can only achieve a BER of 10^{-3} or lower in around 93% of the

world than in the simulation to achieve the same order of BER. Therefore, we choose a lower order of modulation scheme to have more successful measurements to compare FEC I and II in the real world.

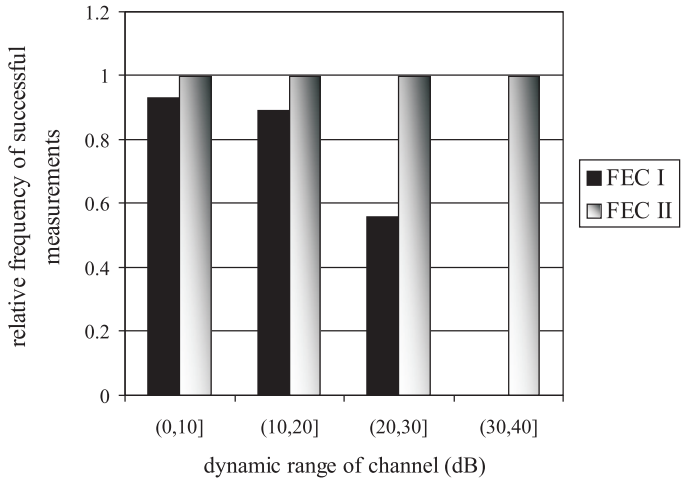

Fig. 6.16: The comparison between FEC I and FEC II in the probability of successful measurements for each $\mathcal{D}$ range over 89 measurements. For FEC I, successful measurement means BER $< 10^{-3}$. For FEC II, measurement succeeds only it has the error-free quality.

measurements while FEC II gives us the error-free quality in all the measurements at $\mathcal{D} \in$ (0,10] dB. That shows FEC II is more robust to the imperfections in the real world than FEC I. Furthermore, FEC I fails in more than 40% of the measurements at $\mathcal{D} \in$ (20,30] dB and it can not survive in the measurements at $\mathcal{D} \in$ (30,40] dB. From this point, we already can conclude that FEC II works better than FEC I in practice.

Both FEC I and II succeed in 77 measurements, where the SNR of the received signal ranges from 12 dB to 25 dB. In order to investigate whether FEC II can endure higher level of noise floor (i.e. lower SNR) than FEC I, we add extra white noise to the received signal in the software. It is difficult to have the same SNR range in all measurements, so we evaluate their practical performance by analyzing the statistical characteristics of measurements.

Here, we define $\mathrm{SNR_I}$ as the minimum SNR for FEC I to achieve a BER of 10^{-3} or lower and $\mathrm{SNR_{II}}$ as the minimum SNR for FEC II to have the error-free quality for each measurement. The difference between $\mathrm{SNR_I}$ and $\mathrm{SNR_{II}}$ is expressed as:

$$\Delta = \mathrm{SNR_I} - \mathrm{SNR_{II}} \tag{6.4}$$

If $\Delta > 0$ (i.e. $\mathrm{SNR_I} > \mathrm{SNR_{II}}$), FEC I needs higher SNR (i.e. lower level of noise floor) to achieve BER $< 10^{-3}$ than FEC II at BER $= 0$. $\Delta < 0$ is for the opposite case.

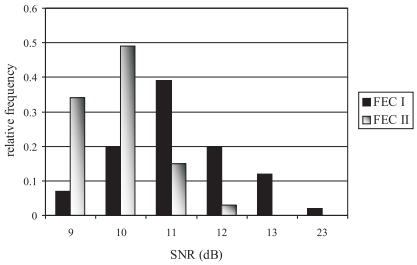

(a) Histogram of $\mathrm{SNR_I}$ and $\mathrm{SNR_{II}}$ for $\mathcal{D} \in$ (0,10] dB.

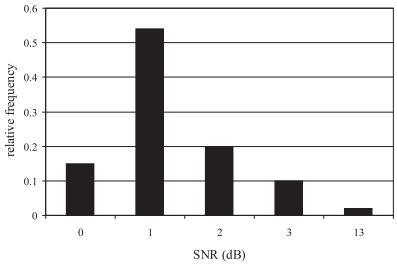

(b) Histogram of Δ for $\mathcal{D} \in$ (0,10] dB

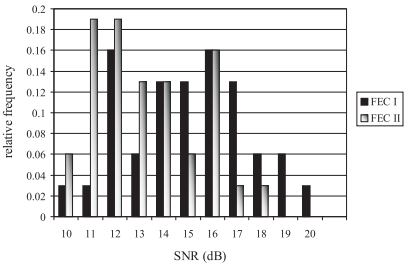

(c) Histogram of $\mathrm{SNR_I}$ and $\mathrm{SNR_{II}}$ for $\mathcal{D} \in$ (10,20] dB.

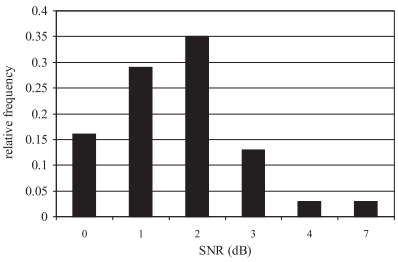

(d) Histogram of Δ for $\mathcal{D} \in$ (10,20] dB

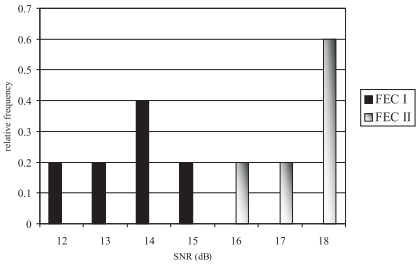

(e) Histogram of $\mathrm{SNR_I}$ and $\mathrm{SNR_{II}}$ for $\mathcal{D} \in$ (20,30] dB.

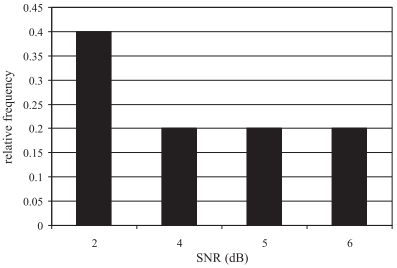

(f) Histogram of Δ for $\mathcal{D} \in$ (20,30] dB

Fig. 6.17: Histogram of $\mathrm{SNR_I}$, $\mathrm{SNR_{II}}$ and Δ for measurements at $\mathcal{D} \in$ (0,10], (10,20] and (20,30] dB.

Figure 6.17 shows the statistical characteristics of $\mathrm{SNR_I}$, $\mathrm{SNR_{II}}$ and Δ at $\mathcal{D} \in$ (0,10] dB, (10,20] dB and (20,30] dB, respectively.

- In the case of $\mathcal{D} \in$ (0,10] dB, around 80% of $\mathrm{SNR_I}$ is in the range of [10,12] dB and around 85% of $\mathrm{SNR_{II}}$ is in the range of [9,10] dB, as shown in Figure 6.17(a).

That already presents that FEC II needs less SNR to have BER = 0 than FEC I to reach BER $< 10^{-3}$. Figure 6.17(b) shows whether SNR_I is always larger than SNR_II in every measurement at $\mathcal{D} \in$ (0,10] dB. Around 15% of measurements have the same SNR for both FEC I and II to reach their required BER. For the other 85% of measurements, SNR_I is larger than SNR_II. Their difference in around 50% of measurements is about 1 dB. On average, SNR_I is around 11.4 dB, SNR_II is around 9.9 dB and Δ is around 1.5 dB. With SNR_I, the average BER of FEC I is around 10^{-4}. That concludes FEC II has a SNR gain of around 1.5 dB to reach the error-free quality comparing to FEC I at BER = 10^{-4} at $\mathcal{D} \in$ (0,10] dB.

- In the case of $\mathcal{D} \in$ (10,20] dB, both SNR_I and SNR_II have a wider range with respect to $\mathcal{D} \in$ (0,10] dB, as we can see in Figure 6.17(b) and 6.17(c). Around 67% of SNR_I is in the range of [11,16] dB while around 87% of SNR_II lies in the same range. Figure 6.17(d) shows that SNR_I is also not smaller than SNR_II in the measurements at $\mathcal{D} \in$ (10,20] dB. Around 16% of measurements have the same SNR for FEC I and II to have successful measurements. In those 31 measurements at $\mathcal{D} \in$ (10,20] dB, the average SNR_I is around 15 dB, the average SNR_II is around 13.3 dB and their average difference Δ is around 1.7 dB. With SNR_II in Figure 6.17(c), the average BER of FEC I is around 1.4×10^{-4}. Therefore, we can conclude that FEC II has a SNR gain of around 1.7 dB to have BER = 0 in comparison with FEC I to reach BER = 1.4×10^{-4} at $\mathcal{D} \in$ (10,20] dB.

- In the case of $\mathcal{D} \in$ (20,30] dB, SNR_I and SNR_II have different range to have successful measurements. SNR_I lies in the range of [16,18] dB while SNR_II is in the range of [12,15] dB. That means that FEC I always needs a higher SNR to achieve a BER of 10^{-3} or lower than FEC II to have the error free quality. On average, SNR_I is around 17.4 dB, SNR_II is around 13.6 dB and Δ is around 3.8 dB. In addition, the average BER of FEC I is around 3×10^{-4} with SNR_I. For the measurements at $\mathcal{D} \in$ (20,30] dB, we can say that FEC II has a SNR gain of around 3.8 dB to have no bit errors with respect to FEC I at BER = 3×10^{-4}.

As mentioned earlier, FEC I fails in the measurement at $\mathcal{D} \in$ (30,40] dB but FEC II survives. By adding extra white noise, FEC II still have the error-free quality at SNR = 14 dB. In general, FEC II performs better than FEC I in practice. To have successful measurement, their minimum SNR difference Δ becomes larger as $\mathcal{D}$ increases. That is also shown in the simulation.

6.2.5 Conclusions

Opportunistic error correction based on fountain codes is specially beneficial for OFDM systems to lower the power consumption in ADCs. The key idea is to lower the dynamic range of the channel by discarding part of the channel with deep fading. By transmitting one packet over a single sub-carrier, fountain codes can reconstruct the original file by only using the packets transmitted over the sub-carriers with high

energy. In such case, the resolution (i.e. the power consumption) of ADCs can be reduced. Correspondingly, the noise floor can be increased. With the same effective throughput, simulation results showed that this new cross coding scheme saves around 52% of energy in ADCs comparing to the joint coding scheme defined in the IEEE 802.11a system [40]. With the same code rate, it has a SNR gain of around 8.5 dB over Channel Model A with respect to the joint coding scheme used in the current WLAN system [24]. However, it is not clear whether this new method also performs better than the traditional joint coding scheme over a narrow-band channel.

We have investigated its performance over the TGn channel with different dynamic range and bandwidth in the simulation under the condition of the same code rate (i.e. $R = 0.5$) and the same modulation scheme (i.e. QAM-16). We compare three FEC schemes in the simulation: the LDPC code from the IEEE 802.11n standard (i.e. FEC I), fountain codes with the (175,255) LDPC code plus 7-bit CRC using the transmission Mode I (i.e. opportunistic error correction, FEC II) and fountain codes with the (175,255) LDPC code plus 7-bit CRC using the transmission Mode II (i.e. FEC III). In comparison with FEC I at a BER of 10^{-5} or lower, FEC II has a SNR loss of around 1 dB at $\mathcal{D} \in$ [0,10] dB, but it has a SNR gain of around 1 dB at $\mathcal{D} \in$ (10,20] dB, around 6 dB at $\mathcal{D} \in$ (20,30] dB, around 10.5 dB at $\mathcal{D} \in$ (30,40] dB and around 13.5 dB at $\mathcal{D} \in (40,+\infty)$ dB. Comparing to FEC III at the error-free quality, FEC II has the same performance at $\mathcal{D} \in$ [0,10] dB, but it has a SNR gain of around 1 dB at $\mathcal{D} \in$ (10,20] dB, around 3 dB at $\mathcal{D} \in$ (20,30] dB, around 7 dB at $\mathcal{D} \in$ (30,40] dB and around 11 dB at $\mathcal{D} \in (40,+\infty)$ dB. Therefore, our conclusion is that opportunistic error correction works better than the joint coding scheme at $\mathcal{D} \in (20,+\infty)$ dB. In addition, FEC II performs better than the joint coding scheme (i.e. FEC I and III) over the TGn channel at 5 MHz, 10 MHz and 20 MHz. If the wireless channel at a certain BW has $\mathcal{D} > 20$ dB, this novel cross coding scheme allows us to have higher level of noise floor than the joint coding scheme.

Furthermore, we evaluate the performance of opportunistic error correction in practice. With the same code rate, FEC I and II are compared in the experimental communication testbed. Due to the noise floor of the testbed, we choose QPSK instead of QAM-16 as the modulation scheme to have more successful measurement at a high range of $\mathcal{D}$. Although FEC I works better than FEC II when $\mathcal{D} \in$ [0,10] dB in the simulation, it does not happen in the real world. That means opportunistic error correction is more robust to the imperfections in the real world than the joint coding scheme. More measurements succeed in FEC II than in FEC I. With respect to the joint coding scheme (i.e. FEC I), on average, opportunistic error correction has a SNR gain of around 1.5 dB at $\mathcal{D} \in$ (0,10] dB, around 1.7 dB at $\mathcal{D} \in$ (10,20] dB and around 3.8 dB at $\mathcal{D} \in$ (20,30] dB. Besides, FEC II can offer us the error-free quality but FEC I can only achieve a BER of 10^{-4} at $\mathcal{D} \in$ (0,10] dB, 1.4×10^{-4} at $\mathcal{D} \in$ (10,20] dB and 3×10^{-4} at $\mathcal{D} \in$ (20,30] dB. The performance difference between FEC I and II becomes larger as $\mathcal{D}$ increases, as shown in the simulation and in the practical measurement. Therefore, we conclude that opportunistic error correction works better than the joint coding scheme.

Chapter 7

Conclusions and Recommendations

7.1 Conclusions

The wireless channel is a hostile environment, so the error correction coding is always required to mitigate the noise and interference encountered during the signal transmission. However, the current design of error correction codes does not take the power consumption in ADCs into account. ADCs consume about 50% of the total base-band power. The power-efficiency of ADCs does not increase in the same speed as the baseband signal processing. Given the same specification, the power consumed in ADCs halves every 2.7 years but the power consumption in the baseband signal processing decreases a factor of 10 every 5 years. In the case of RF signal processing, its power efficiency is limited by the technology. Therefore, ADCs are the main bottleneck for an energy-efficient wireless receiver.

Quantized channels arise in practical communication systems where ADCs are used to sample analog signals corresponding to the transmitted data. Conventional narrow-band systems usually do not take quantization into account, which is reasonable since a large number of quantization levels is used. In this case the difference between the quantized and unquantized channel can be neglected. To lower the resolution of ADCs in the narrow-band wireless system, we need to take the quantization into account. In Chapter 2, we have investigated reliable communication over quantized channels from the information theoretical point of view. With a proper design of a quantization scheme, $d+1$ or $d+2$ quantized bits are already enough when d source bits are mapped into conventional PAM and transmitted over an AWGN channel. Furthermore, we have derived a coded modulation scheme based on multi-level coding and binary linear

block codes to achieve the theoretical limits. For the block length of 10^4 bits, a low bit error rate (i.e. BER $< 10^{-4}$) is achievable at only 1.5 dB from the Shannon limit for $d = 2$ and at 1.4 dB for $d = 3$.

High-resolution ADCs are also applied in the wide-band wireless system. The multi-path effect makes the equalizer in the single-carrier wide-band wireless receiver complicated. OFDM is a common technology to simplify the equalizer in the wide-band communication. The disadvantage of OFDM is the high PAPR. When signal peaks in the OFDM signal are clipped, all sub-carriers are affected. Due to the frequency selectivity of the wide-band wireless channel, some sub-carriers suffer deep fading which can not afford any distortion. Consequently, unreliable communication happens. That urges to use high-resolution ADCs in the OFDM system. The ADC applied in the current OFDM-based wireless receiver are designed for worst-case channel conditions. However, the worst case does not always happen. Therefore, we propose to use resolution adaptive ADCs in this thesis. In such case, the ADC can be designed for each channel realization instead of being fixed for the worst-case channel condition. Correspondingly, the power consumption in ADCs can be reduced.

A further resolution reduction in ADCs can be achieved by using an energy-efficient error correction scheme. Current OFDM systems utilize the joint coding scheme. With this method, source data is encoded over all the sub-carriers. The joint coding scheme works better than the separate coding scheme, as it employs the fact that sub-carriers with high energy can compensate for sub-carriers with low-energy. Its drawback is that each sub-carrier must be correctly decoded. Hence, the maximum level of noise floor endured by the joint coding scheme is limited to the dynamic range of the channel. Correspondingly, the minimum resolution of the ADC required by the joint coding scheme in a certain channel condition is dependent on the dynamic range of the channel. A way to reduce the dynamic range of the channel is to neglect the deep-fading part of the channel and to take care of the high-energy part only. Obviously, the joint-coding scheme can not achieve it. Therefore, we propose an energy-efficient error correction scheme based on fountain codes for OFDM systems. Fountain codes can reconstruct the original source file by only collecting enough number of fountain-encoded packets. It does not matter which packet is received but only need to receive enough number of packets. In other words, fountain-encoded packets are independent with respect to each other. Since fountain codes are designed for erasure channels, error correction codes are required to transfer the noisy wireless channel into an erasure channel. That inspires us to exchange the code rate of error correction codes with the number of sub-carriers with deep fading. In this case, the resolution of ADCs can have another reduction.

It is called opportunistic error correction based on resolution adaptive ADCs and fountain codes. It can be applied in any OFDM systems.

- In the case of SISO-OFDM systems, we have shown that more than 70% of the energy consumption in the ADCs can be saved compared with the conventional IEEE 802.11a WLAN system under the same channel conditions and throughput. In addition, it requires 7.5 dB less SNR than the 802.11a system. Furthermore,

measurement results show that the FEC layer used in the WLAN system consumes at least 26 times of the amount of power in ADCs comparing to the proposed cross-layer method.

- In the case of OFDM-based broadcasting systems, around 84% of the energy consumption in ADCs can be saved compared with the conventional mobile TV system under the same channel conditions. To achieve a data rate of 9.5 Mbits/s, this new approach has a SNR gain of at least 10 dB with the perfect channel knowledge and 11 dB with the non-perfect channel knowledge comparing to the current FEC layer in the DVB-T2 standard. With a low-complexity interpolation-based channel estimation algorithm, opportunistic error correction offers us a QEF (Quasi Error Free) quality with a maximum DF (Doppler Frequency) of 40 Hz but the current DVB-T2 FEC layer can only provide a BER of 10^{-7} quality after BCH decoding with a maximum DF of 20 Hz.

- In the case of MIMO-OFDM systems, this approach allows around 83% of power saving in ADCs for a 2×2 system and 90% for a 4×4 system. With the current FEC scheme defined in the IEEE 802.11n standard, a 4×4 system requires twice amount of power in ADCs as a 2×2 system when receiving the same amount of information with the same power. However, using opportunistic error correction in a 4×4 system costs only around 1.4 times amount of energy in ADCs comparing to a 2×2 system. The coarse quantization means this new method can afford a higher level of noise floor. At the same code rate, simulation results show that opportunistic error correction works better (i.e. requires lower SNR) than the FEC layers defined in the IEEE 802.11n standard. Comparing to RCPC with interleaving, the SNR gained by opportunistic error correction decreases as the multiplexing gain increases. In addition, we evaluate their performance in the real world. This novel approach does not have the same SNR gain in practice as in the simulation, comparing to the FEC layers in the IEEE 802.11n standard. Measurement results show that this new scheme survives in the most channel conditions (i.e. 92%) with respect to RCPC with interleaving (i.e. 86%) and the LDPC code from the IEEE 802.11n standard (i.e. around 80%).

In Chapter 6, we have shown at which environment opportunistic error correction works best. Simulation results show that, with the same code rate, the joint coding scheme works better than opportunistic error correction when the dynamic range of the channel $\mathcal{D}$ is within 10 dB. However, opportunistic error correction starts to show its advantage over the joint coding scheme at $\mathcal{D} > 10$ dB. Their performance difference becomes larger as $\mathcal{D}$ increases. Furthermore, practical measurements show that it is more robust to the imperfections in the real world than the joint coding scheme. More measurements succeed in opportunistic error correction than in the joint coding scheme. This new scheme works better in practice than the joint coding scheme over the wireless channel at any $\mathcal{D}$. With respect to the LDPC code from the IEEE 802.11n standard, on average, this novel approach gains a SNR of around 1.5 dB at $\mathcal{D} \in$ (0,10] dB, around 1.7 dB at $\mathcal{D} \in$ (10,20] dB and around 3.8 dB at $\mathcal{D} \in$ (20,30] dB. Besides, opportunistic error correction can offer us the error-free

quality but the LDPC code defined in the IEEE 802.11n standard can only achieve a BER of 10^{-4} at $\mathcal{D} \in$ (0,10] dB, 1.4×10^{-4} at $\mathcal{D} \in$ (10,20] dB and 3×10^{-4} at $\mathcal{D} \in$ (20,30] dB. Their performance difference becomes larger as $\mathcal{D}$ increases, as shown in the simulation and in the practical measurement. Therefore, we can conclude that opportunistic error correction works better than the joint coding scheme.

7.2 Recommendations

In this section, we make the following recommendations on the possible future work based on the research carried out in this thesis.

- In this thesis, fountain codes allow us to exchange the code rate of error correction codes with the number of discarded sub-carriers. Chapter 2 - 5 has shown that this trade is profitable from the ADC power consumption point of view and the SNR gain point of view. Instead of trading the code rate with the sub-carriers in deep fading, there is another possibility to achieve this gain by using a higher order modulation scheme for each fountain-encoded packet comparing to the joint coding scheme.

- Based on the above point, it is recommendable to investigate the possibility to improve the performance of the current opportunistic error correction by choosing a suitable code rate and a certain modulation order.

- Opportunistic error correction is generic. Except fountain codes, any erasure codes can be applied. Same for the error correcting codes. In this thesis, we choose LT codes and the (175,255) LDPC code with 7-bit CRC to prove the concept. Although this combination gives us a good result in the MIMO-OFDM sytem, their advantage over the FEC layers in the IEEE 802.11n standard decreases as the number of antennas M increases. Therefore, it is recommendable to investigate whether the parameters (i.e. the type of error correcting codes, the code rate and the type of modulation scheme) of opportunistic error correction should be adjusted according to M.

- Opportunistic error correction allows us to neglect the sub-carriers with deep fading. That means this method is robust to the situation with at least narrow-band interference. Therefore, it is recommendable to look at its performance with respect to the interference (i.e. the narrow-band interference and the wide-band interference).

Bibliography

[1] J. Proakis and M. Salehi, *Digital Communications*. McGraw-hill New York, 1995.

[2] D. Tse and P. Viswanath, *Fundamentals of Wireless Communication*. New York, NY, USA: Cambridge University Press, 2005.

[3] T. Rappaport, *Wireless Communications: Principles and Practice*. Prentice Hall PTR Upper Saddle River, NJ, USA, 2001.

[4] J. Bingham, "Multicarrier Modulation for Data Transmission: An Idea Whose Time Has Come," *IEEE Communications magazine*, vol. 28, no. 5, pp. 5–14, 1990.

[5] J. Cioffi, "A Multicarrier Primer," *ANSI T1E1*, vol. 4, pp. 91–157, 1991.

[6] M. Fossorier, M. Mihaljevic, and H. Imai, "Reduced Complexity Iterative Decoding of Low-Density Parity Check Codes Based on Belief Propagation," *IEEE Transactions on Communications*, vol. 47, no. 5, pp. 673–680, 1999.

[7] I. Telatar, "Capacity of Multi-Antenna Gaussian Channels," *European transactions on telecommunications*, 1999.

[8] "MIMO in Mass-Market: Shifting the MIMO paradigm towards robustness and low cost."

[9] B. Murmann and B. Boser, *Digitally Assisted Pipeline ADCs: Theory and Implementation*. Kluwer Academic Pub, 2004.

[10] G. Moore *et al.*, "Progress in Digital Integrated Electronics," *SPIE MILESTONE SERIES MS*, vol. 178, pp. 179–181, 2004.

[11] J. Thomson, B. Baas, E. M. Cooper, J. M. Gilbert, G. Hsieh, P. Husted, A. Lokanathan, J. S. Kuskin, D. McCracken, B. McFarland, T. H. Meng, D. Nakahira, S. Ng, M. Rattehalli, J. L. Smith, R. Subramanian, L. Thon, Y.-H. Wang, R. Yu, and X. Zhang, "An Integrated 802.11a Baseband and MAC Processor," *Solid-State Circuits Conference, 2002. Digest of Technical Papers. ISSCC. 2002 IEEE International*, vol. 1, pp. 126–451 vol.1, 2002.

[12] B. Murmann, "A/D Converter Trends: Power Dissipation, Scaling and Digitally Assisted Architectures," in *IEEE Custom Integrated Circuits Conference, 2008. CICC 2008*, pp. 105–112, 2008.

[13] A. Bahai, B. Saltzberg, and M. Ergen, *Multi-carrier Digital Communications: Theory and Applications of OFDM*. Springer, 2004.

[14] H. Liu and G. Li, *OFDM-Based Broadband Wireless Networks: Design and Optimization*. Wiley-Interscience, 2005.

[15] M. Engels, *Wireless OFDM Systems: How to Make Them Work?* Kluwer Academic Publishers, 2002.

[16] G. Li, *OFDM-based Broadband Wireless Networks: Design and Optimization*. Wiley-Blackwell, 2005.

[17] IEEE, "Wireless LAN Medium Access Control (MAC) and Physical Layer (PHY) Specifications, High-Speed Pysical Layer in the 5 GHz Band (IEEE 802.11a Standard, Part 11)," 1999.

[18] X. Shao and C. Slump, "Quantization Effects in OFDM Systems," in *Proceedings of 29th Symposisum on Information Theory in the Benelux*, (Leuven), May 2008.

[19] G. Faria, J. A. Henriksson, E. Stare and P. Talmola, "DVB-H: Digital Broadcast Services to Handheld Devices," in *Proceedings of the IEEE*, vol. 94, Jan. 2006.

[20] European Telecommunications Standards Institute, "Digital Video Broadcasting (DVB); Framing Structure, Channel Coding and Modulation for Digital Terrestrial Television," 2004.

[21] D. J. C. MacKay, "Fountain Codes," *IEE Communications*, vol. 152, no. 6, pp. 1062–1068, 2005.

[22] European Telecommunications Standards Institute, "Framing Structure, Channel Coding and Modulation for A Second Generation Digital Terrestrial Television Broadcasting System (DVB-T2)," June 2008.

[23] IEEE, "Draft Standards for Wireless LAN Medium Access Control (MAC) and Physical Layer (PHY) Specifications, Enhancements for Higher Throughput (IEEE 802.11n Standard, Part 11)," Jan, 2007.

[24] X. Shao, C.H. Slump, "A Novel Cross Coding Scheme for OFDM Systems," in *IEEE Information Theory Workshop*, 2009.

[25] X. Shao and H. Cronie, "Modulation and coding for quantized channels," in *Proceedings of SPS-DARTS 2007, the third annual IEEE Benelux/DSP Valley Signal Processing Symposium, Antwerp, Belgium* (W. Philips, ed.), (Antwerp), pp. 179–183, IEEE Benelux/DSP, March 2007.

[26] J. Reed, *Software Radio: a Modern Approach to Radio Engineering*. Prentice Hall Press Upper Saddle River, NJ, USA, 2002.

[27] R. Schiphorst, "Software-defined radio for wireless local-area networks," 2004.

[28] Gallager, R.G., *Information Theory and Reliable Communication*. John Wiley & Sons, Inc. New York, NY, USA, 1968.

[29] S. Ross, *Introduction to Probability Models*. Academic Pr, 2006.

[30] S. Axler, F.W. Gehring and K.A. Ribet, *Linear Algebra*. Springer, 1997.

[31] R. Gray and D. Neuhoff, "Quantization," *IEEE Transactions on Information Theory*, vol. 44, no. 6, pp. 2325–2383, 1998.

[32] S. Lloyd, "Least squares quantization in PCM," *IEEE Transactions on Information Theory*, vol. 28, no. 2, pp. 129–137, 1982.

[33] J. Max, "Quantizing for Minimum Distortion," *IRE Transactions on Information Theory*, vol. 6, no. 1, pp. 7–12, 1960.

[34] U. Wachsmann, R. Fischer, and J. Huber, "Multilevel Codes: Theoretical Concepts and Practical Design Rules," *IEEE Transactions on Information Theory*, vol. 45, no. 5, pp. 1361–1391, 1999.

[35] H. Imai and S. Hirakawa, "A new multilevel coding method using error-correcting codes," *IEEE Transactions on Information Theory*, vol. 23, no. 3, pp. 371–377, 1977.

[36] H. Cronie, "Superposition Coding for Power-and Bandwidth Efficient Communication Over the Gaussian Channel," in *IEEE International Symposium on Information Theory, 2007. ISIT 2007*, pp. 2311–2315, 2007.

[37] T. Richardson and R. Urbanke, *Modern Coding Theory*. Cambridge University Press, 2008.

[38] T. Richardson, M. Shokrollahi, and R. Urbanke, "Design of Capacity-Approaching Irregular Low-Density Parity-Check Codes," *IEEE Transactions on Information Theory*, vol. 47, no. 2, pp. 619–637, 2001.

[39] Chung, S.Y. and Forney, G.D. and Richardson, T.J. and Urbanke, R., "On the Design of Low-Density Parity-Check Codes within 0.0045 dB of the Shannon Limit," *IEEE Communications Letters*, vol. 5, no. 2, pp. 58–60, 2001.

[40] X. Shao, R. Schiphorst, and C. H. Slump, "An Opportunistic Error Correction Layer for OFDM Systems," *EURASIP Journal on Wireless Communications and Networking*, 2009.

[41] X. Shao, R. Schiphorst, and C. Slump, "Opportunistic Error Correction for WLAN Applications," *Proceedings of the 4th IEEE International Conference on Wireless Communications, Networking and Mobile Computing*, 2008.

[42] D. MacKay, "Fountain Codes," *IEE Communications*, vol. 152, no. 6, pp. 1062–1068, 2005.

[43] M. Luby, "LT Codes," *Proceedings of the 43rd Annual IEEE Symposium on Foundations of Computer Science*, pp. 271–282, 2002.

[44] A. Shokrollahi, "Raptor Codes," *IEEE Transaction on Information Theory*, vol. 52, 2006.

[45] H. Zhu, C. Zhang, and J. Lu, "Designing of Fountain Codes with Short Code-Length," *Signal Design and Its Applications in Communications, 2007. IWSDA 2007. 3rd International Workshop on*, pp. 65–68, 2007.

[46] A. Bogdanov, M. C. Mertens, C. Paar, J. Pelzl, and A. Rupp, "A Parallel Hardware Architecture for Fast Gaussian Elimination over GF(2)," *14th Annual IEEE Symposium on Field-Programmable Custom Computing Machines*, 2006.

[47] Y. Kou, S. Lin, and M. Fossorier, "Low-Density Parity-Check Codes Based on Finite Geometries: A Rediscovery and New Results," *Information Theory, IEEE Transactions on*, vol. 47, no. 7, pp. 2711–2736, 2001.

[48] C. Berrou, A. Glavieux, and P. Thitimajshima, "Near Shannon Limit Error-Correcting Coding and Decoding: Turbo-Codes.," in *Communications, 1993. ICC 93. Geneva. Technical Program, Conference Record, IEEE International Conference on*, vol. 2, 1993.

[49] E. Jacobsen, "LDPC FEC for 802.11 n Application," *IEEE*, 2003.

[50] S. Nahata, K. Choi, and S. Yoo, "A High-Speed Power and Resolution Adaptive Flash Analog-to-Digital Converter," *SOC Conference, 2004. Proceedings. IEEE International*, pp. 33–36, 12-15 Sept. 2004.

[51] S. Ross, *Introduction to Probability Models*. Orlando, FL, USA: Academic Press, Inc., 2003.

[52] A. Doufexi, S. Armour, P. Karlsson, A. Nix, and D. Bull, "A Comparison of HIPERLAN/2 and IEEE 802.11 a," *IEEE Comminication Magazine*, 2002.

[53] X. Shao, C.H. Slump, "Practical Evaluation of Opportunistic Error Correction," in *IEEE Global Telecommunications Conference (GLOBECOM)*, (Honolulu, USA), December 2009.

[54] D. MacKay, *Information Theory, Interference, and Learning Algorithms*. Cambridge, UK: Cambridge University Press, 2003.

[55] T. Schmidl and D. Cox, "Robust Frequency and Timing Synchronization for OFDM," *IEEE Transactions on Communications*, vol. 45, no. 12, pp. 1613–1621, 1997.

[56] X. Shao, R. Schiphorst and C.H. Slump, "Energy Efficient Error Correction in Mobile TV," in *IEEE International Conference on Communications (ICC)*, (Dresden, Germany), June 2009.

[57] R. van de Plassche, *CMOS Integrated Analog-to-Digital and Digital-to-Analog Converters*. Kluwer Academic Publishers, 2003.

[58] X. Shao, R. Schiphorst and C.H. Slump, "An Opportunistic Error Correction Layer for OFDM Systems," *EURASIP Journal on Wireless Communications and Networking*, submitted for publication.

[59] X. Shao, R. Schiphorst and C. H. Slump, "Opportunistic Error Correction for WLAN Applications," in *Proceedings of the 4th IEEE International Conference on Wireless Communications, Networking and Mobile Computing*, (Da Lian, China), Oct. 2008.

[60] X. Shao, C. H. Slump, "Opportunistic Error Correction for OFDM-based DVB Systems," *IEEE Transactions on Wireless Communications*, submitted for publication.

[61] A.R.S. Bahai, B.R. Saltzberg, and M. Ergen, *Multi-Carrier Digital Communications: Theory and Applications of OFDM*. Springer Verlag, 2004.

[62] European Telecommunications Standards Institute, "Digital Video Broadcasting (DVB); Transmission System for Handheld Terminals (DVB-H)," November 2004.

[63] U. Reimers, *DVB: the Family of International Standards for Digital Video Broadcasting*. Springer Verlag, 2005.

[64] A.B. Carlson, *Communication Systems: An Introduction to Signal and Noise in Electrical Engineering*. New York: McGraw-Hill, 1986.

[65] Gallager, R.G., *Low-Density Parity-Check Codes*. MIT Press, 1963.

[66] D. MacKay and R. Neal, "Good Codes Based on Very Sparse Matrices," *Cryptography and coding*, pp. 100–111, 1995.

[67] T. Richardson, M. Shokrollahi, and R. Urbanke, "Design of Capacity-Approaching Irregular Low-Density Parity-Check Codes," *IEEE Transactions on Information Theory*, vol. 47, no. 2, pp. 619–637, 2001.

[68] S. Lin and D. Costello, *Error Control Coding: Fundamentals and Applications*. Prentice-hall Englewood Cliffs, NJ, 1983.

[69] M. Mitzenmacher, "Digital Fountains: A Survey and Look Forward," in *IEEE Information Theory Workshop, 2004*, pp. 271–276, 2004.

[70] X. Shao, R. Schiphorst and C.H. Slump, "An Opportunistic Error Correction Layer for OFDM Systems," *EURASIP Journal on Wireless Communications and Networking*, 2009.

[71] M. Failli, "Digital Land Mobile Radio Communications COST 207," *European Commission, EUR*, vol. 12160.

[72] P. Maymounkov, "Online Codes," *Research Report TR2002-833, New York University*, 2002.

[73] X. Shao and C.H. Slump, "A Novel Cross Coding Scheme for OFDM Systems," in *IEEE Information Theory Workshop (ITW)*, (Taormina, Italy), October 2009.

[74] Y. Kou, S. Lin and M.P.C Fossorier, "Low-Density Parity-Check Codes Based on Finite Geometries: a Rediscovery and New Results," *IEEE Transactions on Information Theory*, vol. 47, no. 7, pp. 2711–2736, 2001.

[75] W. Peterson and D. Brown, "Cyclic Codes for Error Detection," *Proceedings of the IRE*, vol. 49, no. 1, pp. 228–235, 1961.

[76] M. Speth, S. Fechtel, G. Fock and H. Meyr, "Optimum Receiver Design for OFDM-based Broadband Transmission-Part II: A Case Study," *IEEE Transactions on Communications*, vol. 49, no. 4, pp. 571–578, 2001.

[77] S. Coleri, M. Ergen, A. Puri and A. Bahai, "Channel Estimation Techniques Based on Pilot Arrangement in OFDM Systems," *IEEE Transactions on Broadcasting*, vol. 48, no. 3, pp. 223–229, 2002.

[78] ETSI, "Implementation Guidelines for DVB Terrestrial Services: Transmission Aspects," tech. rep., ETSI Technical Report TR 101 190v1. 1.1 (1997-12).

[79] X. Shao and C. H. Slump, "Opportunistic Error Correction for MIMO," in *The 20th Personal, Indoor and Mobile Radio Communications Symposium 2009 (PIMRC'09)*, (Tokyo, Japan), September 2009.

[80] M. Mitzenmacher, "Digital Fountains: A survey and Look Forward," in *IEEE Information Theory Workshop*, pp. 271–276, 2004.

[81] A. Shokrollahi, "Raptor codes," *Information Theory, IEEE Transactions on*, vol. 52, no. 6, pp. 2551–2567, 2006.

[82] X. Shao, C. H. Slump, "Opportunistic Error Correction for MIMO-OFDM Systems: from Theory to Practice," *IEEE Transactions on Wireless Communications*, submitted for publication.

[83] A. Paulraj, R. Nabar, and D. Gore, *Introduction to Space-Time Wireless Communications*. Cambridge University Press, 2003.

[84] T. Kaiser and A. Bourdoux, *Smart Antennas: State of the Art*. Hindawi Pub Corp, 2005.

[85] E. Biglieri, R. Calderbank, and A. Constantinides, *MIMO Wireless Communications*. Cambridge Univ Pr, 2007.

[86] K. Fazel and S. Kaiser, *Multi-Carrier and Spread Spectrum Systems*. Wiley, 2003.

[87] M. Gast, *802.11 Wireless Networks: the Definitive Guide*. O'Reilly Media, Inc., 2005.

[88] G. Li and G.L. Stüber, *Orthogonal Frequency Division Multiplexing for Wireless Communications*. Springer, 2006.

[89] J. Heiskala and J. Terry, *OFDM Wireless LANs: A Theoretical and Practical Guide*. Sams Indianapolis, IN, USA, 2001.

[90] R. Prasad, *OFDM for Wireless Communications Systems*. Artech House Publishers, 2004.

[91] M. Bossert, *Channel Coding for Telecommunications*. John Wiley & Sons, Inc. New York, NY, USA, 1999.

[92] A. Carlson, *Communication Systems*. McGraw-Hill New York, 1975.

[93] V. Erceg, L. Schumacher, P. Kyritsi, *et al.*, "TGn Channel Models," *IEEE 802.11 document 802.11-03/940r4*, 2004.

[94] L. Schumacher and B. Dijkstra, "Description of a MATLAB® Implementation of the Indoor MIMO WLAN Channel Model Proposed by the IEEE 802.11 TGn Channel Model Special Committee," *Implementation note version*.

[95] G. Foschini and M. Gans, "On Limits of Wireless Communications in a Fading Environment when Using Multiple Antennas," *Wireless personal communications*, vol. 6, no. 3, pp. 311–335, 1998.

[96] I. Telatar, "Capacity of Multi-antenna Gaussian Channels," *European transactions on telecommunications*, 1999.

[97] R. Prasad, M. Rahman, and S. Das, *Single-and Multi-Carrier MIMO Transmission for Broadband Wireless Systems*. River Publishers, 2009.

[98] C. Berrou, A. Glavieux, P. Thitimajshima, *et al.*, "Near Shannon Limit Error Correcting Coding and Decoding: Turbo-Codes (1)," in *IEEE International Conference on Communications*, pp. 1064–1064, 1993.

[99] T. Rappaport *et al.*, *Wireless Communications: Principles and Practice*. Prentice Hall PTR New Jersey, 2002.

[100] H.S. Cronie, F.W. Hoeksema and C.H. Slump, "A CSP-based Processing Architecture for a Flexible MIMO-OFDM Testbed," in *Proceedings of the Communicating Process Architectures Symposium*, (Enschede, The Netherlands), 2003.

[101] K. Akita, R. Sakata, and K. Sato, "A phase compensation scheme using feedback control for IEEE 802.11 a receiver," in *2004 IEEE 60th Vehicular Technology Conference, 2004. VTC2004-Fall*, vol. 7, 2004.

[102] European Telecom Standards Institue, "Channel Models for HIPERLAN/2 in Different Indoor Scenarios," 1998.

[103] X. Shao, C. H. Slump, "Opportunistic Error Correction: When does it Work Best for OFDM Systems?," *IEEE Transactions on Communications*, submitted for publication.

[104] T. Chiueh and P. Tsai, *OFDM Baseband Receiver Design for Wireless Communications*. Wiley, 2007.

[105] P.S. Medbo, "Channel Models for HIPERLAN/2," *ETSI/BRAN*, no. 3ERI085R, 1998.

Acknowledgements

This thesis would not have reached the current format without the help of many people. Here, I would like to thank all those who supported me during the last 4 years, while working on this Ph.D project.

First and foremost, I would like to express my sincere gratitude to my professor, Kees Slump. Thank him for giving me the opportunity to work on this Ph.D project and for all the freedom that he gave me in my research. Thanks to this freedom, I finally found out that the research work can be interesting. Also, I thank him for all the understanding and support during my tough times in the last 4 years.

This work was carried out within the framework of the "MIMO in a mass market" project. I would like to acknowledge the funding from the Dutch Ministry of Economic Affairs and I would like to thank all the project partners for the useful discussions during the project meetings. I especially acknowledge Frans Willems and Wu Yan for the fruitful discussions during all the meetings.

I would like to thank the other members of my graduation committee, Prof.dr.ir. B. Nauta, Prof.dr. P. Havinga, Prof.dr.ir. A.B. Smolders, Dr.ir. M.J. Bentum and Dr.ir. F.M.J. Willems. Thank them for taking time to read my thesis and be part of the opposition during the ceremony.

I have to thank a few former and present members in the Radio sub-group. Thank Harm for supervising me in the first year of my Ph.D. Thank Roel for the collaborations. Thank Marnix for helping me find out the hardware bugs and for some nice discussions. Thank Geert-Jan for building the MIMO testbed and all the technique help during my measurements. Many thanks to Niels for all the help during my Ph.D.

My thank goes to Anneke for all the administration help and for improving my dutch. Thank Gerbert for sharing the office with me, for all the nice conversations and for translating the summary of this thesis into dutch. Thank all the SAS colleagues for giving me a pleasant working environment.

I thank my previous and current flatmates, Denny, Francesca, Jincy, Shuhan and Xinyan, for sharing this cozy home with me. Many thanks to Shuhan for taking care of me and for arranging all the wonderful trips, especially our birthday trip in Vienna. Also, I thank all my friends in Enschede for sharing nice moments with me and thank all my friends in China for keeping a nice eye on me.

Last but not least, I thank my family in the Netherlands and in China. Thank my uncle Dazhong and his family, and my cousin Hui and her family for all the support and caring during my stay in the Netherlands. Because of them, I have never had home sick since I came here. I thank my mother, my brother, my sister-in-law and

my grandmother for their endless support and unconditional love.

Xiaoying

Enschede, April 2010.

Curriculum Vitae

Xiaoying Shao was born in Wenzhou, China. She received her B.Sc degree from Hangzhou Dianzi University in 2003. Afterwards, she did one-year Master study there. In 2004, she went to the Netherlands and continued her master study in University of Twente. She did her internship in Twente Institute for Wireless and Mobile Communications (WMC) from July to September in 2005. She received her M.Sc degree from University of Twente in 2006. In May 2006, she started working toward the Ph.D degree at the Signals and Systems Group, University of Twente. In her Ph.D study, she was working in the 'MIMO in a Mass Market' project which cooperate with Technische Universiteit Eindhoven and Delft University of Technology. Her research interest mainly lies in signal processing and information theory for communication systems.